AN ABSTRACT OF THE DISSERTATION OF

Riana I. Wernick for the degree of Doctor of Philosophy in Zoology presented on June 2, 2016.

Title: Evolutionary Genomic Responses to Mitochondrial Dysfunction in *Caenorhabditis elegans*

Abstract approved: _____

Dee R. Denver

Understanding the impact of mitochondrial dysfunction on genome evolution has the potential not only to provide new insights on the basic evolutionary processes influencing mitochondrial and nuclear genomes, but may also reveal novel avenues for evolutionary adaptive recovery from harmful mutations. Aberrant mitochondrial activity is fundamental to the pathology of mitochondrial diseases in addition to neurodegenerative disorders. While the effects of mitochondrial dysfunction have received much attention, less is known about their impact on genome evolution and potential target mechanisms for ameliorating the harmful effects of mitochondrial impairment. Characterizing genome modifications in animal populations predisposed to mitochondrial dysfunction may identify novel genes, mechanisms, and physiological pathways to target for recovery and provides a genome-wide perspective on the impact of aberrant mitochondrial activity.

This dissertation research investigates how mitochondrial and nuclear genomes evolve in organisms genetically predisposed to mitochondrial dysfunction and contrasts genomic evolution in large and small population sizes. This work furthers understanding

of the impact of evolutionary forces which influence genome evolution in population with reduced fitness, and reveals new insights into genomic responses to mitochondrial dysfunction. Chapters 2 and 3 of this dissertation focus on genome evolution using a set of mitochondrial respiratory chain mutant (*gas-1* strain) and wild-type (N2 strain) *Caenorhabditis elegans* mutation-accumulation (MA) lines that experienced single-worm bottlenecking. The N2 MA lines, derived from a previous experiment, were bottlenecked for 250 generations. The *gas-1* MA lines were created for this research, and bottlenecked in the laboratory for a maximum of 50 generations. Chapter 2 investigates mitogenomic evolution and heteroplasmic inheritance patterns evolving under extreme drift in *gas-1* and N2 MA lines. Chapter 3 analyzes nuclear genome evolution using this same set of *gas-1* and N2 MA lines. In contrast, Chapter 4 provides a complementary perspective, analyzing mitochondrial and nuclear genome evolution in twenty-four *gas-1* 'recovery line' (RC) populations, evolved in large population sizes for sixty generations. Bioinformatic methods and computational simulations were applied to characterize and evaluate genome evolution and provide a comprehensive investigation of the impact of mitochondrial dysfunction within a population genetics framework.

In Chapter 2 our results of inherited mitochondrial DNA (mtDNA) heteroplasmy are in alignment with predictions of theories where a small subset of mtDNA molecules from the parental generation repopulates the mitochondrial genome pool for the progeny. Comparisons between Chapter 2 and 4 suggest that in both *gas-1* and N2 strains organelle genome copy number is elevated in an environment characterized with extreme genetic drift but is less impacted throughout evolution in large populations when the force of genetic drift is reduced.

Investigation of nuclear genome evolution in Chapter 3 revealed putative beneficial nuclear mutations in bottlenecked *gas-1* populations. Additionally, compared to the N2 MA lines, the *gas-1* MA lines were also observed to have a greater number of mutations located within the *gas-1* gene interaction network. These observations reveal new insights into the potential fitness landscape for beneficial mutation and how nuclear genome evolution differs when predisposed to mitochondrial dysfunction in an environment characterized by extreme genetic drift.

In Chapter 4, focusing on evolution in large populations, we observed parallel and potentially compensatory mitochondrial mutations indicative of positive selection in the gas-*1* RC lines. Identified at heteroplasmy levels near-fixation, these mtDNA mutations were located in genes predicted to physically interact with the *gas-1* gene. As signatures of positive selection were not detected in the mitochondrial genomes of *gas-1* MA lines analyzed in Chapter 2, this work suggests that the processes by which beneficial mtDNA mutations rise to homoplasmy within the population may be less likely to occur in small populations. Additionally, we determined the evolutionary rate of nuclear genome change in Chapter 4 to be three times slower than published mutations rate values for *C. elegans* suggesting the influence of purifying selection in RC lines. Given that a quarter of nuclear mutations were located in genes exhibiting interactions within two-degrees of *gas-1* it is likely that positive selection also influenced nuclear genome evolution. Overall, this research demonstrates that although adaptation from harmful mutation may occur in small or large populations, the observed paths to evolutionary adaptive recovery involve different mechanisms and suggests that although an environment with pervasive genetic drift may permit the fixation of beneficial nuclear mutations, the processes by

which beneficial mtDNA mutations rise to homoplasmy within the population may be less permissive.

Evolutionary Genomic Responses to Mitochondrial Dysfunction in *Caenorhabditis elegans*

by
Riana I. Wernick

A DISSERTATION

submitted to

Oregon State University

in partial fulfillment of
the requirements for the
degree of

Doctor of Philosophy

Presented June 2, 2016
Commencement June 2016

Doctor of Philosophy dissertation of Riana I. Wernick presented on June 2, 2016.

APPROVED:

_____

Major Professor, representing Zoology

_____

Chair of the Department of Integrative Biology

_____

Dean of the Graduate School

I understand that my dissertation will become part of the permanent collection of Oregon State University libraries. My signature below authorizes release of my dissertation to any reader upon request.

_____

Riana I. Wernick, Author

ACKNOWLEDGEMENTS

I would especially like to thank my advisor, Dr. Dee Denver for taking me on as a student and providing me with wisdom and insight into the world of evolutionary biology and pursuit of scientific endeavors. Throughout the past five years, he continually supported me during my successes and failures. He provided me with opportunities to grow not only as a scientist but also as a person, and through conversation, critical feedback and answering many questions both big and small, helped me to achieve my goals.

I would also like to thank my committee members Drs. Suzanne Estes, Viviana Perez, Barbara Taylor, and Daniel Rockey for their thoughtful feedback and support throughout my PhD. I am thankful for our interactions as they provided me with a diversity of scientific perspectives and an intellectually stimulating environment.

I would like to thank my collaborators who were instrumental to this research. Dr. Suzanne Estes collaborated with me on many projects and my writing and analytical skills greatly improved as a result of my many interactions with her. I'd also like to thank the Estes Lab at Portland State University for working together on collaborative projects and always providing fun conversation.

I thank IGERT for providing me with opportunities to discuss aging biology and learn about aging from a multitude of perspectives. Specifically, through classes and conversation Drs. Viviana Perez and Tory Hagen, my knowledge on homeostatic mechanisms and the biological aging process developed considerably. I also thank Anne Hatley for her friendship and support.

I'd like to thank the Zoology/Integrative Biology faculty for departmental support. I thank Tara Bevandich, Tori Givigliano, Traci Durrell-Khalife, Trudy Powell, and Jane Van Order for their help on many occasions. I would like to thank my teachers who inspired and challenged me. In particular, Shawn O'Neil who taught me how to think like a programmer and write Python and Unix/Liux.

ACKNOWLEDGEMENTS (Continued)

The CGRB provided sequencing support and I would like to specifically thank Mark Desenko for his assistance.

The entire Denver lab both past and present has both supported and motivated me over the past five years: Dr. Katie Clark, Dr. Amanda Brown, Dr. Michael Raboin, Dana Howe, Emily Bellis, Ian Morelan, Ahn Ha, Sulochana Wasala, and Danielle Tom. In particular, I owe a debt of gratitude to Dana Howe who reliably and diligently performed many aspects on my projects and who personally guided me as I learned to work with the *C. elegans* system and prepare DNA for sequencing (without never losing her positivity and optimism!) I would also like to thank our amazing team of undergraduate researchers, specifically Sita Ping, Jonathan Seng, Jeremey Northway, Levi Dettwyler, and Schunyce Dayton who welcomed me to the lab, helped me with my projects, and provided me with positivity.

The Zoology/ Integrative Biology graduate students have been wonderfully supportive and I am very grateful for our friendship. First and foremost a special thanks to my academic twin sister, Emily Bellis, for being there for me since day one, always supporting me and providing much needed humor! I also want to thank Trang Dang who is one of the funniest and most insightful scientists I know. Caroline Glidden and Vanessa Constant for always supporting and cheering me on. I'd also like to thank Dr. Nathan Brown from Microbiology, for his friendship, fun conversations and support and Keaton Lesnik from Bioengineering for his friendship and encouragement.

Lastly, I would like to thank my dad and mom, Arnie and Lorrie Wernick, for their never-ceasing support, encouragement and for my mom calling me every morning while I was working on my dissertation. I thank my brothers, Forrest and Grant Wernick, and my sister-in-law Julie Kuo for supporting me and making me laugh everyday.

ACKNOWLEDGEMENTS (Continued)

CONTRIBUTION OF AUTHORS

Chapter 2: Dana K. Howe performed the backcrossing work of the *gas-1* progenitor used to propagate *gas-1* MA lines, helped prepare the *gas-1* MA lines for Illumina Sequencing and provided integral assistance in writing. Drs. Suzanne Estes and Dee Denver helped conceive the research design, provided valuable input in data analysis and assistance in writing.

Chapter 3: Dana K. Howe performed the backcrossing work of the *gas-1* progenitor used to propagate *gas-1* MA lines, helped prepare the *gas-1* MA lines for Illumina Sequencing, isolated a strain with the three MA431 Chromosome III SNPs and backcrossed the SNPs onto the *gas-1* and Denver-lab N2 progenitor strains. Mitochondrial phenotyping assays (ROS and ATP output) as well as fitness assays were conducted in Dr. Suzanne Estes' Lab at Portland State University by Suzanne Estes, Stephen Christy and Michael Lue. Drs. Suzanne Estes and Dee Denver helped conceive the research design and provided valuable input in data analysis.

Chapter 4: Dana K. Howe performed the backcrossing work of the *gas-1* progenitor used to propagate *gas-1* RC lines and performed DNA extraction of synchronized *gas-1* RC lines and the *gas-1* and N2 progenitors. Jennifer Sullins from Dr. Suzanne Estes' Lab at Portland State University propagated the *gas-1* RC lines. Stephen Christy performed fitness assays of the *gas-1* RC lines and statistical analysis of fitness recovery. Dr. Suzanne Estes helped conceive the research design. Dr. Dee Denver also helped conceive the research design and provided valuable input in data analysis.

TABLE OF CONTENTS

TABLE OF CONTENTS (Continued)

TABLE OF CONTENTS (Continued)

TABLE OF CONTENTS (Continued)

LIST OF FIGURES

LIST OF FIGURES (Continued)

LIST OF TABLES

LIST OF APPENDIX FIGURES

LIST OF APPENDIX TABLES

LIST OF APPENDIX TABLES (Continued)

LIST OF ABBREVIATIONS

ADP	adenosine diphosphate
ANT	adenine nucleotide translocator
ATG6	autophagy-related protein 6
ATP	adenosine triphosphate
CED-12	cell death abnormality protein 12
CGC	Caenorhabditis Genetic Center
CGRB	Center for Genome Research and Biocomputing
COX	cytochrome c oxidase, complex IV
EMS	ethyl methanesulfonate
ER	endoplasmic reticulum
ETC	electron transport chain
FAD/FADH$_2$	flavin adenine dinucleotide
FMN	flavin mononucleotide
FOXO	mammalian forkhead transcription factor
FOXO	Forkhead box O3
GAS-1	general anesthetic sensitivity protein 1
HTS	high-throughput sequencing
IGF	insulin/insulin growth factor-like
IIS	insulin/insulin growth factor-like signaling
IMM	inner mitochondrial membrane
IMS	intermitochondrial space
LHON	Leber's hereditary optic neuropathy
LRBA	LPS-responsive vesicle trafficking, beach and anchor containing
LSP	light strand promoter
MA	mutation-accumulation
MAPK	mitogen-activated protein kinase

MELAS	mitochondrial encephalomyopathy, lactic acidosis, and strok-like episodes
mGSH	mitochondrial glutathione reductase
mtDNA	mitochondrial DNA
mTOR	mammalian target of rapamycin
NAD^+/NADH	nicotinamide adenine dinucleotide
nDNA	nuclear DNA
NGLY1	N-glycanase 1
OXPHOS	oxidative phosphorylation
PCR	polymerase chain reaction
PDK1	phosphoinositide-dependent kinase-1
PGC-1α	peroxisome proliferator activated receptor gamma, coactivator 1 alpha
PI3K/PKB	phosphoinositide 3-kinase / protein kinase B
PIP2	phosphatidylinositol-(4,5)-biphosphate
PIP2	phosphatidylinositol-(4,5)-biphosphate
PIP3	phosphatidylinositol (3,4,5)-triphosphate
Prx3	peroxiredoxin III
RC	*gas-1* recovery line
RHEB01	Ras homolog enriched in brain
ROS	reactive oxygen species
SNP	single-nucleotide polymorphism
SOD	superoxide dismutase
TAPT1	transmembrane anterior posterior transformation 1
TOR	target of rapamycin
Trx2	thioredoxin 2
Ts	Transition

TSC1/TSC1	tuberous sclerosis complex 1/2
Tv	Transversion
UPR^{mt}	mitochondrial unfolded protein response
VNTR	variable number tandem repeat

DEDICATION

There are seven people and two cats who sparked my curiosity into the world of evolutionary biology. My brothers, Forrest and Grant Wernick, and my sister-in-law Julie Kuo, who continually express genuine interest in my work and ask many thought-provoking questions that help me grow as a scientist. My cats Pollyanna (Polymerase Gamma) and K.C. (Kitty Cat) who always puzzle me with their non-human behaviors such as love of dirt baths and kneading blankets, and change the way I perceive intelligence. Polly, you enriched my life and I will always love you. My mom, Lorrie Wernick, who earned a doctoral degree in education at the age of 50, and my dad, Arnie Wernick, who shares my love of biology and accompanied me to scientific conferences on the West Coast. My boyfriend, Connor Driscoll, for his never-ending support, good-natured humor, and eagerness to discuss evolutionary processes. And finally, my new nephew, Asher Wernick, not yet two months old- may you enjoy exploring questions unknown.

1. GENERAL INTRODUCTION

The acquisition of mitochondria and the origin of the eukaryotic life were plausibly the same event (Martin and Müller, 1998). This endosymbiosis transformed evolutionary pressures acting on eukaryotes and drove the evolution of unique eukaryotic traits including the presence of a nucleus, meiotic sex, and phagocytosis (Lane, 2014). As the majority of genes for mitochondrial metabolism are encoded in the nuclear genome, functional oxidative respiration which occurs across the inner mitochondrial membrane, requires the coevolution of the mitochondrial and nuclear genomes (Lane, 2011; Tuppen et al., 2010a). While the coadaptation of mitochondrial and nuclear genomes has been well-studied, how mitochondrial dysfunction impacts genome evolution has yet to receive as much attention. Moreover, the evolutionary paths of the nuclear and mitochondrial genomes are influenced by the population size. Evolving the impaired mitochondrial Complex I electron transport chain (ETC) *gas-1* mutant *Caenorhabditis elegans* strain in bottlenecked and large population sizes, the research presented in this dissertation investigates how the nuclear and mitochondrial genomes evolve in response to mitochondrial dysfunction and how the evolutionary paths differ when propagated in small versus large population sizes.

1.1   Mitochondria organelles

Mitochondria are double-membrane-bound bioenergetic organelles located in the cytoplasm of most eukaryotic cells (de Paula et al., 2013). The outer mitochondrial membrane is permeable to most molecules less than 10kDa and plays key roles in mitochondrial biogenesis and organelle structure. The inner membrane forms convoluted,

folded structures termed cristae that encompass the mitochondrial matrix where mtDNA is harbored. The inner membrane is rich in proteins, impermeable to ions and most metabolites, and contains transporters that mediate metabolic communication with other cellular organelles and compartments. (Tsang and Lemire, 2003). In addition to generating most of the cellular energy in the form of adenosine triphosphate (ATP) through oxidative phosphorylation and β-oxidation, mitochondria also play key roles in calcium homeostasis, heme synthesis and FeS center assembly, gluconeogenesis, steroid hormone biosynthesis, ammonia detoxification via ureagenesis, ketogenesis in the liver, lipid metabolism and integration of cellular signals for apoptosis and autophagy (Galluzzi et al., 2012; Guha and Avadhani, 2013; Mayr, 2014).

Highly dynamic, mitochondrial organelles respond to cellular stressors through changes in overall mass, interconnectivity and sub-cellular localization (Księzakowska-Łakoma et al., 2014). Modifications in overall mass is accomplished through altered mitochondrial biogenesis (changes in mtDNA replication and quantity of mitochondrial proteins) and rate of mitophagy (selective degradation mitochondria) (Księzakowska-Łakoma et al., 2014). Anterograde signaling (nucleus to organelle) activates mitochondrial biogenesis through activation of nuclear transcription and cytoplasmic mRNA translation (Guha and Avadhani, 2013). Retrograde signaling, in contrast, is a process in which mitochondria communicate with the nucleus; inducing mechanisms include defects in mitochondrial ETC components, mtDNA mutations, alterations in mtDNA copy number, and some models also suggest reactive oxygen species (ROS) (Butow and Avadhani, 2004; Guha and Avadhani, 2013).

The degree to which mitochondrial organelles are interconnected (they can form continuous units) is determined by the extent of fusion which concatenates mitochondria, and fission, which results in fragmented mitochondria (Escobar-Henriques and Anton, 2013). Mitochondria have been shown to undergo constant modifications of fusion and fission as a part of adaptation to the bioenergetics status of the cell (Chevrollier et al., 2012). Accumulating data suggest that impairments in mitochondrial dynamics (fission and fusion) may play a key role both sporadic and familial Parkinson's Disease (Santos et al., 2015).

The cellular location of mitochondrial organelles is also variable (Saxton and Hollenbeck, 2012). Under hypoxic conditions, mitochondria have been shown to exhibit increased perinuclear localization (Al-Mehdi et al., 2012). In neurons mitochondria are located at axonal termini (Knott et al., 2008). To promote mitophagy, mitochondria traverse along microtubules toward lysosomes (Twig and Shirihai, 2011). Altered mitochondrial dynamics, changes in mitochondrial mass and sub-cellular spatial organization are all critical factors that when modified can exhibit harmful effects on organismal function (Księzakowska-Łakoma et al., 2014).

Oxidative phosphorylation, the production of ATP in mitochondria, is also a quintessential function modulating mitochondrial homeostasis and organismal fitness. The reduced molecules nicotinamide adenine dinucleotide (NADH) and $FADH_2$ produced through β-oxidation and the Krebs cycle located in mitochondrial matrix, are further utilized by these organelles in the mitochondrial electron transport chain (ETC) for energy production (Benard et al., 2011). The ETC is comprised of five complexes (I-V) that couple the transfer of electrons with the pumping of protons (H+ ions) across the mitochondria

inner membrane to generate a electrochemical gradient that is ultimately harnessed by Complex V, ATP synthase, in order to synthesize ATP (Benard et al., 2011; Fassone and Rahman, 2012). Two electrons donated from NADH to Complex I (also known as NADH dehydrogenase) or from succinate to Complex II (also referred to as succinate dehydrogenase) are transferred to ubiquinone, a hydrophobic and unanchored electron carrier, (also referred to as coenzyme Q) forming the intermediate ubisemiquinone (QH$^.$) and then the reduced form, ubiquinol (QH$_2$). Reduced ubiquinol then transfers the electrons to Complex III (also termed cytochrome *bc1*) which passes them to cytochrome C, a water soluble electron carrier located within the intermembrane space. From cytochrome c, the electrons flow to Complex IV (also known as cytochrome c oxidase or COX) and finally to $1/2$ O_2 forming H_2O (Alberts B, Johnson A, Lewis J, 2002; Wallace, 2005). Complex V (commonly referred to as ATP Synthase) couples the return of protons that have been pumped across the mitochondrial inner membrane to ATP generation (Figure 1.1).

Over 90% of cellular oxygen is utilized in mitochondria in the production of ATP and although this is a fairly efficient process, approximately 3% of oxygen evades complete reduction to water and becomes a potential source of reactive oxygen species (ROS) (Karthikeyan and Resnick, 2005). While ROS are acknowledged to be key players in the complex signaling network of cells, they are also capable of damage biomolecules including proteins, lipids, and nucleic acids (Michelakis, 2008; Mittler et al., 2011). Complex I is thought to produce ROS through two main mechanisms: (1) when mitochondria are not making ATP and consequently have a high proton motive force and reduced ubiquinol pool (for example during reverse electron transport) and (2) when there

is a high NADH/NAD$^+$ ratio in the matrix (for example during ETC impairment when there is less ATP production) (Murphy, 2009).

Mitochondrial antioxidants aid in the scavenging of ROS and convert them to non-toxic forms. Two manganese containing superoxide dismutase (SOD) enzymes exhibit activity in mitochondrial organelles: SOD2 localizes to the mitochondrial matrix and SOD1 localizes to the mitochondrial inner membrane in addition to the cytoplasm (Vendelbo and Nair, 2011). Most mitochondria lack catalase, although thioredoxin 2 (Trx2) mitochondrial glutathione reductase (mGSH), glutathione peroxidase (GPX1) and peroxiredoxin 3 (Prx3) also exhibit antioxidant activity in the organelle (Ribas et al., 2014; Song et al., 2011; Thu et al., 2010; Vendelbo and Nair, 2011). When high mitochondrial ROS levels overwhelm antioxidant mechanisms, apoptosis may be triggered (Fleury et al., 2002). The brain which accounts for 20% of total body oxygen is thought to contain postmitotic neurons and the central nervous system is believed to be especially sensitive to oxidative stress (Emerit et al., 2004; Santos et al., 2011). The activation of apoptosis via ROS is suggested to play a central role in neurodegenerative disease such as Alzheimer's Disease, Parkinson's Disease, Huntington's disease and amyotrophic lateral sclerosis (Kiriyama and Nochi, 2015).

1.2   mtDNA

As mitochondrial DNA (mtDNA) is localized near the site of ROS production, and because mitochondria lack histones and do not exhibit the same capacity for DNA repair as the nuclear genome, mtDNA has increased susceptibility to accumulate mutations. mtDNA exhibits a higher mutation rate than nuclear DNA (Bergstrom and Pritchard, 1998;

Karthikeyan and Resnick, 2005). The evolution rate of mtDNA is around ten to thirty times faster than nuclear genes in most animals (Lane, 2011).

In mammals, mtDNA codes for thirteen proteins, two ribosomal RNA sequences and twenty-two tRNA genes (Busch et al., 2014). Once free living organisms (α-proteobacteria) the majority of genes for mitochondrial function and metabolism are now nuclear encoded (~1,000 genes) (Holt et al., 2014). mtDNA in mammals encodes seven subunits for Complex I (NADH dehydrogenase) while forty are nuclear encoded. None of the subunits for Complex II (Succinate dehydrogenase) are encoded in mtDNA; all four subunits are encoded in the nuclear genome. One of the eleven Complex III (Ubiquinol cytochrome C oxidoreductase) are encoded in mtDNA. mtDNA encodes three of the thirteen Complex IV (Cytochrome C oxidase or COX) subunits and two of the seventeen Complex V (ATP synthase) subunits (Benard et al., 2011).

mtDNA differs from nuclear DNA in many ways. Unlike the linear nuclear DNA which is inherited from two parents and present in two copies in a cell, mtDNA is circular, generally exhibits uniparental inheritance, and as each mitochondrion harbors their own pool of mtDNAs, mitochondrial DNA is present in numerous copies within a single cell (polyploidy) (Busch et al., 2014; Wallace and Chalkia, 2013a). Homoplasmy refers to a state in which all mtDNA molecules are identical (Taylor and Turnbull, 2005). Heteroplasmy, in contrast, refers to a state in which mtDNA molecules differ from one another and can co-occur within the same mitochondrion, within a single cell, and among tissues in an individual (Figure 1.2) (Stewart and Chinnery, 2015). The degree of heteroplasmy can greatly range; a single mutant mtDNA may harbor a sequence variant or conversely, heteroplasmy levels can exceed 99% of the total mtDNA pool (Holt et al.,

2014). Regardless of the magnitude of severe consequences, any deleterious mutation in mtDNA can persist in a mitochondria, cell or tissue as long as it coexists with wildtype mtDNA molecules present at levels sufficient for compensation (Holt et al., 2014).

Mitochondrial dysfunction and mitochondrial DNA mutations and heteroplasmies underlie and contribute to many diseases and cellular senescence (Park and Larsson, 2011; Wallace and Chalkia, 2013a; Ziegler et al., 2015). Complex I impairment has been observed in neurodegenerative diseases including Alzheimer's and Parkinson's Disease (Fato et al., 2008; Johri and Beal, 2012; Moreira et al., 2010). Complex I deficiency is also the most commonly encountered biochemical defect in childhood-onset mitochondrial disease including Leigh syndrome, mitochondrial encephalomyopathy lactic acidosis and stroke-like episodes (MELAS) syndrome (Fassone and Rahman, 2012).

Studies in genetically-tractable model organisms have been used to establish the role of mtDNA mutations in these pathologies. The availability of mutants exhibiting mitochondrial dysfunction combined with the experimental system of *Caenorhabditis elegans* provides a relevant and unique model to investigate the impact of mitochondrial dysfunction on mitochondrial and nuclear genomes. Research employing *C. elegans* to investigate mitochondrial and mtDNA unknowns has potential to reveal new avenues for ameliorating the harmful effects of mitochondrial dysfunction and Complex I impairment.

1.3   Background on *Caenorhabditis elegans*

Caenorhabditis elegans is a globally distributed 1 mm long, free-living soil nematode (Dexter et al., 2012; Wood, 1988). For the past forty years, the laboratory wild-type strain (N2) has served as an invaluable research model for animal development, programmed cell death and RNA interference (*C.elegans* II, 1997). *C. elegans* feeds

primarily on bacteria (e.g. *Escherichia coli*) and has an average lifespan of about two

weeks (Dexter et al., 2012). Primarily a self-fertilizing hermaphrodite, males are

maintained in wild-type populations at low frequency (Chasnov and Chow, 2002).

Producing both eggs and sperm, under optimal conditions hermaphrodites reproduce

approximately three days following hatching, and lay about 300 eggs during their

reproductive life span of approximately four days (Wood, 1988). The complete cell lineage

of every somatic cell in *C. elegans* has been mapped out (959 in the adult hermaphrodite;

1031 in the adult male) (Bratic et al., 2010). The genome of *C. elegans* has been fully

sequenced and totals 100,291,840bp which are distributed among five autosomes and a sex

(X) chromosome and encode approximately 20,000 protein-coding genes (Consortium,

1998).

There are differences between mitochondria organelles and mtDNA in humans

and *C. elegans*. Notably, mitochondrial gene transcription is markedly different in *C.

elegans* from humans and even most sequenced metazoans, as mtDNA genes are all

transcribed in the same direction from the promoter that corresponds to the mammalian

mtDNA light strands promoter (LSP) (Okimoto et al., 1992). Unlike humans which use

Coenzyme Q10, *C. elegans* employs Coenzyme Q9 (containing nine isoprenyl repeats) as

an electron carrier in the mitochondrial ETC (Dancy et al., 2015). The mitochondrial

genome in *C. elegans* lacks the *atp-8* gene (Leung et al., 2013). Additionally, compared to

humans, there are fewer copies of mtDNA per a cell in *C. elegans* (Dancy et al., 2015).

Though the overlap between humans and (*C. elegans*) is not as extensive as

humans and more complex model organisms, the *C. elegans* system enables the study of

gene functions and interactions contributing to basic cellular pathways relevant to human

disease (Dexter et al., 2012). Further, it is estimated that *C. elegans* harbors orthologs to approximately 70% of genes involved in human disease (Bratic et al., 2010). Mitochondrial functions including the TCA cycle, oxygen consumption profiles, and supercomplex formation of the mitochondrial ETC complexes are relatively well conserved between humans and *C. elegans* (Dancy et al., 2015). Like humans, mtDNA in *C. elegans* is polyploidy, maternally inherited and may exhibit heteroplasmy (Addo et al., 2010). Furthermore, the phenotypes observed in *C. elegans* mutant and knockdown animals mirror those documented for genetic mitochondrial disorders in human patients (Dancy et al., 2015).

At 13,794bp, the size of the *C. elegans* mitochondrial genome is comparable to humans (16,649bp) and encodes similar content to the human mitochondrial genome (Leung et al., 2013). As in humans, *C. elegans* also exhibits a large increase in mtDNA copy number with age and the mitochondrial genome levels can be significantly altered by the *C. elegans* diet (Reinke et al., 2010; Tsang and Lemire, 2002). Additionally, like the human mitochondrial genome, mtDNA in *C. elegans* encodes seven subunits of the ETC Complex I with approximately thirty Complex I genes encoded in the nuclear genome; in humans about thirty-nine Complex I genes are nuclear encoded (Schon et al., 2012; Stiernagle, 2006). The individual respiratory chain subunits between *C. elegans* and humans exhibit extensive homology (40%-99% protein identity) and on the order of over 82% protein identity of the nuclear-encoded Complex I subunits (Falk et al., 2008). Moreover, numerous well-characterized *C. elegans* strains harboring mutations in nuclear-encoded mitochondrial proteins may be readily obtained (*Caenorhabditis* Genetics Center,

WormBase). In the research presented here, we employed the *gas-1* fc21 mutant strain which exhibits mitochondrial impairment (Kayser et al., 2001a).

1.4   *gas-1* (fc21) mutant strain

Investigations focusing on the *gas-1* mutant strain of *C. elegans* and the *gas-1* gene were conducted throughout this dissertation research. The *gas-1* gene encodes the GAS-1 protein which is 83.% similar at the amino acid level relative to the protein in humans (Kayser et al., 2011). The *gas-1* mutant strain exhibits mitochondrial impairment due to harboring a nuclear missense mutation in the 49kDa Complex I ETC subunit (NDUFS2, Nuo4) which alters an evolutionary strictly conserved arginine (R290K) (Kayser et al., 2001b, 2011). The *gas-1* mutation was generated through the mutagenic compound ethyl methanesulfonate (EMS) which is predicted to cause cytosine to thymine transition mutations (Kayser et al., 1999a; Kim et al., 2006). Originally identified for hypersensitivity to volatile anesthetics (isoflurane, halothane and enflurane), *gas-1* was named for general anesthetic sensitivity (Kayser et al., 1999).

Past studies on *gas-1* mutant worms have reported notable phenotypic changes from the N2-wildtype strain including reduced brood size, shortened lifespan, increased production of ROS coupled to decreased ATP output and a 75% reduction in Complex I activity (Kayser et al., 2001b, 2004b, 2011; Sedensky and Morgan, 2006; Vasta et al., 2011a). Additionally, increased mitochondrial mass has been observed in *gas-1* worms which may be a compensation mechanism. Similarily, an increase in Complex II respiration has been documented in *gas-1* animals (Dancy et al., 2015).

GAS-1 is located in the hydrophilic, peripheral arm of Complex I (Pätsi et al., 2008). There are three functional modules of Complex I: the electron input (N) module, the

electron output (Q) module, and the proton translocase (P) module (Figure 1.3) (Fassone and Rahman, 2012). The N and Q modules project into the mitochondrial matrix and the comprising subunits are all nuclear-encoded. In contrast, the seven subunit that compromise the P module that is located within the hydrophobic membrane arm, are all encoded in the mitochondrial genome. At the matrix-end of the peripheral arm, NADH is oxidized and the electrons are passed to Flavin mononucleotide (FMN) followed by a chain of seven iron-sulphur (Fe-S) clusters and then transferred to ubiquinone which undergoes reduction near the junction of the peripheral and membrane arms (Fassone and Rahman, 2012). Along with another core subunit (PSST), GAS-1 forms the catalytic core of Complex I and holds the terminal iron sulfur cluster N2 (Figure 1.2) (Kayser et al., 2011; Pujol et al., 2013). The ubiquinone-binding site is thought to be located in the contact region between these two proteins and the hydrophobic arm (Pätsi et al., 2008).

Complex I is thought to contribute a major proportion of ROS (Murphy, 2009). As *gas-1* mutant worms exhibit increased ROS output, the proximity of the GAS-1 location to the pathway of electron transfer may be a substantial factor responsible for the increased oxidant production in *gas-1* mutant worms (Dingley et al., 2010; Kayser et al., 2011; Murphy, 2009). The short lifespan, near-exclusive hermaphroditic nature, fully sequenced mitochondrial and nuclear genomes and relevance of the *gas-1* mutant strain to mitochondrial pathologies observed in human diseases, the *C. elegans* offers unique opportunities for investigating mitochondrial and mtDNA unknowns using experimental evolution and bioinformatic approaches.

1.5   Experimental evolution and high-throughput sequencing approaches

Experimental evolution approaches provide a valuable and direct methodology to determine the influence and consequences of various evolutionary forces on fundamental processes including genome evolution, adaptation to new environments, and extinction. The fate of a mutation (whether it is lost, fixed, or a fluctuating polymorphism) is dependent not only on its fitness effect but also strongly determined by population size (Bromham, 2009; Wang et al., 2014). In the research presented here, we evolved the *gas-1* mutant strain in small and large population sizes.

Evolving laboratory populations in small population sizes creates an environment in which natural selection is overpowered by genetic drift and chance governs the outcome of the majority of mutations (Bromham, 2009). As the majority of new mutations are thought to be neutral or slightly deleterious, a proportion of slightly deleterious mutations will arise to fixation in small populations simply as a function of chance. (Bataillon, 2003; Bromham, 2009; Eyre-Walker and Keightley, 1999). Further, advantageous mutations which in large population size would likely rise to fixation due to selection, have an increased risk of being removed when in a small population (Wright, 1931). Ultimately, this process may lead to mutationally degraded genomes and extinction of population (Lynch et al., 1993). Mutation accumulation (MA) lines, in which populations are bottlenecked, provide the opportunity to investigate the effects of extreme genetic drift on population genetic variation and organismal fitness (Bataillon, 2003; Mukai, 1964; Rutter et al., 2012). As *C. elegans* primarily reproduces through selfing, *C. elegans* MA lines are derived from a nearly homozygous progenitor. In addition, the hermaphroditic nature of *C. elegans* permits populations to be bottlenecked to the effective population size of one, creating an environment in which natural selection is minimized and genetic drift is extensive. The reduced force of natural selection

coupled with extreme genetic drift predicts that a proportion of slightly deleterious alleles will accumulate in genomes of MA lines and conversely, beneficial genetic variants will have an increased probability of not being maintained.

In contrast to MA approaches, evolving experimental laboratory populations in large population sizes permits natural selection to overpower the influence of genetic drift (Bromham, 2009). Maintenance of laboratory populations in large population sizes enables investigation into the process of adaptation and adaptive recovery from deleterious mutation (Denver et al., 2010). This methodology permits insight into questions such as the rate of adaptive evolution, how fitness changes are the population approaches an optimum, and the types of genetic change that underlie adaptation and compensatory evolution (Orr, 2005). Combining experimental evolution with whole-genome sequencing approaches, enables the identification of specific genetic modifications that take place across generations. High-throughput sequencing (HTS) approaches such as Illumina-MiSeq and Illumina-HiSeq are two technologies that can be employed in order to obtain genome-wide data.

Referred to as next-generation sequencing (NGS), both Illumina-MiSeq and Illumina-HiSeq are "sequencing by synthesis" technologies that sequence a large number of DNA molecules in parallel (Schadt et al., 2010). Prior to sequencing, NGS required a preparation of libraries in which fragments of DNA molecules are fused with platform-specific adapters (van Dijk et al., 2014). These adapters permit binding of the DNA fragments to the Illumina flow cell which is coated with single-stranded oligonucleotides (Schadt et al., 2010). DNA polymerase and dNTPs are added to the flow cell and the bound single-stranded DNA fragments then undergo bridge amplification to generate dense clusters of double-stranded DNA fragments. The original strand is then washed away leaving only the fragments that

have been synthesized to the oligos attached to the flow cell. The process of bridge amplification and denaturation is repeated for many cycles after which fluorescently labeled nucleotides are added to the flow cell. In parallel, clusters are sequenced by synthesis of the DNA fragments by incorporating the fluorescently labeled nucleotides which are then imaged and sequenced base-by-base (Illumina Sequencing, 2010).

There are opportunities present for bias and errors in sequencing data at different steps of the process and include bias and errors induced in the library preparation, sequencing process, and mapping and assembly of sequencing data. In library preparation of DNA fragments, bias is present in the fragmentation and PCR step. Euchromatin are more efficiently sonicated than heterochromatin and as such more than one fragmentation step is recommended. PCR amplification is known to introduce bias as not all fragments, such as those rich in AT-sequences, have equal amplification efficiency. PCR amplification in the library preparation and Illumina sequencing process may generate sequencing artifacts which are especially common in homopolymer and repeat sequences (Schloss et al., 2011). Furthermore, an error introduced through PCR has opportunity to proliferate in abundance and may appear as a experimentally generated mutation. To increase accuracy, various polymerases are available that may reduce PCR bias for AT or GC-rich genomes. Additionally, verifying a variety of start and end positions for reads containing putative mutations reduce the likelihood of reporting a PCR artifact (van Dijk et al., 2014). Homopolymer and repeat sequences are still problematic and may require additional technologies (e.g. Sanger Sequencing) for verification.

The error rate of Illumina MiSeq is published to be range from 0.1%- 0.80% (Loman et al., 2012; Quail et al., 2012). The error rate of Illumina HiSeq 3000 is not yet published,

however, the UC Davis Genome Center reports online an error rate of 0.35% for forward

reads and 0.61% for reverse reads (Froenicke, 2015). Illumina MiSeq can produce longer

reads than Illumina HiSeq (2 x 300bp vs 2 x 150bp, respectively). However, Illumina HiSeq

produces many more reads than Illumina MiSeq increasing coverage depth per a read.

Following sequencing, reads can be assembled and mapped to reference genome (if

available) and allow opportunity to survey all genome-wide changes in experimental studies.

1.6   Overview of research chapters

The dissertation research presented here has five chapters, all focusing on evolution

at the genomic level ad involving the *gas-1* mutant of *C. elegans*. In Chapter 2 we

investigated mitogenomic evolution in bottlenecked reference (N2) and *gas-1* mutant

strains of *C. elegans*. Employing the *gas-1* mutant strain permitted insight into how

mitochondrial genome evolution would be affected by mitochondrial dysfunction and

Complex I impairment when natural selection is minimized and genetic drift is extensive.

Analysis of the N2-wildtype strain provided a baseline of mitogenomic evolution in an

environment permissive of genetic drift. Comparing the N2-strain populations to the *gas-1*

mutant populations may evaluate difference in genomic evolutionary responses in

populations predisposed to mitochondrial dysfunction. We applied MA approaches in

which forty-eight biological replicate *gas-1* populations experiencing single-worm

bottlenecking for a maximum of fifty generations with HTS and bioinformatic analysis. We

sequenced and bioinformatically analyzed five randomly selected *gas-1* MA lines, five

previously characterized N2 MA lines that experienced single-worm bottlenecking for 250

generations and the N2 and *gas-1* progenitor strains. Subsequently we performed single-

worm DNA extractions and Sanger Sequencing on a subset of *gas-1* MA lines and *gas-1*

progenitor worms. We determined mitochondrial DNA copy number and identified and characterized all mitochondrial mutations (both single-base substitutions and indels) in all twelve lines.

In Chapter 3, we examined how the nuclear genome evolution in bottlenecked reference and *gas-1* mutant strains of *C. elegans.* Using the five same *gas-1* and N2 MA lines previously analyzed in Chapter two, we investigated how nuclear genome evolution differs when predisposed to mitochondrial impairment. We performed bioinformatic nuclear genome analyses of the same five *gas-1* and N2 MA lines and N2 and *gas-1* progenitor strains analyzed in Chapter two. Analyses were performed to identify and characterize all nuclear mutations, analyze the interactions of genes in which mutations were located and assess the mutation rate. Subsequent analysis of random mutation simulation determined how likely our observed results were due to chance. Additionally, we also evaluated nuclear genetic differences between our *gas-1* progenitor strain (which experienced ten rounds of backcrossing to the Denver-Lab N2 strain) and the Denver-Lab N2 progenitor strain. This comparison was performed to evaluate the necessity of backcrossing mutant strains to the wild-type strains prior to experimentation.

In Chapter 4, we investigated the mitochondrial and nuclear genome evolution of *gas-1* populations maintained in large population sizes. Twenty-four biological replicate *gas-1* populations were propagated in large population sizes for sixty generations (termed "recovery (RC) lines"). All twenty-four RC lines along the *gas-1* progenitor population used to initially propagate them and the Denver-Lab N2 strain were sequenced and bioinformatically analyzed. We evaluated mitochondrial DNA copy number, identified and characterized all nuclear and mitochondrial single-base substitution mutations, determined

the evolutionary rate, and analyzed the interactions of genes in which RC nuclear and mitochondrial mutations were located. Subsequent analysis of random mutation simulation that simulated observed nuclear and mitochondrial mutation results determined how likely our results were due to chance. Together, this research provides novel insights on mitochondrial and nuclear genome evolution predisposed to mitochondrial dysfunction and broadens understanding of evolutionary adaptation recovery in small and large population sizes.

1.7 References

Addo, M. G., Cossard, R., Pichard, D., Obiri-Danso, K., Rötig, A., and Delahodde, A. (2010). Caenorhabditis elegans, a pluricellular model organism to screen new genes involved in mitochondrial genome maintenance. *Biochim. Biophys. Acta* 1802, 765–773. doi:10.1016/j.bbadis.2010.05.007.

Alberts B, Johnson A, Lewis J, et al (2002). *Molecular Biology of the Cell*. 4th ed. New York: Garland Science.

Al-Mehdi, a B., Pastukh, V. M., Swiger, B. M., Reed, D. J., Patel, M. R., Bardwell, G. C., et al. (2012). Perinuclear mitochondrial clustering creates an oxidant-rich nuclear domain required for hypoxia-induced transcription. *Sci Signal* 5, ra47. doi:10.1126/scisignal.2002712.

Bataillon, T. (2003). Shaking the "deleterious mutations" dogma? *Trends Ecol. Evol.* 18, 315–317. doi:10.1016/S0169-5347(03)00128-9.

Benard, G., Bellance, N., Jose, C., and Rossignol, R. (2011). "Relationships Between Mitochondrial Dynamics and Bioenergetics," in *Mitochondrial Dynamics and Neurodegeneration* (Dordrecht: Springer Netherlands), 47–68. doi:10.1007/978-94-007-1291-1_2.

Bergstrom, C. T., and Pritchard, J. (1998). Germline bottlenecks and the evolutionary maintenance of mitochondrial genomes. *Genetics* 149, 2135–2146.

Bratic, I., Hench, J., and Trifunovic, A. (2010). Caenorhabditis elegans as a model system for mtDNA replication defects. *Methods* 51, 437–443. doi:10.1016/j.ymeth.2010.03.003.

Bromham, L. (2009). Does nothing in evolution make sense except in the light of population genetics? *Biol. Philos.* 24, 387–403. doi:10.1007/s10539-008-9146-6.

Busch, K. B., Kowald, A., and Spelbrink, J. N. (2014). Quality matters: how does mitochondrial network dynamics and quality control impact on mtDNA integrity? *Philos. Trans. R. Soc. Lond. B. Biol. Sci.* 369, 20130442. doi:10.1098/rstb.2013.0442.

Butow, R. A., and Avadhani, N. G. (2004). Mitochondrial signaling: The retrograde response. *Mol. Cell* 14, 1–15. doi:10.1016/S1097-2765(04)00179-0.

Caenorhabditis Genetics Center Available at: http://cbs.umn.edu/cgc/home# [Accessed June 20, 2004].

Chasnov, J. R., and Chow, K. L. (2002). Why are there males in the hermaphroditic species Caenorhabditis elegans? *Genetics* 160, 983–994.

Chevrollier, A., Cassereau, J., Ferré, M., Alban, J., Desquiret-Dumas, V., Gueguen, N., et al. (2012). Standardized mitochondrial analysis gives new insights into mitochondrial dynamics and OPA1 function. *Int. J. Biochem. Cell Biol.* 44, 980–988. doi:10.1016/j.biocel.2012.03.006.

Consortium, C. elegans S. (1998). Genome sequence of the nematode C. elegans: a platform for investigating biology. *Science* 282, 2012–2018. Available at: http://www.ncbi.nlm.nih.gov/pubmed/9851916.

Dancy, B. M., Sedensky, M. M., and Morgan, P. G. (2015). Mitochondrial bioenergetics and disease in Caenorhabditis elegans. *Front. Biosci. (Landmark Ed.* 20, 198–228. doi:10.2741/4305.

Denver, D. R., Howe, D. K., Wilhelm, L. J., Palmer, C. A., Anderson, J. L., Stein, K. C., et al. (2010). Selective sweeps and parallel mutation in the adaptive recovery from deleterious mutation in Caenorhabditis elegans. *Genome Res.* 20, 1663–1671. doi:10.1101/gr.108191.110.

Dexter, P. M., Caldwell, K. A., and Caldwell, G. A. (2012). A Predictable Worm: Application of Caenorhabditis elegans for Mechanistic Investigation of Movement Disorders. *Neurotherapeutics* 9, 393–404. doi:10.1007/s13311-012-0109-x.

Van Dijk, E. L., Jaszczyszyn, Y., and Thermes, C. (2014). Library preparation methods for next-generation sequencing: Tone down the bias. *Exp. Cell Res.* 322, 12–20. doi:10.1016/j.yexcr.2014.01.008.

Dingley, S., Polyak, E., Lightfoot, R., Ostrovsky, J., Rao, M., Greco, T., et al. (2010). Mitochondrial respiratory chain dysfunction variably increases oxidant stress in Caenorhabditis elegans. *Mitochondrion* 10, 125–136. doi:10.1016/j.mito.2009.11.003.

Emerit, J., Edeas, M., and Bricaire, F. (2004). Neurodegenerative diseases and oxidative stress. *Biomed. Pharmacother.* 58, 39–46. doi:10.1016/j.biopha.2003.11.004.

Escobar-Henriques, M., and Anton, F. (2013). Mechanistic perspective of mitochondrial fusion: Tubulation vs. fragmentation. *Biochim. Biophys. Acta - Mol. Cell Res.* 1833, 162–175. doi:10.1016/j.bbamcr.2012.07.016.

Eyre-Walker, a, and Keightley, P. D. (1999). High genomic deleterious mutation rates in hominids. *Nature* 397, 344–347. doi:10.1038/16915.

Falk, M. J., Zhang, Z., Rosenjack, J. R., Nissim, I., Daikhin, E., Nissim, I., et al. (2008). Metabolic pathway profiling of mitochondrial respiratory chain mutants in C. elegans. *Mol. Genet. Metab.* 93, 388–397. doi:10.1016/j.ymgme.2007.11.007.

Fassone, E., and Rahman, S. (2012). Complex I deficiency: clinical features, biochemistry and molecular genetics. *J. Med. Genet.* 49, 578–590. doi:10.1136/jmedgenet-2012-101159.

Fato, R., Bergamini, C., Leoni, S., Strocchi, P., and Lenaz, G. (2008). Generation of reactive oxygen species by mitochondrial complex I: Implications in neurodegeneration. *Neurochem. Res.* 33, 2487–2501. doi:10.1007/s11064-008-9747-0.

Fleury, C., Mignotte, B., and Vayssière, J.-L. (2002). Mitochondrial reactive oxygen species in cell death signaling. *Biochimie* 84, 131–141. doi:10.1016/S0300-9084(02)01369-X.

Froenicke, L. (2015). First HiSeq 3000 data download. Available at: http://dnatech.genomecenter.ucdavis.edu/2015/05/07/first-hiseq-3000-data-download/ [Accessed April 1, 2016].

Galluzzi, L., Kepp, O., Trojel-Hansen, C., and Kroemer, G. (2012). Mitochondrial control of cellular life, stress, and death. *Circ. Res.* 111, 1198–1207. doi:10.1161/CIRCRESAHA.112.268946.

Guha, M., and Avadhani, N. G. (2013). Mitochondrial retrograde signaling at the crossroads of tumor bioenergetics, genetics and epigenetics. *Mitochondrion* 13, 577–591. doi:10.1016/j.mito.2013.08.007.

Holt, I. J., Speijer, D., and Kirkwood, T. B. L. (2014). The road to rack and ruin: selecting deleterious mitochondrial DNA variants. *Philos. Trans. R. Soc. B Biol. Sci.* 369, 20130451–20130451. doi:10.1098/rstb.2013.0451.

Illumina Sequencing (2010). Available at: http://www.illumina.com/documents/products/techspotlights/techspotlight_sequencing.pdf [Accessed April 1, 2016].

Johri, A., and Beal, M. F. (2012). Mitochondrial dysfunction in neurodegenerative diseases. *J. Pharmacol. Exp. Ther.* 342, 619–630. doi:10.1124/jpet.112.192138.

Karthikeyan, G., and Resnick, M. A. (2005). Impact of mitochondria on nuclear genome stability. *DNA Repair (Amst).* 4, 141–148. doi:10.1016/j.dnarep.2004.07.004.

Kayser, E. B., Morgan, P. G., Hoppel, C. L., and Sedensky, M. M. (2001a). Mitochondrial expression and function of GAS-1 in Caenorhabditis elegans. *J. Biol. Chem.* 276, 20551–20558. doi:10.1074/jbc.M011066200.

Kayser, E. B., Morgan, P. G., Hoppel, C. L., and Sedensky, M. M. (2001b). Mitochondrial Expression and Function of GAS-1 in Caenorhabditis elegans. *J. Biol. Chem.* 276, 20551–20558. doi:10.1074/jbc.M011066200.

Kayser, E. B., Morgan, P. G., and Sedensky, M. M. (1999a). GAS-1: a mitochondrial protein controls sensitivity to volatile anesthetics in the nematode Caenorhabditis elegans. *Anesthesiology* 90, 545–554. doi:10.1097/00000542-199902000-00031.

Kayser, E. B., Suthammarak, W., Morgan, P. G., and Sedensky, M. M. (2011). Isoflurane selectively inhibits distal mitochondrial complex i in caenorhabditis elegans. *Anesth. Analg.* 112, 1321–1329. doi:10.1213/ANE.0b013e3182121d37.

Kayser, E.-B., Morgan, P. G., and Sedensky, M. M. (1999b). GAS-1. *Anesthesiology* 90, 545–554. doi:10.1097/00000542-199902000-00031.

Kayser, E.-B., Sedensky, M. M., and Morgan, P. G. (2004). The effects of complex I function and oxidative damage on lifespan and anesthetic sensitivity in Caenorhabditis elegans. *Mech. Ageing Dev.* 125, 455–464. doi:10.1016/j.mad.2004.04.002.

Kim, Y., Schumaker, K. S., and Zhu, J.-K. (2006). EMS mutagenesis of Arabidopsis. *Methods Mol. Biol.* 323, 101–103. doi:10.1101/pdb.prot4621.

Kiriyama, Y., and Nochi, H. (2015). The Function of Autophagy in Neurodegenerative Diseases. *Int. J. Mol. Sci.* 16, 26797–26812. doi:10.3390/ijms161125990.

Knott, A. B., Perkins, G., Schwarzenbacher, R., and Bossy-Wetzel, E. (2008). Mitochondrial fragmentation in neurodegeneration. *Nat. Rev. Neurosci.* 9, 505–518. doi:10.1038/nrn2417.

Księzakowska-Łakoma, K., Zyła, M., and Wilczyński, J. R. (2014). Mitochondrial dysfunction in cancer. *Prz. Menopauzalny* 18, 136–144. doi:10.5114/pm.2014.42717.

Lane, N. (2011). Mitonuclear match: Optimizing fitness and fertility over generations drives ageing within generations. *Bioessays* 33, 860–869. doi:10.1002/bies.201100051.

Lane, N. (2014). Bioenergetic constraints on the evolution of complex life. *Cold Spring Harb. Perspect. Biol.* 6. doi:10.1101/cshperspect.a015982.

Leung, M. C. K., Rooney, J. P., Ryde, I. T., Bernal, A. J., Bess, A. S., Crocker, T. L., et al. (2013). Effects of early life exposure to ultraviolet C radiation on mitochondrial DNA content, transcription, ATP production, and oxygen consumption in developing Caenorhabditis elegans. *BMC Pharmacol. Toxicol.* 14, 9. doi:10.1186/2050-6511-14-9.

Loman, N. J., Misra, R. V, Dallman, T. J., Constantinidou, C., Gharbia, S. E., Wain, J., et al. (2012). Performance comparison of benchtop high-throughput sequencing platforms. *Nat. Biotechnol.* 30, 434–9. doi:10.1038/nbt.2198.

Lynch, M., Bürger, R., Butcher, D., and Gabriel, W. (1993). The mutational meltdown in asexual populations. *J. Hered.* 84, 339–44. Available at: http://www.ncbi.nlm.nih.gov/pubmed/8409355.

Martin, W., and Müller, M. (1998). The hydrogen hypothesis for the first eukaryote. *Nature* 392, 37–41. doi:10.1038/32096.

Mayr, J. A. (2014). Lipid metabolism in mitochondrial membranes. *J. Inherit. Metab. Dis.* 38, 137–144. doi:10.1007/s10545-014-9748-x.

Michelakis, E. D. (2008). Mitochondrial medicine: A new era in medicine opens new windows and brings new challenges. *Circulation* 117, 2431–2434. doi:10.1161/CIRCULATIONAHA.108.775163.

Mittler, R., Vanderauwera, S., Suzuki, N., Miller, G., Tognetti, V. B., Vandepoele, K., et al. (2011). ROS signaling: The new wave? *Trends Plant Sci.* 16, 300–309. doi:10.1016/j.tplants.2011.03.007.

Moreira, P. I., Carvalho, C., Zhu, X., Smith, M. A., and Perry, G. (2010). Mitochondrial dysfunction is a trigger of Alzheimer's disease pathophysiology. *Biochim. Biophys. Acta - Mol. Basis Dis.* 1802, 2–10. doi:10.1016/j.bbadis.2009.10.006.

Mukai, T. (1964). THE GENETIC STRUCTURE OF NATURAL POPULATIONS OF DROSOPHILA MELANOGASTER. I. SPONTANEOUS MUTATION RATE OF POLYGENES CONTROLLING VIABILITY. *Genetics* 50, 1–19.

Murphy, M. P. (2009). How mitochondria produce reactive oxygen species. *Biochem. J.* 417, 1–13. doi:10.1042/BJ20081386.

Okimoto, R., Macfarlane, J. L., Clary, D. O., and Wolstenholme, D. R. (1992). The mitochondrial genomes of two nematodes, Caenorhabditis elegans and Ascaris suum. *Genetics* 130, 471–498.

Orr, H. A. (2005). The genetic theory of adaptation: a brief history. *Nat. Rev. Genet.* 6, 119–127. doi:10.1038/nrg1523.

Park, C. B., and Larsson, N.-G. (2011). Mitochondrial DNA mutations in disease and aging. *J. Cell Biol.* 193, 809–818. doi:10.1083/jcb.201010024.

Pätsi, J., Kervinen, M., Finel, M., and Hassinen, I. E. (2008). Leber hereditary optic neuropathy mutations in the ND6 subunit of mitochondrial complex I affect ubiquinone reduction kinetics in a bacterial model of the enzyme. *Biochem. J.* 409, 129–137. doi:10.1042/BJ20070866.

De Paula, W. B. M., Lucas, C. H., Agip, A.-N. a, Vizcay-Barrena, G., and Allen, J. F. (2013). Energy, ageing, fidelity and sex: oocyte mitochondrial DNA as a protected genetic template. *Philos. Trans. R. Soc. Lond. B. Biol. Sci.* 368, 20120263. doi:10.1098/rstb.2012.0263.

Pujol, C., Bratic-Hench, I., Sumakovic, M., Hench, J., Mourier, A., Baumann, L., et al. (2013). Succinate dehydrogenase upregulation destabilize complex I and limits the lifespan of gas-1 mutant. *PLoS One* 8, e59493. doi:10.1371/journal.pone.0059493.

Quail, M., Smith, M. E., Coupland, P., Otto, T. D., Harris, S. R., Connor, T. R., et al. (2012). A tale of three next generation sequencing platforms: comparison of Ion torrent, pacific biosciences and illumina MiSeq sequencers. *BMC Genomics* 13, 1. doi:10.1186/1471-2164-13-341.

Reinke, S. N., Hu, X., Sykes, B. D., and Lemire, B. D. (2010). Caenorhabditis elegans diet significantly affects metabolic profile, mitochondrial DNA levels, lifespan and brood size. *Mol. Genet. Metab.* 100, 274–282. doi:10.1016/j.ymgme.2010.03.013.

Ribas, V., GarcÃa-Ruiz, C., and FernÃ¡ndez-Checa, J. C. (2014). Glutathione and mitochondria. *Front. Pharmacol.* 5. doi:10.3389/fphar.2014.00151.

Riddle, Donald L. Blementhal, Thomas. Meyer, Barbara J. Priess, J. R. ed. (1997). *C. elegans II*. 2nd editio. New York: Cold Spring Harbor Laboratory Press.

Rutter, M. T., Roles, A., Conner, J. K., Shaw, R. G., Shaw, F. H., Schneeberger, K., et al. (2012). Fitness of arabidopsis thaliana mutation accumulation lines whose spontaneous mutations are known. *Evolution (N. Y).* 66, 2335–2339. doi:10.1111/j.1558-5646.2012.01583.x.

Santos, D., Esteves, A. R., Silva, D., Januário, C., and Cardoso, S. (2015). The Impact of Mitochondrial Fusion and Fission Modulation in Sporadic Parkinson's Disease. *Mol. Neurobiol.* 52, 573–586. doi:10.1007/s12035-014-8893-4.

Santos, R. X., Correia, S. C., Carvalho, C., Cardoso, S., Santos, M. S., and Moreira, P. I. (2011). Mitophagy in neurodegeneration: an opportunity for therapy? *Curr. Drug Targets* 12, 790–799. doi:10.2174/138945011795528813.

Saxton, W. M., and Hollenbeck, P. J. (2012). The axonal transport of mitochondria. *J. Cell Sci.* 125, 2095–2104. doi:10.1242/jcs.053850.

Schadt, E. E., Turner, S., and Kasarskis, A. (2010). A window into third-generation sequencing. *Hum. Mol. Genet.* 19. doi:10.1093/hmg/ddq416.

Schloss, P. D., Gevers, D., and Westcott, S. L. (2011). Reducing the effects of PCR amplification and sequencing Artifacts on 16s rRNA-based studies. *PLoS One* 6. doi:10.1371/journal.pone.0027310.

Schon, E. A., DiMauro, S., and Hirano, M. (2012). Human mitochondrial DNA: roles of inherited and somatic mutations. *Nat. Rev. Genet.* 13, 878–890. doi:10.1038/nrg3275.

Sedensky, M. M., and Morgan, P. G. (2006). Mitochondrial respiration and reactive oxygen species in C. elegans. *Exp. Gerontol.* 41, 957–967. doi:10.1016/j.exger.2006.06.056.

Song, I.-S., Kim, H.-K., Jeong, S.-H., Lee, S.-R., Kim, N., Rhee, B. D., et al. (2011). Mitochondrial Peroxiredoxin III is a Potential Target for Cancer Therapy. *Int. J. Mol. Sci.* 12, 7163–7185. doi:10.3390/ijms12107163.

Stewart, J. B., and Chinnery, P. F. (2015). The dynamics of mitochondrial DNA heteroplasmy: implications for human health and disease. *Nat. Rev. Genet.* 16, 530–42. doi:10.1038/nrg3966.

Stiernagle, T. (2006). Maintenance of C. elegans. *WormBook.* doi:10.1895/wormbook.1.101.1.

Taylor, R. W., and Turnbull, D. M. (2005). Mitochondrial DNA mutations in human disease. *Nat. Rev. Genet.* 6, 389–402. doi:10.1038/nrg1606.

Thu, V. T., Kim, H. K., Ha, S. H., Yoo, J.-Y., Park, W. S., Kim, N., et al. (2010). Glutathione peroxidase 1 protects mitochondria against hypoxia/reoxygenation damage in mouse hearts. *Pflugers Arch.* 460, 55–68. doi:10.1007/s00424-010-0811-7.

Tsang, W. Y., and Lemire, B. D. (2002). Mitochondrial genome content is regulated during nematode development. *Biochem. Biophys. Res. Commun.* 291, 8–16. doi:10.1006/bbrc.2002.6394.

Tsang, W. Y., and Lemire, B. D. (2003). The role of mitochondria in the life of the nematode, Caenorhabditis elegans. *Biochim. Biophys. Acta - Mol. Basis Dis.* 1638, 91–105. doi:10.1016/S0925-4439(03)00079-6.

Tuppen, H. A. L., Blakely, E. L., Turnbull, D. M., and Taylor, R. W. (2010). Mitochondrial DNA mutations and human disease. *Biochim. Biophys. Acta - Bioenerg.* 1797, 113–128. doi:10.1016/j.bbabio.2009.09.005.

Twig, G., and Shirihai, O. S. (2011). The interplay between mitochondrial dynamics and mitophagy. *Antioxid. Redox Signal.* 14, 1939–51. doi:10.1089/ars.2010.3779.

Vasta, V., Sedensky, M., Morgan, P., and Hahn, S. H. (2011). Altered redox status of coenzyme Q9 reflects mitochondrial electron transport chain deficiencies in Caenorhabditis elegans. *Mitochondrion* 11, 136–138. doi:10.1016/j.mito.2010.09.002.

Vendelbo, M. H., and Nair, K. S. (2011). Mitochondrial longevity pathways. *Biochim. Biophys. Acta - Mol. Cell Res.* 1813, 634–644. doi:10.1016/j.bbamcr.2011.01.029.

Wallace, D. C. (2005). A mitochondrial paradigm of metabolic and degenerative diseases, aging, and cancer: a dawn for evolutionary medicine. *Annu. Rev. Genet.* 39, 359–407. doi:10.1146/annurev.genet.39.110304.095751.

Wallace, D. C., and Chalkia, D. (2013). Mitochondrial DNA Genetics and the Heteroplasmy Conundrum in Evolution and Disease. *Cold Spring Harb. Perspect. Biol.* 5, a021220–a021220. doi:10.1101/cshperspect.a021220.

Wang, A. D., Sharp, N. P., and Agrawal, A. F. (2014). Sensitivity of the distribution of mutational fitness effects to environment, genetic background, and adaptedness: A case study with Drosophila. *Evolution (N. Y).* 68, 840–853. doi:10.1111/evo.12309.

Wood, W. B. (1988). *The Nematode Caenorhabditis elegans*. Cold Spring Harbor, N.Y.: Cold Spring Harbor Laboratory.

WormBase *WS242*. Available at: http://www.wormbase.org/#01-23-6 [Accessed June 20, 2004].

Wright, S. (1931). Evolution in Mendelian Populations. *Genetics* 16, 97–159. Available at: http://www.pubmedcentral.nih.gov/articlerender.fcgi?artid=1201091&tool=pmcentrez&rendertype=abstract.

Ziegler, D. V., Wiley, C. D., and Velarde, M. C. (2015). Mitochondrial effectors of cellular senescence: beyond the free radical theory of aging. *Aging Cell* 14, 1–7. doi:10.1111/acel.12287.
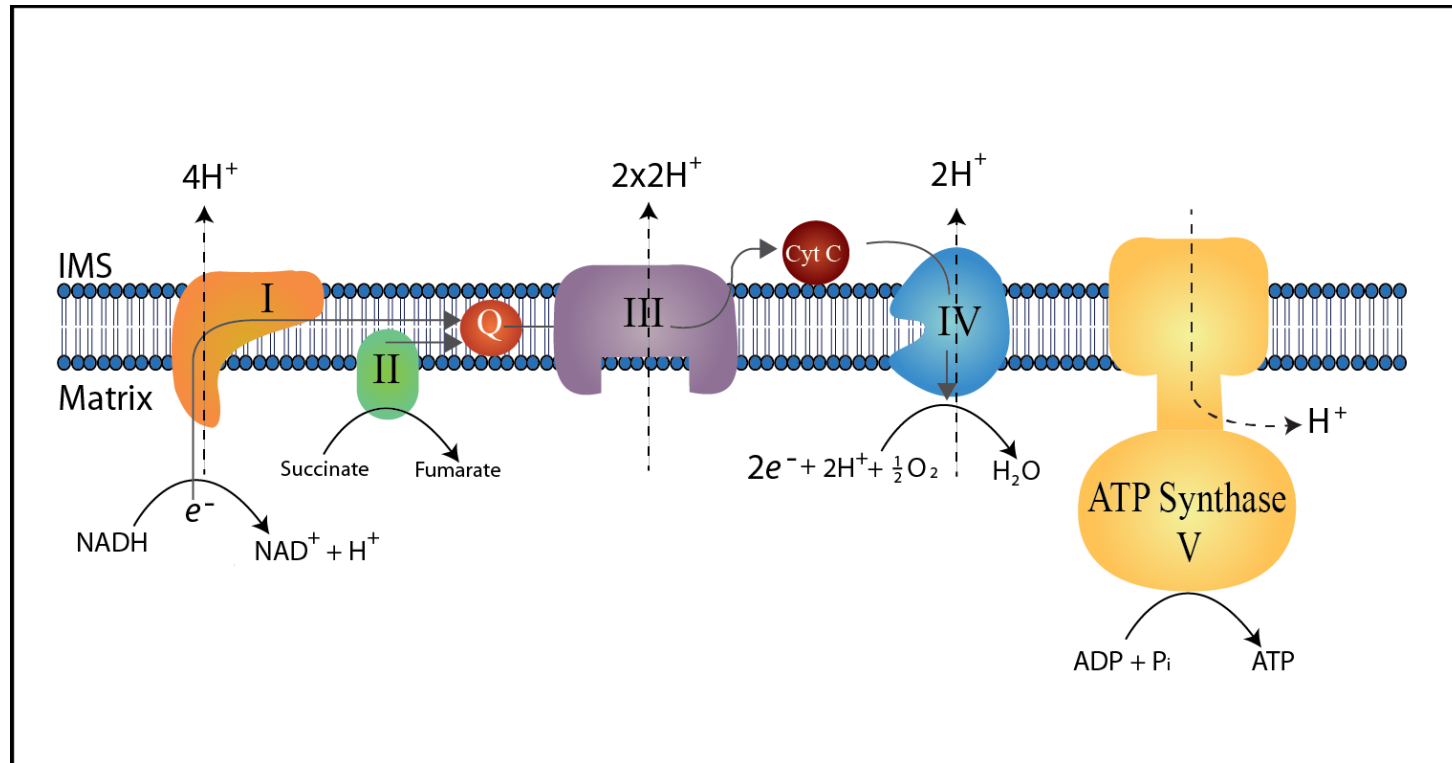
Figure 1.1: Schematic of mitochondrial electron transport chain and process of oxidative phosphorylation. The mitochondrial ETC is comprised of five complexes (I-V) that couple the transfer of electrons with the pumping of protons (H^+) across the inner mitochondrial membrane (IMM) to the intermitochondrial space (IMS). The transfer of electrons generate the membrane potential across the IMM and electrochemical gradient in the form of a proton motive force that is harnessed by ATP Synthase (Complex V) to synthesize ATP (Benard et al., 2011). Electrons donated from NADH to Complex I or from succinate to Complex II are transferred to ubiquinone (represented by the circle labeled "Q") which then transfers the electrons to Complex III. Complex III transfers the electrons to cytochrome C which passes the electrons to Complex IV. Complex IV transfers to electrons to ½ oxygen which leads to the water formation. Complex V couples the return of proton pumped across the IMM to ATP production (Alberts B, Johnson A, Lewis J, 2002; Wallace, 2005). Figure adapted from "Cytochrome C: functions beyond respiration" (Ow et al., 2008).
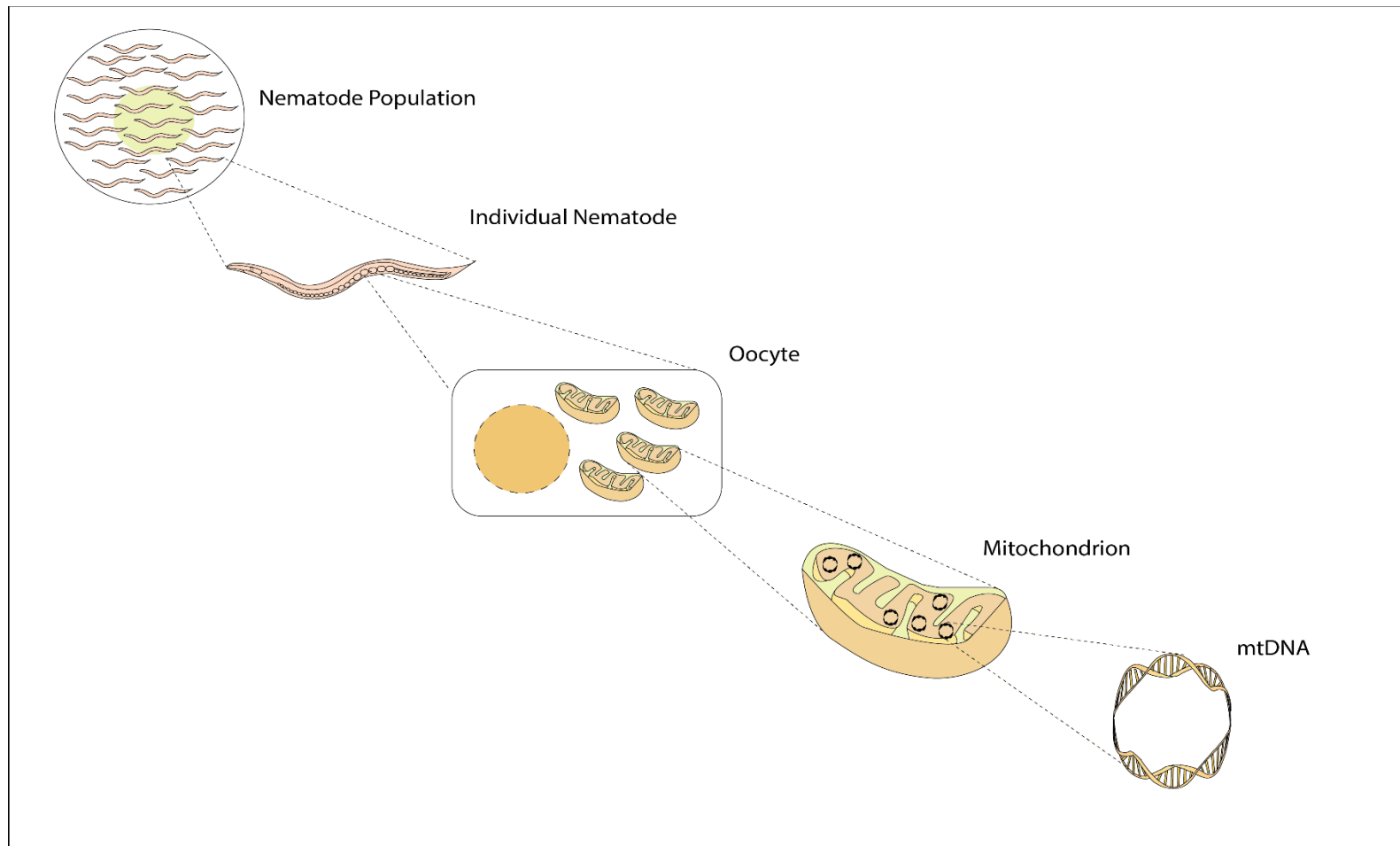
Figure 1.2: Depiction of the hierarchical levels of evolution.
Figure adapted from Phillips et al., 2015.
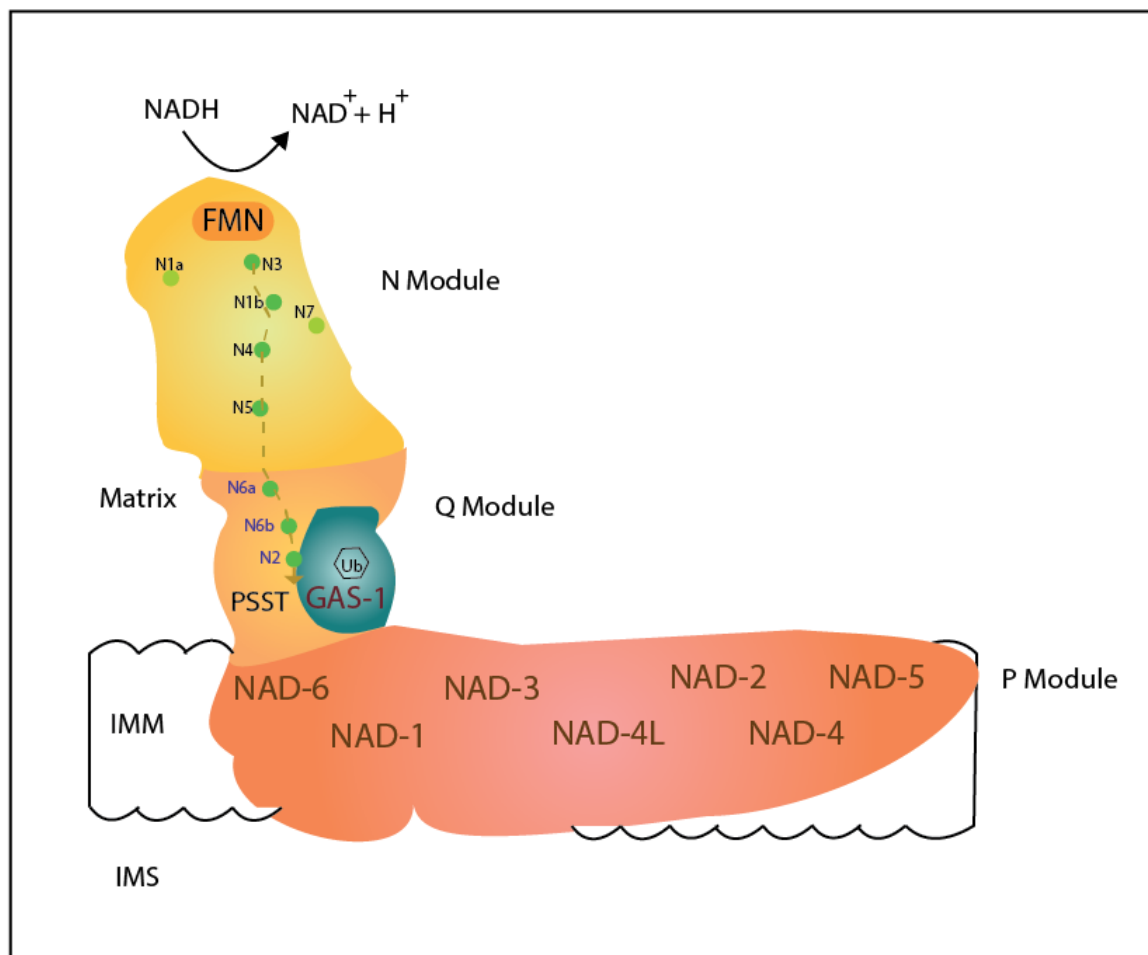
Figure 1.3: Location of GAS-1 subunit in mitochondrial ETC Complex I. There are three functional modules of Complex I: the electron input (N) module (represented by light yellow), the electron output (Q) module (represented by orange shade), and the proton translocase (P) module (represented by pink shade) (Fassone and Rahman, 2012). At the matrix-end of the peripheral arm, NADH is oxidized and the electrons are passed to Flavin mononucleotide (FMN) followed by a chain of iron-sulphur (Fe-S) clusters (represented by the seven green circles: N2, N1b, N4, N5, N6a, N6b, and N2) and then transferred to Coenzyme Q which undergoes reduction near the junction of the peripheral and membrane arms (Fassone and Rahman, 2012). Two additional Fe-S clusters are present (N1a and N7) but do not participate in electron transfer. Along with another core subunit (PSST), GAS-1 forms the catalytic core of Complex I and holds the terminal iron sulfur cluster N2 (Kayser et al., 2011; Pujol et al., 2013). The ubiquinone-binding site (depicted as Ub) is located in the contact region between these two proteins and the hydrophobic arm (Pätsi et al., 2008).

Figure adapted from Patsi et al., 2008.

Chapter 2: Paths of heritable mitochondrial DNA mutation and heteroplasmy in reference and *gas-1* strains of *Caenorhabditis elegans*

Riana I. Wernick[1], Suzanne Estes[2], Dana K. Howe[1], Dee R. Denver[1]

1. Department of Integrative Biology, Oregon State University, Corvallis, Oregon, USA
2. Department of Biology, Portland State University, Portland, Oregon, USA

2.1 Abstract

Heteroplasmy—the presence of more than one mitochondrial DNA (mtDNA) sequence type in a cell, tissue, or individual—impacts human mitochondrial disease and numerous aging-related syndromes. Understanding the trans-generational dynamics of mtDNA is critical to understanding the underlying mechanisms of mitochondrial disease and evolution. We investigated mtDNA mutation and heteroplasmy using a set of wild-type (N2 strain) and mitochondrial electron transport chain mutant (*gas-1*) mutant *Caenorhabditis elegans* mutation-accumulation (MA) lines. The N2 MA lines, derived from a previous experiment, were bottlenecked for 250 generations. The *gas-1* MA lines were created for this study, and bottlenecked in the laboratory for up to 50 generations. We applied Illumina-MiSeq DNA sequencing to L1 larvae from five *gas-1* MA lines and five N2 MA lines to detect and characterize mtDNA mutation and heteroplasmic inheritance patterns evolving under extreme drift. mtDNA copy number increased in both sets of MA lines: 3-fold on average among the *gas-1* MA lines and 5-fold on average among N2 MA lines. Eight heteroplasmic single base substitution polymorphisms were detected in the *gas-1* MA lines; only one was observed in the N2 MA lines. Heteroplasmy frequencies ranged broadly in the *gas-1* MA lines, from as low as 2.3% to complete fixation (homoplasmy). An initially low-frequency (<5%) heteroplasmy discovered in the *gas-1* progenitor was observed to fix in one *gas-1* MA line, achieve higher frequency (37.4%) in another, and be lost in the other three lines. A similar low-frequency heteroplasmy was detected in the N2 progenitor, but was lost in all five N2 MA lines. We identified three insertion-deletion (indel) heteroplasmies in *gas-1* MA lines and six indel variants in the N2 MA lines, most occurring at homopolymeric nucleotide

runs. The observed bias toward accumulation of single nucleotide polymorphisms in *gas-1* MA lines is consistent with the idea that impaired mitochondrial activity renders mtDNA more vulnerable to this type of mutation. The consistent increases in mtDNA copy number imply that extreme genetic drift provides a permissive environment for elevated organelle genome copy number in *C. elegans* reference and *gas-1* strains. This study broadens our understanding of the heteroplasmic mitochondrial mutation process in a multicellular model organism.

2.2 Introduction

"Storing genes, vulnerable informational systems in the immediate vicinity of the mitochondrial respiratory chains, which leak destructive free radicals, is equivalent to storing a valuable library in the wooden shack of a registered pyromaniac"
    -Nick Lane

Nearly all lifeforms observable with the naked eye are composed of eukaryotic cells, most all of which harbor multiple mitochondria (Lane, 2011). These organelles are fundamental to eukaryotic life. In humans, approximately 10% of an individual's body mass is comprised of mitochondria (Nisoli and Carruba, 2006). Mitochondria supply the majority of cellular energy necessary for cell functioning and are central to growth, development, immune response, and reproductive pathways (Dromparis and Michelakis, 2013). Mitochondria respond to cellular stressors (e.g., changes in redox state and substrate availability) and maintain metabolic homeostasis in addition to many other processes necessary for homeostasis (Dromparis and Michelakis, 2013).

The mitochondrial genome is a circular, double-stranded DNA molecule that is nearly always uniparentally inherited—typically from mothers to offspring (Chinnery et al., 2000; Wallace and Chalkia, 2013b). Mitochondrial genomes lack histones and many DNA repair systems, potentially contributing to the higher mutation rates observed in

mitochondrial DNA (mtDNA) versus nuclear DNA in metazoans (Denver et al., 2000). Although some mtDNA mutations may be beneficial (Wallace and Youle, 2013), most are known to be deleterious and contribute to neurodegeneration and many debilitating mitochondrial diseases (Kennedy et al., 2012; Wallace and Chalkia, 2013b). Previously thought to be rare, mtDNA disorders are now known to affect ~1 in 4,300 people (Stewart and Chinnery, 2015). In addition to mutation-generated disease, dysregulation of mtDNA copy number is associated with Alzheimer's Disease and many other pathologies (Lynch et al., 2011; Pyle et al., 2016; Rice et al., 2014). Each mitochondrion contains multiple genome copies (Wallace, 2005), the regulation of which is essential for maintaining proper mitochondrial activity (Lynch et al., 2011). Changes in mtDNA copy number and associated organelle dysfunction may induce mitochondrial retrograde signaling (mitochondria-to-nucleus) as a cellular adaptive response (Guha and Avadhani, 2013). As fluctuations in mtDNA copy number may signify alterations in cellular activity, recent studies in humans and model organisms support the use of mtDNA copy number as a biomarker for aging-related diseases and metabolic syndromes (Lynch et al., 2011; Podlesniy et al., 2013).

Because each cell contains multiple mitochondria, each with multiple genome copies, new mtDNA mutations originate in low-frequency heteroplasmic states; i.e., one copy per cell and organism. We continue to lack a basic understanding of how mtDNA heteroplasmies arise, and how their subsequent frequencies and fates are affected by evolutionary forces operating at different levels (intracellular, between cells, between individuals). Along with nuclear mutations encoding for mitochondrial respiratory chain subunits, single nucleotide mutations in mitochondrial DNA are reported to be a common

cause of the childhood disease Leigh syndrome (Chol, 2003; Hadzsiev et al., 2010).
Though undetected in parental generations, mitochondrial heteroplasmies may increase in
the offspring generation to levels exceeding 80% in both brain and muscle tissues
(Hadzsiev et al., 2010). Furthermore, different mitochondrial pathologies are expressed
only beyond a critical threshold level (typically 60-80%) (Stewart and Chinnery, 2015).
The forces controlling the likelihood of transmission of different mtDNA mutation types
and their subsequent evolutionary dynamics remain understudied.

Early research investigating mitochondrial variation in natural populations often
assumed that all mtDNA molecules within an individual were identical (homoplasmy).
Observations of variation in mtDNA, however, reveals that heteroplasmy is a transient
though necessary phase during mtDNA evolution (Rand, 2001). Different mtDNA
molecules in the heteroplasmic pool may be subject to multi-level selection including
selection between mtDNAs in replication, selection at the level of the cell, and selection
on the organism (Rand, 2001). This cross-level selection may contest Muller's ratchet by
providing a mechanism to purge deleterious mutations (Bergstrom and Pritchard, 1998).
In *Drosophilia* smaller mtDNA molecules resulting from VNTR length variation in the
origin of replication region have been observed to increase in frequency across
generations (Solignac et al., 1987). Similarly, heteroplasmic mtDNA molecules
containing large deletions in the *nad5* gene are observed to experience a transmission
advantage over larger intact mtDNA molecules in *Caenorhabditis briggsae* (Clark et al.
2012; Phillips et al. 2015). By contrast, the opposite effect has been observed in in the
soma of *D. melanogaster* where larger mtDNAs outcompeted smaller ones across the
lifespans of female flies (Kann et al., 1998). In mice models past research has

determined that although random genetic drift is pervasive in some tissues, in other

tissues there is evidence for tissue-specific and age-related directional selection for

different heteroplasmic mtDNA genotypes (Jenuth et al., 1997). Given these inconsistent

results in a variety of animal study systems, more research is necessary to understand the

evolutionary dynamics of mtDNA heteroplasmy.

        C. elegans provides an outstanding model for examining mitochondrial biology.

The nuclear and mitochondrial genomes are well-characterized; a variety of genetic

mutants and other community resources enable diverse investigations into mitochondrial

genetic and physiological questions. Additionally, Illumina-MiSeq can be applied to

evolved lines to detect heteroplasmy and assess relative levels of heteroplasmic to wild-

type mtDNA. Sanger sequencing can also be applied to individual worms to detect the

presence of heteroplasmies. Past research employing the *C. elegans* system demonstrated

increases in mtDNA copy number over development, suggesting that mtDNA might have

variable effects across nematode lifespan (Bratic et al., 2009, 2010; Tsang and Lemire,

2002b). Further, *C. elegans* mtDNA copy number increases up to three-fold in response

to diet and environmental stimuli (Reinke et al., 2010).   Thus, mtDNA copy number is

known to be plastic within a nematode generation. However, little is known about the

trans-generational plasticity of, and effects of fundamental evolutionary forces (e.g.,

genetic drift, natural selection), on mtDNA copy number in *C. elegans* or any other

animal system. Past work employing the *C. elegans* system and mutation-accumulation

(MA) approaches has improved our understanding of the rate and spectrum of mtDNA

changes across generations (Denver et al., 2000, 2009b; Tsang and Lemire, 2002b).

Importantly, work in this system revealed that the baseline rate of mtDNA mutation was

two orders of magnitude higher than previously thought and identified homopolymer nucleotide stretches and repeat sequences as insertion-deletion (indel) mutational hotspots, similar to mtDNA variation associated with human pathologies (Denver et al., 2000). Furthermore, mutation patterns analyzed in *C. elegans* MA lines demonstrated a dominant role for purifying natural selection in shaping mtDNA protein-coding genes in natural populations (Denver et al., 2012a).

We employed a MA approach using a well-characterized *C. elegans* mutant, *gas-1*, to study the impact of mitochondrial dysfunction on mtDNA variation. The *C. elegans gas-1* gene is nuclear-encoded and orthologous to human *NDUFS2* (83.4% protein similarity). *gas-1* encodes a 49 kDa subunit of Complex I of the mitochondrial electron transport chain (ETC). The *gas-1* fc21 allele, used here, is a single-base replacement mutation that renders the GAS-1 protein subunit dysfunctional, resulting in significantly increased endogenous reactive oxygen species (ROS) production, along with decreased ATP (Hartman et al., 2001; Kayser et al., 2004b; Pujol et al., 2013). The *gas-1* mutation reduces ETC Complex I efficiency by 75%, a mitochondrial phenotype commonly observed in many neurodegenerative pathologies such Alzheimer's and Parkinson's Disease (Schulz et al., 2012; Vasta et al., 2011b). Moreover, Complex I deficiencies are the most common cause of mitochondrial disease in both adults and children. *NDUFS2* mutations are reported in fatal infantile lactic acidosis (FILA), Leigh Syndrome, and hypertrophic cardiomyopathy (van den Ecker et al., 2012; Falk et al., 2009; Pujol et al., 2013; Tuppen et al., 2010b). While other *C. elegans* mitochondrial mutants such as *isp-1* and *cyc-1* exhibit extended lifespan in comparison to wild-type, published values for the *gas-1* report a significant decrease in lifespan (Hartman et al., 2001; Kayser et al., 2004b;

Pujol et al., 2013; Van Raamsdonk and Hekimi, 2011). *gas-1* nematodes have reduced

fecundity, delayed growth rates, and exhibit hypersensitivity to oxidative stress as shown

by both hypoxia and paraquat exposure (Hartman et al., 2001; Kayser et al., 2001b).

Employing the *gas-1* strain therefore provides a disease-relevant context for studying

mtDNA variation. We applied Illumina MiSeq technology to analyze five different *gas-1*

MA lines that were bottlenecked for an average of 43 generations, alongside five N2 MA

lines from a previous study, bottlenecked for 250 generations (Baer et al., 2005c).

Bioinformatic analysis identified mitochondrial genomic changes including mtDNA copy

number shifts, and heteroplasmic single-base substitutions and indels.

2.3 Materials and Methods

2.3.1 Strains and backcrossing of *gas-1* mutant

This study utilized the *gas-1* (fc21) mutant containing a C $\rightarrow$ T point mutation

that replaces a highly conserved arginine with lysine in the GAS1 protein, a central

component of mitochondrial ETC Complex I. Because *gas-1* (fc21) originated from an

ethyl methanesulfonate (EMS) mutagenesis screen, the strain was likely to contain many

other mutations (Kayser et al., 1999b). We therefore backcrossed the *gas-1* strain,

CW152, obtained from the *Caenorhabditis* Genetics Center (University of Minnesota) to

our wild-type N2 strain for ten generations to create an isogenic mutant strain. Briefly, a

N2 male was first mated to a *gas-1* hermaphrodite, producing *gas-1* heterozygous

progeny at the F1 generation. Several single heterozygous hermaphrodite offspring were

isolated and mated with a N2 male, producing the F2 generation. The F2 progeny were

screened for the presence of the *gas-1* mutation using PCR and direct Sanger sequencing

of the amplicon (forward primer: ATCTCCTCAATACGGCACAAG; reverse primer:

ATCGTCTCGATTACGTCTCCA), and only hermaphrodites retaining the *gas-1*

mutation were maintained. This sequencing confirmation was continued for backcross

generations F3-F10 and only *gas-1* heterozygous hermaphrodites were used at each

crossing. After ten sequential backcrosses, the resulting *gas-1* heterozygous lineages were

allowed to self and the offspring were screened to find nematodes homozygous for the

fc21 allele. These *gas-1* homozygous lineages were used to initiate MA lines. All

nematodes were cultured under standard laboratory conditions at 20ºC on standard NGM

agar plates seeded with OP50 *Escherichia coli.*

2.3.2 Nematode strains and culture conditions

We studied two sets of MA lines generated from either a *gas-1* mutant or a Bristol

N2 wild-type (G0) progenitor. A set of 48 *gas-1* MA lines was derived from the offspring

of a single backcrossed *gas-1* hermaphrodite. Lines were maintained by transferring

single fourth-larval stage (L4) offspring to fresh plates at 4-day intervals for an average

of 43 generations (35-47 MA generations; G43 MA) (Supplementary Figure A1), after

which time they were stored cryogenically at -80°C (Stiernagle, 2006). The MA process

minimizes the power of natural selection and maximizes genetic drift, allowing all but the

most highly deleterious mutations to accumulate in an effectively neutral fashion

(Halligan and Keightley, 2009). At each transfer, the prior generation was maintained at

10ºC. In the case of a sterilizing or lethal mutation, a replacement L4 nematode was

selected at random from these "backup" plates. This resulted in fewer generations

propagated for some MA lines (Supplementary Table A1). We also utilized five MA

lines generated from N2 as part of a previous experiment (Baer et al., 2005c), and for

which mutational declines in fitness, whole-nuclear genome sequence, ROS and

oxidative DNA damage levels are available (Clark et al., 2012; Denver et al., 2009; Joyner-Matos et al., 2013). These MA lines were initiated from the offspring of a single, highly inbred N2 hermaphrodite and evolved in the manner described above for an maximum of 250 generations (G250 MA) (Baer et al., 2005c).

2.3.3 L1 stage DNA preparation for Illumina-MiSeq MA lines

Twelve nematode strains—five randomly selected *gas-1* MA lines, five previously-studied N2 MA lines (Baer et al., 2005c), and their respective ancestral strains, N2 and the backcrossed *gas-1*—were developmentally synchronized by bleaching according to standard protocols (Wood, 1988). First larval (L1) stage nematodes were harvested and DNA was purified using Qiagen DNeasy Blood & Tissue kit (Valencia, CA) with one modification to the manufacturer's protocol. Prior to adding AL buffer, worms in a solution of M9 buffer, ATL, and Proteinase K were subjected to five cycles of freezing and thawing to break worm cuticles and allow efficient DNA extraction. DNA was prepared for sequencing using standard Illumina TruSeq protocols for genomic DNA. Samples were individually barcoded and pooled for two runs (one per a background), both sequenced using the Illumina MiSeq Genome Analyzer operated by the Oregon State University Center for Genome Research and Biocomputing. All sequences were deposited to NCBI under SRA: accession number SRP069774.

2.3.4 Illumina-MiSeq read mappings and analyses

Following each IlluminaMiSeq run, reads were aligned to the *C. elegans* genome (version WS242) using CLC Genomics Workbench (CLC Bio-Qiagen, Aarhus, Denmark). All reads were paired-end (2 x 150bp) and mapped using the following parameters: No masking, mismatch cost = 2, insertion cost = 3, deletion cost = 3, length

fraction = 0.98, read fraction = 0.98, global alignment = no, non-specific match

handling= map randomly.

2.3.5 Bioinformatic analyses of mtDNA copy number

mtDNA copy number was normalized by nuclear DNA (nDNA) content.

Specifically, relative mtDNA for each line was calculated as the line-specific average

mtDNA coverage divided by the line-specific average coverage of three single-copy

nuclear genes: *ama-1*, *ego-1*, and *efl-2*. The AT-rich region of the mitochondria genome

was not considered in these calculations due to inconsistencies during sequencing created

by its repetitive nature (Table 2.1) (Figure 2.1).

We tested normalized mtDNA copy number data for normality and consistent

variance. A Levene's test determined that the data had inconsistent variance (P= 3.3×10^{-16}) among lines, and a box and whiskers plot displayed the non-normality of the data

(Supplementary Figure A1). We applied the non-parametric Kruskal Wallis H Test with

strain as an explanatory variable to evaluate if there was a statistically significant increase

in mtDNA copy number following bottlenecking. Using normalized mitochondrial DNA

coverage for twelve mitochondrial genes and two ribosomal sequences in each of the

progenitors and respective five MA lines, the analysis determined strain was a significant

factor (P = 2.2×10^{-16}, Kruskal Wallis H Test) (Supplementary Table A2).Post-hoc

analysis applied a Kruskal Multiple Comparison test in order to evaluate the significance

of mtDNA copy number among pairwise comparisons of all lines (Supplementary Table

A3).

2.3.6 Bioinformatic identification of mtDNA variants

Potential line-specific mtDNA variant sites were identified as mitochondrial

genome positions differing from the *C. elegans* reference genome (WS242) and not fixed

within our wild-type N2 lab strain. Site-specific variant frequency was calculated by

dividing the number of variant calls by the total site coverage. To eliminate false

positives resulting from sequencing artifacts, at least six variant calls were required for a

variant to be considered a potential mtDNA heteroplasmy. Furthermore, sites were

required to be within one standard deviation of the line-specific per-site mean

mitochondrial coverage and to have a variant frequency greater than two standard

deviations above the line-specific mean variant frequency to be considered a mtDNA

heteroplasmy (Tables 2.2 and 2.3) (Figure 2.2).

2.3.7 Sanger sequencing assay of bulk and individual nematodes

Sanger sequencing was applied to individual and bulk L1 nematodes to screen for

presence of a specific heteroplasmic site, initially detected by Illumina sequencing,

occurring at low-frequency in the *gas-*1 progenitor and in three of its descendant *gas-1*

MA lines (Supplementary Tables A3-A9). Analysis of L1 individuals should provide the

most accurate reflection of inherited levels of mtDNA heteroplasmy since these

nematodes have not yet undergone the mtDNA copy number expansions occurring at L4

and young adult stages (Tsang and Lemire, 2002b). For all bulk extractions, DNA was

harvested from L1 worms and purified as described above. DNA from individual L1

nematodes was harvested from single worms placed in standard worm lysis buffer

solution prior to the five freeze-thaw cycles (Williams et al., 1992). Following DNA

extraction, mitochondrial DNA was amplified using two primers flanking the

heteroplasmic site of interest (forward primer: TCGGTGGTTTTGGTAACTGA; reverse

primer: CAACACCTGTCAACCCACCT). PCR products were purified through solid

phase reversible immobilization (SPRI) techniques(Elkin et al., 2001). The amplicon was

Sanger sequenced using an internal primer: AGCAGCCGAAAAATAAGCAC.

A total of eighteen *gas-1* progenitor worms, seventeen *gas-1* MA 412 worms,

eighteen *gas-1* MA 429 worms, and seventeen *gas-1* MA 438 worms were individually

assayed (Supplementary Tables A3-A6). Bulk extractions were harvested from both the

gas-1 and N2 progenitor in addition to fourteen *gas-1* MA lines (Supplementary Tables

A8 and A9). Phred scores were used to indicate the uncertainty of Sanger sequencing in

identifying a specific base in a heteroplasmic state. No candidate heteroplasmic sites

were excluded on the basis of Phred score; Phred scores were used to validate

heteroplasmies that evaluated by Sanger sequencing. We used low-quality Phred scores

as an indicator of heteroplasmy, reflecting the presence of more than one nucleotide

signal. To ensure that low Phred scores were a product of heteroplasmy rather than poor

sequence quality, Phred scores for the heteroplasmic site were compared to the average

Phred score for the 50 base pairs flanking the heteroplasmy in both directions (Figure

2.3).

2.4 Results

To investigate mtDNA mutation and heteroplasmy, we analyzed mtDNA

genomes of the N2 and backcrossed *gas-1 C. elegans* progenitors, five randomly selected

gas-1 MA lines, and five previously-studied N2 MA lines using Illumina MiSeq

technology (Denver et al., 2009, 2012). In all lines, over 80% of reads mapped to the *C.*

elegans WS242 reference genome with a mean nDNA coverage of 14.5X and a mean

mtDNA coverage of 378.4X per line (Table 2.1). Analysis of Illumina nDNA sequence

data showed that all *gas-1* MA lines remained homozygous for the *gas-1* mutant allele. Analyses of nuclear genome mutation from these lines will be reported in a separate paper.

2.4.1 Changes in mtDNA copy number

Relative mtDNA copy number (mtDNA coverage normalized by coverage at single-copy nuclear regions – see Materials and Methods for details) was not statistically different between the N2 and *gas-1* progenitor strains. (9.4 and 7.2 respectively) (Supplementary Table A3). Three *gas-1* MA lines (MA412, MA431, and MA438) as well as one N2 MA line (MA523) were not significantly different than the *gas-1* and N2 progenitors (Supplementary Table A3). The six remaining MA lines MA419, MA429, MA526, MA529, MA553 and MA74 showed significant increases in relative mtDNA copy number compared to their respective progenitor strains (Supplementary Table A3). In the *gas-1* MA lines, mean normalized mtDNA copy number was 22.4X, or on average 3-fold higher than in the *gas-1* progenitor (range = 2.2-3.4X higher). Similarly, mean relative mtDNA copy number for the N2 MA lines was 47.7X, 5-fold higher than in the N2 progenitor (range = 1.8-6.0X higher). Coverage patterns across sites were consistent among lines, indicating that mtDNA copy number had increased at all sites (i.e., increases in complete mitogenome copy number) rather than at isolated sections of the mitochondrial genome.

2.4.2 mtDNA variants

We identified and characterized all mitochondrial variants (both heteroplasmic and fixed) in all progenitor and MA lines. Candidate heteroplasmic single-nucleotide polymorphisms (SNPs) were filtered to eliminate false-positives (see Materials and

Methods). Compared to the *C. elegans* reference genome, the N2 progenitor harbored a low-frequency heteroplasmic base substitution in the *COX-1* gene (Table 2.2); this SNP was lost in all of the five N2 MA lines analyzed. A *tRNA-C* deletion was lost in all five *gas-1* MA lines analyzed, while a *gas-1* progenitor *COX-I* heteroplasmy was transmitted to some MA lines (discussed in more detail below). This *COX-1* SNP detected in the N2 progenitor was not detected in the *gas-1* progenitor or its MA lines; however, the *gas-1* progenitor did contain a low-frequency heteroplasmy at a different *COX-I* site in addition to a single-nucleotide deletion in the *tRNA-C* gene (Table 2.3).

Twelve unique heteroplasmic variants were identified in the *gas-1* MA line set: seven SNPs and five indels (Tables 2.2 and 2.3). In the case of the heteroplasmy at position 211, where MA431 and MA438 experienced an identical heteroplasmy event, the heteroplasmy was counted twice. Likewise, as four *gas-1* MA lines experienced an indel event at position 3235 in the *ATP6* gene, this event was counted four times. In contrast, when the heteroplasmy was present in the progenitor, the event was only counted once. The *COX-I* (position 8439) variant present in the *gas-1* progenitor was lost (or present at undetectable levels) in three *gas-1* MA lines and inherited by the remaining two. Of the two lines that inherited this SNP, one (MA412) harbored it at moderate levels (37%) and the other (MA438) harbored it at 100% (homoplasmic) frequency (Table 2.2). Of the new (undetected in progenitors) variants in the *gas-1* MA lines, two were located in the *NAD-6* gene. One of these was shared by two *gas-1* MA lines (MA431 and MA438) and present at similarly low levels – 3.6% and 2.3%, respectively (Tables 2.2 and 2.4). Five of the *gas-1* MA-specific SNP heteroplasmies were present in a single *gas-1* MA line, MA431; these include the two occurring in the *NAD-6* gene and one in each

of the *cyt-b*, *NAD-4*, and *NAD-5* genes. The *NAD-4* heteroplasmy was present at the highest frequency (10%). Only one mtDNA indel (a single bp deletion), occurring within a homopolymeric run within the *ATP6* gene, was detected in the *gas-1* MA line set. This variant was shared among four of the five *gas-1* MA lines at low frequency (<5%) (Tables 2.3 and 2.4; Figure 2.2).

Nine mtDNA heteroplasmies were detected in the five N2 MA lines—one SNP in the *COX-I* gene and eight indel mutations (Tables 2.2 and 2.3). The new SNP heteroplasmy in *COX-1* was found in only one N2 MA line, MA523. Conversely, every N2 MA line contained at least one indel, the majority comprising single-bp deletions compared to the reference genome (Table 2.3). All five N2 MA lines analyzed contained the same *ATP6* variant detected in four of the *gas-1* MA lines (Fig. 2.3) at frequencies ranging from 4%-80% (Tables 2.3 and 2.4). In addition to the *ATP6* variant, N2 MA526 also contained a single-bp insertion in the *COX-I* gene while MA523 and MA574 shared the same heteroplasmic insertion variant located at 11721bp in the *NAD-5* gene. Most indel variants in the N2 MA lines were present at very low frequencies (<7%) (Tables 2.3 and 2.4).

2.4.3 Inheritance patterns of *gas-1* progenitor SNP heteroplasmy

Bioinformatic analysis of Illumina sequence for the *gas-1* MA lines set revealed variable inheritance outcomes for the heteroplasmic SNP in *COX-1*, initially present in the *gas-1* progenitor at about ~5%: (1) Loss or dramatically reduced frequency in three of the five MA lines, (2) increased frequency (up to 37%) in MA412 and (3) complete fixation at 100% in MA438 (Table 2.2). To investigate the inheritance patterns of this heteroplasmic SNP on a finer scale, Sanger sequencing was applied to survey for its

presence in many individual L1 nematodes of the *gas-1* progenitor (Supplementary Table A4) and from three of the five sequenced *gas-1* MA lines (Supplementary Tables A3-A5). Due to the nature of the Sanger sequence data, we were unable to quantify heteroplasmic frequencies, but instead characterized our results based on three electropherogram categories: SNP absent, SNP fixed, and SNP still segregating with wild-type base.

The presence of this focal heteroplasmy varied among individual *gas-1* progenitor nematodes; the heteroplasmy was absent in some individuals and still segregating or fixed in others (Supplementary Table A4). Analysis of individual nematodes from *gas-1* MA412, MA429, and MA438 lines revealed substantial variation among MA lines in the frequency of the 8439 heteroplasmy, but far less inter-individual (or intra-line) variation compared to the *gas-1* progenitor. Namely, in agreement with Illumina sequence results (Tables 2.2 and 2.4), all MA412 worms analyzed harbored the 8439 heteroplasmy in addition to wild-type genomes (Figure 2.3; Supplementary Table A3), all MA429 worms lacked the 8439 heteroplasmy (Figure 2.3; Supplementary Table A6), and all MA438 worms were homoplasmic for the variant (Figure 2.3; Supplementary Table A7).

To further explore the heteroplasmic inheritance patterns of the 8439 *COX-I* heteroplasmy, we applied Sanger sequencing to bulk DNA extractions of nematodes from an additional 11 *gas-1* MA lines alongside the *gas-1* and N2 progenitors. This heteroplasmy was found to be fixed in two of the 11 lines, present as a still-segregating heteroplasmic variant in two others, and lost or undetectable in the remaining seven MA lines (Supplementary Table A9).

2.5 Discussion

Our study reports observed patterns of mitochondrial genome change in wild-type (N2) and mitochondrial ETC mutant (*gas-1*) *C. elegans*, evolving in the lab under extreme drift. Increased mtDNA copy number was consistently observed in all MA lines initiated from both strains. Of the thirteen indels identified across MA lines (including instances of parallel indel heteroplasmy observed in more than one line), the majority occurred in N2 MA lines. Of the eleven total SNPs identified (again including instances of parallel changes), the majority occurred in *gas-1* MA lines, which evolved for less than one fifth the number of MA generations experienced by the wildtype N2 lines. The application of high-throughput DNA sequencing allowed us to gain insights into mitochondrial genome copy number changes, and to detect low-frequency heteroplasmic variants not possible with PCR/Sanger sequencing approaches applied in the past (Denver et al., 2000).

2.5.1 mtDNA copy number

Our observation that N2 and *gas-1* derived MA lines both experienced increased mtDNA content across generations suggests that single-worm bottlenecking may lead to elevated mtDNA copy number in *C. elegans* wildtype and *gas-1* strains (Figure 2.1). All MA lines were observed to increase in mtDNA copy number relative to the respective progenitor strain.Two of out five *gas-1* MA lines and four out of five N2-derived MA lines had significant changes in mtDNA copy as determined by Kruskal Multiple Comparison's test. N2-derived MA lines experienced bottlenecking for 250 generations and exhibited an average five-fold increase in mtDNA relative to the wild-type progenitor, which translates to a ~2% increase in mtDNA copy number per a generation. Similarly, the *gas-1* derived MA-lines were bottlenecked for an average 43 generations,

experienced on average a three-fold elevation in mtDNA copy number which translates to a ~7% increase in mtDNA copy number per a generation. No *gas-1* MA lines actually achieved G50. An important caveat to interpreting our mtDNA copy number results is that interim generational values for mtDNA quantity were not obtained and further experimentation would be needed to address any occurrence of fluctuating mtDNA copy number across generations. Our trans-generational analysis demonstrates that mtDNA copy number can increase across generations in *C. elegans* wildtype and *gas-1* strains, adding to previous studies showing that mtDNA copy number increases during development within a single *C. elegans* generation (Bratic et al., 2009). Furthermore, our results were observed for *C. elegans* reference and *gas-1* strains and may not extrapolate to other *C. elegans* strains.

The evolutionary and molecular causes underlying the variation we observed in mtDNA copy number are not fully understood, although our study suggests three hypotheses: increased oxidative stress, extreme drift and smaller mtDNA molecules. As past research has suggested that oxidative damage to DNA may result in increased mtDNA copy number, particularly in certain cell types (i.e., leukocytes), one hypothesis is that oxidative damage may be contributing to increases in mitogenome copy number (Liu et al., 2003). The *gas-1* progenitor exhibits elevated endogenous ROS levels and a study conducted on N2 MA lines demonstrated that these lines evolved higher endogenous ROS levels due to bottlenecking (Joyner-Matos et al., 2013). Because both the *gas-1* progenitor and N2 MA lines exhibit elevated ROS levels, future work studying wild-type MA lines at earlier generations (where ROS levels might be lower) will be required to disentangle the influences of drift and oxidative damage on mtDNA copy

number increase. Alternatively, there could be a break down in retrograde signaling during mutation accumulation that could initiate a feedback loop generating increased copy number. Due to the extreme drift imposed on *C. elegans* and lack of competition for resources during bottlenecking, the quality-control mechanism eliminating mitochondrial genomes may have been disturbed. The extreme drift on the organismal level may have imposed downstream effects on the level of mitochondria resulting in relaxed selection on mtDNA populations within the organelle and causing massive imbalance of mtDNA content in cells. Extreme drift may eliminate selection on the level of the mitochondrion, creating an imbalance in mitochondrial quality-control and lead to increased mtDNA copy number to compensate for dysfunctional mitochondrial genomes in *C. elegans* N2 wildtype and *gas-1* mutant strains. A third hypothesis is that smaller mtDNA molecules may have evolved. As our analysis excluded the AT-rich region located after the tRNA-alanine sequence, we are unable to detect if the AT-region may have experienced deletions resulting in smaller molecules. It is possible that smaller mtDNA molecules with a replicative advantage increased in proliferation (Phillips et al., 2015; Rand, 2001). The AT-region is highly repetitive and problematic to sequence, making this hypothesis difficult to evaluate and future experimental is needed to investigate these possibilities.

2.5.2 Indel mutations

A previous analysis found homopolymers to be hotspots for indel mutation in *C. elegans* mtDNA (Denver et al., 2000); we also observed numerous indel mutations in this study and, applying improved sequencing technology, were able to provide quantitative estimates of heteroplasmic indel frequencies. All N2 derived MA lines and four *gas-1* derived MA lines harbored indel heteroplasmies in the *ATP6* gene sequence, with no

evidence for the heteroplasmy in either the N2 or *gas-1* progenitor (Table 2.4). This result

suggests that this specific site may be a hotspot for indel mutation in *C. elegans*.

Similarly, as two N2 derived MA lines (MA523 and MA 574) experienced insertion of a

'T' allele at site 11721 located in the *NAD-5* gene, and the N2 progenitor was observed to

only harbor the wild-type allele at this position, the N2 strain may have predisposition for

insertion events at this site. We cannot, however, rule out that these indels may have been

segregating at extremely low (undetectable) frequencies in the N2 ancestor.

The fact that we observed more indel variants in N2 derived lines compared to -

gas-1 nematodes is consistent with their much larger number of MA generations.

However, the higher mtDNA copy number in N2 versus *gas-1* MA lines may also

contribute to this finding. Studies in mice have determined elevated mtDNA copy

number to be associated with impaired replication, which may result in mtDNA deletions

(Fan et al., 2008).

2.5.3 SNP mutations

Our study found more mtDNA base substitution events among the *gas-1* G43 MA

lines compared to the N2 G250 MA lines (Figure 2.2). The larger number of

heteroplasmic SNPs observed in the *gas-1* derived lines may be a product of impaired

mitochondrial activity and/or high ROS levels reported as phenotypes for the *gas-1*

mutant (Pujol et al., 2013). However, our numbers of detected SNPs were small (only

two SNPs in N2 lines and seven in *gas-1* lines), and further work will be required to

establish whether any relationship exists between mitochondrial ETC dysfunction and

mtDNA mutation. We preferred to take a conservative approach to identifying putative

heteroplasmies because our coverage was not extraordinarily high (mean mtDNA

coverage = 545X, Table 2.1). We recognize that our analysis likely results in false negatives although this approach minimizes the possibilities of false positives.

A previous study of mtDNA mutations in *C. elegans* N2 MA lines found homopolymer runs to be mutation hotspots, although there was no evidence for putative base-substitution hotspot sites (e.g., parallel mutation) (Denver, 2000). Here, two *gas-1* MA lines (MA431 and MA438) experienced the same heteroplasmic mutation at 211bp located in the *NAD-6* gene. As this mutation was absent from both wild-type and *gas-1* progenitor, as well as all N2-derived MA lines, this result is consistent with this site being a mutation hotspot.

We observed a low-frequency heteroplasmy in the *gas-1* progenitor at position 8439bp in the *COX-1* gene. The same heteroplasmy was observed to fix in one line (MA438) and achieve a relatively high frequency (>37%) in another (MA412) (Table 2.4). Results of Sanger sequencing revealed that this heteroplasmy was maintained at various levels among individual nematodes sampled from the *gas*-1 progenitor, including complete absence (non-detectable) in some individuals and fixation in others. Furthermore, one explanation for the rapid shift in mitochondrial genotypes observed trans-generationally is a mitochondrial genetic 'bottleneck' (high genetic drift) where only a small proportion of mitochondrial genomes repopulate the subsequent generation (Chinnery et al., 2000). Our results may be in alignment with predictions of these theories where only a small subset of mtDNA molecules from the parental generation repopulate the mitochondrial genome pool for the progeny. However, an important caveat should be noted: the studies referenced here used mammalian models and were not conducted on *C.*

elegans. It still unknown how many mtDNA molecules from the mother are used to proliferate the population of mtDNA in germ cells in the *C. elegans* model.

Eight out of eighteen individual *gas-1* progenitor worms contained the *COX-1* 8439 heteroplasmy. This observation highlights the reality that there exists variation among individuals in the progenitor lab population, and that subsequent observations in lab-evolved lines will be affected by the particular nematode randomly chosen to initiate each plate. Moreover, three of the fourteen *gas-1* derived MA lines analyzed by Sanger sequencing were found to harbor homoplasmic genomes fixed for the 8439bp mutation. In light of both these observations, it is highly likely that the *gas-1* progenitor employed to generate the *gas-1* MA lines harbored the *COX-1* heteroplasmy at moderately high levels. Our results indicate that mtDNA heteroplasmies can become fixed in individuals from lineages evolving under minimized natural selection.

2.6 Conclusion

This study provides new insights into the heteroplasmic paths of mutation in an animal mitochondrial genome. Our study of mtDNA variation across experimental generations revealed increases in mtDNA copy number in *C. elegans* wildtype and *gas-1* strains across generations under extreme genetic drift, adding to previous studies demonstrating increased mtDNA copy number across nematode development (Bratic et al., 2009). The higher frequency of detected single-base substitution mutations in *gas-1* MA-line genomes relative to that of indels may suggest increased vulnerability of the *gas-1* genotype to experience single-base substitution events relative to wild-type MA lines. It is, however, unclear whether the differences in mtDNA mutation type observed between the two sets of MA lines are a consequence of differences in underlying rates of

mutation to each type and/or of subsequent evolutionary dynamics. Further insights into the heteroplasmic mtDNA mutation process will benefit from approaches that consider many generational timepoints, a variety of starting genotypes, and more careful examination of the specific progenitor individuals used to initiate experimental evolution.

2.7 References

Baer, C. F., Shaw, F., Steding, C., Baumgartner, M., Hawkins, A., Houppert, A., et al. (2005). Comparative evolutionary genetics of spontaneous mutations affecting fitness in rhabditid nematodes. *Proc. Natl. Acad. Sci. U. S. A.* 102, 5785–5790. doi:10.1073/pnas.0406056102.

Bergstrom, C. T., and Pritchard, J. (1998). Germline bottlenecks and the evolutionary maintenance of mitochondrial genomes. *Genetics* 149, 2135–2146.

Bratic, I., Hench, J., Henriksson, J., Antebi, A., Bürglin, T. R., and Trifunovic, A. (2009). Mitochondrial DNA level, but not active replicase, is essential for Caenorhabditis elegans development. *Nucleic Acids Res.* 37, 1817–1828. doi:10.1093/nar/gkp018.

Bratic, I., Hench, J., and Trifunovic, A. (2010). Caenorhabditis elegans as a model system for mtDNA replication defects. *Methods* 51, 437–443. doi:10.1016/j.ymeth.2010.03.003.

Chinnery, P. F., Thorburn, D. R., Samuels, D. C., White, S. L., Dahl, H. H. M., Turnbull, D. M., et al. (2000). The inheritance of mitochondrial DNA heteroplasmy: Random drift, selection or both? *Trends Genet.* 16, 500–505. doi:10.1016/S0168-9525(00)02120-X.

Chol, M. (2003). The mitochondrial DNA G13513A MELAS mutation in the NADH dehydrogenase 5 gene is a frequent cause of Leigh-like syndrome with isolated complex I deficiency. *J. Med. Genet.* 40, 188–191. doi:10.1136/jmg.40.3.188.

Clark, K. a., Howe, D. K., Gafner, K., Kusuma, D., Ping, S., Estes, S., et al. (2012). Selfish little circles: Transmission bias and evolution of large deletion-bearing mitochondrial DNA in caenorhabditis briggsae nematodes. *PLoS One* 7, 1–8. doi:10.1371/journal.pone.0041433.

Denver, D. R. (2000). High Direct Estimate of the Mutation Rate in the Mitochondrial Genome of Caenorhabditis elegans. *Science (80-.).* 289, 2342–2344. doi:10.1126/science.289.5488.2342.

Denver, D. R., Dolan, P. C., Wilhelm, L. J., Sung, W., Lucas-Lledo, J. I., Howe, D. K., et al. (2009a. A genome-wide view of Caenorhabditis elegans base-substitution mutation processes. *Proc. Natl. Acad. Sci.* 106, 16310–16314. doi:10.1073/pnas.0904895106.

Denver, D. R., Morris, K., Lynch, M., Vassilieva, L. L., and Thomas, W. K. (2000). High direct estimate of the mutation rate in the mitochondrial genome of Caenorhabditis elegans. *Science* 289, 2342–2344. doi:10.1126/science.289.5488.2342.

Denver, D. R., Wilhelm, L. J., Howe, D. K., Gafner, K., Dolan, P. C., and Baer, C. F. (2012). Variation in base-substitution mutation in experimental and natural lineages of caenorhabditis nematodes. *Genome Biol. Evol.* 4, 513–522. doi:10.1093/gbe/evs028.

Dromparis, P., and Michelakis, E. D. (2013). Mitochondria in Vascular Health and Disease. *Annu. Rev. Physiol.* 75, 95–126. doi:10.1146/annurev-physiol-030212-183804.

Van den Ecker, D., van den Brand, M. A., Ariaans, G., Hoffmann, M., Bossinger, O., Mayatepek, E., et al. (2012). Identification and functional analysis of mitochondrial complex I assembly factor homologues in C. elegans. *Mitochondrion* 12, 399–405. doi:10.1016/j.mito.2012.01.003.

Elkin, C. J., Richardson, P. M., Fourcade, H. M., Hammon, N. M., Pollard, M. J., Predki, P. F., et al. (2001). High-throughput plasmid purification for capillary sequencing. *Genome Res.* 11, 1269–1274. doi:10.1101/gr.167801.

Falk, M. J., Rosenjack, J. R., Polyak, E., Suthammarak, W., Chen, Z., Morgan, P. G., et al. (2009). Subcomplex Ilambda specifically controls integrated mitochondrial functions in Caenorhabditis elegans. *PLoS One* 4. doi:10.1371/journal.pone.0006607.

Fan, W., Waymire, K. G., Narula, N., Li, P., Rocher, C., Coskun, P. E., et al. (2008). A mouse model of mitochondrial disease reveals germline selection against severe mtDNA mutations. *Science* 319, 958–962. doi:10.1126/science.1147786.

Guha, M., and Avadhani, N. G. (2013). Mitochondrial retrograde signaling at the crossroads of tumor bioenergetics, genetics and epigenetics. *Mitochondrion* 13, 577–591. doi:10.1016/j.mito.2013.08.007.

Hadzsiev, K., Maasz, A., Kisfali, P., Kalman, E., Gomori, E., Pal, E., et al. (2010). Mitochondrial DNA 11777C>A Mutation Associated Leigh Syndrome: Case Report with a Review of the Previously Described Pedigrees. *NeuroMolecular Med.* 12, 277–284. doi:10.1007/s12017-010-8115-9.

Halligan, D. L., and Keightley, P. D. (2009). Spontaneous Mutation Accumulation Studies in Evolutionary Genetics. *Annu. Rev. Ecol. Evol. Syst.* 40, 151–172. doi:10.1146/annurev.ecolsys.39.110707.173437.

Hartman, P. S., Ishii, N., Kayser, E. B., Morgan, P. G., and Sedensky, M. M. (2001). Mitochondrial mutations differentially affect aging, mutability and anesthetic sensitivity in Caenorhabditis elegans. *Mech. Ageing Dev.* 122, 1187–1201. doi:10.1016/S0047-6374(01)00259-7.

Jenuth, J. P., Peterson, a C., and Shoubridge, E. a (1997). Tissue-specific selection for different mtDNA genotypes in heteroplasmic mice. *Nat. Genet.* 16, 93–95. doi:10.1038/ng0597-93.

Joyner-Matos, J., Hicks, K. A., Cousins, D., Keller, M., Denver, D. R., Baer, C. F., et al. (2013). Evolution of a Higher Intracellular Oxidizing Environment in Caenorhabditis elegans under Relaxed Selection. *PLoS One* 8, e65604. doi:10.1371/journal.pone.0065604.

Kann, L. M., Rosenblum, E. B., and Rand, D. M. (1998). Aging, mating, and the evolution of mtDNA heteroplasmy in Drosophila melanogaster. *Proc. Natl. Acad. Sci. U. S. A.* 95, 2372–7. doi:10.1073/pnas.95.5.2372.

Kayser, E. B., Morgan, P. G., Hoppel, C. L., and Sedensky, M. M. (2001). Mitochondrial Expression and Function of GAS-1 in Caenorhabditis elegans. *J. Biol. Chem.* 276, 20551–20558. doi:10.1074/jbc.M011066200.

Kayser, E.-B., Morgan, P. G., and Sedensky, M. M. (1999). GAS-1. *Anesthesiology* 90, 545–554. doi:10.1097/00000542-199902000-00031.

Kayser, E.-B., Sedensky, M. M., and Morgan, P. G. (2004). The effects of complex I function and oxidative damage on lifespan and anesthetic sensitivity in Caenorhabditis elegans. *Mech. Ageing Dev.* 125, 455–464. doi:10.1016/j.mad.2004.04.002.

Kennedy, S. R., Loeb, L. A., and Herr, A. J. (2012). Somatic mutations in aging, cancer and neurodegeneration. *Mech. Ageing Dev.* 133, 118–126. doi:10.1016/j.mad.2011.10.009.

Lane, N. (2011). Mitonuclear match: Optimizing fitness and fertility over generations drives ageing within generations. *Bioessays* 33, 860–869. doi:10.1002/bies.201100051.

Liu, C.-S., Tsai, C.-S., Kuo, C.-L., Chen, H.-W., Lii, C.-K., Ma, Y.-S., et al. (2003). Oxidative stress-related alteration of the copy number of mitochondrial DNA in human leukocytes. *Free Radic. Res.* 37, 1307–1317.

Lynch, S. M., Weinstein, S. J., Virtamo, J., Lan, Q., Liu, C.-S., Cheng, W.-L., et al. (2011). Mitochondrial DNA copy number and pancreatic cancer in the alpha-tocopherol beta-carotene cancer prevention study. *Cancer Prev. Res. (Phila).* 4, 1912–1919. doi:10.1158/1940-6207.CAPR-11-0002.

Nisoli, E., and Carruba, M. O. (2006). Nitric oxide and mitochondrial biogenesis. *J. Cell Sci.* 119, 2855–2862. doi:10.1242/jcs.03062.

Phillips, W. S., Coleman-Hulbert, A. L., Weiss, E. S., Howe, D. K., Ping, S., Wernick, R. I., et al. (2015). Selfish Mitochondrial DNA Proliferates and Diversifies in Small, but not Large, Experimental Populations of Caenorhabditis briggsae. *Genome Biol. Evol.* 7, 2023–37. doi:10.1093/gbe/evv116.

Podlesniy, P., Figueiro-Silva, J., Llado, A., Antonell, A., Sanchez-Valle, R., Alcolea, D., et al. (2013). Low cerebrospinal fluid concentration of mitochondrial DNA in preclinical Alzheimer disease. *Ann. Neurol.* 74, 655–668. doi:10.1002/ana.23955.

Pujol, C., Bratic-Hench, I., Sumakovic, M., Hench, J., Mourier, A., Baumann, L., et al. (2013). Succinate dehydrogenase upregulation destabilize complex I and limits the lifespan of gas-1 mutant. *PLoS One* 8, e59493. doi:10.1371/journal.pone.0059493.

Pyle, A., Anugrha, H., Kurzawa-Akanbi, M., Yarnall, A., Burn, D., and Hudson, G. (2016). Reduced mitochondrial DNA copy number is a biomarker of Parkinson's disease. *Neurobiol. Aging* 38, 216.e7–216.e10. doi:10.1016/j.neurobiolaging.2015.10.033.

Van Raamsdonk, J. M., and Hekimi, S. (2011). FUdR causes a twofold increase in the lifespan of the mitochondrial mutant gas-1. *Mech. Ageing Dev.* 132, 519–521. doi:10.1016/j.mad.2011.08.006.

Rand, D. M. (2001). The Units of Selection on Mitochondrial DNA. *Annu. Rev. Ecol. Syst.* 32, 415–448. doi:10.1146/annurev.ecolsys.32.081501.114109.

Reinke, S. N., Hu, X., Sykes, B. D., and Lemire, B. D. (2010). Caenorhabditis elegans diet significantly affects metabolic profile, mitochondrial DNA levels, lifespan and brood size. *Mol. Genet. Metab.* 100, 274–282. doi:10.1016/j.ymgme.2010.03.013.

Rice, A. C., Keeney, P. M., Algarzae, N. K., Ladd, A. C., Thomas, R. R., and Bennett, J. P. (2014). Mitochondrial DNA copy numbers in pyramidal neurons are decreased and mitochondrial biogenesis transcriptome signaling is disrupted in Alzheimer's disease hippocampi. *J. Alzheimer's Dis.* 40, 319–330. doi:10.3233/JAD-131715.

Schulz, K. L., Eckert, A., Rhein, V., Mai, S., Haase, W., Reichert, A. S., et al. (2012). A new link to mitochondrial impairment in tauopathies. *Mol. Neurobiol.* 46, 205–216. doi:10.1007/s12035-012-8308-3.

Solignac, M., Gnermont, J., Monnerot, M., and Mounolou, J.-C. (1987). Drosophila mitochondrial genetics: Evolution of heteroplasmy through germ line cell divisions. *Genetics* 117, 687–696.

Stewart, J. B., and Chinnery, P. F. (2015). The dynamics of mitochondrial DNA heteroplasmy: implications for human health and disease. *Nat. Rev. Genet.* 16, 530–42. doi:10.1038/nrg3966.

Stiernagle, T. (2006). Maintenance of C. elegans. *WormBook*. doi:10.1895/wormbook.1.101.1.

Tsang, W. Y., and Lemire, B. D. (2002). Stable heteroplasmy but differential inheritance of a large mitochondrial DNA deletion in nematodes. *Biochem. Cell Biol.* 80, 645–654. doi:10.1139/o02-135.

Tuppen, H. A. L., Hogan, V. E., He, L., Blakely, E. L., Worgan, L., Al-Dosary, M., et al. (2010). The p.M292T NDUFS2 mutation causes complex I-deficient Leigh syndrome in multiple families. *Brain A J. Neurol.* 133, 2952–2963. doi:10.1093/brain/awq232.

Vasta, V., Sedensky, M., Morgan, P., and Hahn, S. H. (2011). Altered redox status of coenzyme Q9 reflects mitochondrial electron transport chain deficiencies in Caenorhabditis elegans. *Mitochondrion* 11, 136–138. doi:10.1016/j.mito.2010.09.002.

Wallace, D. C. (2005). A mitochondrial paradigm of metabolic and degenerative diseases, aging, and cancer: a dawn for evolutionary medicine. *Annu. Rev. Genet.* 39, 359–407. doi:10.1146/annurev.genet.39.110304.095751.

Wallace, D. C., and Chalkia, D. (2013). Mitochondrial DNA genetics and the heteroplasmy conundrum in evolution and disease. *Cold Spring Harb. Perspect. Biol.* 5. doi:10.1101/cshperspect.a021220.

Wallace, D. C., and Youle, R. eds. (2013). *Mitochondria*. Cold Spring Harbor, New York: Cold Spring Harbor Laboratory Press.

Williams, B. D., Schrank, B., Huynh, C., Shownkeen, R., and Waterston, R. H. (1992). A genetic mapping system in Caenorhabditis elegans based on polymorphic sequence-tagged sites. *Genetics* 131, 609–624.

Wood, 1988). *The Nematode Caenohabditis Elegans*. Cold Spring Harbor, New York: Cold Spring Harbor Laboratory doi:10.1101/087969307.17.1.
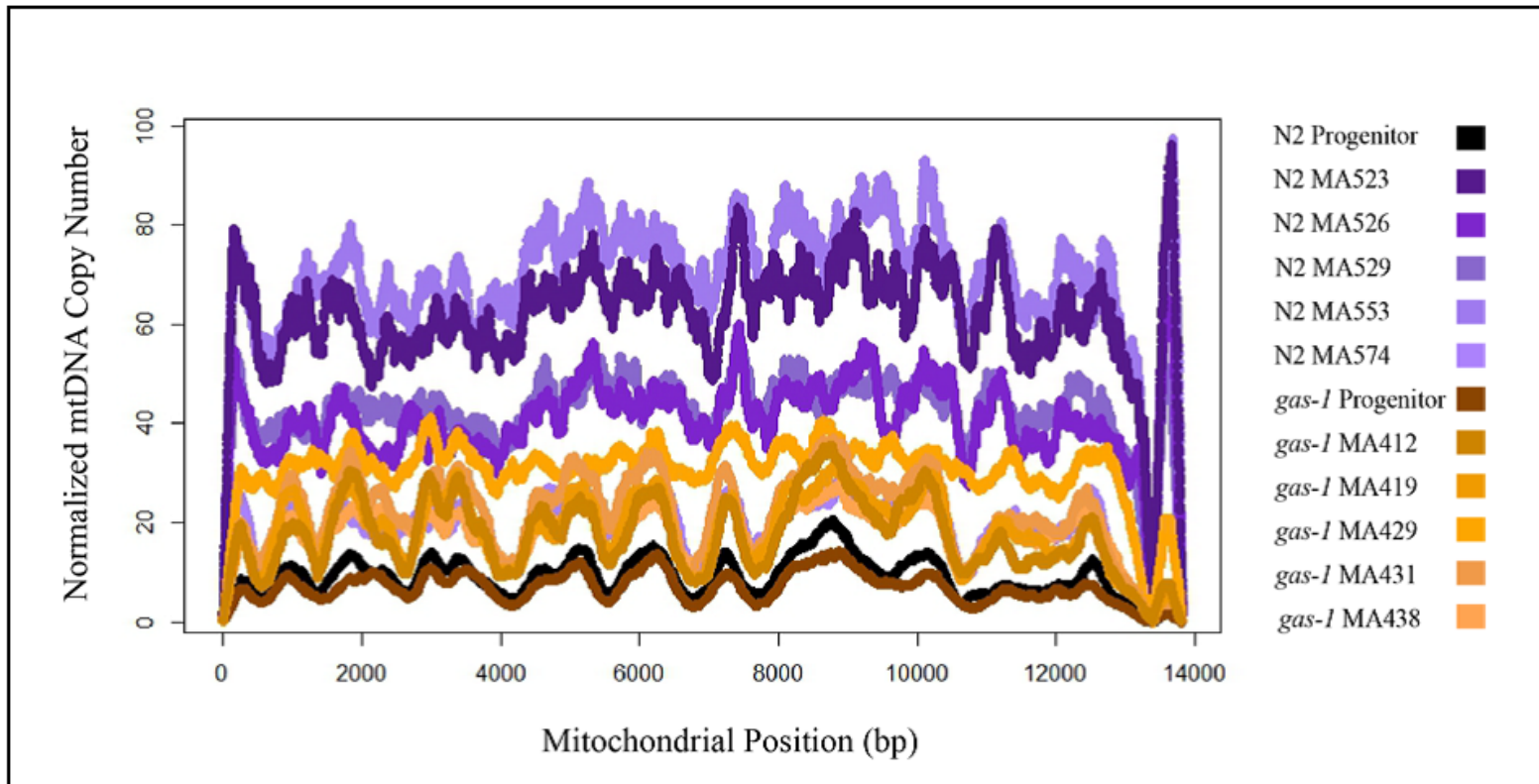
Figure 2.1: mtDNA copy number N2 and *gas-1* progenitor vs. MA lines. All nematodes at L1 stage. N2 MA lines bottlenecked for 250 generations. *gas-1* MA lines bottlenecked for a maximum 50 generations. mtDNA copy number normalized by corresponding line-specific coverage of single-copy nuclear genes: *ama-1*, *ego-1* and *efl-3*. N2 MA lines mean mtDNA copy number = 47.43; standard deviation = 19.9. *gas-1* MA mean mtDNA copy number = 12.89, standard deviation 5.63. The AT-rich region was excluded from analysis.

59

Figure 2.2: **Schematic of Mitochondrial Indel and Single-Base Substitution Heteroplasmies.** All indel and single-base substitution events for all wild-type N2 and *gas-1* lines.
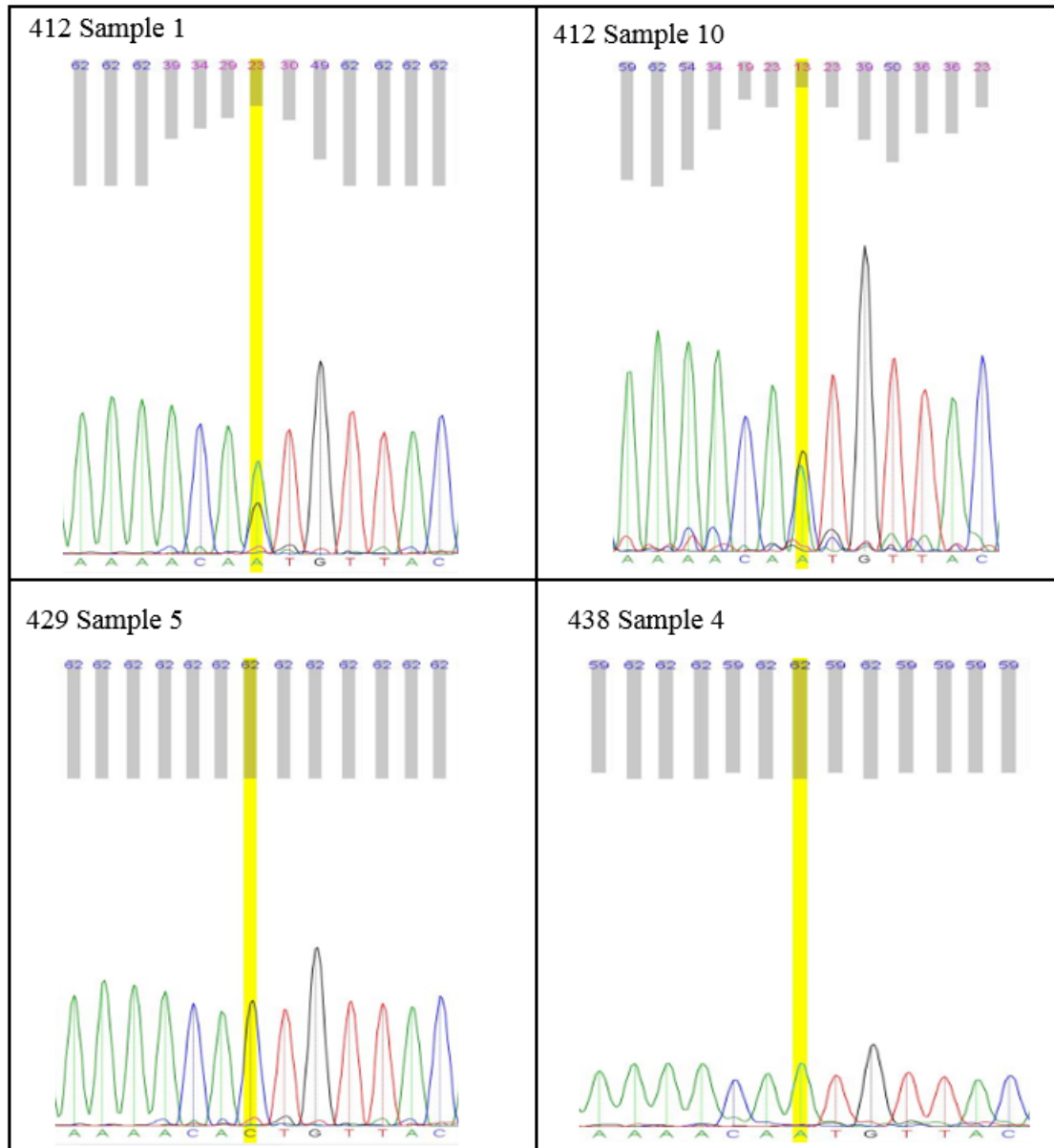
Figure 2.3: **Individual L1's Sanger Electropherogram.** Sanger results for mitochondrial position 8439 heteroplasmy of individual *gas-1* worms. Electropherograms for MA412 samples display presence of both 'A' and 'C' alleles. MA429 is, fixed for the wild-type 'C' allele. MA438 is fixed for the alternate 'A' allele. Lower phred scores, displayed above electropherograms, indicate uncertainty in base calling associated with heteroplasmic sites.

Table 2.1: Illumina-MiSeq Sequencing Run Statistics and Normalization of Mean mtDNA Copy Number. All reads 150bp, paired end. All nematodes at L1 stage. Assembled using WS242 *C. elegans* reference genome in CLC with following parameters: no masking, mismatch cost= 2, insertion cost=3, deletion cost= 3, length fraction= 0.98, read fraction= 0.98, global alignment= no, non-specific match handling= map randomly. mtDNA copy number normalized by mean coverage of corresponding single-copy nuclear genes (Norm mtDNA). mtDNA mean coverage calculated excluding AT-region (Avg mtDNA Cov). Overall nuclear coverage (Avg Nuc Cov) calculated for entire nuclear genome per a line. Average single-copy nuclear coverage (Avg Single-Copy) calculated from average of three single copy genes: *ama-1*(Avg *ama-1 Cov*), *ego-1*(Avg *ego-1 Cov*), *efl-3* (Avg *efl-3 Cov*). Standard deviation of the mean displayed in parentheses adjacent to mean values.

Line	Total Reads	% Mapping	Avg Nuc Cov	Avg mtDNA Cov	Norm mtDNA	Avg Single-Copy	Avg *ama-1* Cov	Avg *ego-1* Cov	Avg *efl-3* Cov
N2									
Progenitor	12,474,086	87.7	27.3 (54.7)	330.7 (128.0)	9.4	37.0	36.3 (13.7)	39.0 (11.4)	35.7 (14.2)
MA523	8,162,820	92.7	11.3 (15.1)	241.6 (62.8)	19.8	12.2	10.4 (3.3)	13.1 (3.5)	13.1 (3.1)
MA526	6,698,142	89.5	8.9 (13.1)	636.2 (85.7)	71.1	9.0	7.4 (2.7)	9.3 (3.4)	10.2 (4.4)
MA529	6,799,824	93.0	9.4 (12.2)	414.2 (52.8)	42.4	9.8	8.9 (3.2)	10.1 (3.2)	10.3 (3.0)
MA553	7,846,166	92.0	10.7 (15.9)	569.1 (74.1)	51.4	11.1	9.1 (3.6)	12.1 (4.6)	12.0 (4.5)
MA574	6,271,490	93.2	8.7 (12.4)	449.5 (67.9)	50.1	9.0	7.1 (3.3)	9.2 (4.3)	10.7 (4.1)
gas-1									
Progenitor	10,725,726	88.6	23.7 (36.9)	221.3 (86.2)	7.2	30.8	26.2 (9.6)	35.0 (9.2)	31.2 (11.2)
MA412	7,558,954	83.4	15.6 (14.5)	324.5 (79.9)	18.0	18.1	13.8 (5.5)	20.3 (5.8)	20.1 (7.3)
MA419	6,843,258	82.5	14.0 (13.7)	308.9 (99.9)	28.3	10.9	10.6 (4.3)	14.9 (4.2)	7.3 (5.9)
MA429	7,351,108	86.8	15.9 (12.3)	498.8 (74.2)	29.1	17.2	11.7 (5.0)	20.0 (6.8)	19.8 (6.2)
MA431	6,896,562	80.6	13.7 (13.7)	286.6 (98.4)	19.4	14.8	10.9 (4.2)	17.4 (4.5)	15.9 (6.8)
MA438	6,998,936	83.4	14.4 (17.4)	259.6 (100.1)	17.1	15.2	11.1 (4.8)	17.3 (5.6)	17.1 (6.4)

Table 2.2: Mitochondrial Heteroplasmic Single-Nucleotide Polymorphisms. Ref Base= Reference Allele. Var Base= Variant Allele. Ref Codon = Reference Codon. Ref AA= Reference Amino Acid. Var Codon= Variant Codon. Var AA= Variant Amino Acid. Site specific variant frequency (Var Freq) calculated by dividing number of variant calls (Var Counts) by the total coverage at the position (Var Counts + Ref Counts). SNPs required to be within one standard deviation of the line-specific per-site mean mitochondrial coverage, have a variant frequency greater than two standard deviations above the line-specific mean variant frequency and at least six variant calls per SNP.

Line	Pos	Gene	Ref Base	Ref Counts	Var Base	Var Counts	Var Freq	Ref Codon	Ref AA	Var Codon	Var AA	Type
N2												
Progenitor	8274	*COX-I*	G	495	A	21	0.041	GGG	Gly	GAG	Glu	Non-Syn
MA523	8731	*COX-I*	C	292	A	18	0.058	GCT	Ala	GAT	Asp	Non-Syn
gas-1												
Progenitor	8439	*COX-I*	G	344	T	18	0.050	GTG	Val	TTG	Leu	Non-Syn
MA412	8439	*COX-I*	G	259	T	155	0.374	GTG	Val	TTG	Leu	Non-Syn
MA431	211	*NAD-6*	A	238	T	9	0.036	CTA	Leu	CTT	Leu	Syn
	450	*NAD-6*	A	140	T	6	0.041	CTA	Leu	CTT	Leu	Syn
	5422	*Cyt-b*	A	261	T	7	0.026	ACC	Thr	ACT	Thr	Syn
	7176	*NAD-4*	T	312	C	36	0.103	TTA	Leu	TCA	Ser	Non-Syn
	11965	*NAD-5*	T	203	A	6	0.029	CTA	Leu	CAA	Gln	Non-Syn
MA438	211	*NAD-6*	A	252	T	6	0.023	CTA	Leu	CTT	Leu	Syn
	8439	*COX-I*	G	0	T	447	1.000	GTG	Val	TTG	Leu	Non-Syn

Table 2.3: Mitochondrial Heteroplasmic Indel Variants. Site specific variant frequency calculated by dividing number of variant calls by the total coverage at the position. Indels required to be within one standard deviation of the line-specific per-site mean mitochondrial coverage, have a variant frequency greater than two standard deviations above the line-specific mean variant frequency and at least six variant calls per indel. Dashes in the reference allele column (Ref Allele) indicate an insertion and that the base missing from reference genome. Dashes in variant allele column (Var allele) indicate a deletion; base missing from experimental line.

Line	Pos	Gene	Ref Allele	Ref Counts	Var Allele	Var Counts	Var Freq	Homopoly Len	Type
N2									
MA523	3235	*ATP6*	A	211	-	11	.0495	11	Deletion
	11721	*NAD-5*	-	193	T	13	0.063	8	Insertion
MA526	3235	*ATP6*	A	113	-	441	.796	11	Deletion
	8653	*COX-I*	-	611	A	11	0.018	2	Insertion
MA529	3235	*ATP6*	A	372	-	15	.0388	11	Deletion
MA553	3235	*ATP6*	A	493	-	21	.041	11	Deletion
MA574	3235	*ATP6*	A	255	-	136	.348	11	Deletion
	11721	*NAD-5*	-	236	T	152	0.392	8	Insertion
gas-1									
Progenitor	9954	*tRNA-C*	T	235	-	11	0.0447	2	Deletion
MA419	3235	*ATP6*	A	370	-	11	0.029	11	Deletion
MA429	3235	*ATP6*	A	502	-	25	.047	11	Deletion
MA431	3235	*ATP6*	A	375	-	17	0.043	11	Deletion
MA438	3235	*ATP6*	A	321	-	11	0.033	11	Deletion

Table 2.4: SNPs and Indels frequencies For All Mitochondrial Sites Containing Variants. Each site which experienced a variant in any of the twelve lines is listed by reference position in WS242 (base pair). Frequencies which appear in tables 2 and 3 are in bold. A value of '0' indicates no variant allele occurred for at this site for the line.

Site	N2 Prog	MA523	MA526	MA529	MA553	MA574	gas-1 Prog	MA412	MA419	MA429	MA431	MA438
SNPs												
211	0.008	0.003	0.004	0.006	0.002	0.002	0.000	0.011	0.020	0.018	**0.036**	**0.023**
450	0.000	0.000	0.000	0.008	0.000	0.000	0.007	0.000	0.006	0.002	**0.041**	0.007
5422	0.000	0.000	0.008	0.004	0.000	0.002	0.006	0.008	0.009	0.004	**0.026**	0.013
8274	**0.041**	0.000	0.001	0.002	0.000	0.000	0.000	0.000	0.008	0.000	0.002	0.000
8439	0.002	0.000	0.000	0.000	0.000	0.000	**0.050**	**0.374**	0.000	0.000	0.000	**1.000**
8731	0.001	**0.060**	0.002	0.000	0.000	0.002	0.000	0.000	0.000	0.002	0.000	0.000
Indels												
3235	0.021	**0.050**	**0.796**	**0.038**	**0.041**	**0.348**	0.013	0.021	**0.029**	0.047	**0.043**	**0.033**
8653	0.001	0.003	**0.018**	0.000	0.000	0.000	0.003	0.002	0.000	0.000	0.002	0.000
9954	0.002	0.000	0.000	0.000	0.000	0.000	**0.045**	0.000	0.000	0.000	0.000	0.002
11721	0.000	**0.063**	0.090	0.002	0.000	**0.392**	0.000	0.000	0.003	0.002	0.004	0.000

Chapter 3: Nuclear genome evolution in bottlenecked populations of

C. elegans N2-reference and *gas-1* mutant strains

Riana I. Wernick[1], Suzanne Estes[2], Stephen Christy[2], Michael Lue[2], Dana K. Howe[1],

Dee R. Denver[1]

1. Department of Integrative Biology, Oregon State University, Corvallis, Oregon, USA
2. Department of Biology, Portland State University, Portland, Oregon, USA

3.1 Abstract

Exposed to extreme genetic drift, changes in the nuclear genome may impose many different consequences on organismal fitness and function. Mutations that accumulate under bottlenecking, while frequently deleterious, have the potential to be beneficial. Understanding how the nuclear genome evolves in response to mitochondrial dysfunction is essential for perceiving the consequences of mitochondrial dysfunction on nuclear mutation and creating therapeutic interventions. We examined how the nuclear genome changes when predisposed to mitochondrial impairment in the mitochondrial electron transport chain (*gas-1*) mutant and wild-type (N2 strain) *Caenorhabditis elegans* mutation-accumulation (MA) lines. The *gas-1* MA lines were created for this study, and bottlenecked in the laboratory for a maximum of fifty generations. The N2 MA lines, derived from a previous experiment, were bottlenecked for 250 generations (Baer et al., 2005). We applied Illumina-MiSeq DNA sequencing to L1 larvae from five *gas-1* MA lines and five N2 MA lines to investigate nuclear genome response to mitochondrial dysfunction. Mutation rate in the *gas-1* MA lines was observed to be comparable to the published N2 mutation rate. While mutations in N2 MA lines were observed to occur randomly within the nuclear genome, analysis suggests that the *gas-1* MA line nuclear mutations were influenced by natural selection, potentially evolving in compensatory response to mitochondrial dysfunction imposed by the *gas-1* mutation. For example, four mutations observed in one MA line appear to have potential for ameliorating mitochondrial impairment. Assays evaluating fecundity and ROS on the *gas-1* and N2 progenitor strains with the inclusion of these four SNPs suggested improvement of fitness

through nuclear mutation under bottlenecking. This study provides new insights on the potential for beneficial mutations under bottlenecking and how the nuclear genome evolves in *C. elegans* when nematodes are predisposed to mitochondrial impairment.

3.2 Introduction

"Nothing in evolution makes sense except in the light of population genetics"
-Michael Lynch

New mutations are the original source of genetic variation (Fisher, 1930; Kondrashov, 1988; Lynch et al., 1999). The fate of a mutation (whether it is lost, fixed, or a fluctuating polymorphism) is dependent not only on its fitness effect but also strongly determined by population size (Bromham, 2009; Wang et al., 2014). In a small population in which selection is overpowered by genetic drift, chance governs the outcome of the majority of mutations (Bromham, 2009). Generally, it is accepted that the majority of new mutations are either neutral or slightly deleterious and only a small fraction of mutations are advantageous (Bataillon, 2003; Eyre-Walker and Keightley, 1999; Shaw et al., 2003). Population bottlenecks, in which the population size is significantly reduced, diminishes natural selection and increases genetic drift (Amos and Harwood, 1998). Exposed to genetic drift as a function of bottlenecking, fitness is expected to decrease and genetic variation within the population is predicted to rise (Bergstrom and Pritchard, 1998). Simply as a function of chance, the lack of selection and extreme genetic drift are predicted to fix a proportion of slightly deleterious mutations in a small population (Bromham, 2009). Further, advantageous mutations which in large population size would likely rise to fixation due to selection, have an increased risk of being removed due to drift alone when in a small population (Wright, 1931).

The theory of Muller's Ratchet, in which the genotypes harboring the lowest amount of deleterious alleles are lost in the subsequent generation due to drift, predicts that small asexual populations will accumulate an ever-increasing deleterious mutation load (Muller, 1964). The effects of deleterious mutation accumulation due to Muller's Ratchet have been observed in experimental evolution approaches employing RNA viruses, bacteria and yeast (Andersson and Hughes, 1996; Chao, 1990; Zeyl et al., 2001). Much research has examined the effects of deleterious mutations, which are frequently observed and occur on short time scales. In contrast, advantageous mutations, which thought to be are rare and occur on an evolutionary time scale, have yet to receive as much experimental attention (Orr, 1998). However, beneficial mutations may be more common than previous assumed (Hall et al., 2008). Mutations enhancing fitness have been observed in *Arabidopsis thaliana* and *Saccharomyces cerevisiae* MA lines (Hall and Joseph, 2010; Rutter et al., 2012; Wloch et al., 2001). In *Caenorhabditis briggsae,* although fecundity was reduced, compensatory mitochondrial mutations under bottlenecking were observed (Howe and Denver, 2008). Therefore, although deleterious mutations exhibit a high rate of incidence, beneficial mutations are possible under extreme genetic drift.

Mutation accumulation (MA) lines, derived from a nearly homozygous progenitor, provide the opportunity to investigate the effects of extreme genetic drift on population genetic variation and organismal fitness (Bataillon, 2003; Mukai, 1964; Rutter et al., 2012). It is assumed that the near-absence of natural selection in MA approaches will result in the perpetuation of slightly deleterious mutations in the population and organismal fitness is predicted to decline as a consequence. Employing a MA approach not only permits the study of genome changes in wildtype individuals but also allows

insight into the effects of genetic drift on individuals exhibiting decreased fitness. In addition, because the majority of slightly deleterious mutations are likely to be maintained due to the absence of selection, MA studies provide a valuable avenue to access mutation rate.

In investigating evolutionary population genetics through MA approaches, new insights into the evolution of nuclear genomes predisposed to mitochondrial dysfunction may be gained. Reliant on genes coded both within the mitochondrial and nuclear genome, mitochondrial function has potential to both increase and diminish organismal function as a result of evolutionary change. Although there are many modes of counter-acting mitochondrial dysfunction, there are numerous affects that exacerbate mitochondrial function and lower organismal fitness. On one hand, mitochondria are key promoters of organismal health. Mitochondria produce most of the energy for the cell and mediate critical responses to infection and cellular imbalance (Michelakis, 2008). On the other hand, mitochondria are also critical components of cell death and are intricately involved with disease (Michelakis, 2008; Wallace, 2007).

There are many hypotheses and claims focused on ameliorating reduced organismal fitness caused by mitochondrial dysfunction; exercise may generate repairs in mitochondrial DNA (mtDNA) mutations (Safdar et al., 2015), the overexpression of specific genes, such as TRAP1, may protect cells from mitochondrial-induced damage (Zhang et al., 2015), and antioxidants may target, amend, and protect cells from mitochondrial-generated impairment (Cai et al., 2016; Ramis et al., 2015). Although mitochondrial dysfunction plays critical roles in disease, aging and neurodegeneration (Park and Larsson, 2011; Wallace and Chalkia, 2013b; Wallace, 2005), a paradox was

found in 1995 when researchers discovered that by disrupting a gene required for the

synthesis of ubiquinone (the molecule which transports electrons from complexes I and II

in the mitochondrial electron transport chain (ETC)) longevity in *C. elegans* was extended

(Wong et al., 1995). Termed the "mit mutants", several *C. elegans* strains have since been

generated that exhibit decreased function of various ETC subunits due to either RNAi

knockdown or mutation (Munkacsy and Rea, 2014). Paradoxically, although the mit

mutants reduce mitochondrial ETC function, lifespan is augmented (Dancy et al., 2015;

Munkacsy and Rea, 2014). Substantial research has delineated this paradox, proposing

that life-extension occurs as a by-product of compensatory processes and demonstrating

that the *C. elegans* "Mit mutants" only exhibit life augmentation within a defined window

of mitochondrial dysfunction (Rossignol et al., 2003; Ventura and Rea, 2007). The

Mitochondrial Threshold Effect Theory suggests that cells can tolerate a certain level of

mitochondrial dysfunction until a critical threshold is reached (Ventura and Rea, 2007).

Experimental evidence suggests several underlying factors for the mitochondrial threshold

effects including, mtDNA heteroplasmy, age-related mitochondrial modifications and

compensatory mitochondrial biochemical pathways (Rossignol et al., 2003).

Activation of the mitochondrial unfolded protein response (UPR[mt]) is one critical

compensatory process thought to counteract mitochondrial dysfunction imposed by the

mit mutants (Wang and Hekimi, 2015). The UPR[mt] is a protective or adaptive

transcriptional response that promotes survival during mitochondrial stress or dysfunction

(Pellegrino and Haynes, 2015). Mitochondrial homeostasis is dependent on control

mechanisms to regulate the quantity and quality of mitochondria (Groenewoud and

Zwartkruis, 2013). Mitochondrial perturbation, such as mtDNA mutations or excessive

ROS production, may cause damaged or improperly folded proteins (Groenewoud and Zwartkruis, 2013). In response, mitochondrial chaperone and protease genes are transcribed, stabilizing protein-folding within mitochondria (Groenewoud and Zwartkruis, 2013; Pellegrino and Haynes, 2015). As the vast majority of mitochondrial proteins are nuclear-encoded, signaling pathways are required to regulate nuclear transcription of mitochondrial genes (Guha and Avadhani, 2013). The target of rapamycin (TOR) signaling pathway is a critical signaling pathway for regulation of nuclear-encoded mitochondrial-related genes (Butow and Avadhani, 2004).

The *C. elegans* TOR pathway is simplified but comparable to the pathway in mammalian taxa and as in mammalians the *C. elegans* TOR functions as two complexes, TORC1 and TORC2 (Figure 3.1). RHEB-1 responds to nutrient flux and activates TORC1. Activation of TORC1 inhibits expression of lipolysis, and detoxification-associated pathways and may inhibit autophagy however it is unclear if TORC1 or TORC2 are inhibitors for that process in *C. elegans* (Lapierre and Hansen, 2012). In contrast, IGF-1 signaling is initiated by DAF-2 in *C. elegans*, the tyrosine kinase receptor which binds insulin and other growth factors on the plasma membrane. DAF-2 activates through autophosphorylation and recruits AGE-1 (orthologue of the mammalian PI3K) to produce PIP3 and activate downstream kinases which ultimately prohibits DAF-16/FOXO from entering the nucleus and enhancing activity in detoxification and anti-inflammation pathways (Figure 3.2). *daf-2* mutants, which are long lived, have been shown to be dependent on the activity of the transcription factor DAF-16 which regulates numerous environmental stresses including high temperature, oxidative stress, and ionizing radiation (Honda and Honda, 1999; Iser and Wolkow, 2007). TORC1 activity, initiated by RHEB-1

in *C. elegans*, also inhibits DAF-16 activity although unlike DAF-2 may inhibit lipolysis and not inhibit DAF-16 detoxification (Lapierre and Hansen, 2012). Like *daf-2* mutants, knockdown of *rheb-1* in *C. elegans* also enhances longevity (Honjoh et al., 2009).

In addition to *daf-2* and *rheb-1 C. elegans* studies, the *C. elegans* system is a useful tool for studying impaired mitochondrial activity and mitochondrial genome evolution. As mitochondrial functions are relatively well conserved between *C. elegans* and humans, investigating mitochondrial dysfunction and mtDNA evolution *C. elegans* provides a relevant context for mitochondrial diseases and aberrations associated with human pathologies and neurodegeneration (Addo et al., 2010; Johri and Beal, 2012; Moreira et al., 2010). Furthermore, due to *C. elegans* primarily self-reproducing (hermaphroditic) nature, short lifespan, and rapid reproductive schedule, the *C. elegans* system is ideal for experimental evolution studies (Bratic et al., 2010; Chasnov and Chow, 2002).

In this experiment, we minimized natural selection and exposed *C. elegans* worms to extreme drift through mutation-accumulation (MA) approaches. We used a well-characterized *C. elegans* mutant, *gas-1* (see Chapter 1) to investigate how the nuclear genome responds to mitochondrial dysfunction. We applied Illumina MiSeq technology to analyze five different *gas-1* MA lines that were bottlenecked for an average of 43 generations, alongside five N2 MA lines from a previous study, bottlenecked for 250 generations (Baer et al., 2005) (See Chapter 1). Comparing the nuclear mutation results of the *gas-1* and wildtype MA lines allowed us to observe if and how the nuclear genome responds to mitochondrial dysfunction. Bioinformatic analysis identified and characterized nuclear mutations in both wildtype and *gas-1* progenitor and MA lines. Interactome

analysis determined if nuclear mutations were either located in genes exhibiting interactions with the *gas-1* gene or located in genes that directly interacted with *gas-1* (i.e. exhibiting interactions within two-degrees of the *gas-1* gene).

Due to small population size, the nuclear genome is predicted to accumulate deleterious mutations with harmful consequences on organismal fitness (Bergstrom and Pritchard, 1998; Howe et al., 2010). Therefore we predicted that the *gas-1* bottlenecked lines would become mutationally degraded due to extreme genetic drift. We also predicted that given the high ROS production in *gas-1* worms, ROS would damage biomolecules including DNA leading to an increased mutation rate. This study provides a novel approach to investigate how nuclear genomes respond to mitochondrial dysfunction imposed by the *gas-1* mutation when natural selection is minimized and genetic drift is extensive.

3.3 Materials and methods

3.3.1 Strains and backcrossing of *gas-1* mutant

This study utilized the *gas-1* (fc21) mutant containing a C $\rightarrow$ T point mutation that replaces a highly conserved arginine with lysine in the GAS-1 protein, a central component of mitochondrial ETC Complex I. Because *gas-1* (fc21) originated from an ethyl methanesulfonate (EMS) mutagenesis screen, the strain was likely to contain many other mutations (Kayser et al., 2001a). To reduce EMS-induced mutations, the *gas-1* strain, CW152, obtained from the *Caenorhabditis* Genetics Center (University of Minnesota) was backcrossed to the Denver-lab N2 strain for ten generations to create an isogenic mutant strain. *gas-1* homozygous lineages were used to initiate MA lines. All nematodes were cultured under standard laboratory conditions at 20ºC on standard NGM

agar plates seeded with OP50 *Escherichia coli.* For further detail on the backcrossing and

maintenance of the *gas-1* strain please refer to Materials and Methods in Chapter two.

3.3.2 L1 stage DNA preparation for Illumina-MiSeq MA lines

Twelve nematode strains—five randomly selected *gas-1* MA lines, five

previously-studied N2 MA lines, and the Denver-Lab N2 and *gas-1* progenitor strains,

were developmentally synchronized by bleaching according to standard protocols (Baer et

al., 2005d) (Wood, 1988). Following MA propagation for a maximum of fifty generations,

DNA was prepared from five randomly selected *gas-1* MA lines, five previously studied

N2 MA lines, and the *gas-1* and N2 progenitor strains for Illumina-MiSeq. First larval

(L1) stage nematodes were harvested and the DNA was purified using Qiagen DNeasy

Blood & Tissue kit (Valencia, CA) with one modification to the manufacturer's protocol:

prior to adding AL buffer, worms in a solution of M9 buffer, ATL, and Proteinase K were

subjected to five cycles of freezing and thawing to break worm cuticles and allow efficient

DNA extraction. DNA was prepared for sequencing using standard Illumina TruSeq

protocols for genomic DNA. Samples were individually barcoded and pooled for two runs

(one per a background), both sequenced using the Illumina MiSeq Genome Analyzer

operated by the Oregon State University Center for Genome Research and Biocomputing.

3.3.3 Illumina MiSeq read mappings and analyses

Following each Illumina MiSeq run, reads were aligned to the *C. elegans* genome

(version WS242) using CLC Genomics Workbench (CLC Bio-Qiagen, Aarhus, Denmark).

All reads were paired-end (2 x 150bp) and mapped using the following parameters: No

masking, mismatch cost = 2, insertion cost = 3, deletion cost = 3, length fraction = 0.98,

read fraction = 0.98, global alignment = no, non-specific match handling= map randomly

(Table 3.1).

3.3.4 Characterization of *gas-1* genetic background

There are two potential sources of genetic difference between the *gas-1* and N2

progenitor strains: (1) mutations due to EMS mutagenesis and (2) spontaneous mutations

due replication errors arising during the ten generations of backcrossing (Figure 3.3). EMS

mutagenesis is predicted to induce G:C $\rightarrow$ A:T mutations (Kim et al., 2006). As the *gas-1*

strain originated through EMS mutagenesis, additional mutations were likely induced.

Although numerous mutations may be eliminated through ten generations of backcrossing

gas-1 to Denver-Lab N2 males, backcrossing likely would not remove all EMS-induced

mutations, particularly those closely linked to the *gas-1* locus. Moreover, *C. elegans*

experiences mutations at the rate of approximately two mutations per a generation and

therefore approximately twenty mutations were expected due to the backcrossing process.

In order to ensure mutations were not located in critical genes and affecting interpretation

of our findings, all mutations in the *gas-1* progenitor were bioinformatically identified and

characterized (Table 3.2). Potential mutations were identified in the *gas-1* genome that

differed from the *C. elegans* reference genome (WS242) and not present in our wild-type

Denver-Lab N2 strain. To eliminate false positives resulting from sequencing artifacts,

candidate mutations were eliminated in which the candidate coverage was not equal or

greater to the average coverage of the *gas-1* candidate SNPs (18X). In addition the

following criteria were applied: (*i*) 100% of reads indicated a single non-reference base,

(*ii*) at least one read was present from both the reverse and forward strand, and (*iii*) reads

in a given direction varied upon start/end positions.

Mutations of six different possible types were counted in a chromosome-specific

manner. Observed mutation results in the *gas-1* progenitor were compared to published

N2 strain mutation values (Table 3.3) (Denver et al., 2012a). This comparison evaluated if

G:C → A:T mutations were over-represented in the *gas-1* progenitor, as well as tested if

the X chromosome of *gas-1* experienced significant increases of G:C → A:T transitions

and overall mutation quantity. Chi-square tests were applied in order test for significance

(Supplementary Tables B1-B3).

3.3.5 Identification and characterization of *gas-1* MA line mutations

Candidate SNPs in N2 and *gas-1* MA lines were identified as variants that differed

from the *C. elegans* reference genome (WS242) and our wild-type N2 lab strain. To

eliminate false positives resulting from sequencing and PCR artifacts, the following

criteria were applied: (*i*) at least 5-fold coverage, (*ii*) 100% of reads indicated a single non-

reference base, (*iii*) at least one read present from both the reverse and forward strand, and

(*iv*) reads in a given direction varied upon start/end positions. To eliminate false positives

due to cryptic heterozygosity or paralogy, candidate SNPs present in only one of the

twelve strains were retained (Table 3.4).

3.3.6 Mutation rate analysis

Mutation rate was calculated from pooled *gas-1* MA lines with the equation $\mu o_{bs}=$

$m/(LnT)$ where μ_{bs} is the base substitution rate (per nucleotide site per generation), L is the

number of MA lines, m is the number of observed mutations, n is the number of

nucleotide sites, and T is the time in generations as previously described (Denver et al.,

2009) (Supplementary Table B4). Values for n reflect the total number of base pairs

surveyed that met the criteria for consideration of a possible mutation site, including a

coverage range of 6-45X (Supplementary Table B5). This same approach was extended to conditional rate analysis for the six mutation types. Nuclear mutations were pooled for the *gas-1* MA lines and condition rate estimates for six mutation types (A:T → G:C, G:C → A:T, A:T →C:G, G:C → T:A, A:T →T:A, and G:C to C:G) were determined in a non-strand specific manner. Standard errors for conditional rate estimates were approximated as $[\mu_{bs}/ (nT)]^{1/2}$. We compared observed conditional rate estimates in the *gas-1* MA lines to published N2 strain values (Denver et al., 2012).

3.3.7 Interaction analysis of genes experienced in *gas-1* MA lines

We determined if the mutations in the *gas-1* MA lines interacted within 2-degrees of the *gas-1* gene. Using Gene Orienteer, all genes directly interacting with *gas-1* were included (Zhong and Sternberg, 2006). Interactomes, the complete list of all genes that are predicted to directly interact with the gene in question, were constructed using Gene Orienteer version 2.25. Gene Orienteer computationally integrates interactome data (known gene interactions), gene expression data, phenotype data and functional annotation data from three model organisms: *Saccharomyces cerevisiae, C. elegans,* and *Drosophila melanogaster* in order to predict genome-wide interactions in *C. elegans* (Zhong and Sternberg, 2006). Due to intrinsic error rate present in data from different sources and corresponding various predictive strengths, a statistical model was employed to assess likelihood of two gene interacting in *C. elegans.* The Gene Orienteer statistical model employs serial logistic regression to predict whether there is an interaction along with a computations algorithm that calibrates the parameters of the explanatory variables. Using the Inparanoid eukaryotic ortholog database, orthologous gene pairs in *C. elegans* and *D. melanogaster* as well as in *C. elegans* and *S. cerevisiae* were identified (O'Brien et al.,

2005). A likelihood ratio assigned a weighted score to five features: (1) identical

anatomical expression, (2), phenotype, (3) functional annotation, (4) microarray

coexpression, and (5) the presence of interlogs. The likelihood ratio evaluates the

frequency of gene pairs having a specific feature; a value greater than 1 indicates that the

feature is enriched in interacting gene pairs and higher scores are indicative of stronger

predictions. Likelihood scores were then integrated to estimate the overall probability that

the two *C. elegans* genes interact. A filter was applied to minimize false positives and

exclude genetic interactions among genes in the same orthologous group. Interactions with

a predicted value below 0.9 were eliminated although interactions below 4.6 have less

evidence. Approximately 8,137 genes in *C. elegans* in Gene Orienteer have interactions

above 4.6 (Zhong and Sternberg, 2006).

The comprehensive list of first- and second-degree *gas-1* interacting genes is

referred to as the "*gas-1*-centric-interactome". This analysis was extended to the N2 MA

line mutations. After identifying six out of twenty-three non-intergenic *gas-1* MA line and

eleven out of sixty non-intergenic N2 MA lines mutations were located in genes that

exhibited interactions within two-degrees of the *gas-1* gene, we conducted a simulation

analysis in order to assess how likely our result was due to chance. A simulation in Python

was performed to simulate random mutation generation in *C. elegans*. As twenty-three of

the *gas-1* MA line mutations were non-intergenic, twenty-three random mutations located

in genes were randomly generated. This simulation was repeated for one-thousand

iterations after which the average and standard deviation of the number of mutations that

occurred in genes with interaction within 2-degrees of *gas-1* were calculated. This

simulation of random mutation generation was repeated for N2 with the exception that

sixty mutations were generated since sixty N2 MA line mutations were located in either introns or exons. As in the previous analysis, one-thousand iterations of this simulation were performed after which the average and standard deviation of the number of mutations that occurred in genes with interactions within 2-degrees of the *gas-1* gene were calculated.

3.4 Results

We investigated the nuclear genome responses of *C. elegans* N2-wildtype and oxidatively stressed *gas-1* mutant strains to extreme drift. We analyzed the nuclear genomes of N2 and backcrossed *gas-1 C. elegans* progenitors, five randomly selected *gas-1* MA lines, and five previously-studied N2 MA lines using Illumina MiSeq technology (Denver et al., 2009, 2012). In all lines, over 80% of reads mapped to the *C. elegans* WS242 reference genome with a mean nDNA coverage of 14.5X and a mean mtDNA coverage of 378.4X per line (Table 3.1.) No instances of reversion of the *gas-1* allele in *gas-1* MA lines were observed.

3.4.1 Characterization of *gas-1* genetic background

Genetic differences between the backcrossed *gas-1* progenitor strain and the Denver-lab N2 strain and WS242 reference genome were identified and characterized. Bioinformatic analysis of the *gas-1* progenitor strain identified 86 genetic differences relative to the Denver-lab N2 strain (Figure 3.4) (Table 3.2). The X-chromosome of *gas-1* experienced an over-abundance of mutations with approximately 65% of the total amount of mutations genome-wide occurring on the X-chromosome. This result was compared to published N2 data (16.5%) and found to be highly significant (P < 0.00001, X^2 test) (Supplementary Table B1) (Denver et al., 2012). The X-chromosome of *gas-1* also

experienced a highly significant increased proportion of G:C → A:T mutations in comparison to published N2 results (69.6% versus 30.8%) (P < 0.00001, X^2 test) (Supplementary Table B2) (Denver et al., 2012). The occurrence of genome-wide G:C→ A:T mutations in the *gas-1* progenitor was also determined to be highly statistically significant in comparison to published N2 value. (76.5% versus 19.0%) (P < 0.00001, X^2 test) (Supplementary Table B3) (Denver et al., 2012). These patterns support that EMS likely induces many genome-wide mutations and are consistent with the backcrossing strategy to reduce the inclusion of off-target mutations in strains.

3.4.2 Identification and characterization of *gas-1* MA line mutations

Nuclear mutations in all *gas-1* MA lines were identified and bioinformatically characterized. A total of forty mutations were detected in the five *gas-1* MA lines. Of the forty mutations, ten occurred in intron regions, thirteen occurred in exons, and the remaining seventeen mutations were intergenic (Table 3.4). Of the thirteen exon mutations, four were synonymous and nine were non-synonymous (Table 3.4). *gas-1* MA438 experienced the highest number of mutation events (n=11) with *gas-1* MA429 experiencing the lowest amount of mutation events (n=5).

Conditional rate estimates of six different possible mutation categories (A:T → G:C, G:C → A:T, A:T → C:G, G:C → T:A, A:T → T:A and G:C → C:G) were assessed in a non-strand specific manner. The majority of the forty mutations were G:C → A:T transition events (n= 16) (Supplementary Table B6). Compared with conditional rate estimates and corresponding SEM values in published N2 results, only the rate of G:C → A:T transition events was significantly deviated in the *gas-1* MA lines (Figure 3.5) (Denver et al., 2012).

3.4.3 Mutation rate analysis

Following identification of *gas-1* MA line nuclear mutations, mutation rate was

calculated using standard equations (See Materials and Methods). On average, *gas-1* lines

experienced bottlenecking for forty-two generations. These data was applied to determine

per-generation base-substitution mutation rate (μ_{obs}) calculated from pooled *gas-1* MA

lines. Mutation rate in *gas-1* MA lines ($\mu_{obs} = 2..13\ (\pm.34) \times 10^{-9}$) was determined to have

no significant change compared to published N2 rates ($\mu_{obs} = 2.7\ (\pm.4)\ \times 10^{-9}$) as the two

rates were within two standard errors of one another (Denver et al., 2009).

3.4.4 Analysis of interactions of *gas-1* interactions

Analysis of biological interactions of genes in which MA nuclear mutations were

located provided additional knowledge in relation to gene function. In particular,

interactions of genes in which *gas-1* and N2 MA mutations were located were identified

using Gene Orienteer. Gene orienteer employs a serial logistic regression model that

analyzes five types of data from three model organisms to predict gene interactions

(Zhong and Sternberg, 2006) (See Materials and Methods). This research focused on a

subcomponent of the *C. elegans* interactome, the *gas-1* interactome. The *gas-1*

interactome includes all 101 genes that are predicted to directly interact with *gas-1*, and all

genes that interact with the 101 direct-interactors of *gas-1* (i.e. within two-degrees of the

gas-1 gene). Roughly one-thousand genes are included in the *gas-1* interactome in this

research. All genes in which *gas-1* and N2 MA line mutations were located were assessed

for available interactome data and all genes with predicted interactions were evaluated for

interactions with 2-degrees of the *gas-1* gene.

The interactions of the genes that experienced mutation in *gas-1* MA lines were evaluated. Of the twenty-three genes, sixteen had available interactomes in Gene Orienteer (Zhong and Sternberg, 2006). Six of the sixteen genes had interactions within 2-degrees of the *gas-1* gene: ZC8.6, *rheb-1*, *daf-2*, *sel-2*, *smf-3*, and *alh-2* (Table 3.5). *alh-2*, an aldehyde dehydrogenase mitochondrial enzyme directly interacts with the *gas-1* gene. To evaluate the likelihood that these results were due to chance, a simulation of random nuclear mutation was performed using a custom Python script. One-thousand iterations of random mutation simulation in *C. elegans* in which twenty-three genes were chosen at random, revealed that this result of six of the twenty-three genes residing 2-degrees from *gas-1* was most likely not due to chance. Out of one-thousand iterations, the mean number of mutations located in genes with interactions within 2-degrees of *gas-1* was 2.62 with a standard deviation of 1.45 (Figure 3.8). Out of one-thousand iterations, thirty-six iterations had six or more mutations residing in genes that had interactions within 2-degrees of *gas-1*.

This simulation of random mutation generation was repeated for the N2 MA line results. Of the sixty non-intergenic mutations in the N2 MA lines, eleven mutations were located in genes that interacted within 2-degrees of *gas-1*. Out of one-thousand iterations of in which sixty mutations were generated at random, the mean number of mutations residing in genes that interacted within 2-degrees of *gas-1* was 7.2 with a standard deviation of 2.5 (Figure 3.9). One-hundred five iterations had at least eleven mutations located in genes that interacted within 2-degrees of *gas-1*. The observed results in the *gas-1* MA lines were significantly different than predicted simulation values (P= 0.027, X^2

test), however, the difference between the results observed for N2 MA lines and simulation predictions was determined to be non-significant (P= 0.131, X^2 test).

3.5 Discussion

Combining MA approaches with high-throughput DNA sequencing for a set of *gas-1* and wildtype lines, this study reveals new insights on the possible evolutionary paths for populations predisposed to mitochondrial dysfunction and identifies candidate genes and potential target pathways for ameliorating Complex I impairment. While observed patterns in the N2 MA lines were not indicative of beneficial mutations, putative beneficial and potential compensatory mutations in bottlenecked *gas-1* populations were observed. Furthermore, in contrast to the N2 MA lines where few mutations (~18%) occurred in genes that interact within 2-degrees of the *gas-1* gene, ~26% of *gas-1* MA line mutations were located in genes that have interactions within 2-degrees of *gas-1*. Moreover, bioinformatic analysis of the Denver-Lab *gas-1* progenitor strain identified eighty-six mutations, significantly more than the number predicted to occur through ten rounds of backcrossing.

3.5.1 Characterization of *gas-1* genetic background

As additional mutations present in the *gas-1* strain could affect evolutionary genomic responses, we identified and characterized all genetic differences between the *gas-1* progenitor and Denver-lab N2 strain. There were two potential sources of genetic differences between these two strains: (1) mutations due to EMS mutagenesis and (2) spontaneous mutations accumulated during ten generations of backcrossing (Figure 3.3). The *gas-1* fc21 strain was generated in 1994 as a genetic model for studying the mechanism of action of volatile anesthetics (Morgan and Sedensky, 1994). As described

by Brenner in his seminal 1974 paper, nematodes were exposed to the potent mutagen ethylmethanesulfonate (EMS) (Brenner, 1974; Morgan and Sedensky, 1994). According to the authors Morgan and Sedensky, EMS generates on average one mutation per a genome (Morgan and Sedensky, 1994). Following mutation screening, newly isolated mutations were mated to the Morgan and Sedensky Lab N2 strain for a total of three outcrosses (Morgan and Sedensky, 1994). Substantial research has since employed the *gas-1* fc21 strain, most notably for mitochondrial and life span investigations (Dingley et al., 2010; Hartman et al., 2001; Kayser et al., 2004a; Kondo et al., 2005; Van Raamsdonk and Hekimi, 2011; Sedensky and Morgan, 2006). Compared to the N2 strain, *gas-1* is demonstrated to have reduced lifespan, brood size, increased ROS output and decreased ATP production. (Dingley et al., 2010; Hartman et al., 2001; Kayser et al., 2001, 2004). We backcrossed the *gas-1* strain obtained from the Caenorhabditis Genetic Center (CGC) to the Denver-Lab N2 strain. *C. elegans* experiences spontaneous mutations at the rate of two mutations per a generation and as ten round of backcrossing were performed, we predicted twenty mutations would be caused by backcrossing. However, as EMS causes numerous mutations, backcrossing *gas-1* to the Denver-Lab N2 strain would eliminate many of the initial EMS-generated mutations due to recombination.

In most studies employing the *gas-1* fc21 strain, the mutant is obtained from the Caenorhabditis Genetic Center (CGC) without further backcrossing to their lab's N2 strain prior to assays and experimentation (Hartman et al., 2001; Kayser et al., 2003, 2004). Foregoing additional backcrossing, the assumption is that the *gas-1* fc21 strain contains an isolated mutation and lacks any superfluous mutations that may interfere with

interpretation of the experimental results. We demonstrate in our work here, that this assumption is in question.

We tested this prediction by sequencing the *gas-1* strain and identified and characterized all genome-wide genetic differences from the Denver-lab N2 strain (See Materials and Methods). Since the *gas-1* mutation is on the X chromosome, we hypothesized that many EMS-induced mutations on the X chromosome would be linked to the *gas-1* gene and remain after backcrossing to the Denver-Lab N2 strain. Spontaneous single-nucleotide mutations are hypothesized to occur at the rate of 2.7 x 10^{-9} per a generation, approximately two mutations per a generation (Denver et al., 2009). Since we backcrossed the *gas-1* strain to the Denver-Lab N2 strain for ten generations, approximately twenty mutations due to are predicted to occur (Denver et al., 2009).

We discovered a total of eighty-six genetic differences in the *gas-1* strain that are not present in the WS242 reference genome or the Denver-lab N2 strain (including the *gas-1* fc21 mutation in K09A9.5) (Figure 3.4) (Table 3.2). The bulk of the mutations occurred on the X Chromosome (n= 56) with the majority of mutations across all six chromosomes being G:C $\rightarrow$A:T transitions (n= 51) (Table 3.2) (Supplementary Table B1). Statistical tests comparing mutations in the *gas-1* strain to published N2 values determined that the number of mutations located on the X-chromosome as well as the proportion of G:C $\rightarrow$ A:T transitions occurring on the X chromosome were highly significant (P <0.00001, X^2) (Supplementary Tables B1 and B2). Furthermore, the number of G:C $\rightarrow$ A:T transitions genome-wide was also determined to be highly significant (P <0.00001, X^2) (Supplementary Table B3)

As EMS causes alkylation of guanine, over 99% of EMS mutations are predicted to be G:C → A:T transitions (Greene et al., 2003; Kim et al., 2006). Our results in which the majority of mutations in the *gas-1* strain are G:C → A:T transitions indicates that not only does EMS generate significantly more than the one mutation per a genome previously assumed, but also suggests that residual mutations are maintained after extensive backcrossing due to linkage with the *gas-1* mutation. As the *gas-1* strain was not sequenced following acquisition from the CGC prior to backcrossing, we do not know how many mutations were initially present due to EMS but speculate that the number is vastly higher than our observed results following backcrossing.

3.5.2 Identification and characterization of *gas-1* MA line mutations

We identified and characterized all nuclear mutations accumulated during bottlenecking in the *gas-1* MA lines. There were a total of forty mutations in all five lines. Of the forty mutations, thirteen were located in exons, ten were located in introns, and seventeen were intergenic. The number of mutations experienced per a line ranged from five in MA429 to eleven in MA438.

Of the thirteen exon mutations, four were synonymous and nine were non-synonymous. Although the sample size is small and therefore insufficient for dN/dS analysis, the observation that there are twice as many non-synonymous as synonymous mutations is consistent with predictions from the neutral theory of evolution in which approximately 2/3 of non-synonymous mutations and 1/3 of synonymous mutations are expected (Kimura, 1998). Additionally, the ratio of transition to transversion mutations (Ts/Tv) in the *gas-1* MA lines (1.35) is close to Ts/Tv reports on assumed neutral sequences (pseudogenes, intergenic sequences and silent codon positions) in *C. elegans*

natural isolate strains (Denver et al., 2009; Swan et al., 2002; Wicks et al., 2001). The

percentage of exon mutations in the *gas-1* MA lines (32.5%) is slightly less though non-

significantly deviated from N2 MA lines values (37.6%) (Denver et al., 2009).

3.5.3 Mutation rate analysis

Following identification of *gas-1* MA line nuclear mutations, mutation rate was

calculated using the standard equation $\mu_{bs}= m/(LnT)$ from pooled *gas-1* MA lines.

Mutation rate was calculated using the standard equation $\mu_{bs}= m/(LnT)$ (See Materials and

Methods). The mutation rate for *gas-1* MA lines was determined to be 2.13 ($\pm$ 0.34) x 10^{-9}

per a site per a generation. Our observed mutation rate was within two standard errors of

the published N2 strain mutation rate (Denver et al., 2009). Studies employing MA

approaches have determined mutation rate for *Drosophila melanogaster*, *Saccharomyces*

cerevisiae, the fisson yeast *Schizosaccharomyces pombe*, the amoeba *Dictyostelium*

discoidum, and the green algae *Chlamydomas reinhardtii* (Farlow et al., 2015; Keightley

et al., 2009; Ness et al., 2012; Saxer et al., 2012; Zhu et al., 2014). The lowest mutation

rate among these taxa is green algae which has a base-substitution mutation rate of 3.23 x

10^{-10} per a site per a generation. Drosophila melanogaster has the highest among these

organisms with a mutation rate of 3.5 x 10^{-9} per a site per a generation. As ROS decreased

in the *gas-1* MA lines our experiment was unable to access whether or not ROS has an

effect on nuclear mutation rate in *C. elegans* however this data as well as past data on *C.*

elegans suggests that there is much stasis in mutation rate (Denver et al., 2000, 2009).

Although the mutation rate between the *gas-1* MA lines was comprable to

published N2 rates, the conditional rate estimate of G:C $\rightarrow$ A:T transition mutations in the

gas-1 MA lines was significantly elevated in comparison to N2 values (Figure 3.5). 5-

hydroxyuracil, a signiture of ROS-induced DNA damage, is reported to generate G:C →

A:T transition mutations. However assays conducted in Dr. Suzanne Estes' lab at Portland

State University demonstrate ROS decreased in *gas-1* MA lines and the rate of G:C →

T:A transversion mutations, an additional signiture of ROS-induced damage, is within one

SEM of N2 values demonstrating that no significant decrease in the rate of this particular

transversion mutation. Given that nuclear mutation rate in *gas-1* lines was non-

significantly changed from N2 values, our observation of this result suggests three

hypotheses: (1) the *gas-1* strain may exhibit bias to G:C → A:T transition mutations, (2)

this observation may be a consequence of a non-ROS induced mechanism, (3) or this

result is a chance event due to genetic drift. Future experiments which employ the *gas-1*

strain in bottlenecked and non-bottlenecked populations mayprovide help evaluate these

hypotheses.

3.5.4 Putative beneficial nuclear mutations in *gas-1* MA lines

Pooled *gas-1* MA lines were determined to exhibit increased fitness relative to the

gas-1 progenitor strain (assay performed in Suzanne Estes lab at Portland State

University). In particular, *gas-1* MA431 experienced two mutations in intron regions of

genes (*rheb-1* and *daf-2*) that we hypothesized may be generating beneficial effects.

Backcrossing experiments conducted by Dana Howe were performed to isolate the *gas-1*

MA431 *rheb-1* and *daf-2* SNPs and create *gas-1* and N2 progenitor strains harboring each

SNP. However, although we were able to segregate five of the nine *gas-1* MA431 SNPs,

we were unable to isolate the *daf-2, rheb-1*, *sel-2* and C04E12.10 SNPs from one another.

These backcrossing experiments separated the four SNPs (C04E12.10, *sel-2, daf-2,* and

rheb-1) from the other mutations in MA431 and crossed this strain to the wildtype and

gas-1 progenitors. Reproduction in both wildtype and *gas-1* progenitors was improved

with the addition of the four SNPs and ROS significantly decreased in the *gas-1* but not

the N2 progenitor (assays performed in Suzanne Estes lab at Portland State University by

Stephen Christy). These results suggest that the combined effects of these four SNPs

experienced by MA431 may have beneficial effects on fitness and may lead to

compensatory activity for the increased ROS production generated by the *gas-1* mutation.

As *rheb-1*, *daf-2,* and *sel-2* are all located on Chromosome III, it is likely these

genes experience genetic linkage. Located on Chromosome V, the C04E12.10 mutation

may exhibit linkage disequilibrium with one or more of the other three SNPs. It is possible

that an epistatic interaction occurs, and this interaction may be necessary for vitality of the

mutant strain (Figure 3.5). As epistasis may be present between any pair of these SNPs as

well as occurring among multiple SNPs, it is important to consider the effects of these

mutations not only individually but also from an epistatic perspective. Two models of

epistasis are relevant hypotheses here: (1) epistasis between deleterious and beneficial

mutations and, (2) epistasis between mutations that individually impose deleterious effects

(Loewe and Hill, 2010). Model 1, epistasis between a deleterious and beneficial mutation,

refers to a situation in which one mutation is deleterious, the other linked mutation is

beneficial, but the combination of the two has higher beneficial effects than the beneficial

mutation alone. In the case of *gas-1* MA431, it is possible that one or more of the four

mutations are deleterious with the remaining mutations beneficial in isolation and

together, the combination of the four mutations produces a heightened beneficial effect. In

contrast, model 2 occurs when presumed deleterious mutations co-occur. If the mutations

appear together, one may compensate for the other or lead to another local optimum with a

different fitness (Loewe and Hill, 2010). Wright's Shifting Balance Theory of Evolution suggests that this epistatic interaction is common but research has not provided strong evidence for this phenomenon (Coyne et al., 1997, 2000). As we were unable to isolate the four mutations on *gas-1* MA431, both models are a possibility and future studies may determine the isolated versus combinatorial mutation effects.

MA431 contained two non-synonymous exon mutations that we were unable to separate from the intron *daf-2* and *rheb-1* mutations, both non-synonymous mutations. One mutation was located in the *sel-2* gene which replaced an arginine residue with a histidine amino acid; the other was located in C04E12.10 and resulted in substitution of an asparagine residue with a histidine amino acid. SEL-2 is the single *C. elegans* homolog of the human proteins neurobeachin and LRBA (Wang et al., 2001). Research suggests that *sel-2* is involved with endosomal traffic and delivery of cell surface proteins to the lysosome (de Souza et al., 2007). LRBA is upregulated in various human tumor cell lines and has been demonstrated to decrease the sensitivity of cells to apoptosis (Wang et al., 2004). As *gas-1* mutants have increased oxidative stress, the *sel-2* mutation may be modifying apoptosis response to *gas-1* imposed mitochondrial dysfunction although this is speculation and future work is needed to investigate the functional consequences of the *sel-2* mutation (Kayser et al., 1999). As discussed previously, the *sel-2* mutation experienced by MA431 may not be beneficial in isolation.

C04E12.10 is an ortholog of human NGLY1 (N- glycanase 1) (Camon, 2003; Mulder, 2003). NGLY1 is a deglycosylating enzyme that has been demonstrated to be involved in the endoplasmic-reticulum (ER)-associated degradation (ERAD) process (Huang et al., 2015). The exact role of this enzyme is still not understood in detail

although a study on mouse embryonic fibroblast cells reported that elimination of *Ngly1*

causes dysregulation in the ERAD process as shown by delayed degradation and errant

deglycosylation (Huang et al., 2015). As activity of NGLY1 is suggested to have critical

roles in proper folding of glycoproteins, it is possible that the *gas-1* MA431 C04E12.10

SNP modifies ER protein folding activity in *gas-1* worms (Hirsch et al., 2003).

The exact mechanism for improved fitness and mitochondrial function in MA431

is unknown but past studies on *daf-2* mutants and the *rheb-1* gene in *C. elegans* may

provide insights on the pathways affected and consequences for organismal homeostasis.

Past research has elucidated the role of *daf-2* in *C. elegans* (Chen et al., 2015; Halaschek-

Wiener, 2005; Hu et al., 2015; Kondo et al., 2005). *daf-2* codes an integral protein in the

PI 3-kinase/Akt pathway in addition to key activities modulating mitochondrial function

and oxidative-stress response (Brys et al., 2010; Depuydt et al., 2016; Kondo et al., 2005).

The *daf-2* gene encodes the single insulin/insulin growth factor-1 like (IGF) receptor in *C.*

elegans (Chen et al., 2015). The activated DAF-2 insulin/IGF-1-like receptor triggers

downstream kinases which phosphorylate a FOXO transcription factor encoded by *daf-16*

(Figure 3.2)*.*

When DAF-16 protein is phosphorylated it is sequestered in the cytoplasm where it

remains inactive. Reduction or loss-of-function of insulin/insulin growth factor-1-like

signaling (IIS) due to mutation in the *daf-2* gene relocates DAF-16 to the nucleus where it

triggers a genetic program for life extension (Brys et al., 2010). Moreover, *daf-2* loss-of-

function mutants exhibit enhanced resistance to oxidative and thermal stress, most likely

by activating various superoxide dismutase and heat-inducible genes (Honda and Honda,

1999, 2002; Hsu et al., 2003; Lithgow et al., 1995). In addition to exhibiting a lifespan

approximately twice as long as wildtype, the *e1370* mutant allele of *daf-2* has several

defining phenotypes including slender adults, reduced brood size, resistance to hypoxia

and enhanced autophagy (Brys et al., 2010; Kenyon, 2011). Autophagy has been shown to

be essential for lifespan extension of *daf-2* mutants and research suggests that increased

autophagy is accomplished through modification of protein turnover (Depuydt et al., 2016;

Hansen et al., 2008; Meléndez et al., 2003).

A second putative beneficial mutation was observed in the *rheb-1* gene which

encodes the RHEB-1 protein, a central component of the TOR pathway in addition to

playing a fundamental role in the UPR[mt] in *C. elegans* (Martin et al., 2014; Melser et al.,

2013). TOR, originally identified in the budding yeast *Saccharomyces cerevisiase*, is a

highly conserved serine-threonine kinase that plays an important role in cell growth,

autophagy, metabolism in response to growth factors, and energy stress (Groenewoud and

Zwartkruis, 2013; Martin and Hall, 2005). The mammalian TOR signaling pathway

(mTOR), is initiated by a cascade of growth factors which signal to mTORC1 through the

phosphoinositide 3-kinase / protein kinase B (PI3K/PKB) pathway (Martin and Hall,

2005). Phosphorylation of phosphatidylinositol-(4,5)-biphosphate (PIP2) activated by

PI3K generates phosphatidylinositol-(3,4,5)-triphosphate (PIP3) at the plasma membrane

and initiates activation of phosphoinositide-dependent kinase-1 (PDK1) which recruits

PKB to the plasma membrane and inactivates tuberous sclerosis complex 1/2

(TSC1/TSC2) (Groenewoud and Zwartkruis, 2013). Phosphorylation of TSC2 prevents

TSC1/TSC2 complex formation and drives the activation of a GTPase termed Rheb (Ras

homolog enriched in brain) into the GTP-bound active state (Pópulo et al., 2012). Rheb

activates mTORC1. mTORC1 phosphorylates and activates a downstream signaling

cascade that ultimately inhibits autophagy, leads to mRNA translation and subsequent protein biogenesis, activates aerobic glycolysis, and initiates lipid and nucleotide synthesis (Laplante and Sabatini, 2012).

In addition to a key role in TOR signaling, Rheb is also involved in the UPR[mt] in both mammalians and *C. elegans* (Groenewoud and Zwartkruis, 2013). A recent study demonstrated that when mammalian cells are shifted from glucose-containing medium to glucose-free medium with glutamine, there is a subsequent shift from glycolysis to OXPHOS (Melser et al., 2013). This shift occurs without a modification of mitochondrial mass and is accompanied by a selective increase in mitochondrial protein turnover. When Rheb is transiently overexpressed a reduction in mitochondrial mass is observed in both mediums. This results demonstrates that increased OXPHOS leads to a Rheb-mediated mitochondrial biogenesis that prevents accumulation of damaged mitochondria (Melser et al., 2013).

Like DAF-2, RHEB-1 in *C. elegans* also leads to downstream signaling that inhibits detoxification and lipolysis pathways (Figure 3.1) (Lapierre and Hansen, 2012). Knockdown of *rheb-1* through RNAi in *C. elegans* extends lifespan by mimicking caloric-restriction effects (Honjoh et al., 2009). Interestingly, though caloric restriction has been shown to extend lifespan in wide range of taxa, its effects on long-lived species such as primates, remains controversial (Di Francesco and De Cabo, 2015; Solon-Biet et al., 2015). In *C. elegans* there is a single Rheb orthologue, *rheb-1* (Li et al., 2004). *rheb-1* not only mimics caloric-restriction in *C. elegans* but also has effects on longevity by exerting effects on the IGF-like signaling effector DAF-16 (Honjoh et al., 2009). *rheb-1* has also been shown to modulate an adaptive response to transient hypoxia exposure and extend

lifespan in *C. elegans* through mitochondrial ROS-dependent regulation of the activation

of the kinase TOR. Given the wide range and critical roles of *daf-2* and *rheb-1* in protein

homeostasis, mitochondrial function and IGF-like signaling, it is possible that these two

mutations are interacting with one another. Although not explored in this experiment, the

intron mutations in *daf-2* and *rheb-1* may be modifying expression levels, leading to

alternative splicing, or changing developmental onset of gene transcription. Further work

applying RNA-sequencing would be useful to discern these possibilities.

The observation that these mutations are beneficial was not what we predicted, as

bottlenecking frequently lowers organismal fitness (Andersson and Hughes, 1996; Chao,

1990; Zeyl et al., 2001). It is argued that in MA approaches the majority of new mutations

that accumulate within the population are deleterious leading to mutationally degraded

genomes (Bataillon, 2000). In contrast to large populations where beneficial mutations are

frequently fixed and deleterious mutations are only fixed if they impose a small cost or

through genetic hitchhiking; in small populations, beneficial mutations may be frequently

lost due to genetic drift (Silander et al., 2007). Furthermore, in a small population,

slightly deleterious mutations will behave as if they were neutral because their fate is

governed by drift instead of selection leading to a proportion of these detrimental

mutations fixing in the population by chance (Bromham, 2009). Therefore, whether fitness

is improved or impaired in a population of a given size is dependent on the relative rates

of beneficial and deleterious mutation and the magnitude of their effect on fitness within

the population context (Silander et al., 2007).

Muller's ratchet, the loss of the individuals with the smallest number of deleterious

mutations, is predicted to occur in small populations due to lack of selection leading to

mutational decay and an ever-increasing deleterious mutational load (Howe and Denver,

2008; Neher and Shraiman, 2012). Over time, this process may lead to extinction which

will be accelerated when the population size is small and deleterious mutations fix at a

high rate (Neher and Shraiman, 2012). We did observe extinction in five of the forty-eight

biological *gas-1* MA line replicates. The five *gas-1* MA lines experiencing extinction

(MA400, MA403, MA404, MA423 and MA432) went extinct between generation twenty

and generation thirty-seven. However, the large majority of *gas-1* MA line replicates did

not experience extinction and we observed beneficial mutations in at least one of the five

gas-1 MA lines bioinformatically analyzed. Moreover, fitness (fecundity) assays pooling

reproductive production in the *gas-1* MA lines determined a significant increase in

fecundity relative to the *gas-1* progenitor (assays performed in Suzanne Estes lab at

Portland State University).

Small population sizes are not only subject to extreme genetic drift, but also

predicted to have lower fixation rates of beneficial mutations overall as the majority of

mutations are generally assumed to be neutral or slightly deleterious (Bataillon, 2003;

Eyre-Walker and Keightley, 1999; Whitlock, 2000). Beneficial mutations under

bottlenecking, although thought to be are rare, have been observed in past studies (Baer et

al., 2005; Howe and Denver, 2008; Rutter et al., 2012, 2012; Wang et al., 2014). A study

conducted on *Arabidopsis thaliana* MA lines observed that the five sequenced MA lines

frequently outperformed the progenitor under an assortment of conditions (Rutter et al.,

2012). Additional research has also detected a moderate to high rate of beneficial

mutations- up to 15% in viruses, 13% in yeast and a significant number in *D.*

melagnogaster (Azad et al., 2010; Burch and Chao, 1999; Hall and Joseph, 2010; Hall et al., 2008; Silander et al., 2007).

One explanation for the proportion of beneficial mutations is the relative fitness of the ancestral strain employed to propagate MA lines. If the ancestral strain is far from the fitness optimum, a larger proportion of beneficial mutations is predicted under Fisher's geometric model (Fisher, 1930). Considering the undesirable effects imposed by the *gas-1* mutation including decreased brood size, reduced lifespan and increased ROS production coupled to decreased ATP output, the *gas-1* progenitor exhibited significantly decreased fitness relative to the N2-wildtype strain (Kayser et al., 1999b, 2001a; Pujol et al., 2013)

Moreover, it is possible that many deleterious mutations would lead to lethality and/or sterility in *gas-1* worms. Lethal mutations, often overlooked in MA experiments, may be exposed to selection, even in an MA framework (Hall and Joseph, 2010). As our experimental approaches required a living, reproducing worm to propagate the next generation, we may have possibly negated many lethal and sterile mutations in *gas-1* MA lines that did not experience extinction. *gas-1* worms exhibit reduced fitness and lifespan relative to wildtype nematodes, and therefore it is likely that deleterious mutations with lethal and sterile effects would not be maintained (Kayser et al., 2001a). Due to these requirements for propagating MA lines our experimental approach would eliminate the inclusion of deleterious mutations with lethal and sterile consequences in all lines that did not experience extinction.

This phenomena of obviating severely deleterious and lethal mutations is also predicted by Kimura's single site mutation-selection-drift analysis which demonstrated that deleterious mutations with effects beyond a particular threshold have no realistic

chance of getting fixed (Kimura, 1984). Therefore, *gas-1* nematodes, while impaired in mitochondrial function and compromised in organismal fitness, may have much greater potential to improve through beneficial mutations than undergo exacerbation of harmful effects imposed by deleterious mutations as even slightly deleterious mutations may have severe consequences on fitness.

3.5.5 Interaction analysis of nuclear genes experiencing *gas-1* MA mutations

Gene Orienteer was applied to evaluate the predicted interactions of all genes in which *gas-1* and N2 MA line mutations were located. Gene Orienteer employs a serial logistic regression model that analyzes five types of data from three model organisms to predict gene interactions (Zhong and Sternberg, 2006) (See Materials and Methods). Mutations residing in genes with available interactome data were evaluated for interactions with 2-degrees of the *gas-1* gene. The observed results of the *gas-1* MA lines were significantly different than predicted simulation values suggesting that compensatory evolution may have occurred during bottlenecking.

Our observed number of mutations in the *gas-1* MA lines (n=6) that interacted within 2-degrees of the *gas-1* gene was just under three standard deviations beyond our simulated mutation results. A statistical analysis determined this outcome to be significantly different from predicted values of random mutation simulation (P= 0.027, X^2 Test). In contrast, our observed number of mutations in the N2 MA lines that interacted within 2-degrees of the *gas-1* gene (n=11) was within one standard-deviation of our simulated mutation results. A statistical test determined the N2 MA line results was not significantly different than simulation predicted values (P=0.13, X^2 Test). While our results of mutation in the N2 MA lines was achieved or surpassed by 247 out of one-

thousand iterations, only five out of one-thousand iterations was equal or greater to our observed results in the *gas-1* MA lines. The results of one-thousand iterations of random mutation generation for the N2 MA lines and *gas-1* MA lines imply that the nuclear mutations observed in *gas-1* MA lines were most likely in response to the *gas-1* mutation and not due to chance.

The six genes experiencing a mutation in the *gas-1* MA lines that interacted within 2-degrees of the *gas-1* gene are: ZC8.6, *rheb-1*, *daf-2*, *sel-2*, *smf-3*, and *alh-2*. *alh-2* directly interacts with the *gas-1* gene (Zhong and Sternberg, 2006). *alh-2* is an aldehyde dehydrogenase and acts to degrade and detoxify xenobiotic substances and has oxidation-reduction activity (Erkut et al., 2013; Patananan et al., 2015). As the mutation in the *alh-2* gene was non-synonymous (Table 3.4), it is probable that the mutation affects oxidative-reduction efficiency. Functional assays would be useful in order to access the consequences of the *alh-2* mutation experienced by *gas-1* MA438 on ROS and ATP production.

smf-3 experienced a change in an intron sequence in *gas-1* MA438 (Table 3.4). Past research has suggested that deletion of *smf-3* increases tolerance to manganese (Au et al., 2009). Despite being essential for metabolic functions, in high concentrations, manganese can be toxic and may cause extrapyramidal syndrome which resembles idiopathic Parkinson's disease (Au et al., 2009). SMF-3 is the main manganese uptake transporter in *C. elegans* with SMF-1/2 having minor and ancillary roles (Vanduyn et al., 2013). SMF-3 has interactions with many superoxide dismutase (SOD) genes including SOD-1, SOD-2, SOD-3, and SOD-5 indicating that *smf-3* may play a key role in modulating oxidative stress response (Reddi et al., 2009; Zhong and Sternberg, 2006). The

mutation experienced in MA438 in the *smf-3* gene may have effects on ROS production. Future work measuring ROS output and assessing mitochondrial function is necessary to discern the exact consequence of the *smf-3* gene mutation within the context of the *gas-1* mutation.

ZC8.6 is not characterized in detail although it is predicted to interact with two genes that interact with *gas-1*: *vps-34* and *acl-3* (Zhong and Sternberg, 2006). VPS34 forms a complex with ATG6 and is required for the nucleation and assembly of the autophagosome membrane (Kovacs and Zhang, 2010). ACL-3 is a predicted mitochondrial protein that has a key role in triacylglycerol metabolism (Zhang et al., 2013). *gas-1* MA412 experienced a synonymous mutation in an exon region of ZC8.6 and thus, the mutation in ZC8.6 may not have functional consequences (Table 3.4).

Three of the six *gas-1* MA line SNPs exhibiting interactions within the *gas-1-*centric-interactome (*daf-2, rheb-1*, and *sel-2*) were observed to occur in *gas-1* MA431. Both *rheb-1* and *daf-2* are predicted to exhibit numerous interactions with genes located in the *gas-1*-centric-interactome. *rheb-1* is predicted to interact with nine genes that likely interact with *gas-1* and *daf-2* is predicted to interact with twenty-one genes that may directly interact with *gas-1*. In contrast, *sel-2* interacts with only gene that interacts with *gas-1* (*hda-1*).

These three SNPs along with an additional SNP not predicted to have interactions within two-degrees of *gas-1* (C04E12.10), have been crossed to the *gas-1* and N2 progenitor strain. Results on fecundity and ROS assays (conducted in Dr. Suzanne Estes' lab at Portland State University) suggest these SNPs may have beneficial consequences on organismal fitness and/or compensatory effects on ROS production for *gas-1* worms. For

more information on *sel-2, daf-2* and *rheb-1* activity in *C. elegans* please refer to discussion section 3.5.4 detailing putative beneficial mutations in *gas-1* MA lines.

3.6 Conclusion

This study reveals insights into the dynamics of beneficial mutations under bottlenecking and ameliorating mitochondrial dysfunction through nuclear mutations. Our investigation across many generations of experimental evolutional provided insights into how nuclear genome evolution differs when predisposed to mitochondrial dysfunction and the potential fitness landscape for mutation in *gas-1* MA lines. Specific nuclear mutations in the *gas-1* MA lines may have been in response to the initial *gas-1* mutation. In addition, the improved fitness of MA431 and the *gas-1* and N2 progenitors with the four SNPs, may suggest that the C04E12.10, *rheb-1*, *daf-2*, and *sel-2* mutations are beneficial in *C. elegans* and furthermore suggest that these nuclear mutations may have potential for ameliorating mitochondrial function, specifically Complex I impairment. Moreover, this work reveals that modified activity of the general TOR and IGF-1 pathways may have beneficial effects on diseases and pathologies involving Complex I impairment. It would be ideal to isolate the four genes and then create the single, double-mutant and triple-mutant combination strains and compare the results on fitness and mitochondrial ROS production to the quadruple-mutant strain employed in this study.

3.7 References

Addo, M. G., Cossard, R., Pichard, D., Obiri-Danso, K., Rötig, A., and Delahodde, A. (2010). Caenorhabditis elegans, a pluricellular model organism to screen new genes involved in mitochondrial genome maintenance. *Biochim. Biophys. Acta* 1802, 765–773. doi:10.1016/j.bbadis.2010.05.007.

Amos, W., and Harwood, J. (1998). Factors affecting levels of genetic diversity in natural populations. *Philos. Trans. R. Soc. B Biol. Sci.* 353, 177–186. doi:10.1098/rstb.1998.0200.

Andersson, D. I., and Hughes, D. (1996). Muller's ratchet decreases fitness of a DNA-based microbe. *Proc Natl Acad Sci U S A* 93, 906–907. doi:10.1073/pnas.93.2.906.

Au, C., Benedetto, A., Anderson, J., Labrousse, A., Erikson, K., Ewbank, J. J., et al. (2009). SMF-1, SMF-2 and SMF-3 DMT1 orthologues regulate and are regulated differentially by manganese levels in C. elegans. *PLoS One* 4. doi:10.1371/journal.pone.0007792.

Azad, P., Zhang, M., and Woodruff, R. C. (2010). Rapid increase in viability due to new beneficial mutations in Drosophila melanogaster. *Genetica* 138, 251–263. doi:10.1007/s10709-009-9418-3.

Baer, C. F., Shaw, F., Steding, C., Baumgartner, M., Hawkins, A., Houppert, A., et al. (2005a. Comparative evolutionary genetics of spontaneous mutations affecting fitness in rhabditid nematodes. *Proc. Natl. Acad. Sci.* 102, 5785–5790. doi:10.1073/pnas.0406056102.

Bataillon, T. (2000). Estimation of spontaneous genome-wide mutation rate parameters: whither beneficial mutations? *Heredity (Edinb).* 84, 497–501. doi:10.1046/j.1365-2540.2000.00727.x.

Bataillon, T. (2003). Shaking the "deleterious mutations" dogma? *Trends Ecol. Evol.* 18, 315–317. doi:10.1016/S0169-5347(03)00128-9.

Bergstrom, C. T., and Pritchard, J. (1998). Germline bottlenecks and the evolutionary maintenance of mitochondrial genomes. *Genetics* 149, 2135–2146.

Bratic, I., Hench, J., and Trifunovic, A. (2010). Caenorhabditis elegans as a model system for mtDNA replication defects. *Methods* 51, 437–443. doi:10.1016/j.ymeth.2010.03.003.

Brenner, S. (1974). The genetics of Caenorhabditis elegans. *Genetics* 77, 71–94. doi:10.1002/cbic.200300625.

Bromham, L. (2009). Does nothing in evolution make sense except in the light of population genetics? *Biol. Philos.* 24, 387–403. doi:10.1007/s10539-008-9146-6.

Brys, K., Castelein, N., Matthijssens, F., Vanfleteren, J. R., and Braeckman, B. P. (2010). Disruption of insulin signalling preserves bioenergetic competence of mitochondria in ageing Caenorhabditis elegans. *BMC Biol.* 8, 91. doi:10.1186/1741-7007-8-91.

Burch, C. L., and Chao, L. (1999). Evolution by small steps and rugged landscapes in the RNA virus ??6. *Genetics* 151, 921–927.

Butow, R. A., and Avadhani, N. G. (2004). Mitochondrial signaling: The retrograde response. *Mol. Cell* 14, 1–15. doi:10.1016/S1097-2765(04)00179-0.

Cai, X., Bao, L., Ren, J., Li, Y., and Zhang, Z. (2016). Grape seed procyanidin B2 protects podocytes from high glucose-induced mitochondrial dysfunction and apoptosis via the AMPK-SIRT1-PGC-1α axis in vitro. *Food Funct.* 7, 805–15. doi:10.1039/c5fo01062d.

Camon, E. (2003). The Gene Ontology Annotation (GOA) Project: Implementation of GO in SWISS-PROT, TrEMBL, and InterPro. *Genome Res.* 13, 662–672. doi:10.1101/gr.461403.

Chao, L. (1990). Fitness of RNA virus decreased by Muller's ratchet. *Nature* 348, 454–455. doi:10.1038/348454a0.

Chasnov, J. R., and Chow, K. L. (2002). Why are there males in the hermaphroditic species Caenorhabditis elegans? *Genetics* 160, 983–994.

Chen, A. T. Y., Guo, C., Itani, O. A., Budaitis, B. G., Williams, T. W., Hopkins, C. E., et al. (2015). Longevity genes revealed by integrative analysis of isoform-specific daf-16/FoxO mutants of caenorhabditis elegans. *Genetics* 201, 613–629. doi:10.1534/genetics.115.177998.

Coyne, J. A., Barton, N. H., and Turelli, M. (1997). Perspective: A Critique of Sewall Wright's Shifting Balance Theory of Evolution. *Evolution (N. Y).* 51, 643. doi:10.2307/2411143.

Coyne, J., Barton, N., and Turelli, M. (2000). Is Wright's shifting balance process important in evolution? *Evolution (N. Y).* 54, 306–317. doi:10.1554/0014-3820(2000)054[0306:iwssbp]2.0.co;2.

Dancy, B. M., Sedensky, M. M., and Morgan, P. G. (2015). Mitochondrial bioenergetics and disease in Caenorhabditis elegans. *Front. Biosci. (Landmark Ed.* 20, 198–228. doi:10.2741/4305.

Denver, D. R., Dolan, P. C., Wilhelm, L. J., Sung, W., Lucas-Lledo, J. I., Howe, D. K., et al. (2009a. A genome-wide view of Caenorhabditis elegans base-substitution mutation processes. *Proc. Natl. Acad. Sci.* 106, 16310–16314. doi:10.1073/pnas.0904895106.

Denver, D. R., Morris, K., Lynch, M., Vassilieva, L. L., and Thomas, W. K. (2000). High direct estimate of the mutation rate in the mitochondrial genome of Caenorhabditis elegans. *Science* 289, 2342–2344. doi:10.1126/science.289.5488.2342.

Denver, D. R., Wilhelm, L. J., Howe, D. K., Gafner, K., Dolan, P. C., and Baer, C. F. (2012). Variation in base-substitution mutation in experimental and natural lineages of caenorhabditis nematodes. *Genome Biol. Evol.* 4, 513–522. doi:10.1093/gbe/evs028.

Depuydt, G., Shanmugam, N., Rasulova, M., Dhondt, I., and Bart, P. (2016). Increased Protein Stability and Decreased Protein Turnover in the Caenorhabditis elegans Ins / IGF-1 daf-2 Mutant. 00, 1–8. doi:10.1093/gerona/glv221.

Dingley, S., Polyak, E., Lightfoot, R., Ostrovsky, J., Rao, M., Greco, T., et al. (2010). Mitochondrial respiratory chain dysfunction variably increases oxidant stress in Caenorhabditis elegans. *Mitochondrion* 10, 125–136. doi:10.1016/j.mito.2009.11.003.

Erkut, C., Vasilj, A., Boland, S., Habermann, B., Shevchenko, A., and Kurzchalia, T. V. (2013). Molecular Strategies of the Caenorhabditis elegans Dauer Larva to Survive Extreme Desiccation. *PLoS One* 8, e82473. doi:10.1371/journal.pone.0082473.

Eyre-Walker, a, and Keightley, P. D. (1999). High genomic deleterious mutation rates in hominids. *Nature* 397, 344–347. doi:10.1038/16915.

Farlow, A., Long, H., Arnoux, S., Sung, W., Doak, T. G., Nordborg, M., et al. (2015). The spontaneous mutation rate in the fission yeast Schizosaccharomyces pombe. *Genetics* 201, 737–744. doi:10.1534/genetics.115.177329.

Fisher, R. A. (1930). *The genetical theory of natural selection*. Oxford, United Kingdom: Oxfors University Press.

Di Francesco, A., and De Cabo, R. (2015). Two-year trial of human caloric restriction. *Journals Gerontol. - Ser. A Biol. Sci. Med. Sci.* 70, 1095–1096. doi:10.1093/gerona/glv100.

Greene, E. A., Codomo, C. A., Taylor, N. E., Henikoff, J. G., Till, B. J., Reynolds, S. H., et al. (2003). Spectrum of chemically induced mutations from a large-scale reverse-genetic screen in Arabidopsis. *Genetics* 164, 731–740.

Groenewoud, M. J., and Zwartkruis, F. J. T. (2013). Rheb and mammalian target of rapamycin in mitochondrial homoeostasis. *Open Biol.* 3, 130185–130185. doi:10.1098/rsob.130185.

Guha, M., and Avadhani, N. G. (2013). Mitochondrial retrograde signaling at the crossroads of tumor bioenergetics, genetics and epigenetics. *Mitochondrion* 13, 577–591. doi:10.1016/j.mito.2013.08.007.

Halaschek-Wiener, J. (2005). Analysis of long-lived C. elegans daf-2 mutants using serial analysis of gene expression. *Genome Res.* 15, 603–615. doi:10.1101/gr.3274805.

Hall, D. W., and Joseph, S. B. (2010). A high frequency of beneficial mutations across multiple fitness components in Saccharomyces cerevisiae. *Genetics* 185, 1397–1409. doi:10.1534/genetics.110.118307.

Hall, D. W., Mahmoudizad, R., Hurd, A. W., and Joseph, S. B. (2008). Spontaneous mutations in diploid Saccharomyces cerevisiae: another thousand cell generations. *Genet. Res. (Camb).* 90, 229–241. doi:10.1017/S001667230900024X.

Hansen, M., Chandra, A., Mitic, L. L., Onken, B., Driscoll, M., and Kenyon, C. (2008). A role for autophagy in the extension of lifespan by dietary restriction in C. elegans. *PLoS Genet.* 4. doi:10.1371/journal.pgen.0040024.

Hartman, P. S., Ishii, N., Kayser, E. B., Morgan, P. G., and Sedensky, M. M. (2001). Mitochondrial mutations differentially affect aging, mutability and anesthetic sensitivity in Caenorhabditis elegans. *Mech. Ageing Dev.* 122, 1187–1201. doi:10.1016/S0047-6374(01)00259-7.

Hirsch, C., Blom, D., and Ploegh, H. L. (2003). A role for N-glycanase in the cytosolic turnover of glycoproteins. *EMBO J.* 22, 1036–1046. doi:10.1093/emboj/cdg107.

Honda, Y., and Honda, S. (1999). The daf-2 gene network for longevity regulates oxidative stress resistance and Mn-superoxide dismutase gene expression in Caenorhabditis elegans. *FASEB J.* 13, 1385–1393.

Honda, Y., and Honda, S. (2002). Oxidative stress and life span determination in the nematode Caenorhabditis elegans. *Ann.N.Y.Acad.Sci.* 959, 466–474. Available at: http://www.ncbi.nlm.nih.gov/entrez/query.fcgi?cmd=Retrieve&db=PubMed&dopt=Citation&list_uids=11976220.

Honjoh, S., Yamamoto, T., Uno, M., and Nishida, E. (2009). Signalling through RHEB-1 mediates intermittent fasting-induced longevity in C. elegans. *Nature* 457, 726–730. doi:10.1038/nature07583.

Howe, D. K., Baer, C. F., and Denver, D. R. (2010). High rate of large deletions in Caenorhabditis briggsae mitochondrial genome mutation processes. *Genome Biol. Evol.* 2, 29–38. doi:10.1093/gbe/evp055.

Howe, D. K., and Denver, D. R. (2008). Muller's Ratchet and compensatory mutation in Caenorhabditis briggsae mitochondrial genome evolution. *BMC Evol. Biol.* 8, 62. doi:10.1186/1471-2148-8-62.

Hsu, A.-L., Murphy, C. T., and Kenyon, C. (2003). Regulation of Aging and Age-Related Disease by DAF-16 and Heat-Shock Factor. *Science (80-.).* 300, 1142–1145. doi:10.1126/science.1083701.

Hu, J.-P., Xu, X.-Y., Huang, L.-Y., Wang, L., and Fang, N.-Y. (2015). Freeze–thaw Caenorhabditis elegans freeze–thaw stress response is regulated by the insulin/IGF-1 receptor daf-2. *BMC Genet.* 16, 139. doi:10.1186/s12863-015-0298-5.

Huang, C., Harada, Y., Hosomi, A., Masahara-Negishi, Y., Seino, J., Fujihira, H., et al. (2015). Endo-β-N-acetylglucosaminidase forms N-GlcNAc protein aggregates during ER-associated degradation in Ngly1-defective cells. *Proc. Natl. Acad. Sci.*, 201414593. doi:10.1073/pnas.1414593112.

Iser, W. B., and Wolkow, C. A. (2007). DAF-2/Insulin-Like Signaling in C. elegans Modifies Effects of Dietary Restriction and Nutrient Stress on Aging, Stress and Growth. *PLoS One* 2, e1240. doi:10.1371/journal.pone.0001240.

Johri, A., and Beal, M. F. (2012). Mitochondrial dysfunction in neurodegenerative diseases. *J. Pharmacol. Exp. Ther.* 342, 619–630. doi:10.1124/jpet.112.192138.

Kayser, E. B., Morgan, P. G., Hoppel, C. L., and Sedensky, M. M. (2001). Mitochondrial expression and function of GAS-1 in Caenorhabditis elegans. *J. Biol. Chem.* 276, 20551–20558. doi:10.1074/jbc.M011066200.

Kayser, E. B., Sedensky, M. M., and Morgan, P. G. (2004a). The effects of complex I function and oxidative damage on lifespan and anesthetic sensitivity in Caenorhabditis elegans. *Mech. Ageing Dev.* 125, 455–464. doi:10.1016/j.mad.2004.04.002.

Kayser, E.-B., Hoppel, C. L., Morgan, P. G., and Sedensky, M. M. (2003). A mutation in mitochondrial complex I increases ethanol sensitivity in Caenorhabditis elegans. *Alcohol. Clin. Exp. Res.* 27, 584–92. doi:10.1097/01.ALC.0000060524.62805.D2.

Kayser, E.-B., Morgan, P. G., and Sedensky, M. M. (1999). GAS-1. *Anesthesiology* 90, 545–554. doi:10.1097/00000542-199902000-00031.

Kayser, E.-B., Sedensky, M. M., and Morgan, P. G. (2004b). The effects of complex I function and oxidative damage on lifespan and anesthetic sensitivity in Caenorhabditis elegans. *Mech. Ageing Dev.* 125, 455–464. doi:10.1016/j.mad.2004.04.002.

Keightley, P. D., Trivedi, U., Thomson, M., Oliver, F., Kumar, S., and Blaxter, M. L. (2009). Analysis of the genome sequences of three Drosophila melanogaster spontaneous mutation accumulation lines. *Genome Res.* 19, 1195–1201. doi:10.1101/gr.091231.109.

Kenyon, C. (2011). The first long-lived mutants: discovery of the insulin/IGF-1 pathway for ageing. *Philos. Trans. R. Soc. B Biol. Sci.* 366, 9–16. doi:10.1098/rstb.2010.0276.

Kim, Y., Schumaker, K. S., and Zhu, J.-K. (2006). EMS mutagenesis of Arabidopsis. *Methods Mol. Biol.* 323, 101–103. doi:10.1101/pdb.prot4621.

Kimura, M. (1984). *The neutral theory of molecular evolution.* doi:http://dx.doi.org/10.1017/CBO9780511623486.

Kondo, M., Senoo-Matsuda, N., Yanase, S., Ishii, T., Hartman, P. S., and Ishii, N. (2005). Effect of oxidative stress on translocation of DAF-16 in oxygen-sensitive mutants, mev-1 and gas-1 of Caenorhabditis elegans. *Mech. Ageing Dev.* 126, 637–641. doi:10.1016/j.mad.2004.11.011.

Kondrashov, A. S. (1988). Deleterious mutations and the evolution of sexual reproduction. *Nature* 336, 435–440. doi:10.1038/336435a0.

Kovacs, A. L., and Zhang, H. (2010). Role of autophagy in Caenorhabditis elegans. *FEBS Lett.* 584, 1335–1341. doi:10.1016/j.febslet.2010.02.002.

Lapierre, L. R., and Hansen, M. (2012). Lessons from C. elegans: Signaling pathways for longevity. *Trends Endocrinol. Metab.* 23, 637–644. doi:10.1016/j.tem.2012.07.007.

Laplante, M., and Sabatini, D. M. (2012). mTOR Signaling in Growth Control and Disease. *Cell* 149, 274–293. doi:10.1016/j.cell.2012.03.017.

Li, Y., Inoki, K., and Guan, K.-L. (2004). Biochemical and Functional Characterizations of Small GTPase Rheb and TSC2 GAP Activity. *Mol. Cell. Biol.* 24, 7965–7975. doi:10.1128/MCB.24.18.7965-7975.2004.

Lithgow, G. J., White, T. M., Melov, S., and Johnson, T. E. (1995). Thermotolerance and extended life-span conferred by single-gene mutations and induced by thermal stress. *Proc. Natl. Acad. Sci. U. S. A.* 92, 7540–7544. doi:10.1073/pnas.92.16.7540.

Loewe, L., and Hill, W. G. (2010). The population genetics of mutations: good, bad and indifferent. *Philos. Trans. R. Soc. B Biol. Sci.* 365, 1153–1167. doi:10.1098/rstb.2009.0317.

Lynch, M., Blanchard, J., Houle, D., Kibota, T., Schultz, S., Vassilieva, L., et al. (1999). Perspective: Spontaneous Deleterious Mutation. *Evolution (N. Y).* 53, 645. doi:10.2307/2640707.

Martin, D. E., and Hall, M. N. (2005). The expanding TOR signaling network. *Curr. Opin. Cell Biol.* 17, 158–166. doi:10.1016/j.ceb.2005.02.008.

Martin, T. D., Chen, X. W., Kaplan, R. E. W., Saltiel, A. R., Walker, C. L., Reiner, D. J., et al. (2014). Ral and Rheb GTPase Activating Proteins Integrate mTOR and GTPase Signaling in Aging, Autophagy, and Tumor Cell Invasion. *Mol. Cell* 53, 209–220. doi:10.1016/j.molcel.2013.12.004.

Meléndez, A., Tallóczy, Z., Seaman, M., Eskelinen, E.-L., Hall, D. H., and Levine, B. (2003). Autophagy genes are essential for dauer development and life-span extension in C. elegans. *Science* 301, 1387–91. doi:10.1126/science.1087782.

Melser, S., Chatelain, E. H., Lavie, J., Mahfouf, W., Jose, C., Obre, E., et al. (2013). Rheb regulates mitophagy induced by mitochondrial energetic status. *Cell Metab.* 17, 719–730. doi:10.1016/j.cmet.2013.03.014.

Michelakis, E. D. (2008). Mitochondrial medicine: A new era in medicine opens new windows and brings new challenges. *Circulation* 117, 2431–2434. doi:10.1161/CIRCULATIONAHA.108.775163.

Moreira, P. I., Carvalho, C., Zhu, X., Smith, M. A., and Perry, G. (2010). Mitochondrial dysfunction is a trigger of Alzheimer's disease pathophysiology. *Biochim. Biophys. Acta - Mol. Basis Dis.* 1802, 2–10. doi:10.1016/j.bbadis.2009.10.006.

Morgan, P. G., and Sedensky, M. M. (1994). Mutations conferring new patterns of sensitivity to volatile anesthetics in Caenorhabditis elegans. *Anesthesiology* 81, 888–898. Available at: http://www.ncbi.nlm.nih.gov/entrez/query.fcgi?cmd=Retrieve&db=PubMed&dopt=Citation&list_uids=7943840.

Mukai, T. (1964). THE GENETIC STRUCTURE OF NATURAL POPULATIONS OF DROSOPHILA MELANOGASTER. I. SPONTANEOUS MUTATION RATE OF POLYGENES CONTROLLING VIABILITY. *Genetics* 50, 1–19.

Mulder, N. J. (2003). The InterPro Database, 2003 brings increased coverage and new features. *Nucleic Acids Res.* 31, 315–318. doi:10.1093/nar/gkg046.

Muller, H. J. (1964). The relation of recombination to mutational advance. *Mutat. Res.* 106, 2–9. Available at: http://www.ncbi.nlm.nih.gov/pubmed/14195748.

Munkacsy, E., and Rea, S. L. (2014). The paradox of mitochondrial dysfunction and extended longevity. *Exp. Gerontol.* 56, 221–233. doi:10.1016/j.exger.2014.03.016.

Neher, R. A., and Shraiman, B. I. (2012). Fluctuations of Fitness Distributions and the Rate of Muller's Ratchet. *Genetics* 191, 1283–1293. doi:10.1534/genetics.112.141325.

Ness, R. W., Morgan, A. D., Colegrave, N., and Keightley, P. D. (2012). Estimate of the spontaneous mutation rate in Chlamydomonas reinhardtii. *Genetics* 192, 1447–1454. doi:10.1534/genetics.112.145078.

O'Brien, K. P., Remm, M., and Sonnhammer, E. L. L. (2005). Inparanoid: A comprehensive database of eukaryotic orthologs. *Nucleic Acids Res.* 33. doi:10.1093/nar/gki107.

Orr, H. A. (1998). The Population Genetics of Adaptation: The Distribution of Factors Fixed during Adaptive Evolution. *Evolution (N. Y).* 52, 935. doi:10.2307/2411226.

Park, C. B., and Larsson, N.-G. (2011). Mitochondrial DNA mutations in disease and aging. *J. Cell Biol.* 193, 809–818. doi:10.1083/jcb.201010024.

Patananan, A. N., Budenholzer, L. M., Eskin, A., Torres, E. R., and Clarke, S. G. (2015). Ethanol-induced differential gene expression and acetyl-CoA metabolism in a longevity model of the nematode Caenorhabditis elegans. *Exp. Gerontol.* 61, 20–30. doi:10.1016/j.exger.2014.11.010.

Pellegrino, M. W., and Haynes, C. M. (2015). Mitophagy and the mitochondrial unfolded protein response in neurodegeneration and bacterial infection. *BMC Biol.* 13, 22. doi:10.1186/s12915-015-0129-1.

Pópulo, H., Lopes, J. M., and Soares, P. (2012). The mTOR Signalling Pathway in Human Cancer. *Int. J. Mol. Sci.* 13, 1886–1918. doi:10.3390/ijms13021886.

Pujol, C., Bratic-Hench, I., Sumakovic, M., Hench, J., Mourier, A., Baumann, L., et al. (2013). Succinate dehydrogenase upregulation destabilize complex I and limits the lifespan of gas-1 mutant. *PLoS One* 8, e59493. doi:10.1371/journal.pone.0059493.

Van Raamsdonk, J. M., and Hekimi, S. (2011). FUdR causes a twofold increase in the lifespan of the mitochondrial mutant gas-1. *Mech. Ageing Dev.* 132, 519–521. doi:10.1016/j.mad.2011.08.006.

Ramis, M. R., Esteban, S., Miralles, A., Tan, D.-X., and Reiter, R. J. (2015). Protective effects of melatonin and mitochondria-targeted antioxidants against oxidative stress: A review. *Curr. Med. Chem.* 22. doi:10.2174/0929867322666150619104143.

Reddi, A. R., Jensen, L. T., Naranuntarat, A., Rosenfeld, L., Leung, E., Shah, R., et al. (2009). The overlapping roles of manganese and Cu/Zn SOD in oxidative stress protection. *Free Radic. Biol. Med.* 46, 154–162. doi:10.1016/j.freeradbiomed.2008.09.032.

Rossignol, R., Faustin, B., Rocher, C., Malgat, M., Mazat, J.-P., and Letellier, T. (2003). Mitochondrial threshold effects. *Biochem. J.* 370, 751–62. doi:10.1042/BJ20021594.

Rutter, M. T., Roles, A., Conner, J. K., Shaw, R. G., Shaw, F. H., Schneeberger, K., et al. (2012). Fitness of arabidopsis thaliana mutation accumulation lines whose spontaneous mutations are known. *Evolution (N. Y).* 66, 2335–2339. doi:10.1111/j.1558-5646.2012.01583.x.

Safdar, A., Khrapko, K., Flynn, J. M., Saleem, A., De Lisio, M., Johnston, A. P. W., et al. (2015). Exercise-induced mitochondrial p53 repairs mtDNA mutations in mutator mice. *Skelet. Muscle* 6, 7. doi:10.1186/s13395-016-0075-9.

Saxer, G., Havlak, P., Fox, S. A., Quance, M. A., Gupta, S., Fofanov, Y., et al. (2012). Whole Genome Sequencing of Mutation Accumulation Lines Reveals a Low Mutation Rate in the Social Amoeba Dictyostelium discoideum. *PLoS One* 7. doi:10.1371/journal.pone.0046759.

Sedensky, M. M., and Morgan, P. G. (2006). Mitochondrial respiration and reactive oxygen species in C. elegans. *Exp. Gerontol.* 41, 957–967. doi:10.1016/j.exger.2006.06.056.

Shaw, R. G., Shaw, F. H., and Geyer, C. (2003). WHAT FRACTION OF MUTATIONS RED.UCES FITNESS? A REPLY TO KEIGHTLEY AND LYNCH. *Evolution (N. Y).* 57, 686–689. doi:10.1111/j.0014-3820.2003.tb01562.x.

Silander, O. K., Tenaillon, O., and Chao, L. (2007). Understanding the evolutionary fate of finite populations: The dynamics of mutational effects. *PLoS Biol.* 5, 922–931. doi:10.1371/journal.pbio.0050094.

Solon-Biet, S. M., Mitchell, S. J., de Cabo, R., Raubenheimer, D., Le Couteur, D. G., and Simpson, S. J. (2015). Macronutrients and caloric intake in health and longevity. *J. Endocrinol.* 226, R17–R28. doi:10.1530/JOE-15-0173.

De Souza, N., Vallier, L. G., Fares, H., and Greenwald, I. (2007). SEL-2, the C. elegans neurobeachin/LRBA homolog, is a negative regulator of lin-12/Notch activity and affects endosomal traffic in polarized epithelial cells. *Development* 134, 691–702. doi:10.1242/dev.02767.

Swan, K. A., Curtis, D. E., McKusick, K. B., Voinov, A. V., Mapa, F. A., and Cancilla, M. R. (2002). High-throughput gene mapping in Caenorhabditis elegans. *Genome Res.* 12, 1100–1105. doi:10.1101/gr.208902.

Vanduyn, N., Settivari, R., Levora, J., Zhou, S., Unrine, J., and Nass, R. (2013). The metal transporter SMF-3/DMT-1 mediates aluminum-induced dopamine neuron degeneration. *J. Neurochem.* 124, 147–157. doi:10.1111/jnc.12072.

Ventura, N., and Rea, S. L. (2007). Caenorhabditis elegans mitochondrial mutants as an investigative tool to study human neurodegenerative diseases associated with mitochondrial dysfunction. *Biotechnol. J.* 2, 584–595. doi:10.1002/biot.200600248.

Wallace, D. C. (2005). A mitochondrial paradigm of metabolic and degenerative diseases, aging, and cancer: a dawn for evolutionary medicine. *Annu. Rev. Genet.* 39, 359–407. doi:10.1146/annurev.genet.39.110304.095751.

Wallace, D. C. (2007). Why do we still have a maternally inherited mitochondrial DNA? Insights from evolutionary medicine. *Annu. Rev. Biochem.* 76, 781–821. doi:10.1146/annurev.biochem.76.081205.150955.

Wallace, D. C., and Chalkia, D. (2013). Mitochondrial DNA genetics and the heteroplasmy conundrum in evolution and disease. *Cold Spring Harb. Perspect. Biol.* 5. doi:10.1101/cshperspect.a021220.

Wang, A. D., Sharp, N. P., and Agrawal, A. F. (2014). Sensitivity of the distribution of mutational fitness effects to environment, genetic background, and adaptedness: A case study with Drosophila. *Evolution (N. Y).* 68, 840–853. doi:10.1111/evo.12309.

Wang, J. W., Howson, J., Haller, E., and Kerr, W. G. (2001). Identification of a novel lipopolysaccharide-inducible gene with key features of both A kinase anchor proteins and chs1/beige proteins. *J. Immunol.* 166, 4586–4595. doi:10.4049/jimmunol.166.7.4586.

Wang, J.-W., Gamsby, J. J., Highfill, S. L., Mora, L. B., Bloom, G. C., Yeatman, T. J., et al. (2004). Deregulated expression of LRBA facilitates cancer cell growth. *Oncogene* 23, 4089–4097. doi:10.1038/sj.onc.1207567.

Wang, Y., and Hekimi, S. (2015). Mitochondrial dysfunction and longevity in animals: Untangling the knot. *Science (80-.).* 350, 1204–1207. doi:10.1126/science.aac4357.

Whitlock, M. C. (2000). Fixation of new alleles and the extinction of small populations: drift load, beneficial alleles, and sexual selection. *Evolution* 54, 1855–1861. doi:10.2144/05384CI01.

Wicks, S. R., Yeh, R. T., Gish, W. R., Waterston, R. H., and Plasterk, R. H. (2001). Rapid gene mapping in Caenorhabditis elegans using a high density polymorphism map. *Nat. Genet.* 28, 160–164. doi:10.1038/88878.

Wloch, D. M., Szafraniec, K., Borts, R. H., and Korona, R. (2001). Direct estimate of the mutation rate and the distribution of fitness effects in the yeast Saccharomyces cerevisiae. *Genetics* 159, 441–452.

Wong, A., Boutis, P., and Hekimi, S. (1995). Mutations in the clk-1 gene of Caenorhabditis elegans affect developmental and behavioral timing. *Genetics* 139, 1247–1259. doi:10.1007/s11033-011-0852-9.

Wood. (1988). *The Nematode Caenohabditis Elegans*. Cold Spring Harbor, New York: Cold Spring Harbor Laboratory doi:10.1101/087969307.17.1.

Wright, S. (1931). Evolution in Mendelian Populations. *Genetics* 16, 97–159. Available at: http://www.pubmedcentral.nih.gov/articlerender.fcgi?artid=1201091&tool=pmcentrez&rendertype=abstract.

Zeyl, C., Mizesko, M., and de Visser, J. a (2001). Mutational meltdown in laboratory yeast populations. *Evolution* 55, 909–917. doi:10.1111/j.0014-3820.2001.tb00608.x.

Zhang, P., Lu, Y., Yu, D., Zhang, D., and Hu, W. (2015). TRAP1 Provides Protection Against Myocardial Ischemia-Reperfusion Injury by Ameliorating Mitochondrial Dysfunction. *Cell. Physiol. Biochem.* 36, 2072–2082. doi:10.1159/000430174.

Zhang, Y., Zou, X., Ding, Y., Wang, H., Wu, X., and Liang, B. (2013). Comparative genomics and functional study of lipid metabolic genes in Caenorhabditis elegans. *BMC Genomics* 14, 164. doi:10.1186/1471-2164-14-164.

Zhong, W., and Sternberg, P. W. (2006). Genome-wide prediction of C. elegans genetic interactions. *Science* 311, 1481–1484. doi:10.1126/science.1123287.

Zhu, Y. O., Siegal, M. L., Hall, D. W., and Petrov, D. A. (2014). Precise estimates of mutation rate and spectrum in yeast. *Proc. Natl. Acad. Sci. U. S. A.* 111, E2310–8. doi:10.1073/pnas.1323011111.
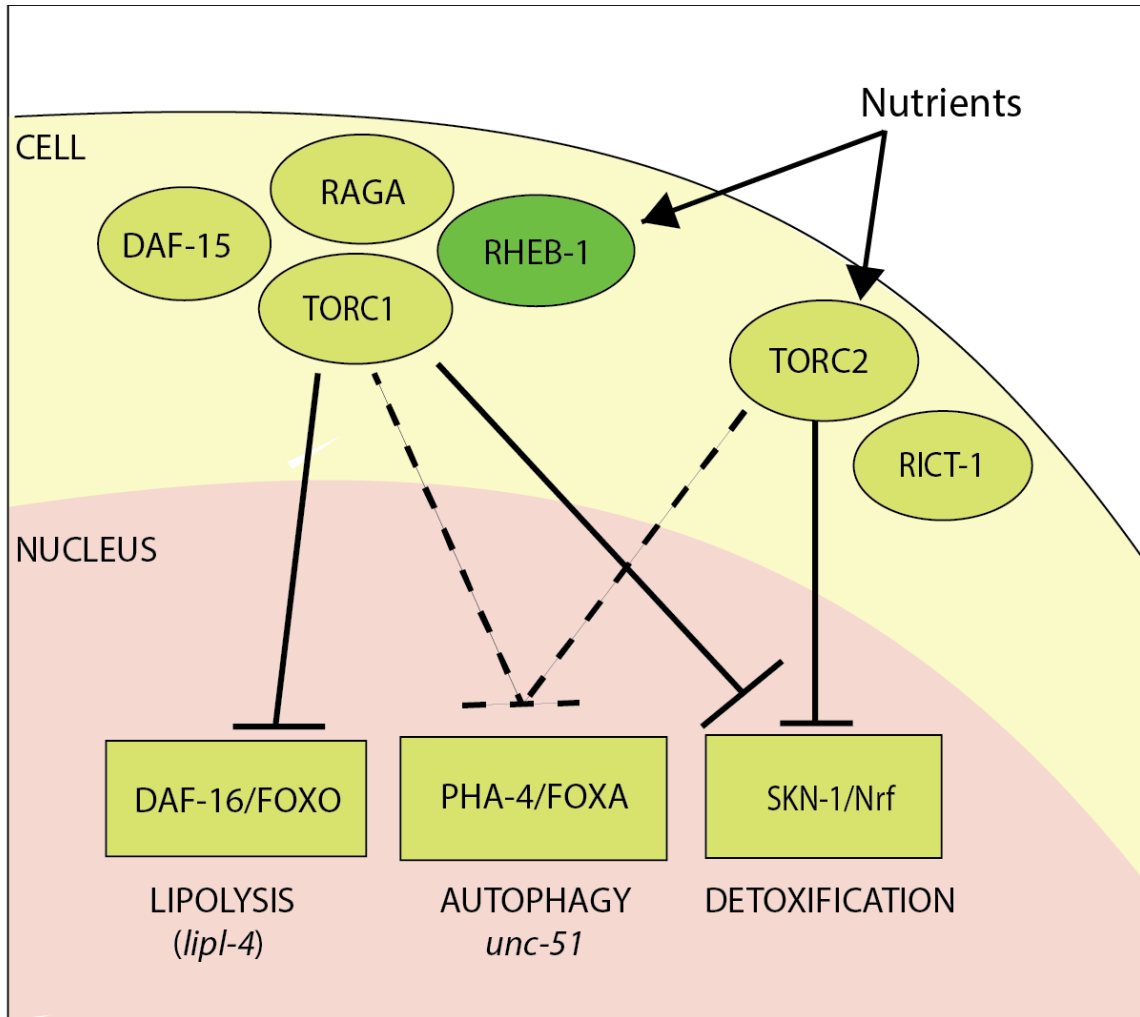
Figure 3.1: **Overview of *C. elegans* TOR signaling.** Ovals with dark green background indicate that the encoding gene experienced a mutation in *gas-1* MA431 (*rheb-1*). TOR responds to nutrient flux and functions in the two complexes, TORC1 and TORC2. As in mammalian systems, TORC1 is reported to interact with DAF-15 (also known as Raptor) and the GTPases RAG and RHEB-1. TORC1 inhibits DAF-16/FOXO and SKN-1/Nrf activity; TORC2 inhibits SKN-1/Nrf activity. It is not known which TOR complex inhibits PHA-4/FOXA which is indicated by dashed lines. The intestine has been linked to longevity mediated by TORC1. Figure and description adapted from "Lessons from *C. elegans*: Signaling pathways for longevity" by authors Lapierre and Hanses, 2012. (Lapierre and Hansen, 2012).
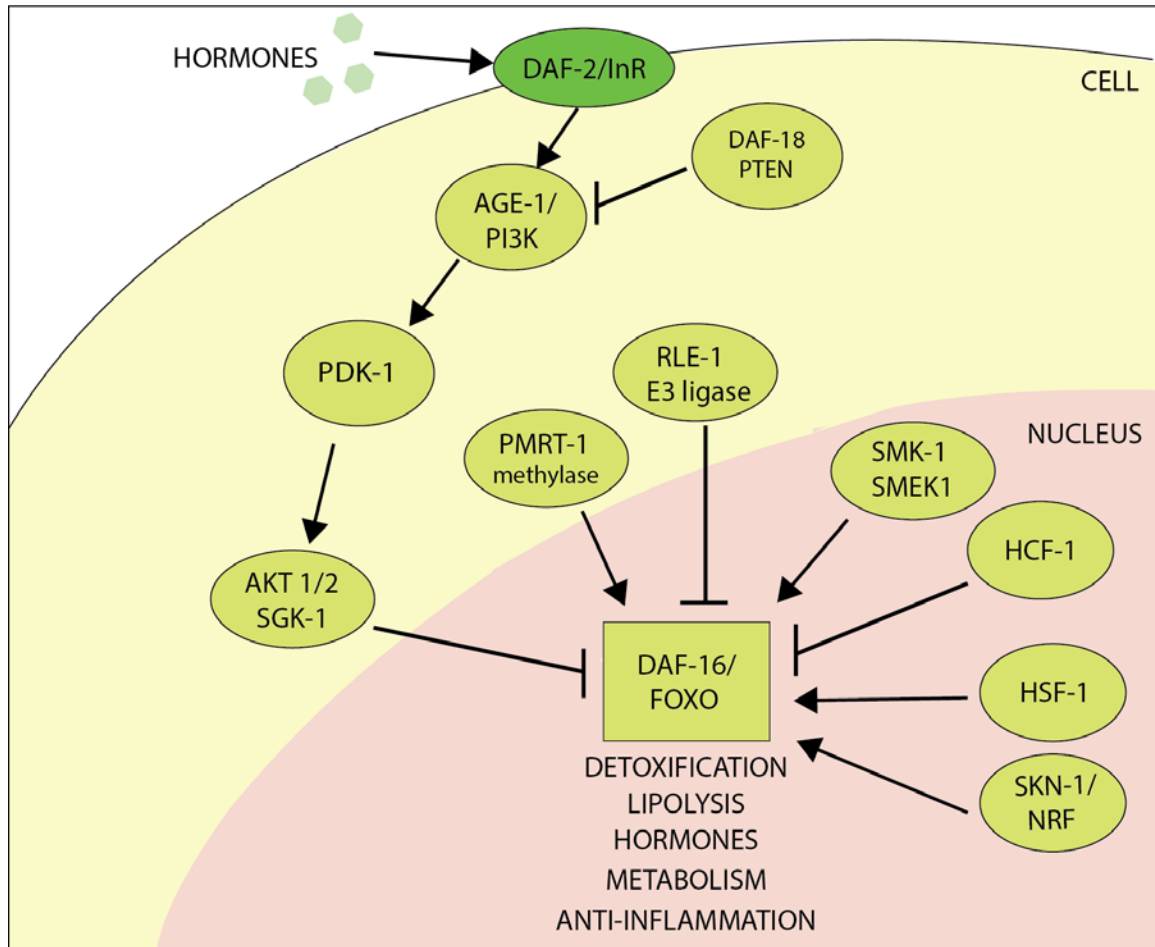
Figure 3.2: Overview of the insulin/IGF-1 signaling *C. elegans*. DAF-2, the insulin receptor (lnR), triggers the insulin signaling pathway in response to insulin-like peptides secreted from neurons to intestinal cells. DAF-2 signaling prevents DAF-16/FOXO from entering the nucleus and activating detoxification activity. DAF-16/FOXO is regulated through other mechanisms including ubiqitination (RLE-1/E3 ligase) and arginine methylation (PMRT-1/methylase). Nuclear-localized DAF-16/FOXO activity is inhibited by HCF-1 and enhanced by SMK-1/SMEK1, HSF-1, and SKN-1/Nrf. Figure and description adapted from "Lessons from *C. elegans*: Signaling pathways for longevity" (Lapierre and Hansen, 2012).
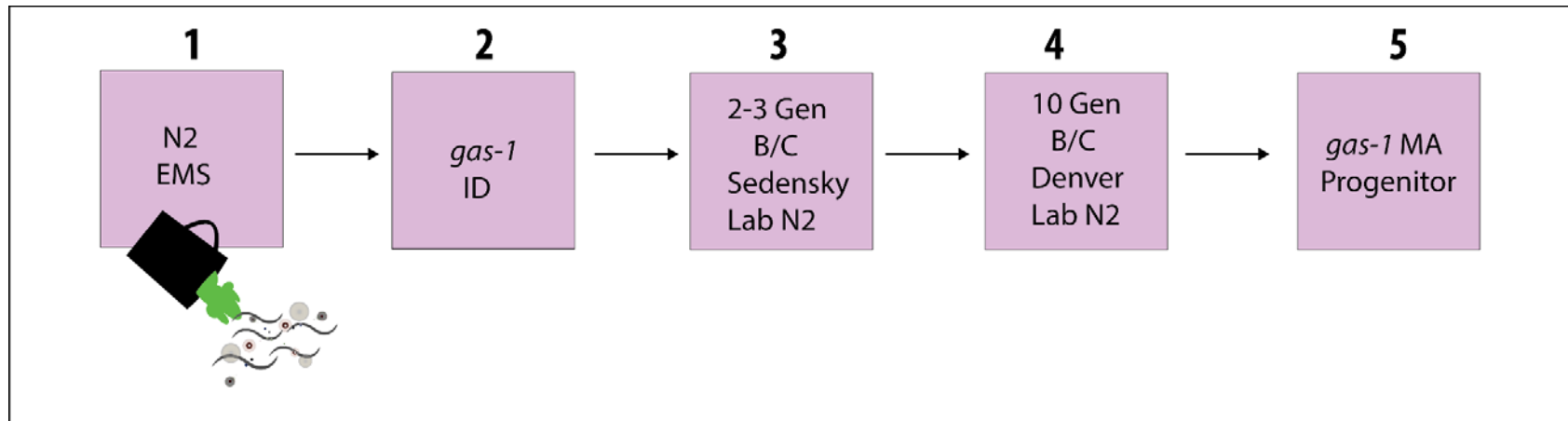
Figure 3.3: **Creation of *gas-1* fc21 mutant strain and steps prior to propagation of *gas-1* MA lines**
Step 1: Ethyl methanesulfate (EMS) induces mutagenesis in *C. elegans* N2 strain
Step 2: Identification of *gas-1* mutation (R290K)
Step 3: Two to three generations of backcrossing to Sedensky-Lab N2 strain; generation of *gas-1* fc21 strain
Step 4: Ten generations of backcrossing to Denver-Lab N2 strain
Step 5: Employment of *gas-1* to propagate forty-eight biological replicates for *gas-1* MA lines
(Kayser et al., 1999a)
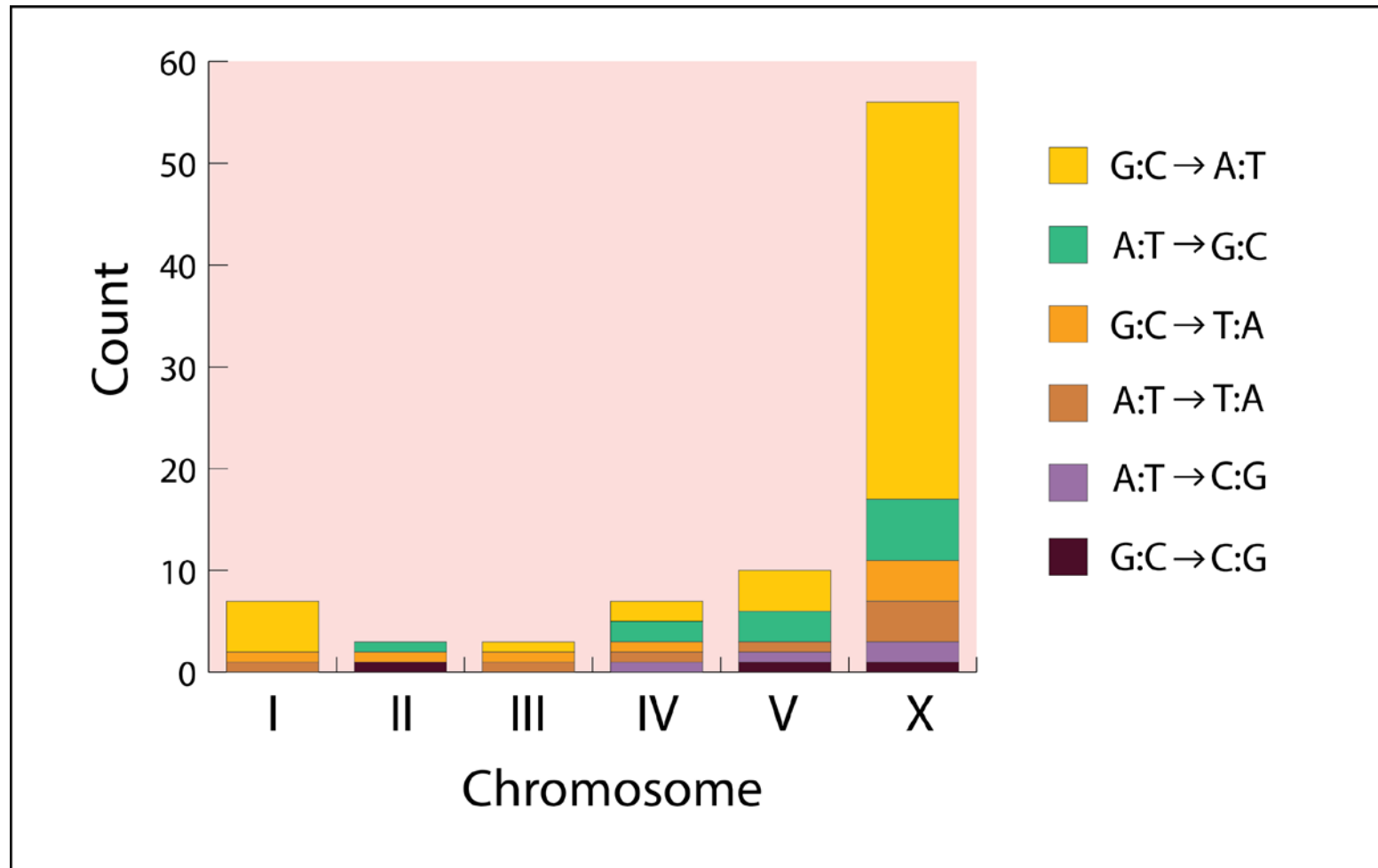
Figure 3.4: Distribution of six mutation types among six chromosomes in Denver-Lab *gas-1* progenitor strain. Count of mutations shown on y-axis. Chromosome depicted on X-axis. Denver-Lab *gas-1* progenitor strain obtained from CGC and backcrossed for ten generations to Denver-Lab N2 strain. There are a total of 86 mutations in the Denver-Lab *gas-1* progenitor strain.
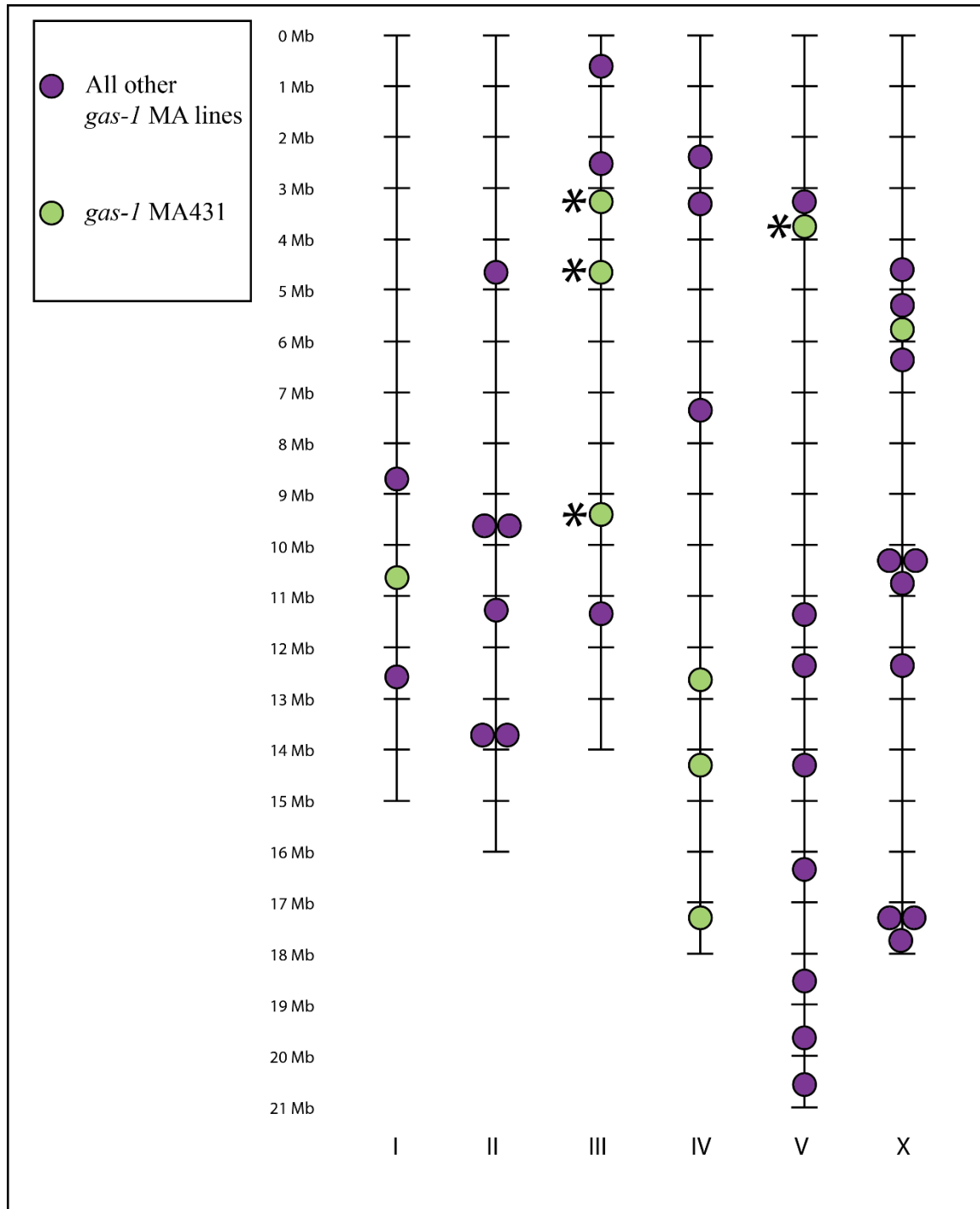
Figure 3.5: **Location of *gas-1* MA line mutations among six *C. elegans* chromosomes.** *gas-1* MA431 experienced SNPs in green; asterisks indicate the three isolated SNPs that were backcrossed to the N2 and *gas-1* progenitor. With introduction of these three SNPs, both progenitors exhibited increased fitness and the *gas-1progenitor/*+SNPs exhibited decreased ROS production.
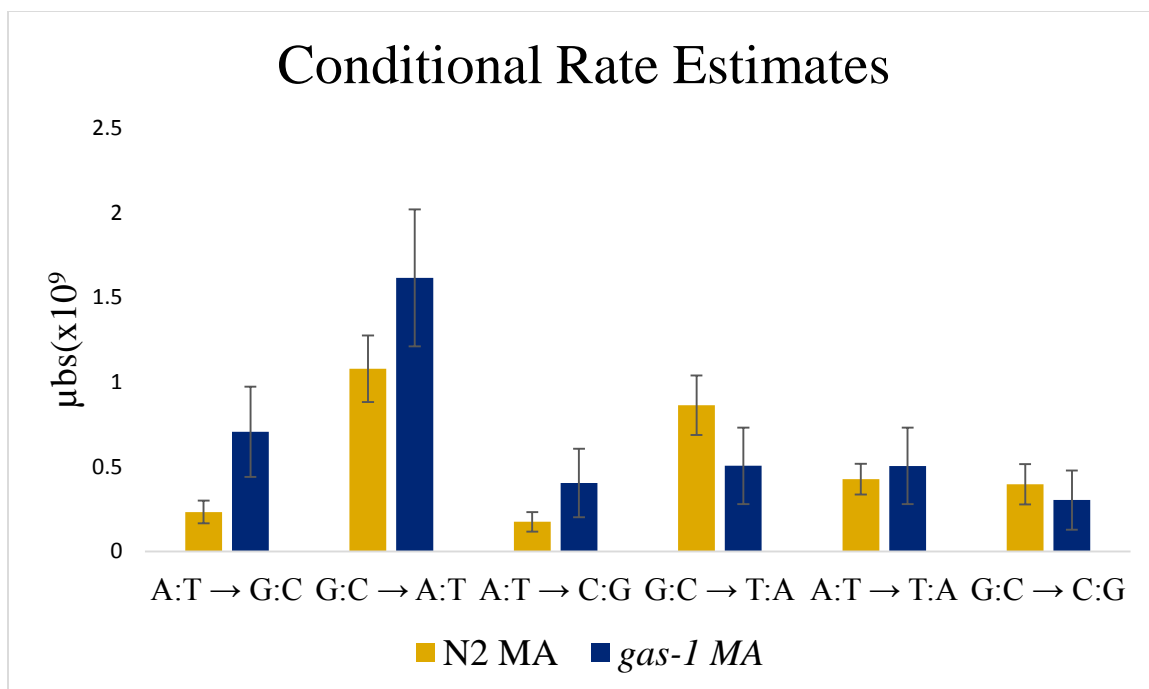
Figure 3.6: Conditional rate estimate for *gas-1* MA lines. Conditional rate estimates for six possible mutation types for pooled *gas-1* MA data. Standard errors showed by error bars.
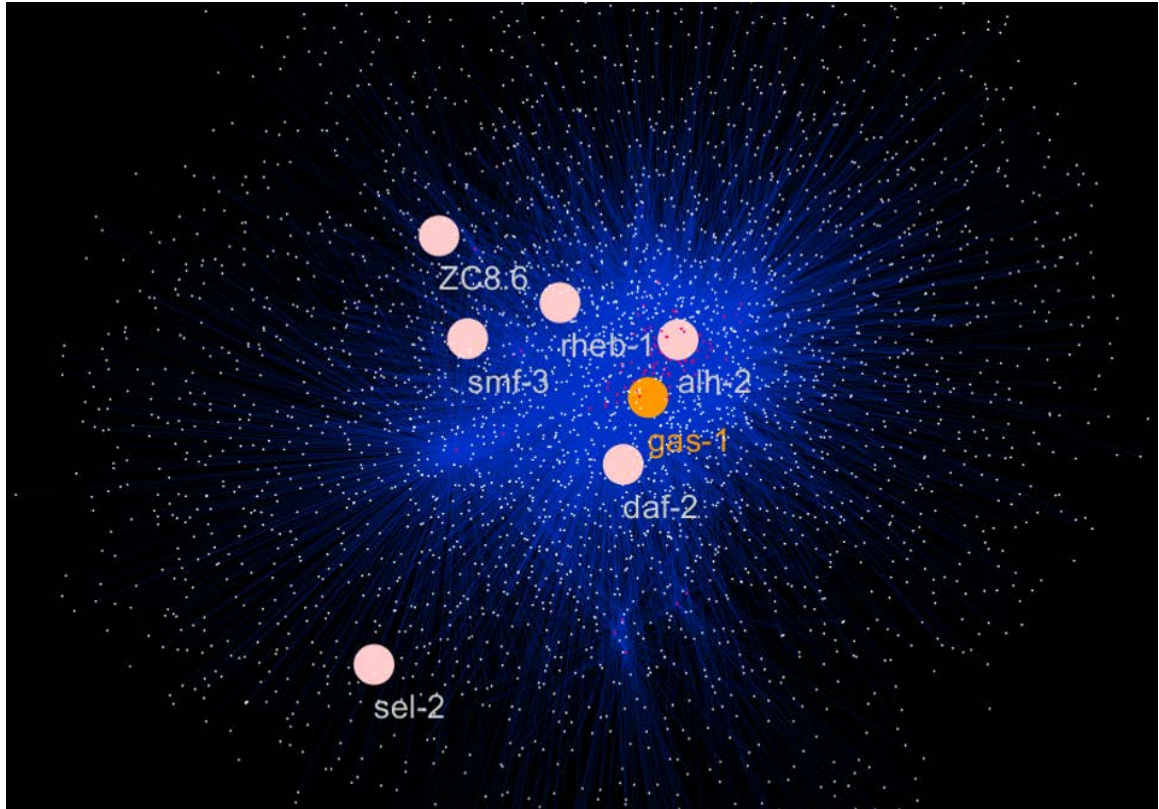
Figure 3.7: "*gas-1*-centric-interactome" depiction of genes that interact within 2-degrees of *gas-1* gene and interacting *gas-1*. Figure depicting all genes that interact within 2-degrees of *gas-1* gene. *gas-1* MA line mutations shown in pink, *gas-1* gene displayed in yellow. Genes that interact directly with *gas-1* shown in red. Gene proximity to *gas-1* correlates with number of interactions within the *gas-1*-centric-interactome.
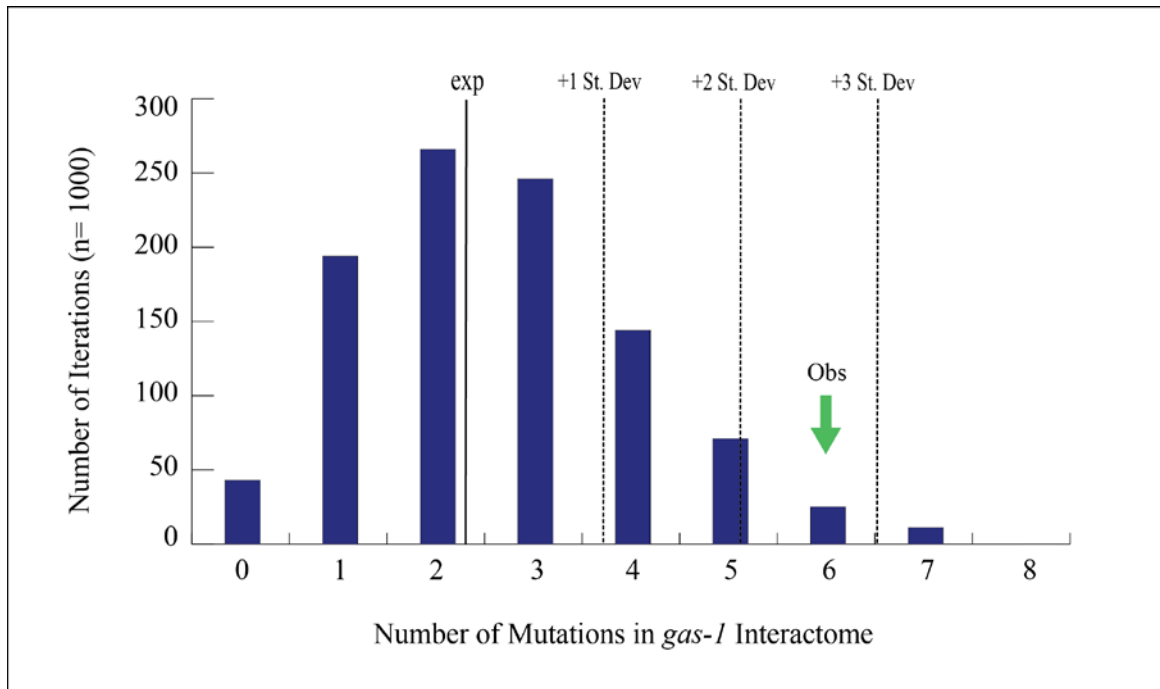
Figure 3.8: *gas-1* **MA Line Simulation Results of One Thousand Iterations of Random Mutation Generation.** Plot depicting proportion of 1000 iterations of random mutation generation in which specific number of mutations were included in *gas-1* interactome. Simulates *gas-1* MA lines mutation results in which 16 *gas-1* MA line mutations fell in coding regions and had available interactomes. Exp= mean number of expected mutations within 2-degrees of *gas-1* network by chance. Obs= observed experimental value (n=6) of mutations within 2-degrees of *gas-1* network.
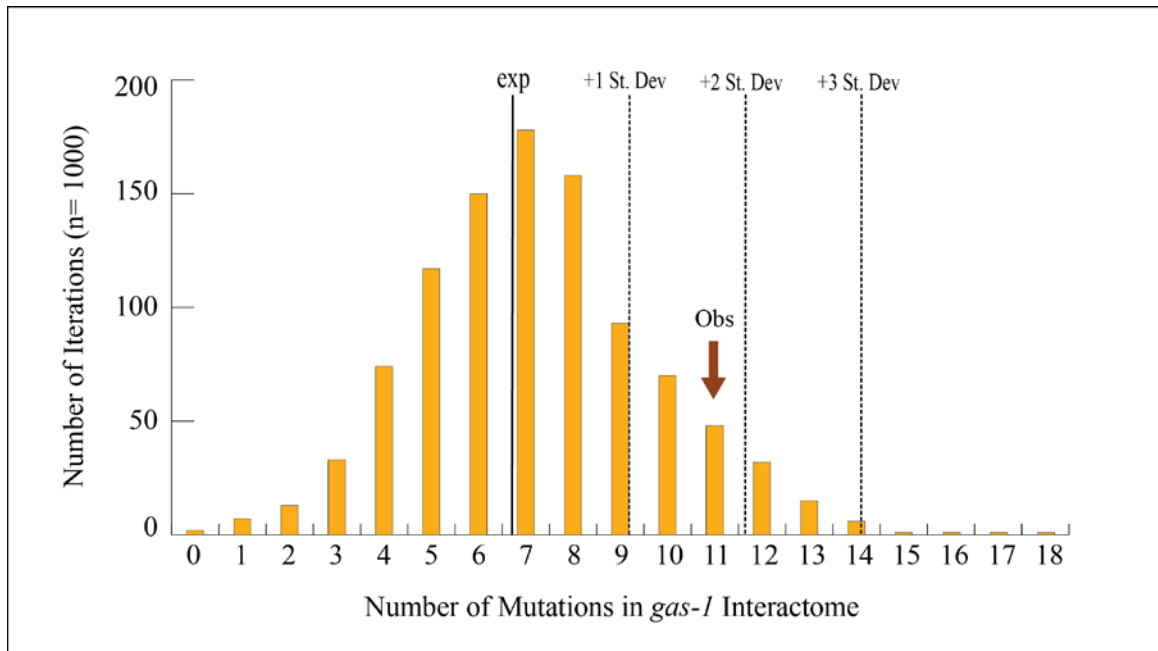
Figure 3.9: N2 Simulation Results of One Thousand Iterations of Random Mutation Generation. Plot depicting proportion of 1000 iterations of random mutation generation in which specific number of mutations were included in *gas-1* interactome. Simulates N2 MA lines mutation results in which 60 N2 MA line mutations had available interactomes and fell in coding regions. Exp= mean number of expected mutations within 2-degrees of *gas-1* network by chance. Obs= observed experimental value (n=11) of mutations within 2-degrees of *gas-1* network.

Table 3.1: Illumina-MiSeq Sequencing Run Statistics. All reads 150bp, paired end. All nematodes at L1 stage. Assembled using WS242 *C. elegans* reference genome in CLC with following parameters: no masking, mismatch cost= 2, insertion cost=3, deletion cost= 3, length fraction= 0.98, read fraction= 0.98, global alignment= no, non-specific match handling= map randomly. Standard deviation of the mean displayed in parentheses adjacent to mean values.

Line	Total Reads	% Mapping	Average Nuclear Coverage
N2 Progenitor	12,474,086	87.7	27.3 (54.7)
N2 MA523	8,162,820	92.7	11.3 (15.1)
N2 MA526	6,698,142	89.5	8.9 (13.1)
N2 MA529	6,799,824	93.0	9.4 (12.2)
N2 MA553	7,846,166	92.0	10.7 (15.9)
N2 MA574	6,271,490	93.2	8.7 (12.4)
gas-1 Progenitor	10,725,726	88.6	23.7 (36.9)
gas-1 MA412	7,558,954	83.4	15.6 (14.5)
gas-1 MA419	6,843,258	82.5	14.0 (13.7)
gas-1 MA429	7,351,108	86.8	15.9 (12.3)
gas-1 MA431	6,896,562	80.6	13.7 (13.7)
gas-1 MA438	6,998,936	83.4	14.4 (17.4)

Table 3.2: *gas-1* **Progenitor Mutations.** Table display of all mutations in *gas-1* progenitor compared to Wildtype (N2) reference strain sequence. Chromo= chromosome, Mut Type= mutation type, Ref Codon= reference codon in N2 sequence, Ref AA= reference amino acid in N2 sequence, Mut Codon= mutation codon in *gas-1* progenitor, Mut AA= mutation amino acid in *gas-1* progenitor, Syn/Non= synonymous/ non-synonymous mutation.

Chromo	Position	Mut Type	Gene	Classification	Ref Codon	Ref AA	Mut Codon	Mut AA	Syn/Non
I	677,471	G:C → A:T		Intergenic					
I	1,253,398	G:C → A:T	Y48G8AL.1/*herc-1*	Exon	TTC	Phe	TTT	Phe	Syn
I	1,287,970	G:C → A:T		Intergenic					
I	2,933,110	G:C → A:T	Y71F9AM.4a	Intron					
I	4,610,900	G:C → T:A	C44E4.1a/*ubr-4*	Intron					
I	10,357,050	A:T → T:A	ZC434.9	Exon	TAT	Tyr	TTT	Phe	Non
I	11,776,568	G:C → A:T	ZK1151.1/*vab-10*	Exon	GAG	Glu	GAA	Glu	Syn
II	1,302,680	G:C → C:G	Y57G7A.10/*emc-2*	Exon	GTC	Val	GTG	Val	Syn
II	7,021,989	G:C → T:A		Intergenic					
II	13,514,494	A:T → G:C	F54F11.2/*nep-17*	Exon	GAT	Asp	GGT	Gly	Non
III	2,252,260	A:T → T:A	T20H9.5/*fbxa-68*	Pseudogene					
III	4,627,853	G:C → T:A	F10F2.2	Intron					
III	10,691,565	G:C → T:A		Intergenic					
IV	2,035,212	A:T → C:G	Y76B12C.9	Intron					
IV	2,749,785	A:T → T:A		Intergenic					
IV	8,310,095	G:C → A:T	F35H10.10	Exon	TGC	Cyc	TAC	Tyr	Non
IV	11,232,104	G:C → A:T	C05C12.6	Intron					
IV	11,418,983	A:T → G:C	F22B3.7	Intron					
IV	15,921,236	G:C → T:A		Intergenic					
IV	16,361,450	A:T → G:C		Intergenic					
V	89,752	A:T → G:C		Intergenic					
V	378,596	G:C à A:T	Y39D8B.3/mltn-8	Intron					

Table 3.2 (Continued)

V	4,234,497	A:T → G:C		Intergenic					
V	4,361,567	A:T → C:G		Intergenic					
V	4,437,706	G:C → A:T		Intergenic					
V	7,192,185	G:C → A:T	F09G2.8	Intron					
V	10,973,142	G:C → A:T	F52B7.5	Exon	GTT	Val	ATT	Ile	Non
V	14,420,082	A:T → G:C		Intergenic					
V	15,847,287	G:C → C:G	K08G2.2	Pseudogene					
V	18,718,740	A:T → T:A	Y17D7C.2	Intron					
X	2,227,737	A:T → G:C		Intergenic					
X	2,246,104	A:T → T:A	AH9.1	Intron					
X	2,445,717	A:T → T:A	T07D1.4/*fox-1*	Intron					
X	3,093,297	A:T → T:A	F52E4.6/*wrt-2*	Exon	TCT	Ser	TCA	Ser	Syn
X	3,161,750	G:C → T:A	C15C7.2/*klp-8*	Exon	ATC	Ile	ATA	Ile	Syn
X	4,282,858	G:C → A:T	C52B9.2/*ets-9*	Exon	AAC	Asn	AAT	Asn	Syn
X	4,998,983	G:C → A:T		Intergenic					
X	6,117,228	G:C → A:T	C15H9.3	Exon	TCC	Ser	TCT	Ser	Syn
X	6,228,286	A:T → T:A	C14F11.3/*lite-1*	Intron					
X	6,507,975	G:C → T:A	F22A3.3/*glr-8*	Exon	TTG	Phe	TTT	Phe	Syn
X	6,540,619	G:C → A:T		Intergenic					
X	6,575,703	G:C → T:A		Intergenic					
X	6,735,763	G:C → A:T		Intergenic					
X	7,487,190	G:C → A:T	F48E3.1/*gly-12*	Intron					
X	8,091,471	G:C à A:T	K07E3.7/catp-5	Exon	ATG	Met	ATA	Ile	Non
X	8,457,385	A:T à G:C		Intergenic					
X	8,469,059	G:C à A:T	F16F9.5/mec-10	Exon	GAG	Glu	AAG	K	Non
X	8,859,047	G:C à A:T		Intergenic					

Table 3.2 (Continued)

X	9,219,655	G:C A:T	C35B8.2	Intron						
X	9,521,874	G:C → A:T		Intergenic						
X	10,047,400	G:C → A:T		Intergenic						
X	10,237,566	G:C → A:T		Intergenic						
X	10,254,086	G:C → A:T		Intergenic						
X	10,304,584	G:C → A:T	F41E7.5/*fipr-21*	Exon	GCT	Ala	GTT	Val	Non
X	10,556,749	G:C → A:T		Intergenic						
X	11,066,118	G:C → A:T	W04G3.3/*lpr-4*	Exon	CCC	Pro	TCC	Ser	Non
X	11,142,075	G:C → A:T		Intergenic						
X	11,160,529	G:C → A:T		Intergenic						
X	11,293,683	A:T → G:C		Intergenic						
X	11,299,794	G:C → A:T		Intergenic						
X	11,636,491	G:C → A:T	Y71H9A.2/*sto-6*	Intergenic						
X	11,936,220	G:C → A:T		Intergenic						
X	12,341,342	G:C → T:A	F42F12.2/*zig-2*	Exon	GCC	Ala	GCA	Ala	Syn
X	12,607,686	G:C → A:T		Intergenic						
X	13,004,573	G:C → A:T		Intergenic						
X	13,055,233	A:T → T:A	K03A11.1	Intergenic						
X	13,754,953	G:C → A:T		Intergenic						
X	14,033,034	G:C → A:T		Intergenic						
X	14,150,227	A:T → C:G	F28H6.1	Intron						
X	14,162,760	G:C → A:T		Intergenic						
X	14,203,413	G:C → A:T	C37E2.5/*ceh-37*	Intron						
X	14,481,964	G:C → C:G	M163.4	Intron						
X	14,762,091	G:C → A:T		Intergenic						
X	14,800,348	G:C → A:T	Y16B4A.2	Exon	GGC	Gly	GAC	Asp	Non

Table 3.2 (Continued)

X	14,811,193	G:C → A:T		Intergenic						
X	15,198,388	G:C → A:T	T10B10.5/*snt-7*	Intron						
X	15,589,151	G:C → A:T	K09A9.5/*gas-1*	Exon						
X	15,600,732	G:C → A:T		Intergenic						
X	15,649,607	G:C → A:T	F59D12.3	Exon	GTT	Val	ATT	Ile	Non	
X	15,933,446	G:C → A:T	E03G2.2/*mrp-3*	Exon	GCT	Ala	ACT	Thr	Non	
X	15,947,532	G:C → A:T	E03G2.3/*mec-5*	Exon	CTC	Leu	CTT	Leu	Syn	
X	16,753,578	A:T → T:A	C10E2.5	Intron						
X	17,173,046	A:T → G:C		Intergenic						
X	17,235,705	G:C → A:T	T25G12.7/*dhs-30*	Exon	GCT	Ala	ACT	Thr	Non	
X	17,293,683	A:T → G:C	C33E10.8	Exon	TCC	Ser	CCC	Pro	Non	
X	17,372,130	G:C → A:T		Intergenic						

Table 3.3: Summary of *gas-1* progenitor mutation types by chromosome. Count of mutation types for each of the six chromosomes (Chromo) in *gas-1* progenitor.

	Chromo I	Chromo II	Chromo III	Chromo IV	Chromo V	Chromo X	Total
A:T → G:C	0	1	0	2	3	6	12
G:C → A:T	5	0	1	2	4	39	51
A:T → C:G	0	0	0	1	1	2	4
G:C → T:A	1	1	1	1	0	4	8
A:T → T:A	1	0	1	1	1	4	8
G:C → C:G	0	1	0	0	1	1	3
Total	7	3	3	7	10	56	86

Table 3.4: *gas-1* MA Line Mutations. Pos = position, Ref Allele = reference allele, Var allele = variant allele, Class= classification, Ref Codon = Reference Codon, Ref AA= reference amino acid, Var Codon = variant codon, Var AA= variant amino acid, Syn or Non = synonymous or non- synonymous mutation, Type Conversion= mutation type. "Intergen" refers to an Intergenic mutation.

Line	Pos	Gene	Ref Allele	Var Allele	Class	Ref Codon	Ref AA	Var Codon	Var AA	Syn or Non	Type Conversion
gas-1 MA412	II: 11,182,784	F37H8.3	A	C	Exon	CCA	Pro	CCC	Pro	Syn	A:T → C:G
gas-1 MA412	II: 13,912,231	W02B8.2	G	A	Exon	GAG	Glu	AAG	Lys	Non	G:C → A:T
gas-1 MA412	V: 11,394,089		A	G	Intergenic						A:T → G:C
gas-1 MA412	V: 12,318,251		T	G	Intergenic						A:T → C:G
gas-1 MA412	V: 19,920,250		A	G	Intergenic						A:T → G:C
gas-1 MA412	V: 20,674,727	*mlt-11*	G	T	Exon	TCG	Ser	TCT	Ser	Non	G:C → T:A
gas-1 MA412	X: 5,107,789		T	C	Intergenic						A:T → G:C
gas-1 MA412	X: 6,529.937		T	C	Intergenic						A:T → G:C
gas-1 MA412	X: 10,265,783		G	C	Intergenic						G:C → C:G
gas-1 MA419	III: 896,522	F23H11.2	G	T	Exon	TGC	Cys	TTC	Phe	Non	G:C → T:A
gas-1 MA419	V: 3,152,259		T	A	Intergenic						A:T → T:A
gas-1 MA419	X: 10.274,961	F41E7.2	C	T	Intron						G:C → A:T
gas-1 MA419	X: 4,975,182	ZC8.6	G	C	Exon	TTC	Phe	TTG	Phe	Syn	G:C → C:G
gas-1 MA419	X: 10,368,359		G	T	Intergenic						G:C → T:A
gas-1 MA419	X: 12,384,471		C	T	Intergenic						G:C → A:T
gas-1 MA429	I:12,870,206		C	T	Intergenic						G:C → A:T
gas-1 MA429	II: 4,663,692	T05A7.11	C	T	Exon	GCA	Ala	ACA	Thr	Non	G:C → A:T
gas-1 MA429	IV: 3,470,137	F58E2.2	G	A	Exon	AAG	Lys	AAA	Lys	Syn	G:C → A:T
gas-1 MA429	X: 17,133,019	K09E3.7	C	T	Exon	GTG	Vak	ATG	Met	Non	G:C → A:T
gas-1 MA429	X: 17,132,998	K09E3.7	T	C	Exon	ACA	Thr	GCA	Ala	Non	A:T → G:C
gas-1 MA431	I: 10,724,831	*srz-85*	A	G	Exon	CAT	His	CAC	His	Syn	A:T → G:C
gas-1 MA431	III: 9,455,062	*rheb-1*	A	T	Intron						A:T → T:A
gas-1 MA431	III: 3,002,544	*daf-2*	G	T	Intron						G:C → T:A

Table 3.4 (Continued)

gas-1 MA431	III: 4,598,014	*sel-2*	C	T	Exon	CGT	Arg	CAT	His	Non	G:C → A:T
gas-1 MA431	IV: 12,986,492		C	T	Intergenic						G:C → A:T
gas-1 MA431	IV: 14,058,054		T	A	Intergenic						A:T → T:A
gas-1 MA431	IV: 17,181,972	C52D10.3	G	A	Intron						G:C → A:T
gas-1 MA431	V: 3,379,498	C04E12.10	G	C	Exon	GAT	Asp	CAT	His	Non	G:C → C:G
gas-1 MA431	X: 5,964,400	R07E4.1	T	A	Intron						A:T → T:A
gas-1 MA438	I: 8,987,554		G	A	Intergenic						G:C → A:T
gas-1 MA438	II: 13,977,894	*sre-48*	G	A	Intron						G:C → A:T
gas-1 MA438	III: 2,792,754	Y71H2AM.24	G	T	Intron						G:C → T:A
gas-1 MA438	III: 11,412,255	*twk-31*	A	C	Intron						A:T → C:G
gas-1 MA438	IV: 2,620,955	*smf-3*	G	A	Intron						G:C → A:T
gas-1 MA438	IV: 7,452,889		G	A	Intergenic						G:C → A:T
gas-1 MA438	V: 14,423,155		C	T	Intergenic						G:C → A:T
gas-1 MA438	V: 1,646,965	*alh-2*	A	C	Exon	TGA	Trp	TGC	Cys	Non	A:T → C:G
gas-1 MA438	V: 18,784,124	Y17D7B.10	T	C	Intron						A:T → G:C
gas-1 MA438	X: 9,580,008		A	T	Intergenic						A:T → T:A
gas-1 MA438	X: 17,456,803		G	A	Intergenic						G:C → A:T

Table 3.5: Summary of *gas-1* MA line SNPs interactions. Display of all *gas-1* MA line SNPs that interact with *gas-1* interacting genes that interact within two-degrees of *gas-1*. *gas-1* gene interactions displayed following *gas-1* MA line SNP interactions. Gene interaction values obtained from Gene Orienteer (Zhong and Sternberg, 2006) (See Materials and Methods).

gas-1 Interaction	Interaction Value	MA Line SNP	MA line
vps-34	10.18	ZC8.6	MA419
acl-3	5.86	ZC8.6	MA419
vps-34	7.74	*rheb-1*	MA431
duox-2	6.02	*rheb-1*	MA431
bli-3	6.02	*rheb-1*	MA431
lpd-5	6.61	*rheb-1*	MA431
DC2.5	5.54	*rheb-1*	MA431
F32A5.8	5.54	*rheb-1*	MA431
sod-5	6.04	*rheb-1*	MA431
hda-1	7.41	*rheb-1*	MA431
sod-1	6.04	*rheb-1*	MA431
vps-34	5.48	*daf-2*	MA431
nuo-5	5.57	*daf-2*	MA431
alh-1	5.36	*daf-2*	MA431
ctl-3	6.48	*daf-2*	MA431
prdx-2	5.76	*daf-2*	MA431
fat-7	5.42	*daf-2*	MA431
T20H4.5	22.89	*daf-2*	MA431
msra-1	23.5	*daf-2*	MA431
nuo-4	22.89	*daf-2*	MA431
dao-3	22.79	*daf-2*	MA431
fat-5	25.38	*daf-2*	MA431
emb-8	26.11	*daf-2*	MA431
cyc-1	24.04	*daf-2*	MA431
sod-5	32.3	*daf-2*	MA431
sod-2	29.6	*daf-2*	MA431
rnr-2	24.19	*daf-2*	MA431
fat-6	25.38	*daf-2*	MA431
sod-1	32.3	*daf-2*	MA431
sod-3	30.4	*daf-2*	MA431
unc-79	20.96	*daf-2*	MA431
hda-1	30.8	*daf-2*	MA431
hda-1	5.73	*sel-2*	MA431

Table 3.5 (Continued)

sod-5	21.45	*smf-3*	MA438
sod-2	6.76	*smf-3*	MA438
sod-3	6.76	*smf-3*	MA438
hda-1	8.26	*smf-3*	MA438
cyc-1	17.07	*alh-2*	MA438
gbh-1	6.83	*alh-2*	MA438
msra-1	7.88	*alh-2*	MA438
C33A12.1	6.42	*alh-2*	MA438
acdh-12	6.44	*alh-2*	MA438
T05H4.4	7.88	*alh-2*	MA438
T05H4.5	7.88	*alh-2*	MA438
gspd-1	9.86	*alh-2*	MA438
prdx-6	8.06	*alh-2*	MA438
duox-2	6.54	*alh-2*	MA438
bli-3	6.54	*alh-2*	MA438
Cyp-44A1	5.57	*alh-2*	MA438
T27E9.2	6.08	*alh-2*	MA438
MTCE.26	6.57	*alh-2*	MA438
ivd-1	5.95	*alh-2*	MA438
LLC1.3	9.27	*alh-2*	MA438
acdh-10	6.67	*alh-2*	MA438
acdh-7	6.67	*alh-2*	MA438
alh-4	11.36	*alh-2*	MA438
alh-5	11.36	*alh-2*	MA438
acdh-10	5.17	*gas-1*	
acdh-7	5.17	*gas-1*	
acdh-12	5.58	*gas-1*	
acl-3	5.56	*gas-1*	
alh-1	5.45	*gas-1*	
alh-2	5.45	*gas-1*	
alh-4	6.39	*gas-1*	
alh-5	6.39	*gas-1*	
bli-3	5.74	*gas-1*	
C25A1.5	6.38	*gas-1*	
C33A12.1	7.27	*gas-1*	
ctl-3	5.23	*gas-1*	
cyc-1	5.31	*gas-1*	
Cyp-44A1	5.89	*gas-1*	

Table 3.5 (Continued)

dao-3	5.13	*gas-1*
DC2.5	5.17	*gas-1*
duox-2	5.74	*gas-1*
emb-8	5.13	*gas-1*
F32A5.8	5.17	*gas-1*
fat-5	6.23	*gas-1*
fat-6	6.43	*gas-1*
fat-7	6.43	*gas-1*
gbh-1	5.13	*gas-1*
gspd-1	5.37	*gas-1*
hda-1	7.14	*gas-1*
ivd-1	6.35	*gas-1*
LLC1.3	5.43	*gas-1*
lpd-5	9.76	*gas-1*
msra-1	6.68	*gas-1*
cox-I (MTCE.26)	5.63	*gas-1*
nuo-4	6.57	*gas-1*
nuo-5	8.5	*gas-1*
prdx-2	5.75	*gas-1*
prdx-6	5.52	*gas-1*
pxn-1	7.06	*gas-1*
pxn-2	7.17	*gas-1*
rnr-2	6.44	*gas-1*
sod-1	7.48	*gas-1*
sod-2	6.5	*gas-1*
sod-3	6.38	*gas-1*
sod-5	7.48	*gas-1*
T05H4.4	5.64	*gas-1*
T05H4.5	5.64	*gas-1*
T20H4.5	9.86	*gas-1*
T27E9.2	6.42	*gas-1*
unc-79	24.14	*gas-1*
vps-34	12.62	*gas-1*

Chapter 4: Evolutionary genome responses to mitochondrial dysfunction in large population sizes of *C. elegans*

Riana I. Wernick[1], Suzanne Estes[2], Stephen Christy[2], Jennifer Sullins[2], Dana K. Howe[1], Dee R. Denver[1]

3. Department of Integrative Biology, Oregon State University, Corvallis, Oregon, USA
4. Department of Biology, Portland State University, Portland, Oregon, USA

4.1 Abstract

Investigating evolutionary adaptive recovery to harmful mutation not only has the potential to provide new insights on the impact of evolutionary forces influencing genetic variation, but may also reveal novel genomic modifications and targets for ameliorating Complex I impairment. Complex I impairment is implicated in mitochondrial diseases and neurodegenerative disorders. While the effects of complex I dysfunction are well-studied in numerous organisms, less is known about the possible avenues for evolutionary adaptive recovery. We characterized how the nuclear and mitochondrial genomes are modified and investigated the potential for adaptation and recovery in populations genetically predisposed to Complex I impairment. Evolving populations of the mitochondrial electron transport chain (*gas-1*) mutant strain of *Caenorhabditis elegans* in large population sizes (N= ~1,000), we applied high-throughput DNA sequencing to examine the influence of evolutionary forces on the potential genomic paths to fitness recovery. Twenty-four biological replicate populations propagated from a single *gas-1* progenitor were evolved for sixty generations. Illumina-Hiseq DNA sequencing was applied to L1 larvae from all twenty-four recovery (RC) lines as well as the *gas-1* and wild-type (N2) strains to investigate nuclear and mitochondrial genome evolution. All nuclear and mitochondrial DNA changes were identified and characterized revealing prospective beneficial and/or compensatory mutations to the *gas-1* mutation. 113 nuclear mutations were identified among the twenty-four *gas-1* RC lines, he majority of which were intergenic (n=63). Nineteen nuclear mutations were located in exons and twenty-one occurred in intron regions. Thirteen single-base substitutions in mtDNA were

observed among the twenty-four *gas-1* RC lines and three single-base substitutions were identified in the N2 progenitor strain.

Calculation of the nuclear genome evolutionary rate suggested influence of natural selection among the *gas-1* RC lines and exhibited an approximate three-fold decrease compared to the published *C. elegans* mutation rate value. Gene network analysis and comparison to simulation predictions revealed a significant number of RC line mutations in genes located in the *gas-1* gene network. These patterns are consistent with both positive and purifying selection influencing nuclear genome evolution.

There were twelve instances of likely *de novo* mitochondrial mutations, and all but two were located in protein-coding regions of the mitochondrial genome. Analysis of mitochondrial DNA mutations within *gas-1* RC lines indicated parallel and potential compensatory evolution in Complex I core subunit genes. This research reveals new insights into the evolution of adaptive recovery from deleterious mutation and provides new knowledge and targets for ameliorating Complex I impairment.

4.2 Introduction

"Natural selection is anything but random"
      -Richard Dawkins

The evolutionary recovery process from deleterious mutations that impose harmful consequences is especially relevant to disease (antibiotic/antiviral resistance), epidemiology (infectious transmission), and conservation efforts (Lande, 1995; Maisnier-Patin et al., 2002; Nagaraja et al., 2015). This process pertains not only on a macro-level (e.g. populations with a large deleterious mutation load) but also on lower hierarchal levels including the cellular level (e.g. cancers), the organelle level (e.g. selfish genetic elements) and the molecular level (e.g. maintenance of RNA and protein secondary structures)

(Kennedy et al., 2012; Phillips et al., 2015; Szamecz et al., 2014). Fitness recovery from deleterious mutations is possible due to three main processes: (1) reversion mutations, (2) beneficial mutations which increase fitness regardless of genetic background, (3) and compensatory epistatic mutations (only increase fitness when co-occurring with the specific deleterious genotype) (Estes and Lynch, 2003). This third process of fitness recovery can be further sub-divided into intra-gene epistasis (i.e. a second mutation within the gene harboring the initial mutation that ameliorates the original allele's effects) and inter-gene epistasis (Denver et al., 2010).

As the target size for compensatory mutations is larger than that for reversion, compensation is generally more probable than reversion of a deleterious variant (Szamecz et al., 2014). This prediction has been widely corroborated in studies employing viruses, bacteria, and eukaryotes (Burch and Chao, 1999; Estes and Lynch, 2003; Maisnier-Patin et al., 2002; Nagaraja et al., 2015; Poon et al., 2005). Analysis of *Caenorhabditis elegans* in which mutation-accumulation (MA) approaches led to deleterious mutations and subsequently evolved population sizes greater than 1,000 worms found that fitness recovery was largely due to compensatory mutation (Denver et al., 2010; Estes and Lynch, 2003).

Though a mutation may theoretically occur in any genome location, mutations located in genes with essential functions may lead to lethal or sterile consequences and thus are likely not to be inherited or maintained in the population. Natural selection has no influence on which parts of the genome undergo mutation- rather natural selection acts on preexisting variation. In contrast to the evolutionary force of genetic drift discussed in

Chapter 3, natural selection is more powerful in large population sizes (Bromham, 2009; Fisher, 1930).

Natural selection can take many forms and act with different intensities (Vasseur and Quintana-Murci, 2013). There are three canonical types of natural selection: Purifying selection, positive selection, and balancing selection. Purifying selection, also referred to as negative selection, is a common type of natural selection and affects most genes (Bamshad and Wooding, 2003; Nielsen et al., 2005). Purifying selection removes variants within a population that are disadvantageous within the environmental context. The degree to which the variant is deleterious determines the magnitude of imposing purifying selection. If a neutral variant happens to be linked to a deleterious variant experiencing purifying selection, it too may experience reduction or elimination from the population a phenomenon known as background selection (Vasseur and Quintana-Murci, 2013). A signature of strong purifying selection is a major deficit of non-synonymous mutations relative to synonymous mutations (Holmes, 2003; Kryazhimskiy and Plotkin, 2008).

Advantageous genetic mutations that increase organismal fitness may increase in frequency within a population when acted upon by positive selection, also referred to as directional selection (Nielsen et al., 2005). Strong positive selection will lead to an increase in the chosen advantageous mutation within the population and as a consequence will eliminate non-associated variation, a process termed a selective sweep, and resulting in an overall reduction of genetic diversity for the locus in question (Bamshad and Wooding, 2003). In contrast, if neutral or slightly deleterious variants are linked to mutations experiencing positive selection they will also experience an increase in frequency within

the population, a process known as genetic hitchhiking (Vasseur and Quintana-Murci, 2013).

Experimental studies on asexual (selfing) or nearly-asexual species, have demonstrated a higher incidence of hitchhiker variants (McDonald et al., 2016). Lacking recombination, beneficial and compensatory mutations do not possess a mechanism to discard neutral or slightly deleterious variants (Cloney, 2016). In order to eliminate the neutral or slightly deleterious variants, selection must act on whole chromosomes (Lane, 2014). This leads to an accumulation of slightly deleterious variants, and reduces genetic variation as selective sweeps for specific variants remove variation in linked genes within the population (selective interference) (Keightley and Otto, 2006).

Selfing also has another detriment- it reduces effective population size through background selection, diminishing neutral variation and reducing the rate of adaptation (Kamran-Disfani and Agrawal, 2014). Outcrossing (sexual reproduction) may increase the rate of adaptation but carries an opportunity cost (Cloney, 2016). In species lacking parental care, all investment in offspring is through gametic maintenance (Chasnov and Chow, 2002). The gender in which fertilization occurs must invest significantly more resources into their gametes yet the opposing gender contributes approximately an equal number of genes. Self-fertilizing hermaphrodites that produce only hermaphroditic offspring could potentially double the number of grandchildren (Smith, 1978). Nevertheless, these costs of sexual reproduction may be outweighed in during times of stress when selfing organisms may benefit from an increase in the outcrossing rate (Morran et al., 2009). Sexual reproduction recombines nuclear genes every generation,

facilitating selection against slightly deleterious variants which in turn may slow the evolution rate (Lane, 2014).

Evolutionary rate is a measure of change in a lineage across generations (Lenski, 2001). Evolutionary rate may differ from mutation rate as deleterious mutations impose a fitness cost and tend to be removed from the population via natural selection (Nishant et al., 2009). The neutral theory of molecular evolution predicts that the evolutionary rate at neutral sites is equal to the mutation rate (Kimura, 1984). Comparison of the evolutionary rate and mutation rate of the same species can be compared to predictions by the neutral theory of evolution and provide opportunity to access the influence of evolutionary forces on a specific population.

Recovery from deleterious mutation facilitated by the evolutionary force of natural selection may be gradual or rapid. Fisher predicted that advantageous mutations with smaller increments should be more common than advantageous mutations with large step sizes (Fisher, 1930). This process of small incremental increases in fitness is predicted to occur more frequently in small populations and for species with reduced mutation rates as the rate of beneficial mutations is estimated to be low (Barroso-Batista et al., 2014). Research on the RNA virus $\Phi6$ which evolved mutationally degraded lines in larger population sizes was also observed to follow Fisher's prediction. Recovery of the viral lines usually exhibited smaller step sizes and step size was proportional to the size of the population (Burch and Chao, 1999). A study on HIV-1 has demonstrated adaptation of the virus to the new host through acquisition of mutations that permit escape from the host immune response and are often accompanied by compensatory mutations that partially recover fitness costs. This work also revealed that HIV-1 reverts mutations that are targeted

in the transmitting host but not in the new host (Nagaraja et al., 2015). Research analyzing bacteriophage ΦΧ174 lines recovering from deleterious mutation revealed that approximately 70% of the mutations responsible for fitness increases were compensatory with only ~30% of the beneficial mutations due to direct mutational reversals (Poon et al., 2005). The study employing the RNA virus Φ6 discussed previously, largely attributes the recovery to compensatory mutation with a minimum contribution of 87%-100% (Burch and Chao, 1999). Investigation on the deleterious effects of antibiotic resistance in *Salmonella typhimurium* lab populations detected over 95% of the beneficial mutations were compensatory (Maisnier-Patin et al., 2002). An experimental evolution study evolving *Caenorhabditis briggsae* in a range of population sizes demonstrated this phenomenon observing that populations of larger sizes were more likely to exhibit a decrease in selfish genetic elements over time. Moreover, it was also observed in some strains evolving in small population sizes that the selfish element accumulated and diversified (Phillips et al., 2015).

In this research we investigate evolutionary adaptive recovery by combing experimental evolution and WGS approaches. We used the same well-characterized *C. elegans gas-1* mutant employed in Chapters 2 and 3 to investigate if and how *gas-1* worms could evolve to recover from the deleterious effects imposed by the *gas-1* mutation. We applied Illumina HiSeq methodology to analyze nuclear and mitochondrial genomes of twenty-four *gas-1* biological replicates maintained in a large population size (N= ~1,0000) for sixty generations. Bioinformatic analysis identified and characterized all mitochondrial and nuclear mutations in all twenty-four recovery (RC) *gas-1* lines and the *gas-1* and N2 progenitor. We then conducted interactome analysis to determine if

nuclear mutations in the *gas-1* RC lines occurred in genes that interacted within 2-degrees of the *gas-1* network. Additional work calculated the evolutionary rate for the twenty-four *gas-1* RC lines and assessed mitochondrial DNA copy number in all twenty-six lines. Fitness assays and male frequency assessments were conducted in Dr. Suzanne Estes' Lab at Portland State University. This work reveals new insights on recovery from mitochondrial dysfunction imposed by the *gas-1* mutation and provides a complementary framework for analysis to Chapters 2 and 3. Comparison of *gas-1* mutant evolution in large population sizes versus populations experiencing bottlenecking permits a comprehensive perspective of genome evolution in response to the *gas-1* gene and how it differs when *gas-1* worms are evolving in a small or large population.

4.3 Materials and Methods

4.3.1 Strains and backcrossing of *gas-1* mutant

This study utilized the *gas-1* (*fc21*) mutant containing a C → T point mutation that replaces a highly conserved arginine with lysine in the GAS1 protein, a central component of mitochondrial ETC Complex I. Because *gas-1* (*fc21*) originated from an ethyl methanesulfonate (EMS) mutagenesis screen, the strain was likely to contain many other mutations (Kayser et al., 1999b). We therefore backcrossed the *gas-1* strain, CW152, obtained from the *Caenorhabditis* Genetics Center (University of Minnesota) to our wild-type N2 strain for ten generations to create an isogenic mutant strain. Briefly, an N2 male was first mated to a *gas-1* hermaphrodite, producing *gas-1* heterozygous progeny at the F1 generation. Several single heterozygous hermaphrodite offspring were isolated and mated with a N2 male, producing the F2 generation. The F2 progeny were screened for the presence of the *gas-1* mutation using PCR and direct Sanger sequencing

of the amplicon (forward primer: ATCTCCTCAATACGGCACAAG; reverse primer: ATCGTCTCGATTACGTCTCCA), and only hermaphrodites retaining the *gas-1* mutation were maintained. This sequencing confirmation was continued for backcross generations F3-F10 and only *gas-1* heterozygous hermaphrodites were used at each crossing. After ten sequential backcrosses, the resulting *gas-1* heterozygous lineages were allowed to self and the offspring were screened to find nematodes homozygous for the fc21 allele. These *gas-1* homozygous lineages were used to initiate MA lines. All nematodes were cultured under standard laboratory conditions at 20ºC on standard NGM agar plates seeded with OP50 *Escherichia coli.*

4.3.2 Nematode strains and culture conditions

We studied twenty-four RC lines generated from a *gas-1* mutant (G0) progenitor. The RC process allows all evolutionary forces to influence population genetics. A set of 24 *gas-1* RC lines were derived from the offspring of a single backcrossed *gas-1* hermaphrodite (Experimental evolution performed in Dr. Suzanne Estes lab at Portland State University by Jennifer Sullins). Lines were maintained in population sizes of approximately 1,000 worms for 60 generations after which time they were harvested for sequencing (Stiernagle, 2006). To maintain age-synchronized populations with approximately 1,000 individuals, a pellet of eggs was transferred into a microcentrifuge tube and resuspended in 1 ML of M9 Buffer. Following brief vortexing to create uniform dispersion within the column, 1 µL of solution was removed and pipetted into eight wells on an eight-well printed slide. An average of eggs in each well was counted and the appropriate volume to obtain 1,000 worms was calculated. Every five generations two

plates of each replicate was produced following age-synchronization with one plate being employed to continue the evolution sequence and the other for freezing samples.

4.3.3 L1 stage DNA preparation for Illumina-HiSeq 3000 RC lines

Twenty-four RC lines propagated from a single *gas-1* progenitor as well as the N2 progenitor and the backcrossed *gas-1* were developmentally synchronized by bleaching according to standard protocols (Wood, 1988). An additional eight *gas-1* MA lines maintained along with the line MA lines from Chapter 2 (See Chapter 2 Materials and Methods) were also synchronized by bleaching according to standard protocols (Wood, 1988). First larval (L1) stage nematodes were harvested and DNA was purified using Qiagen DNeasy Blood & Tissue kit (Valencia, CA) with one modification to the manufacturer's protocol. Prior to adding AL buffer, worms in a solution of M9 buffer, ATL, and Proteinase K were subjected to five cycles of freezing and thawing to break worm cuticles and allow efficient DNA extraction. DNA was prepared for sequencing using standard NanoPrep protocols for genomic DNA by the Oregon State University Center for Genome Research and Biocomputing. Samples were individually barcoded and pooled for a single Illumina-HiSeq 3000 also operated by the Oregon State University Center for Genome Research and Biocomputing.

4.3.4 Illumina-HiSeq 3000 read mappings and analyses

We applied the same criteria to read mappings applied in Chapters 2 and 3. Following our Illumin-HiSeq 3000 run, reads were aligned to the *C. elegans* genome (version WS242) using CLC Genomics Workbench (CLC Bio-Qiagen, Aarhus, Denmark). All reads were paired-end (2 x 150bp) and mapped using the following parameters: No masking, mismatch cost = 2, insertion cost = 3, deletion cost = 3, length

fraction = 0.98, read fraction = 0.98, global alignment = no, non-specific match

handling= map randomly.

4.3.5 Bioinformatic analyses of mtDNA copy number

mtDNA copy number was normalized by nuclear DNA (nDNA) content.

Specifically, relative mtDNA for each line was calculated as the line-specific average

mtDNA coverage divided by the line-specific average coverage of three single-copy

nuclear genes: *ama-1*, *ego-1*, and *efl-2*. The AT-rich region of the mitochondria genome

was not considered in these calculations due to inconsistencies during sequencing created

by its repetitive nature.

We tested normalized mtDNA copy number data for normality and consistent

variance. A Levene's test determined that the data had inconsistent variance (P= 4.96 x

10^{-6}, Levene's test). We applied a Kruskal Wallis H Test with strain as an explanatory

variable to evaluate if there was a statistically significant increase in mtDNA copy

number following evolution in large population sizes. Using normalized mitochondrial

DNA coverage for twelve mitochondrial genes and two ribosomal sequences in each of

the progenitors and respectively twenty-four RC, eight MA lines, and N2 and *gas-1*

progenitors, the analysis determined strain was a significant factor (P = 2.2 x 10^{-16},

Kruskal Wallis H Test). Post-hoc analysis applied a Kruskal Multiple Comparison test in

order to evaluate the significance of normalized mtDNA copy number among pairwise

comparisons of all lines (Supplementary Table C1).

4.3.6 Bioinformatic identification of mtDNA single-base substitution heteroplasmies

Potential line-specific mtDNA variant sites were identified as mitochondrial

genome positions differing from the *C. elegans* reference genome (WS242) and not fixed

within our wild-type N2 lab strain. Heteroplasmy refers to a non-fixed mtDNA variant. Site-specific variant frequency was calculated by dividing the number of variant calls by the total site coverage. To eliminate false positives resulting from sequencing and PCR artifacts, variants were required to be within two standard-deviations of the line-specific mean coverage, have at least six variant calls, and a variant frequency above 2%. We then obtained frequency values of the variant nucleotide for all heteroplasmic sites identified in all RC lines and the N2 and *gas-1* progenitor. These results necessitates subsequent analyses which estimated the HiSeq3000 sequencing error rate in the N2 and *gas-1* progenitor strains. A total of 392 candidate mtDNA single-base substitutions were identified. After filtering candidate mtDNA single-base substitution heteroplasmies, sixteen remained. Three of the sixteen were in the N2 progenitor strain and thirteen were distributed among the *gas-1* RC lines.

Twenty-six of the 392 candidate mtDNA single-base substitutions were a fixed homplasmy located at 12998bp in the *nad-5* gene. This fixed homoplasmic variant is a genetic difference between the Denver-Lab N2 strain and the WS242 *C. elegans* reference genome. Present in both progenitor strains and all twenty-four *gas-1* RC lines, these twenty-six homoplasmic 12998bp variants were eliminated. The 376 eliminated mtDNA single-base substitutions were distributed among 127 mtDNA sites. The majority (n= 317) of these eliminated candidate mtDNA single-base substitutions were located in the AT-rich region (approximately spanning 13327bp-13794bp) and had low-coverage (1-3x) of the variant nucleotide. The remaining fifty-nine candidate mtDNA single-base substitutions were under the required total coverage for the candidate site, which needed to be within two standard-deviations of the line-specific coverage mean and/or did not

meet required coverage for the variant nucleotide (6X). The highest variant coverage in these fifty-nine eliminated candidate sites was 3X.

Sixteen mtDNA single-base substitution heteroplasmies remained after removal of these sixty-two candidates. While this is a conservative approach, likely false-positive mtDNA heteroplasmies and fixed genetic differences between the WS242 *C. elegans* reference genome and the Denver-Lab N2 strain are eliminated.

4.3.7 Determination of Illumina-HiSeq 3000 approximate mtDNA sequencing error rate

For our analysis, the mtDNA sequencing error rate of the *gas-1* and N2 sequenced progenitors was necessary in order to evaluate whether the observed mtDNA heteroplasmies in the *gas-1* RC lines that appeared to be non-inherited from the N2 and *gas-1* progenitors were likely non-inherited (*de novo*) or in contrast, present in the progenitors at low-frequency and inherited. As the error rate of Illumina-HiSeq 3000 sequencing has yet to be determined and as the only source (the UC Davis Genome Center) reports the error rate for 100bp paired-end reads, it was necessary to assess the probable error rate using our own HiSeq 3000 data (Froenicke, 2015). All mitochondrial sites in which a candidate mtDNA heteroplasmy was identified in any RC line and/or the *gas-1* and N2 progenitor strains were excluded from analysis. Eliminating all sites in which potential mtDNA heteroplasmies were located (n=136) provided a data set of non-candidate mtDNA heteroplasmic positions which were in the *gas-1* and N2 progenitors. Analyses for the *gas-1* and N2 progenitor were performed separately with line-specific data.

For each position, the coverage of the four possible nucleotides is known. This allows identification of the majority nucleotide, (i.e. the nucleotide with the greatest coverage). From this subset of mitochondrial DNA positions, the coverage of the three nucleotides that were not the majority nucleotide were summed and used to calculate the site-specific variant frequency and variant count. Variant frequency refers to the summed frequency of the three nucleotides that were not the majority nucleotide and variant coverage refers to the summed coverage of the three nucleotides. The average and standard deviation of the variant frequency and coverage among all non-candidate mtDNA heteroplasmic sites was calculated separately for the *gas-1* and N2 progenitor data. We also assessed how many sites had a variant coverage equal to or greater to the observed heteroplasmy frequency and heteroplasmic coverage in *gas-1* RC line positions of potential parallel evolution. This analysis was also performed in a line-specific manner.

4.3.8 Mitochondrial DNA Mutation Simulation

We conducted a simulation of random mitochondrial single-base mutations in order to assess how likely our results were due to chance. As we observed a total of twelve single-base mitochondrial variants that were not present in either progenitor strain and differed from the *C. elegans* WS242 reference, we employed a custom simulation in Python to generate twelve random mutations in the mitochondrial genome. A total of one-thousand iterations of this simulation were conducted and the outcome was compared to our observed results. In each iteration, the number of random mutations in each of the twelve-protein coding genes was counted and recorded. The number of intergenic tRNA and rRNA mutations were summed together and also counted and

recorded. The intergenic tRNA and rRNA sequences were summed as the emphasis was on protein-coding sequences. In addition to assaying the location of the twelve mutations in each iteration, we also assessed the number of sites which experienced two or more mutations in each iteration which mimicked the result of two independent lines experiencing a mutation at the same site. The number and percentage of synonymous and non-synonymous mutations as well as the ratio of the two mutation types were evaluated and compared to observed results in the *gas-1* RC lines.

We discovered that generating only ten mutations (as this was the number of *de novo* mutations in mtDNA protein-coding regions in the RC lines) produced standard deviations for the percentage of non-synonymous and synonymous mutations that were very large (~15%). The ratio of the two mutation types (approximately 2.2) also had a very large standard deviation (198). Modifying our simulation to generate one-hundred mutations yielded approximately the same percentage of non-synonymous and synonymous mutations (62.4% and 37.6%, respectively), but much lower standard deviations (~4.8%) as well as a moderately lower ratio of non-synonymous to synonymous mutations with a substantially reduced standard deviation (1.7 ± 0.35) (Supplementary Table C2). Comparing these two simulation models in which ten and one-hundred random mutations were generated to published *C. elegans* natural isolate values support the use application of the model in which one-hundred mutations are generated. This simulation is applied in order to predict values expected by chance. Natural isolates are believed to experience strong purifying selection on mtDNA and observed values of non-synonymous and synonymous mutations for these strains are only non-neutral when the simulation model generating one-hundred mutations is applied.

Therefore, the model in which one-hundred mutations are randomly generated is more appropriate for this analysis.

4.3.9 Identification and characterization of *gas-1* RC line nuclear mutations

Candidate SNPs in *gas-1* RC lines were identified as variants that differed from the *C. elegans* reference genome (WS242) and our wild-type N2 lab strain. We applied the same criteria from Chapter 3. To eliminate false positives resulting from sequencing and PCR artifacts, the following criteria were applied: (*i*) at least 5-fold coverage, (*ii*) 100% of reads indicated a single non-reference base, (*iii*) there was at least one read presents from both the reverse and forward strand, and (*iv*) reads in a direction varied upon start/end positions. To eliminate false positives due to cryptic heterozygosity, candidate SNPs present in only one of the twelve strains were retained.

4.3.10 Evolutionary rate analysis of nuclear genome

Evolutionary rate was calculated from pooled *gas-1* RC lines with the equation $K = m/(LnT)$ where K is the base substitution rate (per nucleotide site per generation), L is the number of RC lines, m is the number of observed mutations, n is the number of nucleotide sites, and T is the time in generations as previously described (Denver et al., 2009). Values for n reflect the total number of base pairs surveyed that met the criteria for consideration of a possible mutation site, including a coverage range of 6-45X (Supplementary Table C3). This same approach was extended to conditional rate analysis for the six mutation types and deviation from *gas-1* and N2 MA lines values were evaluated for significance (Supplementary Tables C4 and C5). Standard errors for mutation type rates were approximated as $[K/(nT)]^{1/2}$. We compared observed

conditional rate estimates in the *gas-1* RC lines to Chapter 3 *gas-1* MA lines and published N2 strain values (Denver et al., 2012).

4.3.11 Interaction analyses of genes experiencing *gas-1* RC mutations

We determined if the genes that the *gas-1* RC lines nuclear and mitochondrial mutations were located in exhibited interactions with the *gas-1* gene or with genes that directly interacted with the *gas-1* gene (with two-degrees of *gas-1*). Using Gene Orienteer version 2.25, all genes directly interacting with *gas-1* and their interacting genes were included (i.e. all genes two-degrees away from the *gas-1* genes) (Zhong and Sternberg, 2006). The comprehensive list of first- and second-degree *gas-1* interacting genes is referred to as the "*gas-1*-centric-interactome".

Gene Orienteer computationally integrates interactome data (known gene interactions), gene expression data, phenotype data and functional annotation data from three model organisms: *Saccharomyces cerevisiae, C. elegans,* and *Drosophila melanogaster* in order to predict genome-wide interactions in *C. elegans* (Zhong and Sternberg, 2006). Gene Orienteer's statistical model employs serial logistic regression to predict whether there is an interaction along with a computations algorithm that calibrates the parameters of the explanatory variables. A likelihood ratio assigned a weighted score to five features: (1) identical anatomical expression, (2), phenotype, (3) functional annotation, (4) microarray coexpression, and (5) the presence of interlogs. The likelihood ration evaluates the frequency of gene pairs having a specific feature; a value greater than 1 indicates that the feature is enriched in interacting gene pairs and higher scores are indicative of stronger predictions. Likelihood scores were then integrated to estimate the overall probability that the two *C. elegans* genes interact. A filter was applied to

minimize false positives and exclude genetic interactions among genes in the same orthologous group. Interactions with a predicted value below 0.9 were eliminated although interactions below 4.6 have less evidence. Approximately 8,137 genes in *C. elegans* in Gene Orienteer have interactions above 4.6 (Zhong and Sternberg, 2006).

A simulation in Python was constructed to simulate random mutation in *C. elegans*. As forty non-intergenic nuclear mutations and six mtDNA single-base substitutions present in moderate to high frequency levels (>10%) were observed among the *gas-1* RC lines, forty-six mutations were generated randomly in the *C. elegans* genome. All *C. elegans* genes were incorporated but no intergenic sequences were included. One-thousand iterations of random mutation generation were performed after which the mean and standard deviation of the number of mutations located in genes with interactions 2-degrees of the *gas-1* gene were calculated.

4.4 Results

To investigate how evolving *gas-1* in large population sizes affects mitochondrial and nuclear genomes, we analyzed mtDNA and nuclear genomic changes in the twenty-four *gas-1* RC lines and the N2 and *gas-1* progenitor (G0) using Illumina-HiSeq 3000. An average of 81% of reads mapped to the *C. elegans* WS242 reference genome in all lines with a mean nuclear coverage of 24.1X and a mean mitochondrial coverage of 1059.8X (Table 4.1). As in Chapter 2, analysis of Illumina nDNA sequence data showed that all *gas-1* MA lines remained homozygous for the *gas-1* mutant allele.

4.4.1 Bioinformatic analyses of mtDNA copy number

We analyzed mtDNA copy number in the *gas-1* RC and progenitor lines using the method from Chapter 2. mtDNA copy number was normalized using the average

coverage of three single-copy nuclear genes (Table 4.2). A Kruskal Multiple Comparison

test determined the N2 and *gas-1* progenitor were not significantly different in

normalized mtDNA copy number from another (120.6X vs 128.2X) (Supplementary

Table C1). All possible pairwise comparisons were evaluated using a Kruskal Multiple

Comparison Test (See Materials and Methods) (Supplementary Table C1). Of the twenty-

four RC lines, only five RC lines were statistically different from the *gas-1* progenitor

(RC 7, RC 8, RC 9, RC 10, RC 11) with the remaining nineteen lines exhibiting no

statistical deviation in mtDNA copy number from the *gas-1* progenitor. The average

normalized mtDNA copy number of RC lines was 157.7X, approximately 1.23 times

higher than the *gas-1* progenitor. This is substantially lower than the increase from

Chapter 2 in the *gas-1* MA lines in which MA lines ranged from 2.2 -3.4 times higher

than the *gas-1* progenitor (See Chapter 2). Coverage patterns across sites were consistent

among lines (Figure 4.1).

4.4.2 Bioinformatic identification of mtDNA variants

All mitochondrial mutations, both fixed changes and heteroplasmies were

identified and characterized in the *gas-1* RC lines and the N2 and *gas-1* progenitors

(Table 4.3). Candidate heteroplasmic single-nucleotide substitutions were filtered to

eliminate false-positives (see Materials and Methods). The N2 progenitor strain harbored

three single-base substitutions that differed from the WS242 *C. elegans* reference strain.

All three were synonymous and two of the three single-base substitutions were in coding

regions. One single-base substitution the N2 progenitor harbored was a variant in the *cytb*

sequence at 99% frequency. This variant was absent in the *gas-1* progenitor and only

detected in one RC line, RC 13, at levels of 6.7%. A second variant in the N2 progenitor

was detected in the *COX-I* sequence at 99% frequency which was not retained in either the *gas-1* progenitor tRNA sequence or any RC lines. The N2 progenitor harbored one single-base variant that occurred in the *tRNA-Gln* sequence. While harbored at nearly fixation (99.5%) this variant was absent in the *gas-1* progenitor as well as all *gas-1* RC lines. The *gas-1* progenitor did not contain any mtDNA single-nucleotide substitutions.

A total of thirteen single-base substitutions in mtDNA among the twenty-four *gas-1* RC lines was observed (Table 4.3). RC 13 harbored the single instance of a likely-inherited mtDNA heteroplasmy. Present in the N2 progenitor strain in the *cytb* gene at levels near fixation, this heteroplasmy was determined to be approximately 6.7% in RC 13. The remaining twelve single-base substitution heteroplasmies identified in the *gas-1* RC lines were likely *de novo*.

These twelve mtDNA mutations were absent in the N2 and *gas-1* progenitors (Table 4.4). Two of the twelve likely *de novo* single-base substitution variants occurred in tRNA and rRNA gene sequences of the mitochondrial genome among the twenty-four *gas-1* RC lines. RC 17 experienced a low–frequency variant in the sequence for *tRNA-Glu* and RC 19 harbored a low-frequency variant in the *16S-rRNA* sequence. Both heteroplasmies were determined to be low-frequency (~3.0%). Ten likely *de novo* single-nucleotide substitution heteroplasmies occurred in protein-coding regions of the mitochondrial genome among the twenty-four *gas-1* RC lines (Table 4.3).

These ten variants were not detected in either the N2 or *gas-1* progenitor strain at frequency levels above the predicted error rate (Table 4.4). A non-synonymous and high-frequency variant located at position 227 in the *NAD-6* gene was shared by three RC lines (RC 13, RC 18 and RC 24). This variant was detected at levels near fixation ranging from

95% in RC 13 to levels greater than 99% in RC 18 and RC 24 (Table 4.3). A second variant was also shared in more than one *gas-1* RC line- a variant at position 1977 located in the *NAD-1* gene sequence. This variant substituted a cytosine nucleotide for a thymine and changed a Serine residue to a Lysine amino acid. *gas-1* RC 5 harbored this variant at high levels (37%) and RC 22 harbored this variant at levels near fixation (>99%). A second *nad-1* heteroplasmic mutation was observed in RC 3 in high-frequency levels (>94%).

Nine out of ten *de novo* single-nucleotide substitution variants were non-synonymous. Three of the ten single-nucleotide substitution variants were located in *nad-3*, three were located in *nad-6*, two occurred in *nad-5,* and two occurred in *cox-I.* RC 3 experienced two single-nucleotide substitution heteroplasmies in coding sequences; one in the *nad-1* sequence at nearly fixed levels that was previously discussed and the other in the *Cox-I* sequence at low-frequency (~2.6%). RC 4 harbored heteroplasmy in the *nad-6* sequence at low frequency (~3.7%). RC 14 harbored the sole synonymous single-nucleotide heteroplasmy in the coding region of *Cox-I* which was present at low levels (~4%). RC 19 harbored a *nad-5* low-frequency (~2.5%) heteroplasmy.

4.4.3   Determination of mtDNA sequencing error rate in progenitor strains

Assessment of the mtDNA sequencing error rate of the *gas-1* and N2 sequenced progenitors was necessary in order to evaluate whether the observed mtDNA heteroplasmies in the *gas-1* RC lines that appeared to be non-inherited from the N2 and *gas-1* progenitors were likely non-inherited (*de novo*) or in contrast, present in the progenitors at low-frequency and inherited. We performed this analysis overall non-candidate sites for each of the two progenitor strains and then conducted additional

analysis specifically to address observed variant frequencies and coverage at mtDNA sites observed to exhibit putative parallel evolution in the *gas-1* RC lines.

In the *gas-1* progenitor, non-candidate mtDNA heteroplasmic sites had a frequency average of 0.21% and a standard deviation of 0.21%. Of the 13,660 non-candidate mtDNA heteroplasmic sites, ~26.1% had a variant frequency of 0. Variant frequency ranged from 0-2.5% in non-candidate mtDNA heteroplasmic sites in the *gas-1* progenitor strain sequenced.

In the N2 progenitor, non-heteroplasmic mtDNA sites had a frequency average of 0.21% and a standard deviation of 0.22%. Of the 13,660 non-heteroplasmic mtDNA sites, ~27.4% had a variant frequency of 0. Variant frequency ranged from 0-2.2% in non-heteroplasmic mtDNA sites in the N2 progenitor strain sequenced.

Variant nucleotide coverage in the *gas-1* progenitor was on average 1.68X with a standard deviation of 1.63X. Of the 13,660 non-heteroplasmic mtDNA sites, ~26.1% had a variant coverage of 0X. Variant coverage ranged from 0X-17X in non-heteroplasmic mtDNA sites in the *gas-1* progenitor strain sequenced.

Variant nucleotide coverage in the N2 progenitor was on average 1.63X with a standard deviation of 1.62X. Of the 13,660 non-heteroplasmic mtDNA sites, ~27.4% had a variant coverage of 0X. Variant coverage ranged from 0X-16X in non-heteroplasmic mtDNA sites in the N2 progenitor strain sequenced.

Variant frequency and coverage values for the *nad-6* 227bp site in the N2 and *gas-1* progenitors was evaluated and compared to how many non-candidate heteroplasmic sites were equal to or greater to the N2 and *gas-1* observed variant frequencies and values. The observed variant frequencies and coverage for the *nad-6*

227bp site in the N2 and *gas-1* progenitor are within estimated sequencing error rates. This analysis was repeated for the *nad-1* 1977bp heteroplasmy. The observed variant frequencies and coverage for the *nad-1* 1977bp site in the N2 and *gas-1* progenitor were also determined to be within estimated sequencing error rates.

4.4.4 Mitochondrial DNA Mutation Simulation

In order to assess how likely chance was responsible for our observed mtDNA mutation results, we conducted one-thousand iterations of a simulation of random mtDNA mutation in which twelve random mtDNA mutations were generated and compared outcomes to our observed results among the *gas-1* RC lines. The simulation, which treated each site in the mitochondrial genome as having an equal chance of experiencing mutation, had on average 4.48% of the twelve mutations generated located in the *nad-6* sequence with a standard deviation of ~6%. Our observed value of 33.33% was substantially greater than the simulation outcome. Compared to the simulation, the percentage of mutations we observed in the *nad-6* gene sequence among the twenty-four *gas-1* RC lines were beyond three standard deviations from the simulation average (Figure 4.2). The observed percentage of mutations in the *nad-6* and *nad-1* gene sequences were substantially beyond corresponding simulation predicted values.

The simulation average for mutations located in the *nad-1* gene sequence was ~8.5% with a standard deviation of approximately 8%. Our observed percentage of mutations in the *nad-1* gene was 25%, two-standard deviations beyond the simulation mean (Figure 4.2) No other mitochondrial protein-coding gene differed between the simulation outcome and our observed values among the *gas-1* RC lines, nor did the intergenic tRNA and rRNA sequences.

The simulation outcomes of the percentage of synonymous and non-synonymous as well as the ratio of non-synonymous to synonymous mutations were compared to our observed values in the *gas-1* RC lines. The simulation model that generated one-hundred random mtDNA mutations was employed for comparison to the observed *gas-1* RC line results as published natural isolate values suggest this model, and not the model that generates ten random mutations, better predicts values expected under neutral evolution. The observed percentage of non-synonymous mutations in the *gas-1* RC lines was beyond five standard deviations of the simulation mean and the observed ratio of the two mutation types was more than twenty standard deviations of the simulation mean indicating that the observed value deviated markedly from simulation predictions (Figure 4.3).

We also assessed how many sites were mutated more than once in the simulation of random mitochondrial mutation. Out of one-thousand iterations, there were ten iterations (1%) which had sites mutated twice and no iterations had sites mutated three or more times. These simulation outcomes contrast to our observed result in the *gas-1* RC lines in which two lines experienced the same mutation in *nad-1* and three *gas-1* RC lines experienced the same mutation in *nad-6*.

4.4.5 Identification and characterization of *gas-1* RC line nuclear mutations

We bioinformatically identified and characterized all nuclear mutations in *gas-1* RC lines. A total of 113 nuclear mutations were detected in the twenty-four *gas-1* RC lines. Of the 113 nuclear mutations, 21 occurred in intron regions, 18 were located in exons, and 64 were intergenic (Table 4.5). Of the 18 exon mutations, 7 were synonymous and 11 were non-synonymous. The average number of mutations experienced by a RC

line was 4.7 with a standard deviation of 2.87. *gas-1* RC 13 experienced the highest

number of mutations events (n= 11) with three *gas-1* RC lines (RC 14, RC 15 and RC 21)

experiencing the lowest amount of mutation events (n= 1) (Table 4.5).

Mutations of six different possible categories were counted and the conditional

rate estimates for the six possible mutation types were calculated. The values from the

gas-1 RC lines were compared to estimates from the *gas-1* MA lines derived in Chapter 2

and published N2 values (Figure 4.4) (Denver et al., 2009). The majority of the 113

mutations were G:C → A:T events (n= 37). The least common mutation event type was

A:T → C:G (n= 9). The condition rate estimates of the six mutation types were compared

to *gas-1* MA line values from Chapter 3 and published N2 MA line values

(Supplementary Tables C4 and C5) (Denver et al., 2012). Like the N2 MA lines, the *gas-1* RC lines demonstrated a significant decrease in the rate of G:C → A:T mutations.

While this mutation type was the most frequently encountered of the six mutation types

in the RC lines, nuclear genome evolution was slower in the RC lines, and therefore the

rate of G:C → A:T transition mutations was still significantly less than the rate exhibited

in the *gas-1* MA lines. Conditional rate estimates for the other five mutation types were

non-significantly changed between the *gas-1* RC and *gas-1* MA lines. The *gas-1* RC lines

exhibited a significant decrease in rate estimates for two mutation types compared to

published N2 values. The rate of G:C → T:A mutations and A:T → T:A transversions

were lower in the *gas-1* RC lines with respect to N2 estimates (Denver et al., 2012). The

remaining four mutation types (A:T → G:C, G:C → A:T, A:T → C:G, and G:C → C:G)

were comparable between published N2 values and *gas-1* RC lines estimates (Figure 4.4).

4.4.6 Evolutionary rate analysis of nuclear genome

Evolutionary rate considers all evolutionary forces influencing inherited genome change across generations. Evolutionary rate was calculated from pooled *gas-1* RC lines (See materials and methods). Evolutionary rate was determined to be $8.02 \times 10^{-10} \pm 7.54 \times 10^{-11}$ per site per generation. This rate of genomic change across time was 2.6 times lower than the mutation rate in *gas-1* MA lines ($2.12 \times 10^{-09} \pm 3.36 \times 10^{-10}$ per a site per a generation) (See Chapter 2) and 3.4 times lower than the mutation rate of published N2 values ($2.7 \times 10^{-09} \pm 1.36 \times 10^{-10}$ per a site per a generation) (Denver et al., 2009). The evolutionary rate value of the *gas-1* RC lines and mutation rate of *gas-1* MA lines and N2 values did not overlap within three-standard errors of the mean, respectively (Supplementary Table C6).

4.4.7 Interaction analyses of genes experiencing *gas-1* RC mutations

We determined if the genes experiencing RC nuclear and mitochondrial mutations exhibited interactions with either *gas-1* or the 101 genes that directly interact with *gas-1* (i.e. within two-degrees of *gas-1*). Using Gene Orienteer version 2.25, all genes directly interacting with *gas-1* and their interacting genes were included (i.e. all genes 2-degrees away from the *gas-1* genes) (Zhong and Sternberg, 2006). The comprehensive list of first- and second-degree *gas-1* interacting genes is referred to as the "*gas-1*-centric-interactome" (Figure 4.2).

We investigated the interaction of all exon and intron nuclear mutations in the *gas-1* RC lines. Of the forty non-intergenic nuclear mutations, ten nuclear mutations and three mtDNA mutations were located in genes that had interactions within two-degrees of the *gas-1* gene and with interactions above 4.6 (Figure 4.5) (Zhong and Sternberg, 2006). The ten nuclear genes with predicted interactions above 4.6 within two-degrees of

the *gas-1* gene were: C55F2.1, *ced-12*, F26F2.7, F10F2.2, *math-33*, *pph-4.1, slt-1*, *syd-2*, *tir-1*, and Y41E3.7 (Table 4.6). An additional ten mutations (F16A11.1, *fer-1, fkh-9*, F54F11.1, *nlp-20, ppfr-1, puf-4,* R05D7.4, *set-29*, T01B6.1) were also predicted to have interactions with many genes that interact with *gas-1* but had prediction interaction scores under the threshold minimum of 4.6 (Table 4.6).

Three of the six mtDNA mutations (all three located in the *nad-1* gene) are predicted to directly interact with the *gas-1* gene with an interaction score above the threshold minimum. Mutations in the mtDNA *nad-1* gene occurred in three *gas-1* RC lines: RC 3, RC 5, and RC 22. RC 5 and RC 22 harbor a heteroplasmy at 1977bp and RC 3 harbors a heteroplasmy at 2154bp (Table 4.3). Notably, mutations in the mtDNA *nad-6* gene at 227bp were observed in three RC lines (RC 4, RC 13, and RC 24), and present at high frequency levels. The *nad-6* gene is predicted to directly interact with *gas-1* but all predicted interactions of *nad-6* are below the threshold minimum (Table 4.6).

RC 13 harbored ten of the *gas-1* interacting nuclear mutations (F10F2.2, C55F2.1, *math-13)* as well as additional mutations in *nad-6* and *fkh-9* which are predicted to have interactions within two-degrees of *gas-1* but not above the threshold of 4.6. RC 5 experienced three mutations that interacted with the *gas-1* gene (*nad-1*, *slt-1,* and *tir-1*). Two mutations located in gene exhibiting predicted interactions within two-degrees of *gas-1* were observed in RC 20 (Y41E3.7 and *syd-2*) and RC 24 (F26F2.7 and *ced-12*). RC 16 had one mutation event that interacted within 2-degrees of the *gas-1* gene (*pph-4.1*) as did RC 22 (*nad-1*) and RC 3 (*nad-1*) (Table 4.6).

We conducted a simulation of one-thousand iterations of random mutation generation in *C. elegans* in which forty-six mutations were randomly generated and

evaluated the mean and standard deviation of mutations that occurred in genes with interaction within two-degrees of the *gas-1* gene (see Materials and Methods). We also determined the frequency of total mutation events that interacted within two-degrees of the *gas-1* gene for each iteration (Figure 4.6). Out of one-thousand iterations of random mutation generation in *C. elegans,* the mean number of mutations occurring in genes that interacted within 2-degrees of the *gas-1* gene was 5.6 with a standard deviation of 2.25. Only two iterations contained thirteen mutations in genes that interacted within two-degrees of the *gas-1* gene; thirteen was the maximum number of mutations located in genes within the *gas-1*-centric-interactome in a single simulation iteration (Figure 4.6). The majority of iterations of random mutation simulation (n= 734) experienced between four to eight mutations that interacted within two-degrees of the *gas-1* genes (Supplementary Table C7) (Figure 4.6).

4.5 Discussion

Our investigation revealed new insights into the specific mechanisms by which natural selection leads to the adaptive recovery from the deleterious effects imposed by the *gas-1* mutation. We evaluated evolutionary rate, mitochondrial DNA copy number, mitochondrial heteroplasmies, nuclear mutations, and investigated the interactome of *gas-1* RC line mutations. Comparison of these outcomes to the results of similar analyses conducted for the *gas-1* MA lines demonstrates an alternate path of evolutionary changes in response to the *gas-1* gene when evolved in small versus large populations (Chapters 2 and 3).

4.5.1 Evolution of mtDNA

Mitochondrial genome evolution was analyzed in all twenty-four *gas-1* RC lines. We observed prevalent stasis in mtDNA copy number, elevated incidence of non-synonymous mtDNA mutations, heightened incidence of mutations located in genes encoding Complex I subunits, and potential parallel and compensatory mtDNA evolution. We then conducted a simulation of random mitochondrial DNA mutation in order assess how likely our observed results in the *gas-1* RC lines were due to chance. This simulation (1) predicted estimates of the proportion of non-synonymous and synonymous mutations as well as the ratio of non-synonymous to synonymous mutations evaluated, (2) evaluated the likelihood that the observed frequency of mutations in gene encoding Complex I subunits was due to chance, and (3) determined the probability of duplicate (parallel mutation). A total of one-thousand iterations of this simulation was performed and in each iteration the number of random mutations generated was equal to the number in our observed results. The mean and standard deviation of the one-thousand iterations was calculated and compared to our observed results in the *gas-1* RC lines.

4.5.1.1 General stasis in mtDNA copy number

Kruskal multiple comparison tests revealed that 25% of the *gas-1* RC lines experienced significant changes in mtDNA copy number relative to the *gas-1* progenitor (Supplementary Table C1) (See Materials and Methods). This result is significantly different than the results in Chapter 2 in which 40% of *gas-1* MA lines experiences significant changes in mtDNA copy number relative to the *gas-1* progenitor (P= 0.001, X^2 test). The results of the *gas-1* RC lines also demonstrated significant outcomes compared to the N2 MA line result in Chapter 2 in which 80% of N2 MA lines experienced

significant changes in mtDNA copy number relative to the N2 progenitor (P <.00001, X^2 test).

Together, the results of mtDNA copy number from bottlenecked lines and large populations suggests that bottlenecking, but not evolution in a large population size leads to an increase in mtDNA copy number in the *gas-1* strain. In Chapter 2 we proposed three hypotheses to explain the observation that mtDNA copy number increased through bottlenecked *gas-1* and N2 MA lines: (1) oxidative stress, (2) extreme drift and, (3) smaller mtDNA molecules. The research evaluating mtDNA copy number in *gas-1* RC lines alone cannot distinguish between these three hypotheses. However, as the number of lines experiencing significant deviations from their respective progenitors is dramatically more significant between the N2 MA lines and *gas-1* RC lines, in comparison to the *gas-1* MA lines, one hypothesis is that the longer *C. elegans* experience bottlenecking the more dramatic the increase in mtDNA copy number that may be observed. Experiments that evaluate ROS and PCR the whole or a proportion of the mitochondrial genome that contains the AT-rich region for both MA and RC lines may be able to discern these possibilities.

4.5.1.2 High incidence of non-synonymous mtDNA single-base substitution heteroplasmies

We observed an elevated incidence of non-synonymous mtDNA single-base substitution heteroplasmies with nine out of ten likely *de novo* mtDNA mutations characterized as non-synonymous among the RC lines (Table 4.2). The percentages of synonymous and non-synonymous mutation as well as the ratio of the two mutation types was compared with outcomes of a random mtDNA mutation simulation (Figure 4.3). The

mtDNA random mutation simulation predicted approximately 62.4% of non-synonymous mutations and 37.6% synonymous mutations. Under a null hypothesis of dN/dS = 1, consistent with neutral evolution, approximately two-thirds of the mutations are predicted to be non-synonymous with the remaining one-third resulting in synonymous changes (Kimura, 1984). Therefore, the proportion of non-synonymous and synonymous mutations are within one standard deviation of the simulation mean to expected values under neutral selection.

These simulation results provide support for the validity of this approach. The observed percentages of non-synonymous and synonymous mutation types in the *gas-1* RC lines were beyond five standard deviations of the simulation mean revealing that our observed values deviate substantially from simulation expected numbers. As the observed percentages of non-synonymous and synonymous mutations deviated significantly from the predicted simulation values, our results are highly unlikely due to chance.

Our results in which nine of the ten single-base substitution heteroplasmies are non-synonymous are in sharp contrast to observed percentages of non-synonymous and synonymous mutations in *C. elegans* natural isolates which have been reported to have low incidence of non-synonymous mutations (Montooth and Rand, 2008). The ratio of non-synonymous to synonymous mutations in *C. elegans* natural isolates is reported to be 3:25 (0.12) indicative of purifying selection eliminating non-synonymous mutations.

Past research on N2 MA lines has observed increased prevalence of non-synonymous mtDNA mutations but not nearly as dramatic as the results observed in this study among the *gas-1* RC lines. Published values for the N2 MA lines report that nine out of fifteen mtDNA mutations were non-synonymous with a ratio of the two mutation

types of 1.5 (Denver et al., 2000). In light of these findings, our observations in which 90% of mtDNA mutations were non-synonymous in the *gas-1* RC lines suggest the influence of positive selection on mtDNA variation. Although this pattern is consistent with positive selection, the influence of purifying natural selection may still be present as the low frequency and non-synonymous heteroplasmies identified may be deleterious and eliminated with further propagation in large population sizes.

4.5.1.3 Elevated frequency of mutations in gene encoding Complex I subunits

Approximately two-thirds of *de novo* mtDNA single-base substitution heteroplasmies in the RC lines were located in genes encoding Complex I subunits (Table 4.2). Three mtDNA mutations were located in the *nad-1* gene, four occurred in the *nad-6* gene, and one occurred in the *nad-5* gene. In addition to the 1977bp heteroplasmy observed in two *gas-1* RC lines, an additional *nad-1* mutation was observed in RC 3 at 2154bp. Present at levels near fixation (>99%) and non-synonymous, these results might indicate the influence of positive selection.

A simulation of random mtDNA mutation was performed to assess how likely our results were due to chance. One-thousand iterations were conducted with parameters that permitted an equal probability for each mitochondrial position to experience a mutation. While this simulation does not account for mutational bias that may alter the propensity of a site to harbor a mtDNA mutation, comparison to this simulation output to observations in experimental and natural isolate studies allows insight into species-specific patterns of mutational bias and the influence of evolutionary forces on mtDNA mutation. Additionally, the emphasis was on the regions (specific protein-coding genes, intergenic tRNA, and rRNA sequences) randomly-generated mutations were located in

rather than the precise base-pair position in the mitochondrial genome in which mutations occurred. As the simulation percentage of predicted mutations in the tRNA intergenic and rRNA sequences was comparable to our observed values, it suggests that the simulation is a reliable source for mitochondrial DNA mutation estimates. Furthermore, published data reporting the distribution of mtDNA single-base substitutions in N2 MA lines are within two standard-deviations of the simulation mean providing support that this simulation is an applicable methodology (Denver et al., 2000).

The percentage of observed mutations in the *gas-1* RC lines that were located in the *nad-6* sequence (33.33%) was substantially beyond three standard deviations of the simulation average (Figure 4.2). The simulation estimated that ~4.5% of mutations should occur in the *nad-6*. The *nad-6* sequence is 436bp long and one of the shortest gene sequences in the mitochondrial genome with only *nad4L* and *nad-3* being smaller in size. In the N2 MA lines analyzed in Chapter 2, no instances of heteroplasmy in the *nad-6* sequence were observed although in the *gas-1* MA lines 50% (three out of six) heteroplasmies located in *nad-6* were identified. Unlike the *nad-6* heteroplasmies observed in the *gas-1* RC lines, the *gas-1* MA line heteroplasmies in the gene were all low-frequency (range 2-4%) (See Chapter 2). A quarter of *de novo* mtDNA single-base substitutions in the *gas-1* RC lines were located in the *nad-1* sequence. Simulation estimates for *nad-1* mutation are predicted to be 8.49% ± 7.96% (Figure 4.2).

Together the estimates of the simulation and the results of the *gas-1* RC lines suggest that *gas-1* populations may have propensity to experience *nad-6* and *nad-1* heteroplasmies. The near-fixation of the non-synonymous *nad-6* heteroplasmy at 227bp harbored by three RC lines and *nad-1* 1977bp heteroplasmy shared by two RC lines, and

the lack of *nad-6* mutations in N2 MA lines from Chapter 2 coupled with simulation predictions for *nad-6* and *nad-1* mutations, suggest that our observed results of *nad-6* and *nad-1* mtDNA single-base substitution heteroplasmies are not due to chance. Therefore the influence of positive selection may be the driver for our observed result of heighted frequency of *nad-6* and *nad-1* heteroplasmies in the RC lines.

4.5.1.4 Potential parallel and compensatory mtDNA evolution

We observed two separate instances of likely parallel mutation: one at a site in the *nad-6* sequence (227bp) that was shared by three RC lines, and another at a site located in the *nad-1* (1977bp) sequence shared by two RC lines. The *nad-6* variation was non-synonymous and near fixation in two RC lines (RC 18; 99.3% and RC 24; 99.8%) and present at very high levels in the other (RC 13, 94.7%) (Table 4.3). The *nad-1* heteroplasmy was also non-synonymous, near fixation in RC 22 and at moderate levels (34%) in RC 3.

In order to determine if these instances of parallel mutation in the *nad-6* and *nad-1* gene sequences were *de-novo* mutations versus heteroplasmies pre-exisiting in the RC line progenitor, an assessment of the sequencing error rate in the N2 and *gas-1* progenitor strains was performed. For both the N2 and *gas-1* progenitor the average variant frequency for non-candidate heteroplasmic sites was approximately 0.21% ± 0.21%. Both the *nad-1* and the *nad-6* variant frequencies and coverage values were within the estimated error rate for the progenitor strains (See Materials and Methods section 4.3.7: Determination of Illumina-HiSeq 3000 approximate mtDNA sequencing error rate and Results section 4.4.3 Determination of mtDNA sequencing error rate in progenitor strain). These results suggest that the *nad-1* 1977bp and the *nad-6 227bp* mtDNA

heteroplasmies were not inherited from pre-existing heteroplasmies from either the *gas-1* or N2 progenitor strain. These observations support that *de novo* and parallel evolution for the *nad-1* 1977bp mtDNA heteroplasmy in RC 5 and RC 22 and for the *nad-6* 227bp heteroplasmy in RC 13, RC 18, and RC 24.

We compared the outcome of random mitochondrial DNA mutation simulation to our observed results of parallel mutation in the *gas-1* RC lines. This simulation did not take into account the nucleotide substitution and thus comparison to our observed results is more conservation as parallel mutation in the *gas-1* RC lines was not only at the same site but also an identical heteroplasmy. Out of one-thousand iterations in which twelve mtDNA mutations were generated, ten iterations (1%) experienced duplicate mutations at identical sites. There were no instances in the simulation of an iteration experiencing three or more mutations at the same site. We did not observe any instances of the same site experiencing three or more mutations until we increased the number of iterations of random mutation generation to 500,000. This outcome of our simulation suggests that our observed results of two RC lines experiencing the same heteroplasmy in *nad-1* and three RC lines harboring identical mutations in *nad-6* are most likely not due to chance. These results further support that selection may be influencing the perpetuation and near-fixation of the *nad-1* and *nad-6* heteroplasmies.

Gene Orienteer provides substantial evidence for a direct interaction between *nad-1* and *gas-1* (a score of 7.58) but a predicted interaction between *nad-6* and *gas-1* in *C. elegans* of 2.05 (Table 4.6) (Zhong and Sternberg, 2006). Studies on *Escherichia coli,* cattle (*Bos taurus*), and bacteria (*Thermus thermophilius*) have demonstrated that in these organisms the NAD-6 and NAD-1 subunits of Complex I are located in the membrane

arm along with the remaining five core subunits (Efremov and Sazanov, 2011; Pätsi et al., 2008; Sazanov, 2015; Vinothkumar et al., 2014). X-ray crystallography, single particle analysis, and cryo-electron microscopy studies on these model organisms suggest that NAD-1 and NAD-6 interface between the hydrophobic membrane arm and the hydrophilic peripheral arm of Complex I in which the GAS-1 subunit is located (Figure 4.7) (Brandt, 2006; Efremov and Sazanov, 2011; Sazanov, 2015).

gas-1 codes for the core 49 kDa subunit which is the immediate electron donor to ubiquinone and together with PSST, forms the quinone-binding pocket of Complex I (Figure 4.7) (Shiraishi et al., 2012; Vasta et al., 2011a). Observations that mutations in the NAD-1 subunit alter ubiquinone reductase activity and past photoaffinity labeling studies propose that along with GAS-1 and PSST, the NAD-1 subunit may contribute to quinone binding by constituting a hydrophobic pocket (Brandt, 2006; Darrouzet et al., 1998; Kurki et al., 2000). In contrast, NAD-6 may not participate directly in ubiquinone binding however there is evidence from kinetic analysis performed on transmitochondrial cybrids that the NAD-6 subunit may be involved with the interaction between Complex I and ubiquinone (Jun et al., 1996). Further work analyzing *E. coli* cybrids suggests that the NAD-6 subunit may contribute a channel through which the binding site becomes accessible and is compatible with the idea that although NAD-6 may not directly participate in the catalytic reaction it may demarcate the binding cavity of ubiquinone (Pätsi et al., 2008). Therefore, as GAS-1 and the NAD-6 and NAD-1 subunits are suggested to be localized near one another, and as evidence suggests that the NAD-1 subunit may be directly involved in ubiquinone binding with NAD-6 indirectly contributing, it is probable that GAS-1 interacts with the NAD-6 and NAD-1 subunits.

Alternate explanations for the high incidence of mtDNA single-base substitution heteroplasmies located in Complex I subunit, specifically the *nad-1* and *nad-6* genes, including chance, mutational bias and off-target evolution are possible. However, past observations on N2 MA lines discovered only three of the fifteen mtDNA single-base substitution heteroplasmies identified were located in the *nad-1* and *nad-6* genes (Denver, 2000). Considering mutational bias, we observed that 66.66% of mtDNA single-base substitution heteroplasmies were transversion mutations with the remaining third transition substitutions (Table 4.2). Likewise, in Chapter 1, five of the six non-inherited mtDNA single-base substitution heteroplasmies were transversion mutations. Although the numbers in both the *gas-1* MA and RC datasets are small, these observations suggest that *gas-1* animals may exhibits mitochondrial mutation bias towards transversion mutations (A:T → C:G, G:C → T:A, A:T → T:A, and G:C → C:G). In contrast, animal mtDNA is characterized by a strong bias for transition mutations (A:T → G:C and G:C → A:T) (Bhatnagar et al., 1994; Lindahl, 1993). Comparison of two *C. elegans* natural isolates and past values determined from N2 MA lines reveal strong bias towards transition mutations and suggest that this pattern is a reflection of the baseline mutation bias and not selection (Denver, 2000). This comparison cannot determine whether our observed results may be driven by natural selection, perhaps in adaptation to the *gas-1* gene, or a mutational bias of *gas-1* worms. Future studies that characterize mtDNA mutations in *gas-1* populations are necessary to discern whether transversion mutation bias is present in the *gas-1* strain.

In light of these findings, the 227bp and 1977bp heteroplasmies in *nad-6* and *nad-1* observed in the *gas-1* RC lines suggest parallel and potential compensatory evolution to

the *gas-1* mutation. Moreover, the near-fixation of all three RC lines harboring the non-synonymous *nad-6* heteroplasmy and moderate to near-fixation of the two RC lines experiencing the non-synonymous *nad-1* heteroplasmy are consistent with patterns of positive selection. Assays which isolate and evaluate the mitochondrial phenotypes of these mtDNA heteroplasmies may determine their functional consequences within the context of the *gas-1* background.

4.5.2 Nuclear genome evolution

We analyzed nuclear genome evolution in all twenty-four *gas-1* RC lines. Using pooled nuclear mutation data, we determined the evolutionary rate of nuclear genomic change, identified and characterized all nuclear mutations, and analyzed the interactions of nuclear mutations in *gas-1* RC lines. In comparison to published mutation rates, we observed in the RC lines, a rate of nuclear genome change approximately three times slower than that observed in MA lines of the same species. Results of nuclear mutation analysis demonstrate that *gas-1* may exhibit bias towards specific mutational types and suggest a decreased proportion of mutations located in exon sequences between *gas-1* RC lines and N2 MA values which may indicate the influence purifying selection on the nuclear genome.

4.5.2.1 Evolutionary rate analysis of nuclear genome change

We assessed the evolutionary rate of nuclear genomic change among the *gas-1* RC lines and compared this value to published mutation rate for *C. elegans.* Evolutionary rate for pooled the twenty-four *gas-1* RC lines was determined to be 8.01 ($\pm$.75) x10^{-10} per a nucleotide per a generation (See Materials and Methods). This rate of genomic change is approximately 3.4 times slower than that of the mutation rate of *gas-1* MA lines

from Chapter 3 (2.12 ± (0.34) x 10^{-09}) and more than three standard errors of the mean (SEM) away from the mutation rate. In contrast to the experimental system applied in this chapter, the MA approaches applied in Chapter 3 and past MA experiments minimize natural selection and expose worms to extreme genetic drift, allowing the accumulation of slightly deleterious mutations (Kimura, 1984). Evolution in large population sizes, such as in the experimental approach applied here to the *gas-1* RC lines, decreases genetic drift and increases the power of natural selection (Phillips et al., 2015).

The slower rate of evolutionary genomic change within *gas-1* RC large population sizes is indicative that natural selection may be eliminating nuclear genome variation either through purifying or directional selection. As MA approaches lead to the accumulation of slightly deleterious mutations it is likely that the influence of natural selection removed harmful mutations in the *gas-1* RC populations. This prediction would correspond with adaptive evolution in which *gas-1* lines were recovering from the undesirable effects imposed by the *gas-1* mutation. However, as the overall numbers of SNPs occurring in exon sequences is small (n=18), a dN/dS analysis cannot be performed. Therefore, it is not possible to distinguish between positive selection which eliminates variation and causes selective sweeps and purifying selection which removes variation and contributes to background selection.

4.5.2.2 Nuclear Mutation Identification

Nuclear mutations were identified and characterized for all twenty-four *gas-1* RC lines using the same criteria applied in Chapter 3 (See Materials and Methods). The results of the six mutation types were compared to the mutation rates exhibited by the *gas-1* MA lines in Chapter 3 and published N2 values (Figure 4.4) (Denver et al., 2012).

The significantly reduced conditional rate of G:C → A:T mutations in the *gas-1* RC lines relative to the *gas-1* MA lines, and the significantly lower conditional rates of G:C →T:A and A:T →T:A transversions in the *gas-1* RC lines relative to the N2 MA lines are indicative of slower nuclear genome evolution and suggest the influence of purifying selection.

In the *gas-1* MA lines, the majority of nuclear mutations (40%) were observed to be G:C →A:T. This was also observed in the *gas-1* RC lines in which the majority (approximately 32.7%) of nuclear mutations were G:C → A:T. The observed results in the *gas-1* MA and RC lines suggest that the *gas-1* strain may have similar mutational bias to experience an increase in A:T → G:C transition mutations, However it should be noted that although the proportion of A:T → G:C mutations differed significantly between the *gas-1* RC lines and published N2 values, the rate of A:T → G:C mutations was nearly identical (Figure 4.4). Therefore the proportion of A:T → G:C mutations in the *gas-1* RC lines is elevated significantly to published N2 values but not the rate at which A:T → G:C mutations occur (Denver et al., 2012).

The transition/transversion (Ts/Tv) base-substitution ratio is 1.35 for the *gas-1* MA lines and 1.04 for the *gas-1* RC lines. Although the Ts/Tv ratio in the N2 MA lines was 0.45 (range of 0.19-0.79), studies investigating neutral sequences (pseudogenes, intergenic sequences and silent codon positions) of *C. elegans* natural isolates report Ts/Tv ratios around 1.3 (Denver et al., 2009; Swan et al., 2002; Wicks et al., 2001). While the Ts/Tv ratio in the *gas-1* MA lines is within predicted values for neutral evolution, the lower Ts/Tv ratio in the *gas-1* RC lines suggests mild to moderate influence of non-neutral evolutionary forces.

There were a total of eleven non-synonymous mutations and seven synonymous mutations in the gas-*1* RC lines. The ratio of non-synonymous to synonymous mutations in the RC lines (1.57) was substantially lower that the ration of nonsynonymous to synonymous mutation value *gas-1* MA lines from Chapter 3 (2.25) and roughly equivalent to published N2 values (1.63) (Denver et al., 2009). Statistical assessments of the percent of mutations located in exon regions revealed a decreased and significant difference between the *gas-1* RC and *gas-1* MA lines (15.9% versus 32.5%, respectively) (P= 0.0004, X^2 test). In addition, the *gas-1* RC lines exhibited lower incidence of exon mutations that were significantly different from the published N2 values (37.6% exon mutations) (P=0.00001, X^2 test) (Denver et al., 2009).

While the ratio of non-synonymous to synonymous mutations may be comparable to N2 values, the dramatically decreased percentage of exon mutations in the *gas-1* RC lines suggests purifying selection. It is possible that while directional natural selection may be influencing the fixation of nuclear mutations in genes that are beneficial and/or compensatory to the *gas-1* mutation, purifying selection is eliminating exon variation. The decreased incidence of exon mutation suggestive of purifying selection is also supported by the evolutionary rate of nuclear genomic change which is significantly lower than published mutation rate values for *C. elegans* (Denver et al., 2009).

4.5.3 Interactome analysis of mitochondrial and nuclear mutations

We discovered that 25% of the forty non-intergenic nuclear mutations and three of the six mitochondrial mutations (50%) with moderate to high-frequency (>10%) heteroplasmic levels, were located in genes that exhibit interactions above the threshold value of 4.6 within 2-degrees of the *gas-1* gene (i.e. the *gas-1*-centric-interactome)

(Figure 4.5) (Table 4.6). This proportion of nuclear mutations that are located in the *gas-1*-centric-interactome is markedly similar to the results observed in the *gas-1* MA lines in which ~26% of mutations were located in genes residing in the *gas-1*-centric-interactome (See Chapter 3). In both the *gas-1* MA and RC lines, statistical tests determined that the number of mutations located in genes residing in the *gas-1*-centric-interactome was significantly elevated compared to simulation predicted values. Additionally, the raw percentage of the number of non-intergenic observed mutations located in the *gas-1*-centric-interactome was more than the number of observed mutations residing in the *gas-1*-centric-interactome in the N2 MA lines (~18.3%, See Chapter 3) and. This evidence suggests that compensatory evolution is occurring in both the *gas-1* MA and RC experimental systems. However, unlike the *gas-1* RC lines, no mitochondrial mutations were observed in moderately-high frequency levels in the *gas-1* MA lines.

Compared to our results of random mutation simulation in which an average of 5.6 mutations were located in genes that exhibit interactions within 2-degrees of the *gas-1* gene, our observed results in which thirteen of the forty-six nuclear and mitochondrial mutations are located within the *gas-1*-centric-interactome are beyond three standard deviations of the simulation mean (Figure 4.6). Ten of the forty RC line non-intergenic nuclear mutations and three of the six mitochondrial mutations occurred in genes that exhibit interactions within 2-degrees of the *gas-1* gene. Statistical analysis found this results to be significant (P= 0.001, X^2 Test). However, out of one-thousand iterations, only two iterations (0.2%) had a result in which thirteen mutations were located in genes that exhibit interactions within 2-degrees of the *gas-1* gene (Figure 4.6). No iterations had greater than thirteen mutations located in genes within the gas-*1*-centric-interactome.

Compared to the N2 and *gas-1* MA line interactome simulation results in Chapter 3, the observed results in the *gas-1* RC lines farther from the simulation predictions (beyond three standard deviations of the simulation mean) have the least amount of iterations that produce an equal or greater result.

The ten RC line nuclear mutations exhibiting interactions within 2-degrees of the *gas-1* gene above the threshold minimum of 4.6 are: F10F2.2, C55F2.1, Y41E3.7, *syd-2,* F26F2.7, *ced-12, tir-1, math-33, slt-1* and *pph-4.1* (Table 4.8). An additional ten RC line nuclear mutations were observed to have interactions within 2-degrees of the *gas-1* gene but do not meet the minimum threshold values (F16A11.1, F54A11.1, *fer-1, fkh-9,* K07C5.2, *ppfr-1, puf-4,* R05D7.4, *set-29*, and T01B6.1. More work is needed to assess if these ten mutations are beneficial or compensatory to the *gas-1* mutation, but studies investigating these ten genes may provide insight into their function and effect on mitochondrial activity in *C. elegans.*

Three RC lines harbored mitochondrial mutations in the *nad-1* gene, which is predicted to directly interact with *gas-1* with interaction values above the threshold minimum of 4.6. Previously discussed, two RC lines were observed to harbor the same mitochondrial mutation located in *nad-1* at 1977bp (RC 5 and RC 22)

An additional and different *nad-1* heteroplasmy was observed in RC 3 at 2154bp present at levels near fixation (>99%) (Table 4.3) Two RC lines were observed to harbor a mtDNA heteroplasmy in the *nad-6* gene but the interaction score of *nad-6* directly interacting with *gas-1* was below the threshold value (Table 4.6). For a detailed discussion on the interactions of *nad-1* and *nad-6* please refer to section 4.5.1.4 on Potential parallel and compensatory mtDNA evolution**.**

An intron mutation in the *tir-1* sequence was experienced in RC 5. A study which inactivated *tir-1* via RNA interference in *C. elegans* revealed that TIR-1 inactivation increased susceptibility to infection. In addition, the F-subunit of ATP synthase was demonstrated to interact with TIR-1 suggesting that this protein may not only have immune related activity but may also be crucial in energy production (Couillault et al., 2004). RC 5 experienced a second intron mutation located in a gene which exhibited interactions within 2-degrees of the *gas-1* gene above the threshold minimum, *slt-1*. Research on *slt-1* gain-of-function and loss-of-function mutations in *C. elegans* supports that SLT-1 is involved in cell and axon guidance and plays a key role in the developing nervous system (Hao et al., 2001). Gene Orienteer predicts that *slt-1* has interactions with many antioxidant genes including *sod-1, sod-3* and *sod-5* but it is unclear how this intron mutation of *slt-1* would affect ROS levels in RC 5. Given the critical role of *slt-1* in the developing nervous system, it may be more likely that the intron mutation in *slt-1* is neutral or slightly deleterious.

RC 13 experienced three intron mutations located in genes that exhibit interactions within 2-degrees from *gas-1* and above the threshold minimum. Not much is known about F10F2.2 but C55F2.1 has been shown to be involved in reproduction and *math-33* has activity in embryo development (Heimbucher et al., 2015; Maeda et al., 2001). MATH-33 also exhibits roles in oxidative stress response, longevity and metabolism by promoting the DAF-16 stabilization (Heimbucher et al., 2015). More work is needed to address the consequences of these three intron mutations which possibly compensate for one another in addition to the *gas-1* mutation.

RC 16 harbored an intron mutation in *pph-4.1*. PPH-4.1 activity is critical in embryo development and loss of PPH-4.1 has been shown to reduce the number of recombination effects and lead to meiotic nondisjunction and embryonic lethality (Han et al., 2009). *pph-4.1* has only one predicted interaction within two-degrees of the *gas-1* gene: *hda-1*. *hda-1* is essential for embryonic viability and gonadogenesis in *C. elegans* (Dufourcq et al., 2002). A reproductive assay on the isolated *pph-4.1* mutation would be useful to discern the consequences of this mutation on reproductive fitness in *C. elegans.*

RC 20 experienced two intron mutations that were located in genes exhibiting interactions above the threshold minimum within two-degrees of the *gas-1* gene: Y41E3.7 and *syd-2* (Table 4.8). Y41E3.7, an ortholog of human TMED8, is predicted to have fatty-acyl-CoA binding activity (Camon, 2003; Mulder, 2003). Acyl-CoA binding proteins buffer the intracellular concentration of unbound acyl-CoA esters (Faergeman and Knudsen, 1997). Studies on the mitochondrial adenine nucleotide translocase (ANT) which catalyzes the exchange of ATP synthesized in the mitochondria for cytosolic ADP demonstrate that activity is the rate-limiting step in mitochondrial energy metabolism (Khopp et al., 1977; Kim et al., 2010; Lemasters and Sowers, 1979). Acyl-CoA esters have revealed to be potent inhibitors of ANT in mitochondria and is possible that the intro mutation in Y41E3.7 is modifying the pool of unbound acyl-CoA esters leading to altered ATP production in mitochondria (Faergeman and Knudsen, 1997). Evaluation of ATP production in an isolated strain harboring the Y41E3.7 intron mutation may provide insight into its effects.

syd-2, the second gene in which RC 20 harbors an intron mutation, is required for establishing appropriate presynaptic density and is expressed in all neuronal and muscle

cell in *C. elegans* (Serra-Pages, 1998; Zhen and Jin, 1999). *syd-2* has one interaction that directly interacts with the *gas-1* gene, *unc-9*. *unc-9* is critical for reproduction and defects in the *unc-9* sequence reduce the egg-laying in *C. elegans* (Barnes and Hekimi, 2002). Interestingly, in some cases, mutations in *unc-9* block hypersensitivity to volatile anesthetics and as a characteristic phenotype of *gas-1* mutants is increased sensitivity to volatile anesthetics, the intron in *syd-2* may be indirectly related to altered sensitivity to volatile anesthetics in RC 20 (Barnes and Hekimi, 2002; Kayser et al., 2001). Exposing a strain of *gas-1* with the isolated *syd-2* mutation to halothane would be relevant to ascertain this hypothesis.

RC 24 experienced two mutations located in genes that have interactions within two-degrees of the *gas-1* gene (Table 4.8). One mutation was located in an exon sequence of *ced-12* and was non-synonymous, substituting a phenylalanine amino acid for a serine residue. The second mutation was in an intron sequence of F26F2.7. CED-12 plays key roles in apoptosis, as the protein is required for phagocytic engulfment of apoptotic cells, in addition to being necessary for cell migration during development (Gumienny et al., 2001). ROS production may lead to activation of apoptosis; as *gas-1* worms have increased ROS production it is possible that the mutation in *ced-12* observed in RC 24 may be modifying the phagocytic processing of apoptotic cells (Kondo et al., 2005; Mates and Sanchez-Jimenez, 2000).Whether this effect is beneficial or deleterious (or even occurs!) could be investigated by assessment of phagocytosis of apoptotic cells by quantification of engulfment.

ced-12 has only one interaction with a gene that directly interacts with *gas-1*, *hda-1* (Table 4.8) (Zhong and Sternberg, 2006). As discussed previously in the interactome

results of RC 16, *hda-1* is required for embryonic viability and gonadogenesis in *C. elegans* (Dufourcq et al., 2002). A reproductive fitness assay would be useful to determine if this non-synonymous mutation alters reproductive production in a strain with the *ced-12* mutation isolated.

F26F2.7, the gene in which the second mutation experienced by RC 24 located in the *gas-1*-centric-interactome is an ortholog of human TAPT1 and is predicted to be involved in embryo development (Maeda et al., 2001). The three genes with which F26F2.7 interacts with that directly interact with *gas-1* are: *ero-1, sod-2* and *sod-3* (Table 4.8). All three of these genes have antioxidant activity and *sod-2* and *sod-3* are have been demonstrated to locate to mitochondria in *C. elegans* (Doonan et al., 2008; Harding et al., 2003; Yanase et al., 2002). Mutant strains with deletion alleles of *sod-2* and *sod-3* have exhibited delayed and reduced reproduction although only the double *sod-2*:*sod-3* mutant demonstrates hypersensitivity to hyperoxia (Doonan et al., 2008). Based on these past findings, assays of reproductive fitness, ROS production, and sensitivity to hyperoxia in an isolate strain with the F26F2.7 intron mutation may provide information on the consequences of the mutation's effects.

4.6 Conclusion

This research demonstrates adaptive recovery to the *gas-1* mutation through alternate evolutionary paths of mitochondrial and nuclear genomic modifications. Our investigation across sixty generations of experimental evolution revealed mtDNA mutations consistent with patterns of parallel and potential compensatory evolution and identified prospective beneficial and/or compensatory nuclear mutations to the *gas-1* mutation. Furthermore, observations of the relative incidence of non-synonymous and

synonymous mtDNA mutations and high-frequency of mtDNA heteroplasmies in the RC

lines suggest the influence of positive selection in shaping mtDNA variation. The results

of this study in which populations were evolved in large population sizes suggest that

mtDNA copy number is more inclined to increase in small but not large populations of *C.

elegans gas-1* nematodes.

There is evidence that is suggestive of both positive and purifying selection

influencing nuclear genome variation among the *gas-1* RC lines. The nuclear

evolutionary rate which is three times lower than the *C. elegans* mutation rate indicates

purifying selection on nuclear DNA. Our observation of a quarter of nuclear mutations

occurring in genes that exhibit interactions two-degrees away from the *gas-1* gene is

suggestive of positive natural selection, in the shape of interlocus compensatory

evolution, on nuclear genome variation and may be compared to future studies which

explore evolutionary adaption to harmful mutation. The lower incidence of exon

mutations indicates purifying selection removing exon variation among *gas-1* RC lines.

Isolation of nuclear mutations located in the *gas-1*-centric-interactome and in RC lines

that significantly recovered from the *gas-1* mutation as well as functional analysis of the

mitochondrial heteroplasmies demonstrating parallel evolution in the *nad-1* and *nad-6*

genes would provide insight on the phenotypic effects of these genomic changes and may

suggest relevant targets for ameliorating Complex I impairment.

4.7 References

Bamshad, M., and Wooding, S. (2003). Signatures of natural selection in the human genome. *Nat. Rev. Genet.* 4, 99–111. doi:10.1038/nrg999.

Barnes, T. M., and Hekimi, S. (2002). The Caenorhabditis elegans Avermectin Resistance and Anesthetic Response Gene unc-9 Encodes a Member of a Protein Family Implicated in Electrical Coupling of Excitable Cells. *J. Neurochem.* 69, 2251–2260. doi:10.1046/j.1471-4159.1997.69062251.x.

Barroso-Batista, J., Sousa, A., Louren??o, M., Bergman, M. L., Sobral, D., Demengeot, J., et al. (2014). The First Steps of Adaptation of Escherichia coli to the Gut Are Dominated by Soft Sweeps. *PLoS Genet.* 10. doi:10.1371/journal.pgen.1004182.

Bhatnagar, A., Suresh Nair, K. R., Kumar, R., Chalapati, K., and Patro, Y. G. K. (1994). Study of Cross Coupling in Transition Bends Using Cascaded Coupler Segment Method. *IEEE Photonics Technol. Lett.* 6, 1004–1007. doi:10.1109/68.313077.

Brandt, U. (2006). Energy converting NADH:quinone oxidoreductase (complex I). *Annu. Rev. Biochem.* 75, 69–92. doi:10.1146/annurev.biochem.75.103004.142539.

Bromham, L. (2009). Does nothing in evolution make sense except in the light of population genetics? *Biol. Philos.* 24, 387–403. doi:10.1007/s10539-008-9146-6.

Burch, C. L., and Chao, L. (1999). Evolution by small steps and rugged landscapes in the RNA virus ??6. *Genetics* 151, 921–927.

Camon, E. (2003). The Gene Ontology Annotation (GOA) Project: Implementation of GO in SWISS-PROT, TrEMBL, and InterPro. *Genome Res.* 13, 662–672. doi:10.1101/gr.461403.

Chasnov, J. R., and Chow, K. L. (2002). Why are there males in the hermaphroditic species Caenorhabditis elegans? *Genetics* 160, 983–994.

Cloney, R. (2016). Molecular evolution: Friends with benefits - sex speeds up adaptation. *Nat. Rev. Genet.* doi:10.1038/nrg.2016.32.

Couillault, C., Pujol, N., Reboul, J., Sabatier, L., Guichou, J.-F., Kohara, Y., et al. (2004). TLR-independent control of innate immunity in Caenorhabditis elegans by the TIR domain adaptor protein TIR-1, an ortholog of human SARM. *Nat. Immunol.* 5, 488–494. doi:10.1038/ni1060.

Darrouzet, E., Issartel, J.-P., Lunardi, J., and Dupuis, A. (1998). The 49-kDa subunit of NADH-ubiquinone oxidoreductase (Complex I) is involved in the binding of piericidin and rotenone, two quinone-related inhibitors. *FEBS Lett.* 431, 34–38. doi:10.1016/S0014-5793(98)00719-4.

Denver, D. R. (2000). High Direct Estimate of the Mutation Rate in the Mitochondrial Genome of Caenorhabditis elegans. *Science (80-.).* 289, 2342–2344. doi:10.1126/science.289.5488.2342.

Denver, D. R., Dolan, P. C., Wilhelm, L. J., Sung, W., Lucas-Lledo, J. I., Howe, D. K., et al. (2009). A genome-wide view of Caenorhabditis elegans base-substitution mutation processes. *Proc. Natl. Acad. Sci.* 106, 16310–16314. doi:10.1073/pnas.0904895106.

Denver, D. R., Howe, D. K., Wilhelm, L. J., Palmer, C. A., Anderson, J. L., Stein, K. C., et al. (2010). Selective sweeps and parallel mutation in the adaptive recovery from deleterious mutation in Caenorhabditis elegans. *Genome Res.* 20, 1663–1671. doi:10.1101/gr.108191.110.

Denver, D. R., Morris, K., Lynch, M., Vassilieva, L. L., and Thomas, W. K. (2000). High direct estimate of the mutation rate in the mitochondrial genome of Caenorhabditis elegans. *Science* 289, 2342–2344. doi:10.1126/science.289.5488.2342.

Denver, D. R., Wilhelm, L. J., Howe, D. K., Gafner, K., Dolan, P. C., and Baer, C. F. (2012). Variation in base-substitution mutation in experimental and natural lineages of caenorhabditis nematodes. *Genome Biol. Evol.* 4, 513–522. doi:10.1093/gbe/evs028.

Doonan, R., McElwee, J. J., Matthijssens, F., Walker, G. A., Houthoofd, K., Back, P., et al. (2008). Against the oxidative damage theory of aging: superoxide dismutases protect against oxidative stress but have little or no effect on life span in Caenorhabditis elegans. *Genes Dev.* 22, 3236–3241. doi:10.1101/gad.504808.

Dufourcq, P., Victor, M., Gay, F., Calvo, D., Hodgkin, J., and Shi, Y. (2002). Functional Requirement for Histone Deacetylase 1 in Caenorhabditis elegans Gonadogenesis. *Mol. Cell. Biol.* 22, 3024–3034. doi:10.1128/MCB.22.9.3024-3034.2002.

Efremov, R. G., and Sazanov, L. A. (2011). Structure of the membrane domain of respiratory complex I. *Nature* 476, 414–420. doi:10.1038/nature10330.

Estes, S., and Lynch, M. (2003). Rapid fitness recovery in mutationally degraded lines of Caenorhabditis elegans. *Evolution* 57, 1022–1030.

Faergeman, N. J., and Knudsen, J. (1997). Role of long-chain fatty acyl-CoA esters in the regulation of metabolism and in cell signalling. *Biochem. J.* 323 (Pt 1, 1–12.

Fisher, R. A. (1930). *The genetical theory of natural selection*. Oxford, United Kingdom: Oxfors University Press.

Froenicke, L. (2015). First HiSeq 3000 data download. Available at: http://dnatech.genomecenter.ucdavis.edu/2015/05/07/first-hiseq-3000-data-download/ [Accessed April 1, 2016].

Gumienny, T. L., Brugnera, E., Tosello-Trampont, A.-C., Kinchen, J. M., Haney, L. B., Nishiwaki, K., et al. (2001). CED-12/ELMO, a Novel Member of the CrkII/Dock180/Rac Pathway, Is Required for Phagocytosis and Cell Migration. *Cell* 107, 27–41. doi:10.1016/S0092-8674(01)00520-7.

Han, X., Gomes, J.-E., Birmingham, C. L., Pintard, L., Sugimoto, A., and Mains, P. E. (2009). The Role of Protein Phosphatase 4 in Regulating Microtubule Severing in the Caenorhabditis elegans Embryo. *Genetics* 181, 933–943. doi:10.1534/genetics.108.096016.

Hao, J. C., Yu, T. W., Fujisawa, K., Culotti, J. G., Gengyo-Ando, K., Mitani, S., et al. (2001). C. elegans slit acts in midline, dorsal-ventral, and anterior-posterior guidance via the SAX-3/Robo receptor. *Neuron* 32, 25–38. doi:10.1016/S0896-6273(01)00448-2.

Harding, H. P., Zhang, Y., Zeng, H., Novoa, I., Lu, P. D., Calfon, M., et al. (2003). An Integrated Stress Response Regulates Amino Acid Metabolism and Resistance to Oxidative Stress. *Mol. Cell* 11, 619–633. doi:10.1016/S1097-2765(03)00105-9.

Heimbucher, T., Liu, Z., Bossard, C., McCloskey, R., Carrano, A. C., Riedel, C. G., et al. (2015). The Deubiquitylase MATH-33 Controls DAF-16 Stability and Function in Metabolism and Longevity. *Cell Metab.* 22, 151–163. doi:10.1016/j.cmet.2015.06.002.

Holmes, E. C. (2003). Patterns of Intra- and Interhost Nonsynonymous Variation Reveal Strong Purifying Selection in Dengue Virus. *J. Virol.* 77, 11296–11298. doi:10.1128/JVI.77.20.11296-11298.2003.

Jun, A. S., Trounce, I. A., Brown, M. D., Shoffner, J. M., and Wallace, D. C. (1996). Use of transmitochondrial cybrids to assign a complex I defect to the mitochondrial DNA-encoded NADH dehydrogenase subunit 6 gene mutation at nucleotide pair 14459 that causes Leber hereditary optic neuropathy and dystonia. *Mol. Cell. Biol.* 16, 771–777. Available at: http://mcb.asm.org/cgi/reprint/16/3/771?view=long&pmid=8622678\npapers3://publication/uuid/0723095B-18F7-4D3C-8753-FEEF567AB8EA.

Kamran-Disfani, A., and Agrawal, A. F. (2014). Selfing, adaptation and background selection in finite populations. *J. Evol. Biol.* 27, 1360–1371. doi:10.1111/jeb.12343.

Kayser, E. B., Morgan, P. G., Hoppel, C. L., and Sedensky, M. M. (2001). Mitochondrial expression and function of GAS-1 in Caenorhabditis elegans. *J. Biol. Chem.* 276, 20551–20558. doi:10.1074/jbc.M011066200.

Kayser, E.-B., Morgan, P. G., and Sedensky, M. M. (1999). GAS-1. *Anesthesiology* 90, 545–554. doi:10.1097/00000542-199902000-00031.

Keightley, P. D., and Otto, S. P. (2006). Interference among deleterious mutations favours sex and recombination in finite populations. *Nature* 443, 89–92. doi:10.1038/nature05049.

Kennedy, S. R., Loeb, L. A., and Herr, A. J. (2012). Somatic mutations in aging, cancer and neurodegeneration. *Mech. Ageing Dev.* 133, 118–126. doi:10.1016/j.mad.2011.10.009.

Khopp, K., Zaidenshnur, G., Beier, R., Kheinrikh, I., and Germann, K. (1977). [Cardiotocographic and electroencephalographic studies in early diagnosis of fetal hypoxia]. *Akush Ginekol (Mosk)*, 27–31.

Kim, E. H., Koh, E. H., Park, J.-Y., and Lee, K.-U. (2010). Adenine Nucleotide Translocator as a Regulator of Mitochondrial Function: Implication in the Pathogenesis of Metabolic Syndrome. *Korean Diabetes J.* 34, 146. doi:10.4093/kdj.2010.34.3.146.

Kimura, M. (1984). *The neutral theory of molecular evolution*. doi:http://dx.doi.org/10.1017/CBO9780511623486.

Kondo, M., Senoo-Matsuda, N., Yanase, S., Ishii, T., Hartman, P. S., and Ishii, N. (2005). Effect of oxidative stress on translocation of DAF-16 in oxygen-sensitive mutants, mev-1 and gas-1 of Caenorhabditis elegans. *Mech. Ageing Dev.* 126, 637–641. doi:10.1016/j.mad.2004.11.011.

Kryazhimskiy, S., and Plotkin, J. B. (2008). The Population Genetics of dN/dS. *PLoS Genet.* 4, e1000304. doi:10.1371/journal.pgen.1000304.

Kurki, S., Zickermann, V., Kervinen, M., Hassinen, I., and Finel, M. (2000). Mutagenesis of three conserved Glu residues in a bacterial homologue of the ND1 subunit of complex I affects ubiquinone reduction kinetics but not inhibition by dicyclohexylcarbodiimide. *Biochemistry* 39, 13496–13502. doi:10.1021/bi001134s.

Lande, R. (1995). Mutation and Conservation. *Conserv. Biol.* 9, 782–791. doi:10.1046/j.1523-1739.1995.09040782.x.

Lane, N. (2014). Bioenergetic constraints on the evolution of complex life. *Cold Spring Harb. Perspect. Biol.* 6. doi:10.1101/cshperspect.a015982.

Lemasters, J. J., and Sowers, A. E. (1979). Phosphate dependence and atractyloside inhibition of mitochondrial oxidative phosphorylation. The ADP-ATP carrier is rate-limiting. *J. Biol. Chem.* 254, 1248–1251.

Lenski, R. E. (2001). "Evolutionary Rate," in *Encyclopedia of Genetics* (Elsevier), 671–672. doi:10.1006/rwgn.2001.0432.

Lindahl, T. (1993). Instability and decay of the primary structure of DNA. *Nature* 362, 709–715. doi:10.1038/362709a0.

Maeda, I., Kohara, Y., Yamamoto, M., and Sugimoto, A. (2001). Large-scale analysis of gene function in Caenorhabditis elegans by high-throughput RNAi. *Curr. Biol.* 11, 171–176. doi:10.1016/S0960-9822(01)00052-5.

Maisnier-Patin, S., Berg, O. G., Liljas, L., and Andersson, D. I. (2002). Compensatory adaptation to the deleterious effect of antibiotic resistance in Salmonella typhimurium. *Mol. Microbiol.* 46, 355–366. doi:10.1046/j.1365-2958.2002.03173.x.

Mates, J. M., and Sanchez-Jimenez, F. M. (2000). Role of reactive oxygen species in apoptosis: implications for cancer therapy. *Int. J. Biochem. Cell Biol.* 32, 157–170. doi:10.1016/S1357-2725(99)00088-6.

McDonald, M. J., Rice, D. P., and Desai, M. M. (2016). Sex speeds adaptation by altering the dynamics of molecular evolution. *Nature*. doi:10.1038/nature17143.

Montooth, K. L., and Rand, D. M. (2008). The Spectrum of Mitochondrial Mutation Differs across Species. *PLoS Biol.* 6, e213. doi:10.1371/journal.pbio.0060213.

Morran, L. T., Cappy, B. J., Anderson, J. L., and Phillips, P. C. (2009). Sexual partners for the stressed: Facultative outcrossing in the self-fertilizing nematode Caenorhabditis elegans. *Evolution (N. Y).* 63, 1473–1482. doi:10.1111/j.1558-5646.2009.00652.x.

Mulder, N. J. (2003). The InterPro Database, 2003 brings increased coverage and new features. *Nucleic Acids Res.* 31, 315–318. doi:10.1093/nar/gkg046.

Nagaraja, P., Alexander, H. K., Bonhoeffer, S., and Dixit, N. M. (2015). Influence of recombination on acquisition and reversion of immune escape and compensatory mutations in HIV-1. *Epidemics*. doi:10.1016/j.epidem.2015.09.001.

Nielsen, R., Bustamante, C., Clark, A. G., Glanowski, S., Sackton, T. B., Hubisz, M. J., et al. (2005). A scan for positively selected genes in the genomes of humans and chimpanzees. *PLoS Biol.* 3, 0976–0985. doi:10.1371/journal.pbio.0030170.

Nishant, K. T., Singh, N. D., and Alani, E. (2009). Genomic mutation rates: what high-throughput methods can tell us. *BioEssays* 31, 912–920. doi:10.1002/bies.200900017.

Pätsi, J., Kervinen, M., Finel, M., and Hassinen, I. E. (2008). Leber hereditary optic neuropathy mutations in the ND6 subunit of mitochondrial complex I affect ubiquinone reduction kinetics in a bacterial model of the enzyme. *Biochem. J.* 409, 129–137. doi:10.1042/BJ20070866.

Phillips, W. S., Coleman-Hulbert, A. L., Weiss, E. S., Howe, D. K., Ping, S., Wernick, R. I., et al. (2015). Selfish Mitochondrial DNA Proliferates and Diversifies in Small, but not Large, Experimental Populations of Caenorhabditis briggsae. *Genome Biol. Evol.* 7, 2023–37. doi:10.1093/gbe/evv116.

Poon, A., Davis, B. H., and Chao, L. (2005). The coupon collector and the suppressor mutation: Estimating the number of compensatory mutations by maximum likelihood. *Genetics* 170, 1323–1332. doi:10.1534/genetics.104.037259.

Sazanov, L. A. (2015). A giant molecular proton pump: structure and mechanism of respiratory complex I. *Nat. Rev. Mol. Cell Biol.* 16, 375–388. doi:10.1038/nrm3997.

Serra-Pages, C. (1998). Liprins, a Family of LAR Transmembrane Protein-tyrosine Phosphatase-interacting Proteins. *J. Biol. Chem.* 273, 15611–15620. doi:10.1074/jbc.273.25.15611.

Shiraishi, Y., Murai, M., Sakiyama, N., Ifuku, K., and Miyoshi, H. (2012). Fenpyroximate Binds to the Interface between PSST and 49 kDa Subunits in Mitochondrial NADH-Ubiquinone Oxidoreductase. *Biochemistry* 51, 1953–1963. doi:10.1021/bi300047h.

Smith, J. M. (1978). *The Evolution of Sex*. Cambridge: Cambridge University Press.

Stiernagle, T. (2006). Maintenance of C. elegans. *WormBook*. doi:10.1895/wormbook.1.101.1.

Swan, K. A., Curtis, D. E., McKusick, K. B., Voinov, A. V., Mapa, F. A., and Cancilla, M. R. (2002). High-throughput gene mapping in Caenorhabditis elegans. *Genome Res.* 12, 1100–1105. doi:10.1101/gr.208902.

Szamecz, B., Boross, G., Kalapis, D., Kovács, K., Fekete, G., Farkas, Z., et al. (2014). The Genomic Landscape of Compensatory Evolution. *PLoS Biol.* 12, e1001935. doi:10.1371/journal.pbio.1001935.

Vasseur, E., and Quintana-Murci, L. (2013). The impact of natural selection on health and disease: uses of the population genetics approach in humans. *Evol. Appl.* 6, 596–607. doi:10.1111/eva.12045.

Vasta, V., Sedensky, M., Morgan, P., and Hahn, S. H. (2011). Altered redox status of coenzyme Q9 reflects mitochondrial electron transport chain deficiencies in Caenorhabditis elegans. *Mitochondrion* 11, 136–138. doi:10.1016/j.mito.2010.09.002.

Vinothkumar, K. R., Zhu, J., and Hirst, J. (2014). Architecture of mammalian respiratory complex I. *Nature* 515, 80–84. doi:10.1038/nature13686.

Wicks, S. R., Yeh, R. T., Gish, W. R., Waterston, R. H., and Plasterk, R. H. (2001). Rapid gene mapping in Caenorhabditis elegans using a high density polymorphism map. *Nat. Genet.* 28, 160–164. doi:10.1038/88878.

Wood. (1988). *The Nematode Caenohabditis Elegans*. Cold Spring Harbor, New York: Cold Spring Harbor Laboratory doi:10.1101/087969307.17.1.

Yanase, S., Yasuda, K., and Ishii, N. (2002). Adaptive responses to oxidative damage in three mutants of Caenorhabditis elegans (age-1, mev-1 and daf-16) that affect life span. *Mech. Ageing Dev.* 123, 1579–1587. doi:10.1016/S0047-6374(02)00093-3.

Zhen, M., and Jin, Y. (1999). The liprin protein SYD-2 regulates the differentiation of presynaptic termini in C. elegans. *Nature* 401, 371–375. doi:10.1038/43886.

Zhong, W., and Sternberg, P. W. (2006). Genome-wide prediction of C. elegans genetic interactions. *Science* 311, 1481–1484. doi:10.1126/science.1123287.
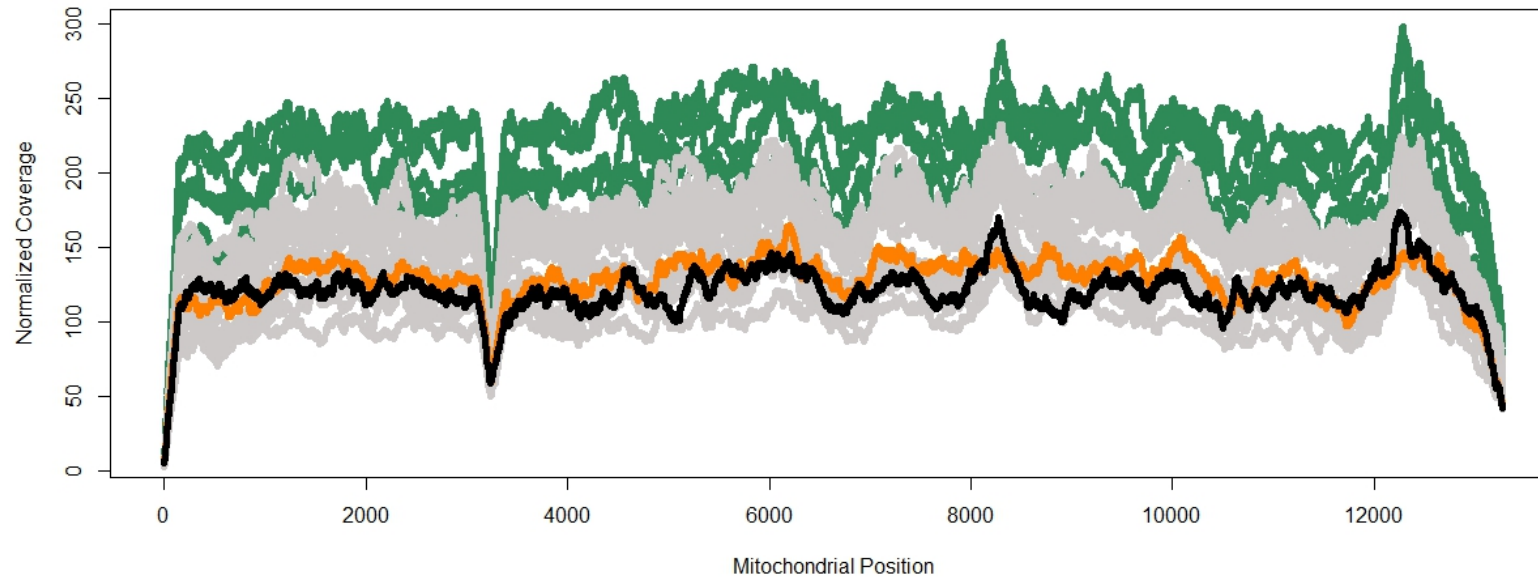
Figure 4.1: Normalized mtDNA copy number *gas-1* and N2 progenitor vs. *gas-1* RC lines. All nematodes at L1 stage. *gas-1* progenitor depicted in orange, N2 progenitor depicted in black. The five RC lines (RC 7, RC 8, RC 9, RC 10, RC 11) exhibiting significantly increased normalized mtDNA copy number relative to the *gas-1* progenitor shown in green, the remaining nineteen *gas-1* RC lines depicted in gray. mtDNA copy number normalized by corresponding line-specific coverage of single-copy nuclear genes: *ama-1*, *ego-1* and *efl-3*. The AT-rich region was excluded from analysis.
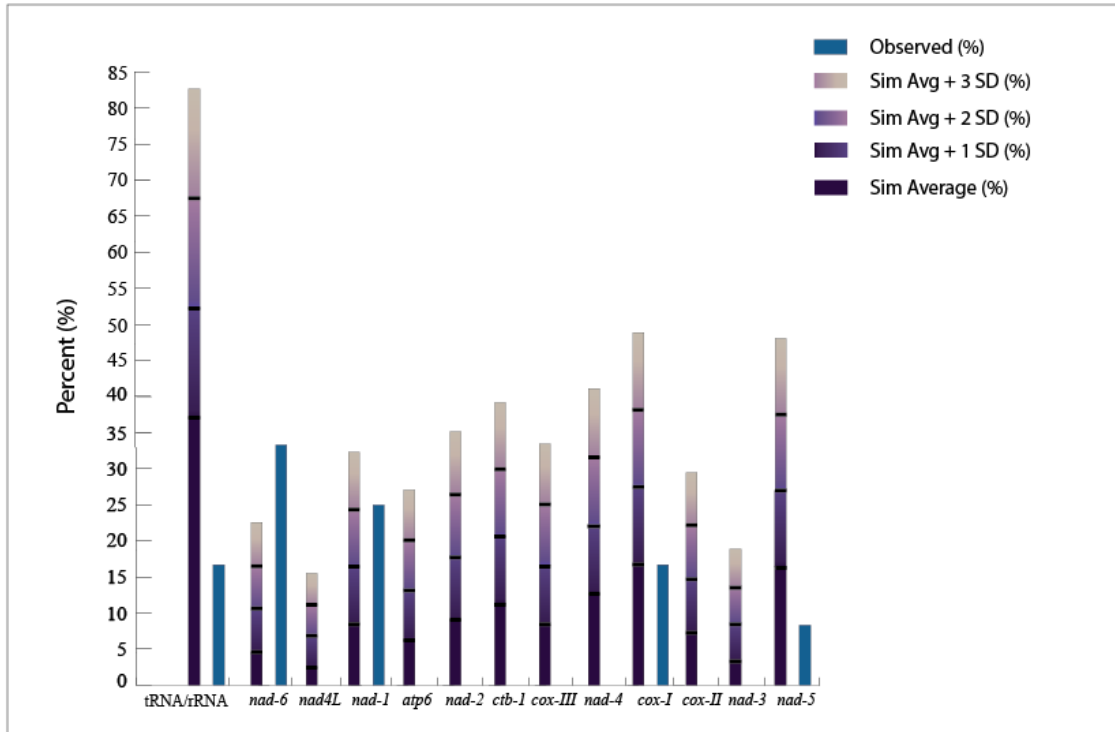
Figure 4.2: Comparison of percentage of mtDNA mutations per twelve protein-coding mtDNA genes and intergenic tRNA and rRNA sequences between mtDNA random mutation simulation and observed *gas-1* RC line results. Horizontal black bars denote the simulation average and standard deviations from the simulation mean.
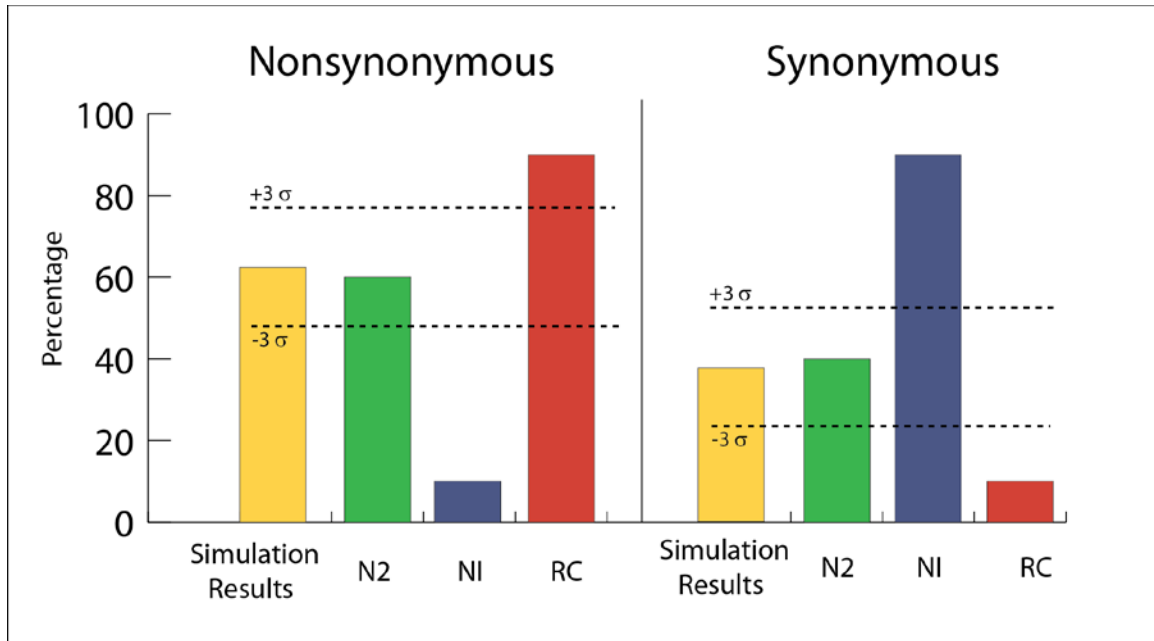
Figure 4.3: Comparison of proportion of non-synonymous and synonymous in mtDNA mutation simulation and observed results in *gas-1* RC lines. Dashed lines indicate three standard deviations above and below the simulation mean. Simulation results demonstrated by yellow bar; N2 MA line results (N2) displayed by green bar; *C. elegans* natural isolate (NI) results indicated by blue bar; *gas-1* RC line results (RC) indicated by red bar.
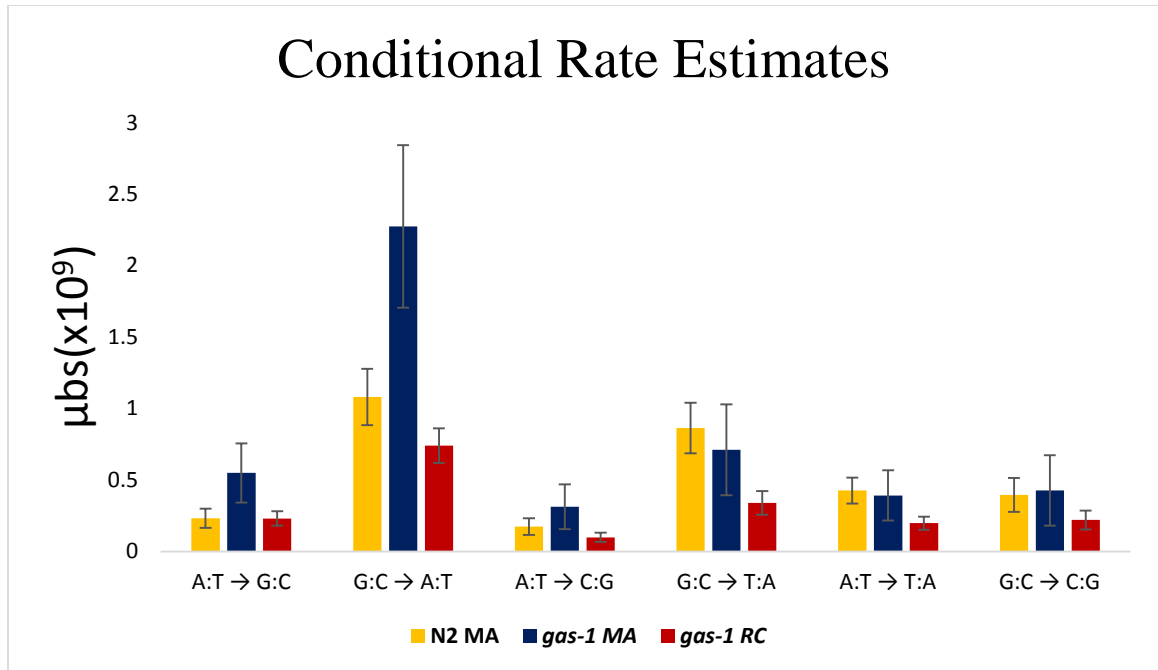
Figure 4.4: Conditional rate estimate for *gas-1* RC line nuclear mutations.
Conditional rate estimates for six possible mutation types for pooled *gas-1* RC line data compared to *gas-1* MA line values from Chapter 3 and published N2 MA line values (Denver et al., 2009c). Standard errors showed by error bars.
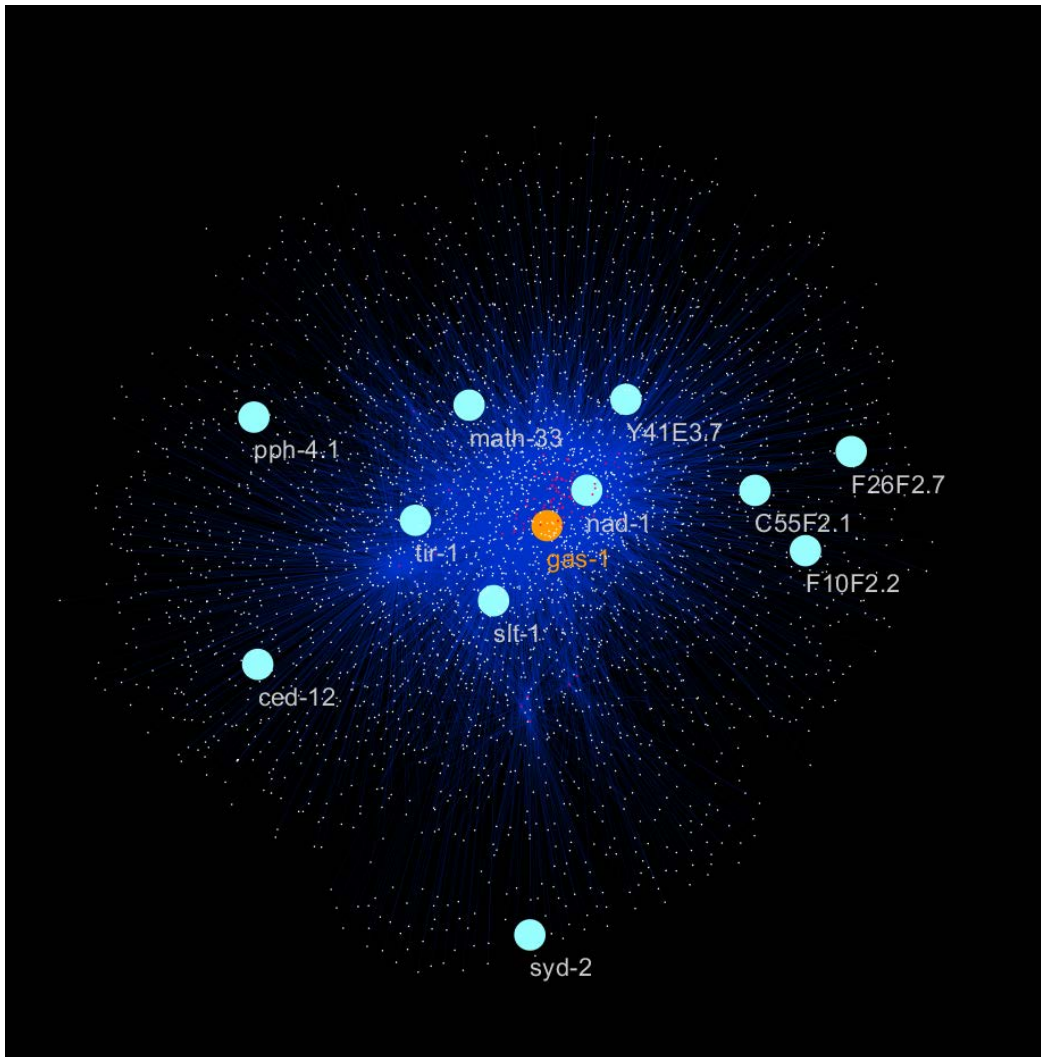
Figure 4.5: "*gas-1*-centric-interactome" depiction of *gas-1* RC line nuclear mutations in genes that interact within 2-degrees of the *gas-1* gene. Figure depicting all *gas-1* RC line nuclear mutations in genes that interact within 2-degrees of *gas-1* gene. *gas-1* RC line mutations shown in pink, *gas-1* gene displayed in yellow. Gene proximity to *gas-1* correlates with number of interactions within the *gas-1*-centric-interactome
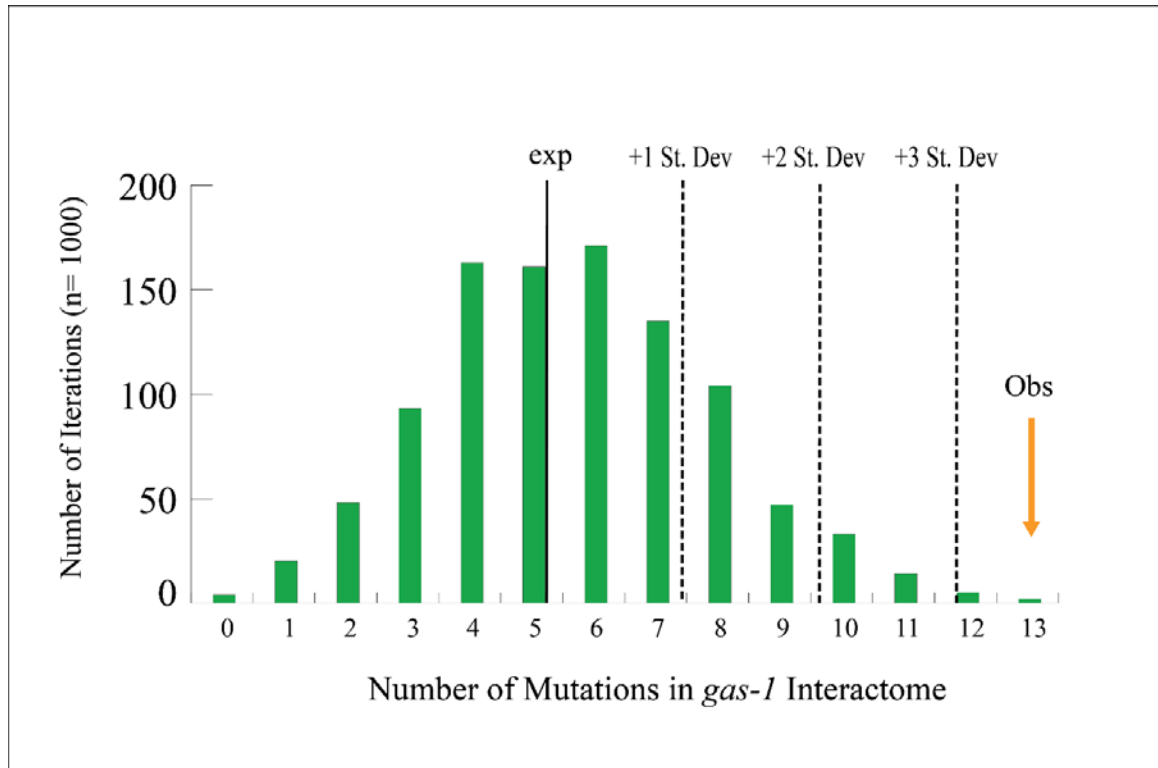
Figure 4.6: Random mutation simulation results of *gas-1* RC line nuclear mutations.
Plot depicting proportion of one-thousand iterations of random mutation generation in
which specific number of mutations were included in *gas-1* interactome. Simulates *gas-1*
RC line nuclear mutation results in which forty non-intergenic nuclear and six mtDNA
mutations with frequency levels greater than 30% mutations were observed (total of
forty-six mutations). Exp= mean number of expected mutations within 2-degrees of *gas-1*
network by chance. Obs= observed experimental value (n=13) of mutations within 2-
degrees of *gas-1* network.
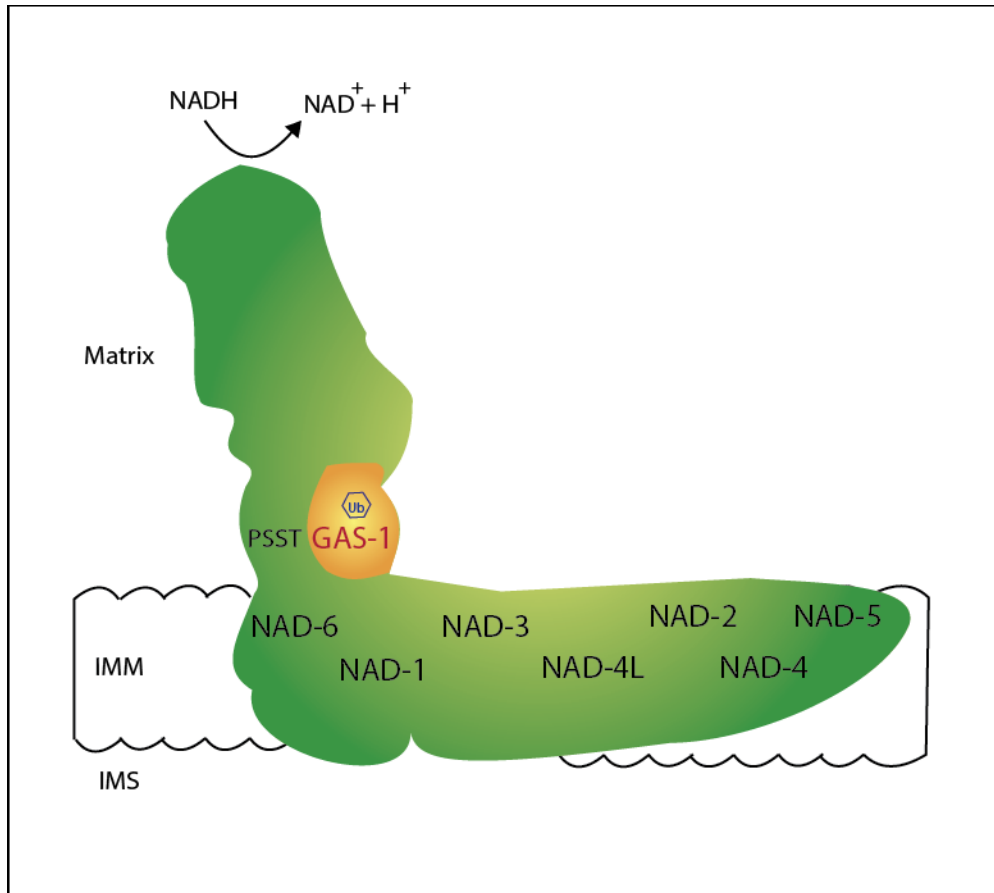
Figure 4.7: Location of GAS-1, NAD-6 and NAD-1 subunits of Complex I. Figure depicting relative location of GAS-1, NAD-6 and NAD-1 subunits inside the L-shaped Complex I of the mitochondrial electron transport chain. NAD-6 and NAD-1 are located in the inner mitochondrial membrane (IMM). GAS-1 along with PSST are located in the peripheral arm of Complex I in the mitochondrial matrix. The four subunits form the interface between the hydrophobic membrane arm and hydrophilic peripheral arm of Complex I. NAD-3, ND4L, NAD-2, NAD-4 and NAD-5 are present in the hydrophobic membrane arm as well. IMS denotes intermembrane space. Ub represents the hypothesized location of ubiquinone binding pocket.

Figure adapted from Patsi et al., 2008.

Table 4.1: Illumina-HiSeq 3000 Sequencing Run Statistics. All reads 150bp, paired end. All nematodes at L1 stage. Assembled using WS242 *C. elegans* reference genome in CLC with following parameters: no masking, mismatch cost= 2, insertion cost=3, deletion cost= 3, length fraction= 0.98, read fraction= 0.98, global alignment= no, non-specific match handling= map randomly. To eliminate false positives resulting from sequencing and PCR artifacts, the following criteria was applied: (*i*) at least 5-fold coverage, (*ii*) 100% of reads indicated a single non-reference base, (*iii*) there was at least one read presents from both the reverse and forward strand, and (*iv*) reads in a direction varied upon start/end positions. To eliminate false positives due to cryptic heterozygosity, candidate SNPs present in only one of the twelve strains were retained. Overall nuclear coverage (Avg Nuc Cov) calculated for entire nuclear genome per a line. Average mitochondrial coverage (Avg mtDNA Cov) calculated for whole mitochondrial genome coverage per a line. Standard deviation of the mean displayed in parentheses adjacent to mean values.

Line	Total Reads	Percent Mapped	Avg Nuc Cov	Avg mtDNA Cov
N2 Progenitor	20,728,966	79.83%	24 (0.6)	783.3 (119.1)
gas-1 Progenitor	18,773,512	79.95%	21.8 (0.7)	835.0 (130.0)
RC 1	19,786,862	81.69%	23.8 (0.7)	918.9 (203.9)
RC 2	19,247,616	81.07%	22.7 (0.7)	1164.8 (182.1)
RC 3	21,439,774	80.93%	25.3 (0.7)	1181.2 (184.9)
RC 4	16,474,084	79.60%	19.2 (0.7)	905.7 (141.7)
RC 5	19,538,046	82.19%	23.5 (0.5)	1093.3 (178.9)
RC 6	19,619,022	81.42%	23.3 (0.5)	1126.8 (200.9)
RC 7	21,495,750	80.90%	25.5 (0.5)	1309.4 (221.6)
RC 8	16,295,230	79.21%	18.7 (0.7)	1267.2 (196.5)
RC 9	22,938,664	82.50%	27.7 (0.7)	1418.3 (276.9)
RC 10	22,568,108	80.31%	26.5 (0.5)	1199.1 (172.4)
RC 11	20,643,212	81.39%	24.7 (0.7)	1475.5 (218.5)
RC 12	18,032,434	78.77%	20.8 (0.7)	987.9 (177.7)
RC 13	21,139,024	80.92%	25.0 (0.8)	975.3 (167.5)
RC 14	20,883,266	81.24%	24.8 (0.7)	1005.6 (167.1)

Table 4.1 (Continued)

RC 15	20,963,736	80.87%	25.0 (0.8)	835.2 (140.4)
RC 16	22,865,822	80.92%	27.0 (0.8)	1200.1 (224.6)
RC 17	21,378,998	82.74%	26.0 (0.8)	1126.3 (183.5)
RC 18	21,058,244	82.17%	25.5 (1.0)	918.8 (156.3)
RC 19	20,711,046	81.42%	24.5 (0.5)	1017.7 (171.5)
RC 20	19,369,868	81.33%	23.0 (0.6)	919.8 (160.9)
RC 21	21,488,148	82.19%	26.0 (0.8)	1179.7 (189.3)
RC 22	20,626,582	82.57%	25.2 (0.7)	965.8 (163.2)
RC 23	20,960,498	82.22%	25.3 (0.7)	1046.2 (189.6)
RC 24	18,399,798	80.77%	21.8 (0.7)	697.0 (123.8)

Table 4.2: Normalization of Mean mtDNA Copy Number. All reads 150bp, paired end. All nematodes at L1 stage. Assembled using WS242 *C. elegans* reference genome in CLC with following parameters: no masking, mismatch cost= 2, insertion cost=3, deletion cost= 3, length fraction= 0.98, read fraction= 0.98, global alignment= no, non-specific match handling= map randomly. mtDNA copy number normalized by mean coverage of corresponding single-copy nuclear genes (Norm mtDNA). mtDNA mean coverage calculated excluding AT-region (Avg Norm mtDNA Cov). Average single-copy nuclear coverage (Avg Single-Copy) calculated from average of three single copy genes: *ama-1*(Avg *ama-1 Cov*), *ego-1*(Avg *ego-1 Cov*), *efl-3* (Avg *efl-3 Cov*). Standard deviation of the mean displayed in parentheses adjacent to mean values.

Line	Avg Norm mtDNA Cov	Avg Single Nuc Cov	Avg *ama-1* Cov	Avg *ego-1* Cov	Avg *efl-1* Cov
N2 Progenitor	120.6 (16.1)	20.5 (6.5)	23.2 (7.0)	26.4 (7.3)	11.8 (7.2)
gas-1 Progenitor	128.2 (16.8)	19.4 (6.5)	19.8 (6.1)	27.0 (8.7)	11.2 (7.3)
RC 1	116.5 (22.9)	20.5 (7.9)	24.4 (8.0)	27.1 (6.8)	9.9 (7.3)
RC 2	157.8 (20.1)	19.3 (7.4)	20.9 (6.4)	27.2 (7.5)	9.8 (5.8)
RC 3	164.2 (20.2)	21.3 (7.3)	24.5 (7.6)	28.1 (7.6)	11.2 (7.7)
RC 4	133.2 (17.6)	18.0 (6.8)	20.3 (6.9)	24.8 (6.8)	8.8 (5.6)
RC 5	153.5 (20.1)	20.5 (7.2)	22.7 (6.7)	28.0 (6.7)	10.9 (7.1)
RC 6	165.7 (23.8)	20.0 (6.9)	24.6 (8.9)	25.1 (7.1)	10.3 (6.1)
RC 7	207.0 (28.8)	22.4 (6.4)	24.4 (6.5)	28.8 (7.3)	13.9 (9.1)
RC 8	223.0 (27.6)	15.3 (5.7)	18.0 (4.9)	20.2 (5.3)	7.8 (5.2)
RC 9	192.1 (33.1)	22.1 (7.4)	23.2 (7.0)	30.1 (8.3)	12.9 (6.5)
RC 10	186.7 (20.1)	22.4 (6.5)	25.9 (7.9)	28.4 (7.8)	13.1 (6.9)
RC 11	230.1 (24.9)	20.3 (6.5)	23.4 (6.8)	26.4 (9.5)	11.2 (6.5)
RC 12	133.7 (20.5)	19.3 (7.4)	20.5 (6.5)	27.6 (7.5)	9.7 (6.0)
RC 13	164.6 (25.3)	20.8 (5.9)	24.6 (6.5)	25.6 (9.5)	12.3 (6.0)
RC 14	123.3 (17.8)	21.5 (8.2)	21.8 (6.6)	31.2 (7.9)	11.5 (6.5)
RC 15	117.2 (17.3)	20.5 (7.1)	24.6 (7.0)	26.6 (6.3)	10.4 (6.5)

Table 4.2 (Continued)

RC 16	172.3 (27.7)	23.6 (7.0)	24.7 (6.8)	31.9 (8.2)	14.2 (8.1)
RC 17	161.1 (20.5)	21.9 (7.1)	23.3 (7.1)	29.9 (9.7)	12.6 (6.8)
RC 18	110.8 (17.0)	21.3 (8.3)	23.5 (7.1)	30.0 (8.5)	10.3 (6.0)
RC 19	165.9 (24.6)	20.2 (6.2)	20.2 (6.2)	27.9 (8.1)	12.5 (7.5)
RC 20	157.7 (25.0)	19.4 (5.8)	20.7 (6.6)	25.5 (6.8)	11.8 (6.3)
RC 21	170.5 (22.1)	22.3 (7.0)	25.8 (9.6)	28.5 (8.2)	12.5 (7.3)
RC 22	156.6 (22.4)	21.1 (6.2)	24.4 (7.1)	26.7 (6.3)	12.1 (7.3)
RC 23	121.9 (19.3)	22.4 (8.6)	23.4 (6.6)	32.3 (9.3)	11.3 (5.9)
RC 24	98.2 (14.7)	19.3 (7.1)	25.0 (7.8)	23.4 (6.3)	9.4 (6.2)

Table 4.3: mtDNA Heteroplasmic Single-Nucleotide Polymorphisms. Variant refers to an allele which differs from the WS242 reference and N2 progenitor. Heteroplasmy refers to a non-fixed variant. mtDNA heteroplasmies that are likely non-inherited are shown in bold. mtDNA heteroplasmies required to be within two standard deviations of the line-specific per-site mean mitochondrial coverage, have a variant frequency greater than two standard deviations above the line-specific mean variant frequency and at least six variant calls per a mtDNA heteroplasmy. Ref Nuc= Reference Nucleotide. Ref Cov = Coverage of reference allele. Var Nuc= Variant nucleotide. Ref Codon = Reference Codon. Ref AA= Reference Amino Acid. Var Codon= Variant Codon. Var AA= Variant Amino Acid. Site specific variant frequency (Var Freq) calculated by dividing number of variant calls (Var Cov) by the total coverage at the position (Ref Cov + Var Cov).

Line	Pos	Gene	Ref Nuc	Ref Cov	Var Nuc	Var Cov	Total Cov	Var Freq	Ref Codon	Ref AA	Var Codon	Var AA
N2 Prog	5079	*CYTB*	G	6	A	640	646	0.9907	GGG	Gly	GGA	Gly
N2 Prog	4391	*tRNA-Gln*	C	3	T	740	743	0.9960				
N2 Prog	8429	*COX-1*	A	5	G	870	875	0.9943	GTA	Val	GTA	Val
RC 3	**2154**	***NAD-1***	**T**	**7**	**C**	**1095**	**1102**	**0.9936**	**ATA**	**Met**	**ACA**	**Thr**
RC 3	**9145**	***COX-1***	**C**	**1246**	**T**	**33**	**1279**	**0.0258**	**CCG**	**Pro**	**CTG**	**Leu**
RC 4	**219**	***NAD-6***	**G**	**772**	**T**	**30**	**802**	**0.0374**	**AGT**	**Ser**	**ATT**	**Met**
RC 5	**1977**	***NAD-1***	**C**	**683**	**T**	**403**	**1086**	**0.3711**	**TCA**	**Ser**	**TTA**	**Leu**
RC 13	**227**	***NAD-6***	**G**	**40**	**T**	**721**	**761**	**0.9474**	**GTT**	**Val**	**TTT**	**Phe**
RC 13	5079	*CYTB*	G	919	A	66	985	0.0670	GGG	Gly	GGA	Gly
RC 14	**8057**	***COX-1***	**T**	**1073**	**A**	**45**	**1118**	**0.0403**	**ATT**	**Met**	**ATA**	**Met**
RC 17	**851**	***tRNA-Glu***	**G**	**1052**	**T**	**39**	**1091**	**0.0357**				
RC 18	**227**	***NAD-6***	**G**	**5**	**T**	**662**	**667**	**0.9925**	**GTT**	**Val**	**TTT**	**Phe**
RC 19	**10846**	***16S-rRNA***	**G**	**939**	**T**	**30**	**969**	**0.0310**				
RC 19	**11734**	***NAD-5***	**G**	**s**	**T**	**23**	**904**	**0.0254**	**GGT**	**Gly**	**GTT**	**Val**
RC 22	**1977**	***NAD-1***	**C**	**1**	**T**	**907**	**908**	**0.9989**	**TCA**	**Ser**	**TTA**	**Leu**
RC 24	**227**	***NAD-6***	**G**	**1**	**T**	**542**	**543**	**0.9982**	**GTT**	**Val**	**TTT**	**Phe**

Table 4.4: Frequencies in each *gas-1* RC line for all mtDNA positions in which a variant or heteroplasmy was identified. Each mtDNA position (Site) in a single-base substitution heteroplasmy occurred in any of the twenty-four *gas-1* RC lines is listed by reference position in WS242 (base pair). Frequencies which appear in Table 4.3 are in bold. A value of '0' indicates no variant allele occurred at this site for the line. N2 prog = N2 progenitor; *gas-1* Prog= *gas-1* progenitor.

	219bp	227bp	851bp	1977bp	2154bp	4391bp	5079bp	8057bp	8429bp	9145bp	10846bp	11734bp
N2 Prog	0.0013	0.0026	0	0	0	0.9933	**0.9846**	0	**0.9943**	0.0027	0.0013	0.0043
gas-1 **Prog**	0.0014	0.0042	0.0028	0.0012	0	0.0012	0.0021	0	0	0	0	0
RC 1	0	0.0012	0	0	0.0011	0	0.0142	0	0.0008	0.0058	0	0.0043
RC 2	0.0019	0.0009	0	0.0017	0.0009	0.0016	0.0031	0	0	0	0.0008	0.0061
RC 3	0	0.0103	0	0.0008	**0.9927**	0.0008	0.0015	0	0	**0.0258**	0.0015	0.001
RC 4	**0.0374**	0.0037	0.0013	0.0032	0.0011	0.0011	0	0.001	0.0009	0.001	0	0.0025
RC 5	0.001	0.001	0	**0.3707**	0	0	0	0	0.0007	0.0008	0	0.0042
RC 6	0.0029	0.003	0.0019	0.0009	0.0009	0	0.0017	0.0015	0.0021	0.0024	0.0009	0.0066
RC 7	0.0025	0.0017	0.0027	0	0.0008	0	0	0.0007	0.0006	0	0.0022	0.0079
RC 8	0	0.0016	0.0023	0	0	0.0007	0	0.0008	0	0.0008	0	0.0028
RC 9	0	0	0.0008	0	0	0	0.0006	0	0.0006	0.0006	0.0007	0.0026
RC 10	0.0016	0.0008	0	0	0	0	0.0008	0	0	0.0008	0.0016	0.0035
RC 11	0.0007	0.0021	0	0.0007	0	0	0	0.0007	0.0019	0.0012	0.0013	0.006
RC 12	0.0042	0.0011	0.0011	0.0019	0	0	0.0038	0.0008	0	0.0046	0	0.0011
RC 13	0.0013	**0.9956**	0.9988	0	0	0	0.0669	0.0009	0.0016	0	0	0.0013
RC 14	0	0	0.9977	0	0	0	0	**0.0402**	0.0016	0.0036	0	0.0024
RC 15	0	0.0032	0.0015	0	0	0	0	0	0.001	0.0011	0.0012	0.0011
RC 16	0.002	0.001	0	0	0	0	0.0027	0.0014	0.0007	0.0029	0.0016	0.0063
RC 17	0	0.0019	**0.0357**	0	0	0.0008	0	0	0.0008	0.0023	0.0026	0.001
RC 18	0.0015	**0.9925**	0.0012	0	0	0	0	0	0.0009	0	0.001	0.0026

Table 4.4 (Continued)

RC 19	0.0013	0	0.0023	0	0	0	0.0078	0	0	0.0008	**0.031**	**0.0254**
RC 20	0	0	0	0	0	0	0	0.0009	0.0019	0	0	0.0095
RC 21	0.0009	0.0027	0.0008	0.0024	0.0009	0	0	0	0.002	0.0008	0.0017	0.0018
RC 22	0.0028	0.0014	0.0011	**0.9978**	0	0	0	0	0	0.0019	0.001	0.0034
RC 23	0.0012	0	0.0012	0.0017	0.001	0	0	0	0.0008	0.0008	0	0.0059
RC 24	0.0046	**0.9963**	0.0016	0	0	0.0014	0	0	0.0012	0.006	0	0.005

Table 4.5: **RC Line Nuclear Mutations.** Mutations identified by mapping to WS424 N2 reference sequence. All mutations in *gas-1* RC lines compared to *gas-1* Progenitor and Wildtype (N2) Denver-Lab reference strain sequence to eliminate Denver-Lab N2 progenitor variants. Chromo= chromosome, Ref Nuc= reference nucleotide, Mut Nuc= mutation nucleotide, Cov= coverage at position, Type categorized as either intergenic (IG), intronic (IN), exonic (EX), or pseudogene (PS). Ref codon= reference codon in WS424 genome. Ref AA = reference amino acid in WS424 genome. Mut codon= mutation codon. Mut AA = mutation amino acid. Syn/Non indicates if mutation was synonymous or non-synonymous.

Line	Chromo	Position	Ref Nuc	Mut Nuc	Cov	Type	Gene	Ref Codon	Ref AA	Mut Codon	Mut AA	Syn/Non
RC 1	I	12,782,722	A	G	6	IG						
RC 1	II	4,642,450	A	T	7	IG						
RC 1	II	14,338,105	G	A	9	IG						
RC 1	V	9,603,829	T	C	7	IG						
RC 1	X	8,651,733	A	T	5	IG						
RC 2	III	7,425,423	C	A	8	IG						
RC 2	IV	7,591,706	A	G	5	EX	F45E4.3/*tag-80*	AAG	Lys	AGG	Arg	Non
RC 2	V	5,084,795	A	G	6	EX	Y58A7A.4	GAT	Asp	GAC	Asp	Syn
RC 2	V	5,084,806	C	A	6	EX	Y58A7A.4	GCA	Ala	TCA	Ser	Non
RC 2	V	17,412,257	C	A	6	IG						
RC 2	X	5,283,318	G	A	5	IN	Y34B4A.2					
RC 3	I	1,413,024	T	C	7	EX	Y92H12BR.6/*set-29*	AAT	Asn	AAC	Asn	Syn
RC 3	I	15,01,842	C	T	11	IN	Y92H12A.5					
RC 3	I	13,203,218	T	G	23	IG						
RC 3	III	7,415,219	A	C	21	IG						
RC 3	V	1,164,088	C	T	24	IN	T21H3.5					
RC 3	V	13,645,972	T	C	8	IG						
RC 3	X	7,607,385	C	T	30	IN	C44E12.3/*twk-17*					

Table 4.5 (Continued)

RC 4	I	10,137,355	C	T	5	IG						
RC 4	X	4,028,900	A	T	7	IG						
RC 5	III	3,386,567	T	A	5	IG						
RC 5	III	3,897,472	A	G	10	IN	F13B10.1/*tir-1*					
RC 5	X	4,037,336	G	A	6	IG						
RC 5	X	14,679,813	T	A	36	IN	F40E10.4/*slt-1*					
RC 5	X	17,447,220	G	A	11	IG						
RC 6	I	8,623,736	A	G	28	EX	F43G9.6/*fer-1*	AGA	Arg	GGA	Gly	Non
RC 6	II	6,669,203	C	T	6	EX	T19D12.1	AAC	Asn	AAT	Asn	Syn
RC 6	III	12,004,543	A	T	6	IG						
RC 6	III	12,004,552	G	A	6	IG						
RC 6	IV	6,794,092	C	T	32	EX	C17H12.3	CTC	Leu	CTT	Leu	Syn
RC 6	IV	8,580,642	T	C	5	IG						
RC 6	X	6,687,376	A	T	21	IG						
RC 6	X	7,206,440	C	T	28	IG						
RC 6	X	13,634,317	A	T	31	IG						
RC 7	III	2,500,192	T	G	6	IG						
RC 7	III	4,947,709	A	G	32	IG						
RC 7	V	19,683,735	G	T	5	IN	Y43F8C.12/*mrp-7*					
RC 7	X	14,763,281	G	T	31	EX	Y16B4A.2	GGG	Gly	GGT	Gly	Syn
RC 8	III	2,282,489	G	T	6	IN	Y54F10BM.3					
RC 8	X	17,441,843	G	A	5	IG						
RC 9	II	4,308,972	A	T	10	IG						
RC 9	V	6,086,004	C	A	5	IG						
RC 10	IV	12,731,956	G	A	5	IG						

Table 4.5 (Continued)

RC 10	V	10,340,073	C	T	28	IN	K07C5.2					
RC 10	X	4,425,834	G	A	22	IG						
RC 11	IV	7,642,263	T	C	22	IN	F45E4.8.2/*nlp-20*					
RC 11	V	5,358,409	T	G	22	IG						
RC 11	X	2,347,297	C	A	17	IN	T01B6.1					
RC 11	X	2,884,067	C	T	16	IG						
RC 12	X	11,976,631	C	G	6	IG						
RC 12	X	14,908,742	G	C	5	IG						
RC 13	I	34,362	C	G	22	IG						
RC 13	I	9,403,794	C	G	24	IN	F16A11.1					
RC 13	I	12,181,325	C	A	23	EX	R05D7.4/*abdh-11.2*	TTC	Phe	TTA	Phe	Syn
RC 13	III	1,849,254	A	T	5	IN	Y39A3CR.7/*pqn-82*					
RC 13	III	4,634,881	C	T	24	IN	F10F2.2					
RC 13	IV	5,871,330	C	T	25	PS	H04M03.5/*srv-18*					
RC 13	IV	7,899,075	G	A	13	IN	C55F2.1/*atic-1*					
RC 13	IV	11,272,487	C	T	22	IG						
RC 13	V	11,114,001	G	A	22	IN	H19N07.2/*math-33*					
RC 13	V	14,297,743	G	A	20	PS	F14D7.4					
RC 13	X	3,821,608	G	T	17	IN	K03C7.2/*fkh-9*					
RC 14	IV	8,574,587	A	T	6	IG						
RC 15	V	9,981,010	G	A	6	IG						
RC 16	II	694,578	T	G	6	IG						
RC 16	II	3,797,273	T	A	13	EX	Y8A9A.2	CTG	Leu	CAG	Gln	Non
RC 16	II	4,260,898	T	C	5	IG						

Table 4.5 (Continued)

RC 16	III	12,347,900	T	C	5	IN	Y75B8A.30/*pph-4.1*					
RC 16	V	4,140,793	G	A	24	EX	Y45G5AL.2/*lgc-29*	ACG	Thr	ACA	Thr	Syn
RC 17	III	5,357,452	C	T	5	IG						
RC 17	V	12,864,657	A	G	11	IN	T07F10.6					
RC 17	V	12,864,661	C	G	11	IN	T07F10.6					
RC 18	I	6,644,090	C	A	18	IG						
RC 18	III	7,415,236	G	A	25	IG						
RC 18	IV	3,208,939	G	C	25	PS	puf-4					
RC 18	IV	17,063,015	A	C	8	IN	Y116A8C.467					
RC 18	V	6,087,148	A	T	6	IG						
RC 18	V	9,603,864	C	T	6	IG						
RC 18	X	17,445,113	G	A	8	IG						
RC 19	I	8,008,052	C	G	27	EX	C54G4.2	CCA	Pro	CGA	Arg	Non
RC 19	III	1,441,904	C	T	21	EX	Y82E9BR.2	CGT	Arg	TGT	Cys	Non
RC 19	IV	7,128,174	A	G	6	IN	C24D4.16/*str-50*					
RC 19	V	2,763,471	A	G	20	IG						
RC 19	X	14,908,867	G	C	9	IG						
RC 20	I	12,360,758	A	T	21	IN	oac-43					
RC 20	II	1,422,675	T	C	14	IN	Y51H7C.10					
RC 20	II	13,505,040	C	T	18	EX	F54F11.1	CAA	Gln	TAA	Stop	Non
RC 20	III	958,048	T	A	35	IG						
RC 20	IV	9,047,795	C	G	5	IG						
RC 20	IV	15,020,193	G	A	23	IN	Y41E3.7					
RC 20	V	14,756,564	C	T	24	IG						
RC 20	X	10,549,806	C	T	21	IN	F59F5.6/*syd-2*					

Table 4.5 (Continued)

RC 20	X	12,276,980	G	T	7	IG						
RC 21	II	696,862	T	C	5	IG						
RC 22	I	10,116,399	C	A	23	EX	Y106G6D.4	GCC	Ala	GAC	Asp	Non
RC 22	I	10,948,653	T	G	8	IG						
RC 22	III	490,793	C	T	27	IG						
RC 22	IV	16,615,359	T	G	17	IG						
RC 22	V	10,379,220	G	C	29	EX	AC3.12	GTA	Val	CTA	Leu	Non
RC 22	X	11,787,528	T	A	9	IG						
RC 23	IV	8,573,847	G	A	9	IG						
RC 23	V	6,173,736	G	T	14	EX	W06H8.8/*ttn-1*	GAA	Glu	TAA	Stp	Non
RC 23	V	17,173,442	C	A	27	IG						
RC 23	X	13,697,074	A	T	27	IG						
RC 24	I	10,225,483	T	C	9	EX	Y106G6E.5/*ced-12*	TTA	Phe	TCA	Ser	Non
RC 24	II	7,026,963	C	A	18	IN	C52E12.1					
RC 24	II	7,188,583	T	G	9	IG						
RC 24	II	7,188,585	G	T	9	IG						
RC 24	IV	11,614,944	C	G	10	IG						
RC 24	V	12,312,064	A	G	14	IG						
RC 24	V	20,588,961	A	G	19	IN	F26F2.7					

Table 4.6: Summary of *gas-1* RC line nuclear SNPs that interact with *gas-1* interacting genes. Summary of *gas-1* RC line SNPs that interact with *gas-1* interacting genes. Interaction values obtained from Gene Orienteer (See Materials and Methods). Asterisks denote interactions below the threshold minimum of 4.6.

gas-1 Interaction	Interaction Value	RC Line SNP	RC Line
C31C9.2	5.68	F10F2.2	RC 13
T22D1.3	21.36	F10F2.2	RC 13
T22D1.3	9.2	C55F2.1	RC 13
Y57G11C.3	13.91	C55F2.1	RC 13
R04B5.6	14.72	C55F2.1	RC 13
T05H4.4	5.35	Y41E3.7	RC 20
T05H4.5	5.35	Y41E3.7	RC 20
F08F8.2	5.35	Y41E3.7	RC 20
unc-9	5.02	*syd-2*	RC 20
ero-1	14.41	F26F2.7	RC 24
sod-3	4.76	F26F2.7	RC 24
sod-2	4.76	F26F2.7	RC 24
hda-1	5.52	*ced-12*	RC 24
gas-1	7.58	*nad-1*	RC 3
gas-1	7.58	*nad-1*	RC 22
gas-1	7.58	*nad-1*	RC 5
hda-1	8.89	*tir-1*	RC 5
bli-3	21.92	*tir-1*	RC 5
duox-2	5.39	*tir-1*	RC 5
emb-8	5.29	*tir-1*	RC 5
vps-34	6.01	*tir-1*	RC 5
lpd-5	7.76	*tir-1*	RC 5
sod-1	6.47	*tir-1*	RC 5
sod-5	6.47	*tir-1*	RC 5
sod-3	5.32	*slt-1*	RC 5
unc-9	5.34	*slt-1*	RC 5
sdha-1	5.69	*slt-1*	RC 5
sdha-2	5.53	*slt-1*	RC 5
sod-1	6.04	*slt-1*	RC 5
sod-5	6.04	*slt-1*	RC 5
hda-1	10.97	*slt-1*	RC 5
hda-1	6.33	*math-33*	RC 13
prdx-2	6.75	*math-33*	RC 13
idh-1	13.18	*math-33*	RC 13

Table 4.6 (Continued)

T22D1.3	15.55	*math-33*	RC 13
hda-1	15.44	*pph-4.1*	RC 16
gas-1	*2.05	*nad-6*	RC 13
gas-1	*2.05	*nad-6*	RC 18
gas-1	*2.05	*nad-6*	RC 24
rnr-1	*0.79	*F16A11.1	RC 13
cts-1	*0.79	*F16A11.1	RC 13
Y56A3A.19	*1.02	*F54F11.1	RC 20
F08F8.2	*1.02	*F54F11.1	RC 20
sod-2	*4.28	*fer-1*	RC 6
sod-3	*4.17	*fer-1*	RC 6
unc-1	*1.61	*fkh-9*	RC 13
sdha-1	*0.86	*K07C5.2	RC 10
shda-2	*0.86	*K07C5.2	RC 10
trxr-1	*0.86	*K07C5.2	RC 10
T27E9.2	*0.86	*K07C5.2	RC 10
ivd-1	*0.86	*K07C5.2	RC 10
acdh-12	*0.86	*K07C5.2	RC 10
Y57G11C.3	*0.86	*K07C5.2	RC 10
DC2.5	*0.86	*K07C5.2	RC 10
let-721	*0.86	*K07C5.2	RC 10
cts-1	*0.86	*K07C5.2	RC 10
hda-1	*2.05	*ppfr-1*	RC 6
sod-1	*2.04	*puf-4*	RC 18
sod-2	*2.04	*puf-4*	RC 18
sod-3	*2.04	*puf-4*	RC 18
hda-1	*2.04	*puf-4*	RC 18
Y56A3A.19	*3.35	*R05D7.4	RC 13
fat-6	*4.37	*R05D7.4	RC 13
fat-7	*4.37	*R05D7.4	RC 13
fat-5	*4.37	*R05D7.4	RC 13
alh-1	*3.13	*set-29*	RC 3
alh-2	*3.13	*set-29*	RC 3
gspd-1	*3.86	*set-29*	RC 3
emb-8	*3.47	*set-29*	RC 3
C31C9.2	*3.13	*set-29*	RC 3
sod-1	*0.97	*T01B6.1	RC 11

Table 4.6 (Continued)

fat-6	*1.32	*T01B6.1*	RC 11
fat-7	*1.32	*T01B6.1*	RC 11
acdh-12	5.58	*gas-1*	
alh-1	5.45	*gas-1*	
alh-2	5.45	*gas-1*	
bli-3	5.74	*gas-1*	
C31C9.2	5.13	*gas-1*	
cts-1	5.4	*gas-1*	
DC2.5	5.17	*gas-1*	
duox-2	5.74	*gas-1*	
emb-8	5.13	*gas-1*	
ero-1	6.42	*gas-1*	
F08F8.2	5.36	*gas-1*	
fat-5	6.23	*gas-1*	
fat-6	6.43	*gas-1*	
fat-7	6.43	*gas-1*	
gspd-1	5.37	*gas-1*	
hda-1	7.14	*gas-1*	
idh-1	5.32	*gas-1*	
ivd-1	6.35	*gas-1*	
let-721	7.31	*gas-1*	
lpd-5	9.76	*gas-1*	
prdx-2	5.75	*gas-1*	
R04B5.6	5.89	*gas-1*	
rnr-1	6.46	*gas-1*	
sdha-1	7.61	*gas-1*	
sdha-2	7.61	*gas-1*	
sod-1	7.48	*gas-1*	
sod-2	6.5	*gas-1*	
sod-3	6.38	*gas-1*	
sod-5	7.48	*gas-1*	
T05H4.4	5.64	*gas-1*	
T05H4.5	5.64	*gas-1*	
T22D1.3	5.25	*gas-1*	
T27E9.2	6.42	*gas-1*	
trxr-1	7.48	*gas-1*	
unc-1	24.25	*gas-1*	
unc-9	20.88	*gas-1*	

Table 4.6 (Continued)

Y56A3A.19	7.11	*gas-1*
vps-34	12.62	*gas-1*
Y57G11C.3	5.17	*gas-1*

5. Dissertation Conclusions

The work presented in this dissertation examines the impact of mitochondrial dysfunction on genome evolution. Three aspects of mitogenomic and nuclear genome evolution were each analyzed and the evolutionary paths of genomic evolution in bottlenecked and large population sizes were compared: (1) dynamics of mtDNA copy number, (2) the mitochondrial genomic landscape of single-base substitution and indel mutations, (3) and trans-generational dynamics of inherited mtDNA mutation. The three aspects of nuclear genome evolution analyzed were: (1) the nuclear genome mutation rate and evolutionary rate, (2) the nuclear genomic landscape of single-nucleotide polymorphisms, and (3) the location of nuclear mutations within the context of the interaction network of the *gas-1* gene.

Chapters 2 and 3 examine how these genomic features evolve in *gas-1* MA-line populations that experienced single-worm bottlenecking for a maximum of fifty generation. Results of genome evolution in *gas-1* MA lines were compared to previously analyzed *C. elegans* N2 wild-type MA lines that experienced single-worm bottlenecking for 250 generations (Baer et al., 2005b). In Contrast, Chapter 4 analyzes genome evolution in large population sizes of the *C. elegans gas-1* strain for sixty generations (RC lines). Bioinformatic methods and computational simulations were applied to examine these aspects in a population genetics context and provide a comprehensive investigation of the impact of mitochondrial dysfunction on mitochondrial and nuclear genome evolution.

Additional analysis characterized the genetic background of the Denver-Lab *gas-1* progenitor strain. Bioinformatic analysis of nuclear mutation discovered eight-six

genetic differences in the *gas-1* strain that are not present in the WS242 reference genome or the Denver-lab N2 strain (Table 3.2). The majority of these genetic difference are located on the X chromosome and are G:C → A:T transitions. The proportion of mutations present on the X chromosome as well as the proportion of G:C → A:T transitions both genome-wide and on the X-chromosome were all determined to be significantly increased compared to the published N2 values. These results indicated that EMS generates numerous mutations and also suggests that residual mutations are maintained after extensive backcrossing due to linkage with the *gas-1* mutation.

5.1. mtDNA copy number is elevated in environments characterized by extreme genetic drift in which natural selection in minimized

Trans-generational changes in mtDNA copy number were assessed in Chapters 2 and 4. Chapter 2 analyzed mtDNA copy number in five *gas-1* MA populations that experienced single-worm bottlenecking for a maximum of fifty generations as well as in five previously analyzed N2 wildtype MA populations that experienced single-worm bottlenecking for 250 generations (Baer et al., 2005b). Chapter 4 analyzed mtDNA copy number in twenty-four *gas-1* RC populations evolved in large population sizes for sixty generations. To assess relative change in mtDNA copy number, MA lines were compared to the N2 and *gas-1* progenitor strain values that were sequenced in the same sample prep and Illumina-MiSeq lane. Likewise RC line relative values in mtDNA copy number were compared to progenitor strain values that were sequenced in the same sample prep and Illumina-HiSeq lane. Our results do not permit the direct comparison of mtDNA copy number between MA and RC line data sets as the coverage for mtDNA was

substantially elevated among lines sequenced with Illumina-HiSeq versus values obtained from Illumina-MiSeq.

Evaluating the proportion of MA and RC lines demonstrating increases relative to progenitor strains suggests that unlike natural selection, the influence of extreme genetic drift provides a permissive environment for elevated organelle genome copy number in *C. elegans* N2 and *gas-1* strains. Furthermore, as the N2 MA lines experienced single-worm bottlenecking over five times as long as the *gas-1* MA lines and demonstrated a substantially more dramatic increase in mtDNA copy number, our results suggest that the degree to which mtDNA copy number is increased may correspond to the number of generations that lines experienced bottlenecking. Future directions for this work include assessing mtDNA copy number in MA and RC lines sequenced in the same HTS analysis. This data has been collected and can be analyzed for assessment. Further work evaluating trans-generational changes in mtDNA copy number in additional *C. elegans* mutant and natural isolate strains experiencing single-worm bottlenecking may reveal if our observed result of elevated organelle genome copy number is a phenomenon isolated to *gas-1* and N2 reference strains or is a general characteristic of *C. elegans*. Moreover, research which determines the outcome of relative mtDNA copy number modifications in other *Caenorhabditis* species experiencing extreme drift may demonstrate if an environment in which natural selection is minimized leads to increased mtDNA copy number elevation. These future endeavors can provide insights on the possible differences and physiological mechanisms behind maintenance of organelle genome copy number.

5.2 Increased incidence of single-base substitution mutations located in mitochondrial-encoded Complex I subunits in *gas-1* populations

Chapters 2 and 4 identified and characterized all mitochondrial single-base substitution heteroplasmies. Chapter 2 analyzed five *gas-1* MA lines bottlenecked for a maximum of fifty generations and chapter 4 analyzed twenty-four *gas-1* RC lines evolved in large population sizes for sixty generations. Incidence of single-base substitution heteroplasmies in mtDNA does not include inherited heteroplasmies or homopolasmies.

Analysis of the five *gas-1* MA lines in Chapter 2 and the twenty-four *gas-1* RC lines in Chapter 4 demonstrated an increased incidence of single-base substitution heteroplasmies in mitochondrial-encoded Complex I subunits. In the *gas-1* MA lines analyzed in Chapter 2, five of the six non-inherited single-base substitution heteroplasmies observed were in mitochondrial-encoded Complex I subunits (*nad-4, nad-5,* and *nad-6)* (Table 2.2). Two *gas-1* MA lines experienced identical mitochondrial heteroplasmies in the *nad-6* gene which were observed in low-frequency in both lines. In the *gas-1* RC lines analyzed in Chapter 4, eight of the twelve non-inherited single-base substitution heteroplasmies observed were in mitochondrial-encoded Complex I subunits (*nad-1, nad-5,* and *nad-6)* (Table 4.3). Furthermore, two separate instances of parallel and potential compensatory evolution were observed in the *gas-1* RC lines, one in the *nad-1* gene and the other in *nad-6*. All instances of heteroplasmic parallel and potential compensatory evolution in the RC lines were observed at moderate to near-fixated levels indicative of positive selection. These observations of mtDNA mutations in the *gas-1* RC lines in Chapter 4 suggest that mitochondrial genome evolution may be driven in response to the *gas-1* mutation which causes Complex I dysfunction (Kayser et al.,

2001a, 2011). Furthermore, our results suggest that the NAD-6 subunit may exhibit interactions with GAS-1.

Future directions for the observed increased incidence of single-base substitutions located in mitochondrially-encoded Complex I subunits include functional analysis of the parallel and potentially compensatory mtDNA mutations in the *nad-1* and *nad-6* genes. Analyses which evaluate mitochondrial phenotypes including ROS and ATP production and fitness assays assessing lifespan and fecundity in *gas-1* and N2 strains which contain the isolated *nad-1* and *nad-1* mutations could demonstrate the compensatory capacity of effects of these mutations. Additional research on *gas-1* experimental populations will be useful to discern if the observation of elevated single-base substitutions located in mitochondrial-encoded Complex I subunits is driven by selection for compensatory and beneficial mutations in mtDNA Complex I subunit genes.

5.3 Evolution in large population sizes leads to a decreased rate of nuclear genomic change

Chapter 3 determined the nuclear mutation rate (per a site per a generation) of the *gas-1* MA lines was within the standard error of previously published nuclear mutation rate for *C. elegans.* Chapter 4 calculated the evolutionary rate of nuclear genomic change for pooled *gas-1* RC lines. Although the equation used to assess mutation rate and evolutionary rate is the same, the evolutionary forces influencing the rate of genomic change is dependent the effective population size. The *gas-1* MA lines analyzed in Chapter 3 experienced extreme genetic drift and minimized natural selection which is in direct contrast to the *gas-1* RC lines analyzed in Chapter 4 which experienced natural selection and minimized genetic drift.

Our results are within expected predictions from population-genetic theory. The three-fold slower evolutionary rate of nuclear genomic change determined in Chapter 4 indicates that natural selection influences genetic variation in large population sizes and suggests the presence of purifying natural selection in elimination of nuclear variation. The increased mutation rate of nuclear genomic change determined in Chapter 3 is characteristic of minimized natural selection and extreme genetic drift influences which permit the accumulation of slightly deleterious mutations. This work suggests that although the *gas-1* lines may exhibit increased ROS production, the results of the rate of nuclear genomic change is still within expectations from population genetic theory. Future work which addresses the mitochondrial mutation and evolutionary rate of genomic change will help discern if the elevated ROS production in *gas-1* worms causes elevated rates of mitochondrial mutations and is generally localized within mitochondrial organelles. Conducting experimental evolution for many generations (100 or more) may lead to an increase in the number of mitochondrial mutations. Additionally, sampling at more than one generation (e.g. generational intervals) could be useful to provide insights on the fluctuating levels of mitochondrial heteroplasmies and evolutionary paths to homoplasmy.

5.4 Enrichment of *gas-1* gene interactors in *gas-1* MA and RC lines

The observed results in the N2 MA lines from Chapter 3 and the simulations of random nuclear and mitochondrial mutation demonstrate that mutations located in genes which exhibit interactions within two-degrees of the *gas-1* gene are expected by chance. However, compared with the N2 wildtype MA lines and the predictions generated by simulations of random nuclear and mitochondrial gene mutation, our results from

Chapters 3 and 4 demonstrate that both the *gas-1* MA and RC lines experienced considerably more mutations in genes exhibiting interactions within two-degrees of the *gas-1* gene. This result was substantially more pronounced in the *gas-1* RC lines and as demonstrated with corresponding interactome simulations, unlikely due to chance. In light of this evidence, it is likely that natural selection is driving nuclear and mitochondrial mutations located within the *gas-1* network suggesting that the functional consequences of these mutations may improve mitochondrial function in *gas-1* worms or alternatively activate compensatory mechanisms. These results indicate increased propensity of nuclear mutations located in genes that interact within two-degrees of the *gas-1* gene in the *gas-1* MA and RC lines and suggest that the fixation of nuclear and mitochondrial mutations in *gas-1* populations may be driven by compensatory and beneficial mutations to the *gas-1* mutation.

5.5 Evidence for recovery to the *gas-1* mutation occurring in both large and small population sizes but beneficial mitochondrial mutations are more likely to arise to fixation in large population sizes

This research suggests that the consequences of the *gas-1* mutation are substantially deleterious and that further harmful mutations may contribute to lethality and/or sterility. Therefore mutations with beneficial and potentially compensatory consequences to the *gas-1* gene may prevail even in an environment characterized by extreme genetic drift. This study reveals that recovery of the *gas-1* mutation may occur through beneficial mutations in an environment characterized by extreme drift in addition to forces of natural selection influencing populations evolving in large effective population sizes.

Among the *gas-1* RC lines analyzed in Chapter 4, observed signatures indicative of positive selection on mtDNA variation were more dramatic (parallel and potential compensatory evolution, high levels of mtDNA heteroplasmy, and majority of non-mutations) than the results among *gas-1* MA lines analyzed in Chapter 2. As beneficial mutations were observed in the nuclear genome but likely absent or infrequent in the mitochondrial genome among *gas-1* MA lines, this work suggests that although an environment with pervasive genetic drift may permit the fixation of beneficial nuclear mutations, the processes by which beneficial mtDNA mutations rise to homoplasmy within the population may be less permissive. Our observations of inherited mtDNA heteroplasmy in Chapter 2 may align with predictions of theories where a small subset of mtDNA molecules from the parental generation repopulate the mitochondrial genome pool for the progeny. Given the polyploidy nature of mtDNA, and the necessary heteroplasmic phase prior to fixation, our work suggests that either the influence of natural selection or a series of states due to chance may be essential for significant increases in heteroplasmic levels and ultimate fixation of a novel homoplasmy within a population.

This dissertation research provides new insights on mitochondrial genome evolution and the evolution of the recovery from harmful mutation. In addition, the work presented in this dissertation suggests potential targets for ameliorating mitochondrial dysfunction and Complex I impairment through nuclear and mitochondrial mutations. Future endeavors which investigate the mode of mtDNA inheritance and the functional consequences of beneficial mitochondrial and nuclear genome mutations could provide an understanding of the physiological processes that may compensate for Complex I

impairment and mitochondrial dysfunction. As existing approaches are incorporated with newly developed technologies, our knowledge of the evolutionary processes influencing mitochondrial and nuclear genome evolution and the recovery from mitochondrial dysfunction and harmful mutation will continue to burgeon and may advance numerous disciplines, from disease research to conservation science.

APPENDICES

APPENDIX A- Supplementary material for Chapter 2

Supplementary Table A1: **Number of Generations of Bottlenecking Per Line.** All lines experienced single-worm bottlenecking. Single worms transferred in 4 day intervals. All nematodes maintained on standard NGM plates.

Line	Number Generations Bottlenecking
N2 Line	
Progenitor	N/A
N2 MA523	250
N2 MA526	250
N2 MA529	250
N2 MA553	250
N2 MA574	250
gas-1 **Line**	
progenitor	N/A
gas-1 MA412	42
gas-1 419	38
gas-1 MA429	43
gas-1 MA431	44
gas-1 MA438	43

Supplementary Table A2: **Kruskal Wallis H Test of mtDNA copy number.** Kruskal Wallis H Test analysis of mtDNA copy number with strain as an explanatory variable. Degrees of freedom (DF) and Chi-Squared value (Chi-Sq).

	DF	Chi-Sq	P-Value
Strain	11	154.2	2.2×10^{-16}

Supplementary Table A3: **Kruskal Multiple Comparison test of mtDNA copy number.** All possible pairwise comparisons of mtDNA copy number between lines. Critical Difference (critical.dif) signifies level delineating significance from non-significance. Observational difference (obs.dif) indicates observed difference between lines. P <0.05 indicates significance of mtDNA copy number difference between two lines indicated by corresponding Output (difference). TRUE signifies the two lines are significantly different in mtDNA copy number, FALSE indicates the two lines are not significantly different from one another.

Line 1	Line 2	obs.dif	critical.dif	difference
N2 Progenitor	*gas-1* Progenitor	6.71429	61.91712	FALSE
N2 Progenitor	MA412	37.9286	61.91712	FALSE
N2 Progenitor	MA419	72.2857	61.91712	TRUE

Supplementary Table A3 (Continued)

N2 Progenitor	MA429	80.2143	61.91712	TRUE
N2 Progenitor	MA431	43.0714	61.91712	FALSE
N2 Progenitor	MA438	30.8571	61.91712	FALSE
N2 Progenitor	MA523	45.5	61.91712	FALSE
N2 Progenitor	MA526	142.5	61.91712	TRUE
N2 Progenitor	MA529	103.714	61.91712	TRUE
N2 Progenitor	MA553	121.5	61.91712	TRUE
N2 Progenitor	MA574	119.429	61.91712	TRUE
gas-1 Progenitor	MA412	44.6429	61.91712	FALSE
gas-1 Progenitor	MA419	79	61.91712	TRUE
gas-1 Progenitor	MA429	86.9286	61.91712	TRUE
gas-1 Progenitor	MA431	49.7857	61.91712	FALSE
gas-1 Progenitor	MA438	37.5714	61.91712	FALSE
gas-1 Progenitor	MA523	52.2143	61.91712	FALSE
gas-1 Progenitor	MA526	149.214	61.91712	TRUE
gas-1 Progenitor	MA529	110.429	61.91712	TRUE
gas-1 Progenitor	MA553	128.214	61.91712	TRUE
gas-1 Progenitor	MA574	126.143	61.91712	TRUE
MA412	MA419	34.3571	61.91712	FALSE
MA412	MA429	42.2857	61.91712	FALSE
MA412	MA431	5.14286	61.91712	FALSE
MA412	MA438	7.07143	61.91712	FALSE
MA412	MA523	7.57143	61.91712	FALSE
MA412	MA526	104.571	61.91712	TRUE
MA412	MA529	65.7857	61.91712	TRUE
MA412	MA553	83.5714	61.91712	TRUE
MA412	MA574	81.5	61.91712	TRUE
MA419	MA429	7.92857	61.91712	FALSE
MA419	MA431	29.2143	61.91712	FALSE
MA419	MA438	41.4286	61.91712	FALSE
MA419	MA523	26.7857	61.91712	FALSE
MA419	MA526	70.2143	61.91712	TRUE
MA419	MA529	31.4286	61.91712	FALSE
MA419	MA553	49.2143	61.91712	FALSE
MA419	MA574	47.1429	61.91712	FALSE
MA429	MA431	37.1429	61.91712	FALSE
MA429	MA438	49.3571	61.91712	FALSE
MA429	MA523	34.7143	61.91712	FALSE
MA429	MA526	62.2857	61.91712	TRUE
MA429	MA529	23.5	61.91712	FALSE

Supplementary Table A3 (Continued)

MA429	MA553	41.2857	61.91712	FALSE
MA429	MA574	39.2143	61.91712	FALSE
MA431	MA438	12.2143	61.91712	FALSE
MA431	MA523	2.42857	61.91712	FALSE
MA431	MA526	99.4286	61.91712	TRUE
MA431	MA529	60.6429	61.91712	FALSE
MA431	MA553	78.4286	61.91712	TRUE
MA431	MA574	76.3571	61.91712	TRUE
MA438	MA523	14.6429	61.91712	FALSE
MA438	MA526	111.643	61.91712	TRUE
MA438	MA529	72.8571	61.91712	TRUE
MA438	MA553	90.6429	61.91712	TRUE
MA438	MA574	88.5714	61.91712	TRUE
MA523	MA526	97	61.91712	TRUE
MA523	MA529	58.2143	61.91712	FALSE
MA523	MA553	76	61.91712	TRUE
MA523	MA574	73.9286	61.91712	TRUE
MA526	MA529	38.7857	61.91712	FALSE
MA526	MA553	21	61.91712	FALSE
MA526	MA574	23.0714	61.91712	FALSE
MA529	MA553	17.7857	61.91712	FALSE
MA529	MA574	15.7143	61.91712	FALSE
MA553	MA574	2.07143	61.91712	FALSE

Supplementary Table A4: Sanger Results for Mitochondrial Position 8439 Heteroplasmy of Individual *gas-1* progenitor L1 Worms. All nematodes at L1 stage. Average flanking Phred score calculated by mean Phred score of 50 bp flanking heteroplasmy in both directions.

gas-1 G0 L1 Sample	Reference Base	Evidence "C" Allele	Evidence "A" Allele	Phred Score	Average Flanking Phred Score
1	C	Heteroplasmy	Heteroplasmy	46	60.02
2	C	Heteroplasmy	Heteroplasmy	12	57.44
3	C	Heteroplasmy	Heteroplasmy	25	59.2
4	C	Heteroplasmy	Heteroplasmy	43	58.7
5	C	Fixed	0	59	59.2
6	C	Heteroplasmy	Heteroplasmy	27	60.44
7	C	Fixed	0	59	57.57
8	C	Fixed	0	62	61.41
9	C	Fixed	0	62	59.23
10	C	Heteroplasmy	Heteroplasmy	34	58.58
11	C	Fixed	0	62	59.68
12	C	Heteroplasmy	Heteroplasmy	18	59.1
13	C	Fixed	0	36	41.07
14	C	Heteroplasmy	Heteroplasmy	34	54.99
15	C	Fixed	0	54	55.82
16	C	Fixed	0	56	40.45
17	C	Fixed	0	59	56.81
18	C	Fixed	0	54	58.7

Supplementary Table A5: Sanger Results for Mitochondrial Position 8439 Heteroplasmy of Individual *gas-1* MA412 L1 Worms. All nematodes at L1 stage. Average flanking Phred score calculated by mean Phred score of 50 bp flanking heteroplasmy in both directions.

gas-1 MA 412 L1 Sample	8439 Allele Call	Evidence "C" Allele	Evidence "A" Allele	Phred Score	Average Flanking Phred Score
1	A	Heteroplasmy	Heteroplasmy	23	59.21
2	C	Heteroplasmy	Heteroplasmy	13	58.15
3	C	Heteroplasmy	Heteroplasmy	34	60.14
4	C	Heteroplasmy	Heteroplasmy	18	59.4
5	A	Heteroplasmy	Heteroplasmy	13	59.6
6	A	Heteroplasmy	Heteroplasmy	18	58.26
7	A	Heteroplasmy	Heteroplasmy	23	59.24
8	C	Heteroplasmy	Heteroplasmy	38	59.53
9	C	Fixed	0	62	60.14
10	C	Heteroplasmy	Heteroplasmy	18	58.63
11	C	Heteroplasmy	Heteroplasmy	35	58.78
12	C	Heteroplasmy	Heteroplasmy	28	58.29
13	C	Heteroplasmy	Heteroplasmy	13	58.75
14	C	Heteroplasmy	Heteroplasmy	27	58.6
15	C	Fixed	0	59	58.98
16	C	Heteroplasmy	Heteroplasmy	18	53.45
17	A	Heteroplasmy	Heteroplasmy	13	50.16

Supplementary Table A6: Sanger Results for Mitochondrial Position 8439 Heteroplasmy of Individual *gas-1* MA429 L1 Worms. All nematodes at L1 stage. Average flanking Phred score calculated by mean Phred score of 50 bp flaning heteroplasmy in both directions.

gas-1 MA 429 L1 Sample	8439 Allele Call	Evidence "C" Allele	Evidence "A" Allele	Phred Score	Average Flanking Phred Score
1	C	Fixed	0	62	61.19
2	C	Fixed	0	62	60.41
3	C	Fixed	0	62	60.97
4	C	Fixed	0	62	60.63
5	C	Fixed	0	62	60.84
6	C	Fixed	0	62	60.81
7	C	Fixed	0	62	60.46
8	C	Fixed	0	62	60.99
9	C	Fixed	0	62	60.76
10	C	Fixed	0	62	59.74
11	C	Fixed	0	62	60.02
12	C	Fixed	0	62	60.26
13	C	Fixed	0	62	60.65
14	C	Fixed	0	62	60.46
15	C	Fixed	0	56	60.14
16	C	Fixed	0	62	60.86
17	C	Fixed	0	62	61
18	C	Fixed	0	54	51.75

Supplementary Table A7: Sanger Results for Mitochondrial Position 8439 Heteroplasmy of Individual *gas-1* MA438 L1 Worms. All nematodes at L1 stage. Average flanking Phred score calculated by mean Phred score of 50 bp flanking heteroplasmy in both directions.

gas-1 MA 438 L1 Sample	8439 Allele Call	Evidence "C" Allele	Evidence "A" Allele	Phred Score	Average Flanking Phred Score
1	A	0	Fixed	62	61.53
2	A	0	Fixed	62	60.85
3	A	0	Fixed	62	60.77
4	A	0	Fixed	62	61.33
5	A	0	Fixed	62	61.2
6	A	0	Fixed	62	61.64
7	A	0	Fixed	62	61.21
8	A	0	Fixed	62	56.56
9	A	0	Fixed	62	59.98
10	A	0	Fixed	62	60.44
11	A	0	Fixed	62	60.48
12	A	0	Fixed	62	59.66
13	A	0	Fixed	62	60.24
14	A	0	Fixed	62	60.73
15	A	0	Fixed	56	58
16	A	0	Fixed	62	60.53
17	A	0	Fixed	62	56.59

Supplementary Table A8: Sanger Results for Mitochondrial Position 8439 Heteroplasmy of Bulk *gas-1* and N2 Progenitor Worms. All nematodes at L1 stage. Average flanking Phred score calculated by mean Phred score of 50 bp flanking heteroplasmy in both directions.

Progenitor Line	8439 Allele	Evidence "C" Allele	Evidence "A" Allele	Phred Score	Average Flanking Score
N2	C	Fixed	0	62	61.62
gas-1	C	Fixed	0	62	61.53

Supplementary Table A9: Sanger Results for Mitochondrial Position 8439 Heteroplasmy of Bulk Extraction *gas-1* MA lines.
All nematodes at L1 stage. Average flanking Phred score calculated by mean Phred score of 50 bp flanking heteroplasmy in both directions.

gas-1 MA Sample	Reference Base	Evidence "C" Allele	Evidence "A" Allele	Phred Score	Average Flanking Phred Score
MA402	C	Fixed	0	62	61.76
MA405	C	Fixed	0	62	61.67
MA412	C	Heteroplasmy	Heteroplasmy	18	58.37
MA415	C	Fixed	0	62	59.59
MA422	C	Fixed	0	62	61.18
MA425	A	Heteroplasmy	Heteroplasmy	18	55.83
MA427	C	Fixed	0	62	61
MA428	C	Fixed	0	62	60.98
MA429	C	Fixed	0	62	58.95
MA432	C	Fixed	0	56	61.01
MA433	C	Fixed	0	62	60.82
MA437	A	0	Fixed	62	61.41
MA438	A	0	Fixed	62	60.18
MA439	A	0	Fixed	62	61.41
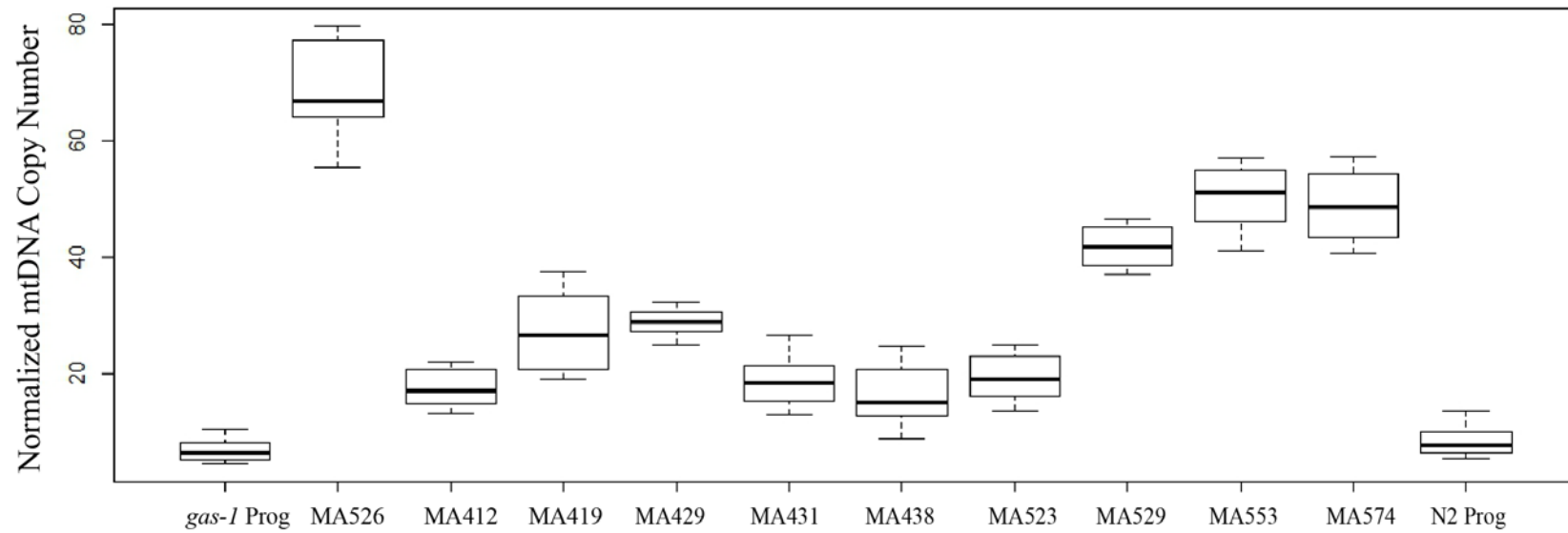
Supplementary Figure A1: Box and whisker plot of Normalized mtDNA copy number per line. Plot depicting variance for normalized mtDNA copy number in all 12 lines. Normalized mtDNA copy number portrayed on Y-axis.

APPENDIX B- Supplementary material for Chapter 3

Supplementary Table B1: Statistical comparison of X chromosome mutation events between *gas-1* progenitor and published wildtype values. Chi-Square (Chi-Sq, X^2) test results comparing percent of X Chromosome mutation events between *gas-1* progenitor (*gas-1* prog) and published wildtype (N2) values (Denver et al., 2009b).

% of Total (N2)	% of Total (*gas-1* prog)
16.46	65.12
Chi-Sq Value	171.6
P-Value	<0.00001

Supplementary Table B2: Statistical comparison of X chromosome G:C → A:T mutation events between *gas-1* progenitor and published wildtype values. Chi-Square (Chi-Sq, X^2) test results comparing percent of X Chromosome G:C → A:T mutation events between *gas-1* progenitor (*gas-1* prog) and published wildtype (N2) values (Denver et al., 2009b).

% of Total (N2)	% of Total (*gas-1* prog)
30.8	69.6
Chi-Sq Value	70.94
P-Value	<0.00001

Supplementary Table B3: Statistical comparison of G:C → A:T genome-wide mutation events between *gas-1* progenitor and published wildtype values. Chi-Square (Chi-Sq, X^2) test results comparing percent of G:C → A:T genome-wide mutation events between *gas-1* progenitor (*gas-1* prog) and published wildtype (N2) values (Denver et al., 2009b).

% of Total (N2)	% of Total (gas-1 prog)
19.0	76.5
Chi-Sq Value	213.85
P-Value	<0.0001

Supplementary Table B4: **Mutation rate and standard error of the mean for *gas-1* MA lines.** Mutation rate (μ) calculated for *gas-1* MA lines using the equation $\mu_{bs} = m/(LnT)$ where μ_{bs} is the base substitution rate (per nucleotide site per generation), L is the number of MA lines, m is the number of observed mutations, n is the number of nucleotide sites, and T is the time in generations (See Materials and Methods). Standard error of the mean (SEM) calculated using the equation $[\mu_{bs}/(nT)]^{1/2}$.

μ (per site/per generation)	2.128×10^{-09}
SEM	3.364×10^{-10}

Supplementary Table B5: **Sites considered for *gas-1* MA lines.** Counts of sites considered for all six chromosomes (I, II, III, IV, V, and X) in all *gas-1* MA lines. All sites with coverage between 6-45X coverage included.

	I	II	III	IV	V	X	Total
MA412	14,321,113	14,655,093	13,042,196	16,778,670	20,067,493	13,042,196	91,906,761
MA419	13,869,054	14,243,096	12,558,505	16,403,499	19,646,528	16,969,433	93,690,115
MA429	10,822,362	11,518,516	9,643,311	13,247,060	16,198,818	14,692,341	76,122,408
MA431	13,760,918	14,191,031	12,492,603	16,296,905	19,525,959	16,895,643	93,163,059
MA438	13,619,888	14,097,877	12,335,145	16,201,381	19,473,365	16,903,661	92,631,317
Total							447,513,660

Supplementary Table B6: Percentage of six mutation types in N2 and *gas-1* MA lines.

	% of Total (N2)	% of Total (*gas-1* MA)
A:T → G:C	10.13	13.48
G:C → A:T	26.58	59.3
A:T → C:G	8.86	4.65
G:C → T:A	26.58	9.30
A:T → T:A	17.72	11.63
G:C → C:G	10.13	4.65

APPENDIX C- Supplementary material for Chapter 4

Supplementary Table C1: Kruskal multiple comparison test of mtDNA copy number. All possible pairwise comparisons of mtDNA copy number between lines. Critical Difference (Critical Diff) signifies level delineating significance from non-significance. Observational difference (Obs Diff) indicates observed difference between lines (Line 1 and Line 2). $P < 0.05$ indicates significance of mtDNA copy number difference between two lines indicated by corresponding Output (Difference). TRUE signifies the two lines are significantly different in mtDNA copy number, FALSE indicates the two lines are not significantly different from one another.

Line 1	Line 2	Obs Diff	Critical Diff	Difference
N2 Progenitor	*gas-1* Progenitor	19.78571	150.5213	FALSE
N2 Progenitor	RC 1	22.07143	150.5213	FALSE
N2 Progenitor	RC 2	121.0714	150.5213	FALSE
N2 Progenitor	RC 3	149.8571	150.5213	FALSE
N2 Progenitor	RC 4	37.57143	150.5213	FALSE
N2 Progenitor	RC 5	107.9286	150.5213	FALSE
N2 Progenitor	RC 6	146.2143	150.5213	FALSE
N2 Progenitor	RC 7	242.8571	150.5213	TRUE
N2 Progenitor	RC 8	262.6429	150.5213	TRUE
N2 Progenitor	RC 9	206.5714	150.5213	TRUE
N2 Progenitor	RC 10	220.2143	150.5213	TRUE
N2 Progenitor	RC 11	271.1429	150.5213	TRUE
N2 Progenitor	RC 12	41.07143	150.5213	FALSE
N2 Progenitor	RC 13	141.0714	150.5213	FALSE
N2 Progenitor	RC 14	1.5	150.5213	FALSE
N2 Progenitor	RC 15	15.78571	150.5213	FALSE
N2 Progenitor	RC 16	162.3571	150.5213	TRUE
N2 Progenitor	RC 17	133.7857	150.5213	FALSE
N2 Progenitor	RC 18	35.92857	150.5213	FALSE
N2 Progenitor	RC 19	146.8571	150.5213	FALSE
N2 Progenitor	RC 20	111.5714	150.5213	FALSE
N2 Progenitor	RC 21	169.5	150.5213	TRUE
N2 Progenitor	RC 22	109.5714	150.5213	FALSE
N2 Progenitor	RC 23	4.714286	150.5213	FALSE
N2 Progenitor	RC 24	63.35714	150.5213	FALSE
gas-1 Progenitor	RC 1	41.85714	150.5213	FALSE
gas-1 Progenitor	RC 2	101.2857	150.5213	FALSE
gas-1 Progenitor	RC 3	130.0714	150.5213	FALSE
gas-1 Progenitor	RC 4	17.78571	150.5213	FALSE
gas-1 Progenitor	RC 5	88.14286	150.5213	FALSE
gas-1 Progenitor	RC 6	126.4286	150.5213	FALSE
gas-1 Progenitor	RC 7	223.0714	150.5213	TRUE

Supplementary Table C1 (Continued)

gas-1 Progenitor	RC 8	242.8571	150.5213	TRUE
gas-1 Progenitor	RC 9	186.7857	150.5213	TRUE
gas-1 Progenitor	RC 10	200.4286	150.5213	TRUE
gas-1 Progenitor	RC 11	251.3571	150.5213	TRUE
gas-1 Progenitor	RC 12	21.28571	150.5213	FALSE
gas-1 Progenitor	RC 13	121.2857	150.5213	FALSE
gas-1 Progenitor	RC 14	18.28571	150.5213	FALSE
gas-1 Progenitor	RC 15	35.57143	150.5213	FALSE
gas-1 Progenitor	RC 16	142.5714	150.5213	FALSE
gas-1 Progenitor	RC 17	114	150.5213	FALSE
gas-1 Progenitor	RC 18	55.71429	150.5213	FALSE
gas-1 Progenitor	RC 19	127.0714	150.5213	FALSE
gas-1 Progenitor	RC 20	91.78571	150.5213	FALSE
gas-1 Progenitor	RC 21	149.7143	150.5213	FALSE
gas-1 Progenitor	RC 22	89.78571	150.5213	FALSE
gas-1 Progenitor	RC 23	24.5	150.5213	FALSE
gas-1 Progenitor	RC 24	83.14286	150.5213	FALSE
RC 1	RC 2	143.1429	150.5213	FALSE
RC 1	RC 3	171.9286	150.5213	TRUE
RC 1	RC 4	59.64286	150.5213	FALSE
RC 1	RC 5	130	150.5213	FALSE
RC 1	RC 6	168.2857	150.5213	TRUE
RC 1	RC 7	264.9286	150.5213	TRUE
RC 1	RC 8	284.7143	150.5213	TRUE
RC 1	RC 9	228.6429	150.5213	TRUE
RC 1	RC 10	242.2857	150.5213	TRUE
RC 1	RC 11	293.2143	150.5213	TRUE
RC 1	RC 12	63.14286	150.5213	FALSE
RC 1	RC 13	163.1429	150.5213	TRUE
RC 1	RC 14	23.57143	150.5213	FALSE
RC 1	RC 15	6.285714	150.5213	FALSE
RC 1	RC 16	184.4286	150.5213	TRUE
RC 1	RC 17	155.8571	150.5213	TRUE
RC 1	RC 18	13.85714	150.5213	FALSE
RC 1	RC 19	168.9286	150.5213	TRUE
RC 1	RC 20	133.6429	150.5213	FALSE
RC 1	RC 21	191.5714	150.5213	TRUE
RC 1	RC 22	131.6429	150.5213	FALSE
RC 1	RC 23	17.35714	150.5213	FALSE
RC 1	RC 24	41.28571	150.5213	FALSE

Supplementary Table C1 (Continued)

RC 2	RC 3	28.78571	150.5213	FALSE
RC 2	RC 4	83.5	150.5213	FALSE
RC 2	RC 5	13.14286	150.5213	FALSE
RC 2	RC 6	25.14286	150.5213	FALSE
RC 2	RC 7	121.7857	150.5213	FALSE
RC 2	RC 8	141.5714	150.5213	FALSE
RC 2	RC 9	85.5	150.5213	FALSE
RC 2	RC 10	99.14286	150.5213	FALSE
RC 2	RC 11	150.0714	150.5213	FALSE
RC 2	RC 12	80	150.521	FALSE
RC 2	RC 13	20	150.521	FALSE
RC 2	RC 14	119.571	150.521	FALSE
RC 2	RC 15	136.857	150.521	FALSE
RC 2	RC 16	41.2857	150.521	FALSE
RC 2	RC 17	12.7143	150.521	FALSE
RC 2	RC 18	157	150.521	TRUE
RC 2	RC 19	25.7857	150.521	FALSE
RC 2	RC 20	9.5	150.521	FALSE
RC 2	RC 21	48.4286	150.521	FALSE
RC 2	RC 22	11.5	150.521	FALSE
RC 2	RC 23	125.786	150.521	FALSE
RC 2	RC 24	184.429	150.521	TRUE
RC 3	RC 4	112.286	150.521	FALSE
RC 3	RC 5	41.9286	150.521	FALSE
RC 3	RC 6	3.64286	150.521	FALSE
RC 3	RC 7	93	150.521	FALSE
RC 3	RC 8	112.786	150.521	FALSE
RC 3	RC 9	56.7143	150.521	FALSE
RC 3	RC 10	70.3571	150.521	FALSE
RC 3	RC 11	121.286	150.521	FALSE
RC 3	RC 12	108.786	150.521	FALSE
RC 3	RC 13	8.78571	150.521	FALSE
RC 3	RC 14	148.357	150.521	FALSE
RC 3	RC 15	165.643	150.521	TRUE
RC 3	RC 16	12.5	150.521	FALSE
RC 3	RC 17	16.0714	150.521	FALSE
RC 3	RC 18	185.786	150.521	TRUE
RC 3	RC 19	3	150.521	FALSE
RC 3	RC 20	38.2857	150.521	FALSE
RC 3	RC 21	19.6429	150.521	FALSE

Supplementary Table C1 (Continued)

RC 3	RC 22	40.2857	150.521	FALSE
RC 3	RC 23	154.571	150.521	TRUE
RC 3	RC 24	213.214	150.521	TRUE
RC 4	RC 5	70.3571	150.521	FALSE
RC 4	RC 6	108.643	150.521	FALSE
RC 4	RC 7	205.286	150.521	TRUE
RC 4	RC 8	225.071	150.521	TRUE
RC 4	RC 9	169	150.521	TRUE
RC 4	RC 10	182.643	150.521	TRUE
RC 4	RC 11	233.571	150.521	TRUE
RC 4	RC 12	3.5	150.521	FALSE
RC 4	RC 13	103.5	150.521	FALSE
RC 4	RC 14	36.0714	150.521	FALSE
RC 4	RC 15	53.3571	150.521	FALSE
RC 4	RC 16	124.786	150.521	FALSE
RC 4	RC 17	96.2143	150.521	FALSE
RC 4	RC 18	73.5	150.521	FALSE
RC 4	RC 19	109.286	150.521	FALSE
RC 4	RC 20	74	150.521	FALSE
RC 4	RC 21	131.929	150.521	FALSE
RC 4	RC 22	72	150.521	FALSE
RC 4	RC 23	42.2857	150.521	FALSE
RC 4	RC 24	100.929	150.521	FALSE
RC 5	RC 6	38.2857	150.521	FALSE
RC 5	RC 7	134.929	150.521	FALSE
RC 5	RC 8	154.714	150.521	TRUE
RC 5	RC 9	98.6429	150.521	FALSE
RC 5	RC 10	112.286	150.521	FALSE
RC 5	RC 11	163.214	150.521	TRUE
RC 5	RC 12	66.8571	150.521	FALSE
RC 5	RC 13	33.1429	150.521	FALSE
RC 5	RC 14	106.429	150.521	FALSE
RC 5	RC 15	123.714	150.521	FALSE
RC 5	RC 16	54.4286	150.521	FALSE
RC 5	RC 17	25.8571	150.521	FALSE
RC 5	RC 18	143.857	150.521	FALSE
RC 5	RC 19	38.9286	150.521	FALSE
RC 5	RC 20	3.64286	150.521	FALSE
RC 5	RC 21	61.5714	150.521	FALSE
RC 5	RC 22	1.64286	150.521	FALSE

Supplementary Table C1 (Continued)

RC 5	RC 23	112.643	150.521	FALSE
RC 5	RC 24	171.286	150.521	TRUE
RC 6	RC 7	96.6429	150.521	FALSE
RC 6	RC 8	116.429	150.521	FALSE
RC 6	RC 9	60.3571	150.521	FALSE
RC 6	RC 10	74	150.521	FALSE
RC 6	RC 11	124.929	150.521	FALSE
RC 6	RC 12	105.143	150.521	FALSE
RC 6	RC 13	5.14286	150.521	FALSE
RC 6	RC 14	144.714	150.521	FALSE
RC 6	RC 15	162	150.521	TRUE
RC 6	RC 16	16.1429	150.521	FALSE
RC 6	RC 17	12.4286	150.521	FALSE
RC 6	RC 18	182.143	150.521	TRUE
RC 6	RC 19	0.64286	150.521	FALSE
RC 6	RC 20	34.6429	150.521	FALSE
RC 6	RC 21	23.2857	150.521	FALSE
RC 6	RC 22	36.6429	150.521	FALSE
RC 6	RC 23	150.929	150.521	TRUE
RC 6	RC 24	209.571	150.521	TRUE
RC 7	RC 8	19.7857	150.521	FALSE
RC 7	RC 9	36.2857	150.521	FALSE
RC 7	RC 10	22.6429	150.521	FALSE
RC 7	RC 11	28.2857	150.521	FALSE
RC 7	RC 12	201.786	150.521	TRUE
RC 7	RC 13	101.786	150.521	FALSE
RC 7	RC 14	241.357	150.521	TRUE
RC 7	RC 15	258.643	150.521	TRUE
RC 7	RC 16	80.5	150.521	FALSE
RC 7	RC 17	109.071	150.521	FALSE
RC 7	RC 18	278.786	150.521	TRUE
RC 7	RC 19	96	150.521	FALSE
RC 7	RC 20	131.286	150.521	FALSE
RC 7	RC 21	73.3571	150.521	FALSE
RC 7	RC 22	133.286	150.521	FALSE
RC 7	RC 23	247.571	150.521	TRUE
RC 7	RC 24	306.214	150.521	TRUE
RC 8	RC 9	56.0714	150.521	FALSE
RC 8	RC 10	42.4286	150.521	FALSE
RC 8	RC 11	8.5	150.521	FALSE

Supplementary Table C1 (Continued)

RC 8	RC 12	221.571	150.521	TRUE
RC 8	RC 13	121.571	150.521	FALSE
RC 8	RC 14	261.143	150.521	TRUE
RC 8	RC 15	278.429	150.521	TRUE
RC 8	RC 16	100.286	150.521	FALSE
RC 8	RC 17	128.857	150.521	FALSE
RC 8	RC 18	298.571	150.521	TRUE
RC 8	RC 19	115.786	150.521	FALSE
RC 8	RC 20	151.071	150.521	TRUE
RC 8	RC 21	93.1429	150.521	FALSE
RC 8	RC 22	153.071	150.521	TRUE
RC 8	RC 23	267.357	150.521	TRUE
RC 8	RC 24	326	150.521	TRUE
RC 9	RC 10	13.6429	150.521	FALSE
RC 9	RC 11	64.5714	150.521	FALSE
RC 9	RC 12	165.5	150.521	TRUE
RC 9	RC 13	65.5	150.521	FALSE
RC 9	RC 14	205.071	150.521	TRUE
RC 9	RC 15	222.357	150.521	TRUE
RC 9	RC 16	44.2143	150.521	FALSE
RC 9	RC 17	72.7857	150.521	FALSE
RC 9	RC 18	242.5	150.521	TRUE
RC 9	RC 19	59.7143	150.521	FALSE
RC 9	RC 20	95	150.521	FALSE
RC 9	RC 21	37.0714	150.521	FALSE
RC 9	RC 22	97	150.521	FALSE
RC 9	RC 23	211.286	150.521	TRUE
RC 9	RC 24	269.929	150.521	TRUE
RC 10	RC 11	50.9286	150.521	FALSE
RC 10	RC 12	179.143	150.521	TRUE
RC 10	RC 13	79.1429	150.521	FALSE
RC 10	RC 14	218.714	150.521	TRUE
RC 10	RC 15	236	150.521	TRUE
RC 10	RC 16	57.8571	150.521	FALSE
RC 10	RC 17	86.4286	150.521	FALSE
RC 10	RC 18	256.143	150.521	TRUE
RC 10	RC 19	73.3571	150.521	FALSE
RC 10	RC 20	108.643	150.521	FALSE
RC 10	RC 21	50.7143	150.521	FALSE
RC 10	RC 22	110.643	150.521	FALSE
RC 10	RC 23	224.929	150.521	TRUE

Supplementary Table C1 (Continued)

RC 10	RC 24	283.571	150.521	TRUE
RC 11	RC 12	230.071	150.521	TRUE
RC 11	RC 13	130.071	150.521	FALSE
RC 11	RC 14	269.643	150.521	TRUE
RC 11	RC 15	286.929	150.521	TRUE
RC 11	RC 16	108.786	150.521	FALSE
RC 11	RC 17	137.357	150.521	FALSE
RC 11	RC 18	307.071	150.521	TRUE
RC 11	RC 19	124.286	150.521	FALSE
RC 11	RC 20	159.571	150.521	TRUE
RC 11	RC 21	101.643	150.521	FALSE
RC 11	RC 22	161.571	150.521	TRUE
RC 11	RC 23	275.857	150.521	TRUE
RC 11	RC 24	334.5	150.521	TRUE
RC 12	RC 13	100	150.521	FALSE
RC 12	RC 14	39.5714	150.521	FALSE
RC 12	RC 15	56.8571	150.521	FALSE
RC 12	RC 16	121.286	150.521	FALSE
RC 12	RC 17	92.7143	150.521	FALSE
RC 12	RC 18	77	150.521	FALSE
RC 12	RC 19	105.786	150.521	FALSE
RC 12	RC 20	70.5	150.521	FALSE
RC 12	RC 21	128.429	150.521	FALSE
RC 12	RC 22	68.5	150.521	FALSE
RC 12	RC 23	45.7857	150.521	FALSE
RC 12	RC 24	104.429	150.521	FALSE
RC 13	RC 14	139.571	150.521	FALSE
RC 13	RC 15	156.857	150.521	TRUE
RC 13	RC 16	21.2857	150.521	FALSE
RC 13	RC 17	7.28571	150.521	FALSE
RC 13	RC 18	177	150.521	TRUE
RC 13	RC 19	5.78571	150.521	FALSE
RC 13	RC 20	29.5	150.521	FALSE
RC 13	RC 21	28.4286	150.521	FALSE
RC 13	RC 22	31.5	150.521	FALSE
RC 13	RC 23	145.786	150.521	FALSE
RC 13	RC 24	204.429	150.521	TRUE
RC 14	RC 15	17.2857	150.521	FALSE
RC 14	RC 16	160.857	150.521	TRUE
RC 14	RC 17	132.286	150.521	FALSE

Supplementary Table C1 (Continued)

RC 14	RC 18	37.4286	150.521	FALSE
RC 14	RC 19	145.357	150.521	FALSE
RC 14	RC 20	110.071	150.521	FALSE
RC 14	RC 21	168	150.521	TRUE
RC 14	RC 22	108.071	150.521	FALSE
RC 14	RC 23	6.21429	150.521	FALSE
RC 14	RC 24	64.8571	150.521	FALSE
RC 15	RC 16	178.143	150.521	TRUE
RC 15	RC 17	149.571	150.521	FALSE
RC 15	RC 18	20.1429	150.521	FALSE
RC 15	RC 19	162.643	150.521	TRUE
RC 15	RC 20	127.357	150.521	FALSE
RC 15	RC 21	185.286	150.521	TRUE
RC 15	RC 22	125.357	150.521	FALSE
RC 15	RC 23	11.0714	150.521	FALSE
RC 15	RC 24	47.5714	150.521	FALSE
RC 16	RC 17	28.5714	150.521	FALSE
RC 16	RC 18	198.286	150.521	TRUE
RC 16	RC 19	15.5	150.521	FALSE
RC 16	RC 20	50.7857	150.521	FALSE
RC 16	RC 21	7.14286	150.521	FALSE
RC 16	RC 22	52.7857	150.521	FALSE
RC 16	RC 23	167.071	150.521	TRUE
RC 16	RC 24	225.714	150.521	TRUE
RC 17	RC 18	169.714	150.521	TRUE
RC 17	RC 19	13.0714	150.521	FALSE
RC 17	RC 20	22.2143	150.521	FALSE
RC 17	RC 21	35.7143	150.521	FALSE
RC 17	RC 22	24.2143	150.521	FALSE
RC 17	RC 23	138.5	150.521	FALSE
RC 17	RC 24	197.143	150.521	TRUE
RC 18	RC 19	182.786	150.521	TRUE
RC 18	RC 20	147.5	150.521	FALSE
RC 18	RC 21	205.429	150.521	TRUE
RC 18	RC 22	145.5	150.521	FALSE
RC 18	RC 23	31.2143	150.521	FALSE
RC 18	RC 24	27.4286	150.521	FALSE
RC 19	RC 20	35.2857	150.521	FALSE
RC 19	RC 21	22.6429	150.521	FALSE
RC 19	RC 22	37.2857	150.521	FALSE

Supplementary Table C1 (Continued)

RC 19	RC 23	151.571	150.521	TRUE
RC 19	RC 24	210.214	150.521	TRUE
RC 20	RC 21	57.9286	150.521	FALSE
RC 20	RC 22	2	150.521	FALSE
RC 20	RC 23	116.286	150.521	FALSE
RC 20	RC 24	174.929	150.521	TRUE
RC 21	RC 22	59.9286	150.521	FALSE
RC 21	RC 23	174.214	150.521	TRUE
RC 21	RC 24	232.857	150.521	TRUE
RC 22	RC 23	114.286	150.521	FALSE
RC 22	RC 24	172.929	150.521	TRUE
RC 23	RC 24	58.6429	150.521	FALSE

Supplementary Table C2: mtDNA mutation simulation output of one-hundred randomly generated non-synonymous and synonymous mutations. Random mutation mtDNA simulation output of percent of nonsynonymous, synonymous and ratio of nonsynonymous to synonymous (Ration Non/Syn) mutations. Average = Avg; Standard deviation = SD; Three standard deviations of the mean = Avg +3SD.

Simulation	Nonsynonymous (%)	Synonymous (%)	Ratio Non/Syn
Avg (%)	62.40	37.60	1.70
SD (%)	4.76	4.76	0.35
Avg + 3 SD (%)	76.68	51.88	2.75

Supplementary Table C3: **Sites Considered for *gas-1* RC lines.** Sites considered for all six chromosomes (Chromo) in all *gas-1* RC lines. All sites with coverage within 6-45X included.

Line	A Count	C Count	T Count	G Count	AT Count	CG Count	Total Count
RC 1	31,280,221	17,205,302	31,290,592	17,183,046	62,570,813	34,388,348	96,959,161
RC 2	31,719,230	17,460,384	31,725,966	17,436,543	63,445,196	34,896,927	98,342,123
RC 3	31,679,941	17,419,387	31,686,161	17,393,610	63,366,102	34,812,997	98,179,099
RC 4	31,514,973	17,384,705	31,521,228	17,361951	63,036,201	34,746,656	97,782,857
RC 5	31,673,861	17,422,196	31,679,955	17,398,606	63,353,816	34,820,802	98,174,618
RC 6	31,570,633	17,337,488	31,578,239	17,316,007	63,148,872	34,653,495	97,802,367
RC 7	31,570,633	17,337,488	31,578,239	17,316,007	63,148,872	34,653,495	97,802,367
RC 8	31,432,128	17,350,845	31,440,475	17,326,927	62,872,603	34,677,772	97,550,375
RC 9	31,019,424	17,038,150	31,030,362	17,013,227	62,049,786	34,051,377	96,101,163
RC 10	31,577,733	17,341,037	31,586,633	17315,785	63,164,366	34,656,822	97,821,188
RC 11	31,756,749	17,450,396	31,760,946	17,426,451	63,517,695	34,876,847	98,394,542
RC 12	31,491,085	17,379,749	31,496,637	17,356,582	62,987,722	34,736,331	97,724,053
RC 13	31,657,617	17,392,096	31,664,411	17,366552	63,322,028	34,758,648	98,,080,676
RC 14	31,718,990	17,432,107	31,726,739	17,407,234	63,445,729	34,839,341	98285,070
RC 15	31,698,606	17,415,187	31,707,508	17,389,696	63,406,114	34,804,883	98,210,997
RC 16	31,411,115	17,259,713	31,419,419	17,234,875	62,830,534	34,494,588	97,325,122
RC 17	31,539,431	17,309,922	31,543,116	17,287,014	63,082,547	34,596,936	97,679,483
RC 18	31,536,594	17,339,032	31,544,478	17,313,560	63,081,072	34,652,592	97,733,664
RC 19	31,751,093	17,448,874	31,756,306	17,424,943	63,507399	34,873,817	98,381,216
RC 20	31,781,357	17,481,623	31,786,741	17,459,040	63,568,098	34,940,663	98,508,761
RC 21	31,484,125	17,230,969	31,491,714	17,207,350	62,975,839	34,438319	97,414,158
RC 22	31,767,617	17,457,684	31,775,080	17,434,383	63,542,697	34,892,067	98,434,764
RC 23	31,629,254	17,382,535	31,637,584	17,358,857	63,266,838	34,741,392	98,008,230

Supplementary Table C3 (Continued)

RC 24	31,654,532	17,423,215	31,662,338	17,398,645	63,316,870	34,821,860	98,138,730
Total	757,916,942	416,700,084	758,090,867	416,126,891	1,516,007,809	832,826,975	2,348,834,784

Supplementary Table C4: Proportion of six mutation types in nuclear mutations in the *gas-1* RC lines and N2 MA lines. Percent of nuclear mutations for each of the six mutation types in the *gas-1* RC lines and published N2 MA lines (Denver et al., 2009c).

	% of Total (N2)	**% of Total (*gas-1* RC)**
A:T → G:C	10.13	18.58
G:C → A:T	26.58	32.74
A:T → C:G	8.86	7.96
G:C → T:A	26.58	15.04
A:T → T:A	17.72	15.93
G:C → C:G	10.13	9.73

Supplementary Table C5: Proportion of six mutation types in nuclear mutations in the *gas-1* RC lines and *gas-1* MA lines from Chapter 3. Percent of nuclear mutations for each of the six mutation types in the *gas-1* RC lines and *gas-1* MA lines from Chapter 3.

	% of Total (*gas-1* MA)	**% of Total (*gas-1* RC)**
A:T → G:C	17.5	18.58
G:C → A:T	40	32.74
A:T → C:G	10	7.96
G:C → T:A	12.5	15.04
A:T → T:A	12.5	15.93
G:C → C:G	7.5	9.73

Supplementary Table C6: Comparison of evolutionary (k) and mutation rate (μ) Values. Comparison of evolutionary rate (k) and mutation rate (μ) values between *gas-1* RC lines (RC), *gas-1* MA lines (MA) and N2 values. *gas-1* MA line values from Chapter 3, N2 values from pervious study (Denver et al., 2009a). Standard error of the mean (SEM) added to RC k values. Standard error of the mean subtracted from *gas-1* MA lines and N2 values.

Line	k/ μ Rate	SEM	± 1 SEM	± 2 SEM	± 3 SEM	± 4 SEM	± 5 SEM
RC	8.02×10^{-10}	7.54×10^{-11}	8.77×10^{-10}	9.52×10^{-10}	1.03×10^{-09}	1.10×10^{-09}	1.18×10^{-09}
MA	2.12×10^{-09}	3.36×10^{-10}	1.78×10^{-09}	1.45×10^{-09}	1.11×10^{-09}	7.74×10^{-10}	4.38×10^{-10}
N2	2.70×10^{-09}	1.36×10^{-10}	2.56×10^{-09}	2.43×10^{-09}	2.29×10^{-09}	2.16×10^{-09}	2.02×10^{-09}

BIBLIOGRAPHY

Addo, M. G., Cossard, R., Pichard, D., Obiri-Danso, K., Rötig, A., and Delahodde, A. (2010). Caenorhabditis elegans, a pluricellular model organism to screen new genes involved in mitochondrial genome maintenance. *Biochim. Biophys. Acta* 1802, 765–773. doi:10.1016/j.bbadis.2010.05.007.

Alberts B, Johnson A, Lewis J, et al (2002). *Molecular Biology of the Cell*. 4th ed. New York: Garland Science.

Al-Mehdi, a B., Pastukh, V. M., Swiger, B. M., Reed, D. J., Patel, M. R., Bardwell, G. C., et al. (2012). Perinuclear mitochondrial clustering creates an oxidant-rich nuclear domain required for hypoxia-induced transcription. *Sci Signal* 5, ra47. doi:10.1126/scisignal.2002712.

Amos, W., and Harwood, J. (1998). Factors affecting levels of genetic diversity in natural populations. *Philos. Trans. R. Soc. B Biol. Sci.* 353, 177–186. doi:10.1098/rstb.1998.0200.

Andersson, D. I., and Hughes, D. (1996). Muller's ratchet decreases fitness of a DNA-based microbe. *Proc Natl Acad Sci U S A* 93, 906–907. doi:10.1073/pnas.93.2.906.

Au, C., Benedetto, A., Anderson, J., Labrousse, A., Erikson, K., Ewbank, J. J., et al. (2009). SMF-1, SMF-2 and SMF-3 DMT1 orthologues regulate and are regulated differentially by manganese levels in C. elegans. *PLoS One* 4. doi:10.1371/journal.pone.0007792.

Azad, P., Zhang, M., and Woodruff, R. C. (2010). Rapid increase in viability due to new beneficial mutations in Drosophila melanogaster. *Genetica* 138, 251–263. doi:10.1007/s10709-009-9418-3.

Baer, C. F., Shaw, F., Steding, C., Baumgartner, M., Hawkins, A., Houppert, A., et al. (2005a). Comparative evolutionary genetics of spontaneous mutations affecting fitness in rhabditid nematodes. *Proc. Natl. Acad. Sci.* 102, 5785–5790. doi:10.1073/pnas.0406056102.

Baer, C. F., Shaw, F., Steding, C., Baumgartner, M., Hawkins, A., Houppert, A., et al. (2005b). Comparative evolutionary genetics of spontaneous mutations affecting fitness in rhabditid nematodes. *Proc. Natl. Acad. Sci.* 102, 5785–5790. doi:10.1073/pnas.0406056102.

Baer, C. F., Shaw, F., Steding, C., Baumgartner, M., Hawkins, A., Houppert, A., et al. (2005c). Comparative evolutionary genetics of spontaneous mutations

affecting fitness in rhabditid nematodes. *Proc. Natl. Acad. Sci. U. S. A.* 102, 5785–5790. doi:10.1073/pnas.0406056102.

Baer, C. F., Shaw, F., Steding, C., Baumgartner, M., Hawkins, A., Houppert, A., et al. (2005d). Comparative evolutionary genetics of spontaneous mutations affecting fitness in rhabditid nematodes. *Proc. Natl. Acad. Sci. U. S. A.* 102, 5785–90. doi:10.1073/pnas.0406056102.

Bamshad, M., and Wooding, S. (2003). Signatures of natural selection in the human genome. *Nat. Rev. Genet.* 4, 99–111. doi:10.1038/nrg999.

Barnes, T. M., and Hekimi, S. (2002). The Caenorhabditis elegans Avermectin Resistance and Anesthetic Response Gene unc-9 Encodes a Member of a Protein Family Implicated in Electrical Coupling of Excitable Cells. *J. Neurochem.* 69, 2251–2260. doi:10.1046/j.1471-4159.1997.69062251.x.

Barroso-Batista, J., Sousa, A., Louren??o, M., Bergman, M. L., Sobral, D., Demengeot, J., et al. (2014). The First Steps of Adaptation of Escherichia coli to the Gut Are Dominated by Soft Sweeps. *PLoS Genet.* 10. doi:10.1371/journal.pgen.1004182.

Bataillon, T. (2000). Estimation of spontaneous genome-wide mutation rate parameters: whither beneficial mutations? *Heredity (Edinb).* 84, 497–501. doi:10.1046/j.1365-2540.2000.00727.x.

Bataillon, T. (2003). Shaking the "deleterious mutations" dogma? *Trends Ecol. Evol.* 18, 315–317. doi:10.1016/S0169-5347(03)00128-9.

Benard, G., Bellance, N., Jose, C., and Rossignol, R. (2011). "Relationships Between Mitochondrial Dynamics and Bioenergetics," in *Mitochondrial Dynamics and Neurodegeneration* (Dordrecht: Springer Netherlands), 47–68. doi:10.1007/978-94-007-1291-1_2.

Bergstrom, C. T., and Pritchard, J. (1998). Germline bottlenecks and the evolutionary maintenance of mitochondrial genomes. *Genetics* 149, 2135–2146.

Bhatnagar, A., Suresh Nair, K. R., Kumar, R., Chalapati, K., and Patro, Y. G. K. (1994). Study of Cross Coupling in Transition Bends Using Cascaded Coupler Segment Method. *IEEE Photonics Technol. Lett.* 6, 1004–1007. doi:10.1109/68.313077.

Brandt, U. (2006). Energy converting NADH:quinone oxidoreductase (complex I). *Annu. Rev. Biochem.* 75, 69–92. doi:10.1146/annurev.biochem.75.103004.142539.

Bratic, I., Hench, J., Henriksson, J., Antebi, A., Bürglin, T. R., and Trifunovic, A. (2009). Mitochondrial DNA level, but not active replicase, is essential for Caenorhabditis elegans development. *Nucleic Acids Res.* 37, 1817–1828. doi:10.1093/nar/gkp018.

Bratic, I., Hench, J., and Trifunovic, A. (2010). Caenorhabditis elegans as a model system for mtDNA replication defects. *Methods* 51, 437–443. doi:10.1016/j.ymeth.2010.03.003.

Brenner, S. (1974). The genetics of Caenorhabditis elegans. *Genetics* 77, 71–94. doi:10.1002/cbic.200300625.

Bromham, L. (2009). Does nothing in evolution make sense except in the light of population genetics? *Biol. Philos.* 24, 387–403. doi:10.1007/s10539-008-9146-6.

Brys, K., Castelein, N., Matthijssens, F., Vanfleteren, J. R., and Braeckman, B. P. (2010). Disruption of insulin signalling preserves bioenergetic competence of mitochondria in ageing Caenorhabditis elegans. *BMC Biol.* 8, 91. doi:10.1186/1741-7007-8-91.

Burch, C. L., and Chao, L. (1999). Evolution by small steps and rugged landscapes in the RNA virus ??6. *Genetics* 151, 921–927.

Busch, K. B., Kowald, A., and Spelbrink, J. N. (2014). Quality matters: how does mitochondrial network dynamics and quality control impact on mtDNA integrity? *Philos. Trans. R. Soc. Lond. B. Biol. Sci.* 369, 20130442. doi:10.1098/rstb.2013.0442.

Butow, R. A., and Avadhani, N. G. (2004). Mitochondrial signaling: The retrograde response. *Mol. Cell* 14, 1–15. doi:10.1016/S1097-2765(04)00179-0.

Caenorhabditis Genetics Center Available at: http://cbs.umn.edu/cgc/home# [Accessed June 20, 2004].

Cai, X., Bao, L., Ren, J., Li, Y., and Zhang, Z. (2016). Grape seed procyanidin B2 protects podocytes from high glucose-induced mitochondrial dysfunction and apoptosis via the AMPK-SIRT1-PGC-1α axis in vitro. *Food Funct.* 7, 805–15. doi:10.1039/c5fo01062d.

Camon, E. (2003). The Gene Ontology Annotation (GOA) Project: Implementation of GO in SWISS-PROT, TrEMBL, and InterPro. *Genome Res.* 13, 662–672. doi:10.1101/gr.461403.

Chao, L. (1990). Fitness of RNA virus decreased by Muller's ratchet. *Nature* 348, 454–455. doi:10.1038/348454a0.

Chasnov, J. R., and Chow, K. L. (2002). Why are there males in the hermaphroditic species Caenorhabditis elegans? *Genetics* 160, 983–994.

Chen, A. T. Y., Guo, C., Itani, O. A., Budaitis, B. G., Williams, T. W., Hopkins, C. E., et al. (2015). Longevity genes revealed by integrative analysis of isoform-specific daf-16/FoxO mutants of caenorhabditis elegans. *Genetics* 201, 613–629. doi:10.1534/genetics.115.177998.

Chevrollier, A., Cassereau, J., Ferré, M., Alban, J., Desquiret-Dumas, V., Gueguen, N., et al. (2012). Standardized mitochondrial analysis gives new insights into mitochondrial dynamics and OPA1 function. *Int. J. Biochem. Cell Biol.* 44, 980–988. doi:10.1016/j.biocel.2012.03.006.

Chinnery, P. F., Thorburn, D. R., Samuels, D. C., White, S. L., Dahl, H. H. M., Turnbull, D. M., et al. (2000). The inheritance of mitochondrial DNA heteroplasmy: Random drift, selection or both? *Trends Genet.* 16, 500–505. doi:10.1016/S0168-9525(00)02120-X.

Chol, M. (2003). The mitochondrial DNA G13513A MELAS mutation in the NADH dehydrogenase 5 gene is a frequent cause of Leigh-like syndrome with isolated complex I deficiency. *J. Med. Genet.* 40, 188–191. doi:10.1136/jmg.40.3.188.

Clark, K. a., Howe, D. K., Gafner, K., Kusuma, D., Ping, S., Estes, S., et al. (2012). Selfish little circles: Transmission bias and evolution of large deletion-bearing mitochondrial DNA in caenorhabditis briggsae nematodes. *PLoS One* 7, 1–8. doi:10.1371/journal.pone.0041433.

Cloney, R. (2016). Molecular evolution: Friends with benefits - sex speeds up adaptation. *Nat. Rev. Genet.* doi:10.1038/nrg.2016.32.

Consortium, C. elegans S. (1998). Genome sequence of the nematode C. elegans: a platform for investigating biology. *Science* 282, 2012–2018. Available at: http://www.ncbi.nlm.nih.gov/pubmed/9851916.

Couillault, C., Pujol, N., Reboul, J., Sabatier, L., Guichou, J.-F., Kohara, Y., et al. (2004). TLR-independent control of innate immunity in Caenorhabditis elegans by the TIR domain adaptor protein TIR-1, an ortholog of human SARM. *Nat. Immunol.* 5, 488–494. doi:10.1038/ni1060.

Coyne, J. A., Barton, N. H., and Turelli, M. (1997). Perspective: A Critique of Sewall Wright's Shifting Balance Theory of Evolution. *Evolution (N. Y).* 51, 643. doi:10.2307/2411143.

Coyne, J., Barton, N., and Turelli, M. (2000). Is Wright's shifting balance process important in evolution? *Evolution (N. Y).* 54, 306–317. doi:10.1554/0014-3820(2000)054[0306:iwssbp]2.0.co;2.

Dancy, B. M., Sedensky, M. M., and Morgan, P. G. (2015). Mitochondrial bioenergetics and disease in Caenorhabditis elegans. *Front. Biosci. (Landmark Ed.* 20, 198–228. doi:10.2741/4305.

Darrouzet, E., Issartel, J.-P., Lunardi, J., and Dupuis, A. (1998). The 49-kDa subunit of NADH-ubiquinone oxidoreductase (Complex I) is involved in the binding of piericidin and rotenone, two quinone-related inhibitors. *FEBS Lett.* 431, 34–38. doi:10.1016/S0014-5793(98)00719-4.

Denver, D. R. (2000). High Direct Estimate of the Mutation Rate in the Mitochondrial Genome of Caenorhabditis elegans. *Science (80-.).* 289, 2342–2344. doi:10.1126/science.289.5488.2342.

Denver, D. R., Dolan, P. C., Wilhelm, L. J., Sung, W., Lucas-Lledo, J. I., Howe, D. K., et al. (2009a). A genome-wide view of Caenorhabditis elegans base-substitution mutation processes. *Proc. Natl. Acad. Sci.* 106, 16310–16314. doi:10.1073/pnas.0904895106.

Denver, D. R., Dolan, P. C., Wilhelm, L. J., Sung, W., Lucas-Lledó, J. I., Howe, D. K., et al. (2009b). A genome-wide view of Caenorhabditis elegans base-substitution mutation processes. *Proc. Natl. Acad. Sci. U. S. A.* 106, 16310–16314. doi:10.1073/pnas.0904895106.

Denver, D. R., Dolan, P. C., Wilhelm, L. J., Sung, W., Lucas-Lledó, J. I., Howe, D. K., et al. (2009c). A genome-wide view of Caenorhabditis elegans base-substitution mutation processes. *Proc. Natl. Acad. Sci. U. S. A.* 106, 16310–4. doi:10.1073/pnas.0904895106.

Denver, D. R., Howe, D. K., Wilhelm, L. J., Palmer, C. A., Anderson, J. L., Stein, K. C., et al. (2010a). Selective sweeps and parallel mutation in the adaptive recovery from deleterious mutation in Caenorhabditis elegans. *Genome Res.* 20, 1663–1671. doi:10.1101/gr.108191.110.

Denver, D. R., Howe, D. K., Wilhelm, L. J., Palmer, C. A., Anderson, J. L., Stein, K. C., et al. (2010b). Selective sweeps and parallel mutation in the adaptive recovery from deleterious mutation in Caenorhabditis elegans. *Genome Res.* 20, 1663–1671. doi:10.1101/gr.108191.110.

Denver, D. R., Morris, K., Lynch, M., Vassilieva, L. L., and Thomas, W. K. (2000). High direct estimate of the mutation rate in the mitochondrial genome of Caenorhabditis elegans. *Science* 289, 2342–2344. doi:10.1126/science.289.5488.2342.

Denver, D. R., Wilhelm, L. J., Howe, D. K., Gafner, K., Dolan, P. C., and Baer, C. F. (2012a). Variation in base-substitution mutation in experimental and natural lineages of caenorhabditis nematodes. *Genome Biol. Evol.* 4, 513–522. doi:10.1093/gbe/evs028.

Denver, D. R., Wilhelm, L. J., Howe, D. K., Gafner, K., Dolan, P. C., and Baer, C. F. (2012b). Variation in Base-Substitution Mutation in Experimental and Natural Lineages of Caenorhabditis Nematodes. *Genome Biol. Evol.* 4, 513–522. doi:10.1093/gbe/evs028.

Depuydt, G., Shanmugam, N., Rasulova, M., Dhondt, I., and Bart, P. (2016). Increased Protein Stability and Decreased Protein Turnover in the Caenorhabditis elegans Ins / IGF-1 daf-2 Mutant. 00, 1–8. doi:10.1093/gerona/glv221.

Dexter, P. M., Caldwell, K. A., and Caldwell, G. A. (2012). A Predictable Worm: Application of Caenorhabditis elegans for Mechanistic Investigation of Movement Disorders. *Neurotherapeutics* 9, 393–404. doi:10.1007/s13311-012-0109-x.

Van Dijk, E. L., Jaszczyszyn, Y., and Thermes, C. (2014). Library preparation methods for next-generation sequencing: Tone down the bias. *Exp. Cell Res.* 322, 12–20. doi:10.1016/j.yexcr.2014.01.008.

Dingley, S., Polyak, E., Lightfoot, R., Ostrovsky, J., Rao, M., Greco, T., et al. (2010). Mitochondrial respiratory chain dysfunction variably increases oxidant stress in Caenorhabditis elegans. *Mitochondrion* 10, 125–136. doi:10.1016/j.mito.2009.11.003.

Doonan, R., McElwee, J. J., Matthijssens, F., Walker, G. A., Houthoofd, K., Back, P., et al. (2008). Against the oxidative damage theory of aging: superoxide dismutases protect against oxidative stress but have little or no effect on life span in Caenorhabditis elegans. *Genes Dev.* 22, 3236–3241. doi:10.1101/gad.504808.

Dromparis, P., and Michelakis, E. D. (2013). Mitochondria in Vascular Health and Disease. *Annu. Rev. Physiol.* 75, 95–126. doi:10.1146/annurev-physiol-030212-183804.

Dufourcq, P., Victor, M., Gay, F., Calvo, D., Hodgkin, J., and Shi, Y. (2002). Functional Requirement for Histone Deacetylase 1 in Caenorhabditis elegans Gonadogenesis. *Mol. Cell. Biol.* 22, 3024–3034. doi:10.1128/MCB.22.9.3024-3034.2002.

Van den Ecker, D., van den Brand, M. A., Ariaans, G., Hoffmann, M., Bossinger, O., Mayatepek, E., et al. (2012). Identification and functional analysis of

mitochondrial complex I assembly factor homologues in C. elegans. *Mitochondrion* 12, 399–405. doi:10.1016/j.mito.2012.01.003.

Efremov, R. G., and Sazanov, L. A. (2011). Structure of the membrane domain of respiratory complex I. *Nature* 476, 414–420. doi:10.1038/nature10330.

Elkin, C. J., Richardson, P. M., Fourcade, H. M., Hammon, N. M., Pollard, M. J., Predki, P. F., et al. (2001). High-throughput plasmid purification for capillary sequencing. *Genome Res.* 11, 1269–1274. doi:10.1101/gr.167801.

Emerit, J., Edeas, M., and Bricaire, F. (2004). Neurodegenerative diseases and oxidative stress. *Biomed. Pharmacother.* 58, 39–46. doi:10.1016/j.biopha.2003.11.004.

Erkut, C., Vasilj, A., Boland, S., Habermann, B., Shevchenko, A., and Kurzchalia, T. V. (2013). Molecular Strategies of the Caenorhabditis elegans Dauer Larva to Survive Extreme Desiccation. *PLoS One* 8, e82473. doi:10.1371/journal.pone.0082473.

Escobar-Henriques, M., and Anton, F. (2013). Mechanistic perspective of mitochondrial fusion: Tubulation vs. fragmentation. *Biochim. Biophys. Acta - Mol. Cell Res.* 1833, 162–175. doi:10.1016/j.bbamcr.2012.07.016.

Estes, S., and Lynch, M. (2003). Rapid fitness recovery in mutationally degraded lines of Caenorhabditis elegans. *Evolution* 57, 1022–1030.

Eyre-Walker, a, and Keightley, P. D. (1999). High genomic deleterious mutation rates in hominids. *Nature* 397, 344–347. doi:10.1038/16915.

Faergeman, N. J., and Knudsen, J. (1997). Role of long-chain fatty acyl-CoA esters in the regulation of metabolism and in cell signalling. *Biochem. J.* 323 (Pt 1, 1–12.

Falk, M. J., Rosenjack, J. R., Polyak, E., Suthammarak, W., Chen, Z., Morgan, P. G., et al. (2009). Subcomplex Ilambda specifically controls integrated mitochondrial functions in Caenorhabditis elegans. *PLoS One* 4. doi:10.1371/journal.pone.0006607.

Falk, M. J., Zhang, Z., Rosenjack, J. R., Nissim, I., Daikhin, E., Nissim, I., et al. (2008). Metabolic pathway profiling of mitochondrial respiratory chain mutants in C. elegans. *Mol. Genet. Metab.* 93, 388–397. doi:10.1016/j.ymgme.2007.11.007.

Fan, W., Waymire, K. G., Narula, N., Li, P., Rocher, C., Coskun, P. E., et al. (2008). A mouse model of mitochondrial disease reveals germline selection

against severe mtDNA mutations. *Science* 319, 958–962. doi:10.1126/science.1147786.

Farlow, A., Long, H., Arnoux, S., Sung, W., Doak, T. G., Nordborg, M., et al. (2015). The spontaneous mutation rate in the fission yeast Schizosaccharomyces pombe. *Genetics* 201, 737–744. doi:10.1534/genetics.115.177329.

Fassone, E., and Rahman, S. (2012). Complex I deficiency: clinical features, biochemistry and molecular genetics. *J. Med. Genet.* 49, 578–590. doi:10.1136/jmedgenet-2012-101159.

Fato, R., Bergamini, C., Leoni, S., Strocchi, P., and Lenaz, G. (2008). Generation of reactive oxygen species by mitochondrial complex I: Implications in neurodegeneration. *Neurochem. Res.* 33, 2487–2501. doi:10.1007/s11064-008-9747-0.

Fisher, R. A. (1930). *The genetical theory of natural selection*. Oxford, United Kingdom: Oxfors University Press.

Fleury, C., Mignotte, B., and Vayssière, J.-L. (2002). Mitochondrial reactive oxygen species in cell death signaling. *Biochimie* 84, 131–141. doi:10.1016/S0300-9084(02)01369-X.

Di Francesco, A., and De Cabo, R. (2015). Two-year trial of human caloric restriction. *Journals Gerontol. - Ser. A Biol. Sci. Med. Sci.* 70, 1095–1096. doi:10.1093/gerona/glv100.

Froenicke, L. (2015). First HiSeq 3000 data download. Available at: http://dnatech.genomecenter.ucdavis.edu/2015/05/07/first-hiseq-3000-data-download/ [Accessed April 1, 2016].

Galluzzi, L., Kepp, O., Trojel-Hansen, C., and Kroemer, G. (2012). Mitochondrial control of cellular life, stress, and death. *Circ. Res.* 111, 1198–1207. doi:10.1161/CIRCRESAHA.112.268946.

Greene, E. A., Codomo, C. A., Taylor, N. E., Henikoff, J. G., Till, B. J., Reynolds, S. H., et al. (2003). Spectrum of chemically induced mutations from a large-scale reverse-genetic screen in Arabidopsis. *Genetics* 164, 731–740.

Groenewoud, M. J., and Zwartkruis, F. J. T. (2013). Rheb and mammalian target of rapamycin in mitochondrial homoeostasis. *Open Biol.* 3, 130185–130185. doi:10.1098/rsob.130185.

Guha, M., and Avadhani, N. G. (2013). Mitochondrial retrograde signaling at the crossroads of tumor bioenergetics, genetics and epigenetics. *Mitochondrion* 13, 577–591. doi:10.1016/j.mito.2013.08.007.

Gumienny, T. L., Brugnera, E., Tosello-Trampont, A.-C., Kinchen, J. M., Haney, L. B., Nishiwaki, K., et al. (2001). CED-12/ELMO, a Novel Member of the CrkII/Dock180/Rac Pathway, Is Required for Phagocytosis and Cell Migration. *Cell* 107, 27–41. doi:10.1016/S0092-8674(01)00520-7.

Hadzsiev, K., Maasz, A., Kisfali, P., Kalman, E., Gomori, E., Pal, E., et al. (2010). Mitochondrial DNA 11777C>A Mutation Associated Leigh Syndrome: Case Report with a Review of the Previously Described Pedigrees. *NeuroMolecular Med.* 12, 277–284. doi:10.1007/s12017-010-8115-9.

Halaschek-Wiener, J. (2005). Analysis of long-lived C. elegans daf-2 mutants using serial analysis of gene expression. *Genome Res.* 15, 603–615. doi:10.1101/gr.3274805.

Hall, D. W., and Joseph, S. B. (2010). A high frequency of beneficial mutations across multiple fitness components in Saccharomyces cerevisiae. *Genetics* 185, 1397–1409. doi:10.1534/genetics.110.118307.

Hall, D. W., Mahmoudizad, R., Hurd, A. W., and Joseph, S. B. (2008). Spontaneous mutations in diploid Saccharomyces cerevisiae: another thousand cell generations. *Genet. Res. (Camb).* 90, 229–241. doi:10.1017/S001667230900024X.

Halligan, D. L., and Keightley, P. D. (2009). Spontaneous Mutation Accumulation Studies in Evolutionary Genetics. *Annu. Rev. Ecol. Evol. Syst.* 40, 151–172. doi:10.1146/annurev.ecolsys.39.110707.173437.

Han, X., Gomes, J.-E., Birmingham, C. L., Pintard, L., Sugimoto, A., and Mains, P. E. (2009). The Role of Protein Phosphatase 4 in Regulating Microtubule Severing in the Caenorhabditis elegans Embryo. *Genetics* 181, 933–943. doi:10.1534/genetics.108.096016.

Hansen, M., Chandra, A., Mitic, L. L., Onken, B., Driscoll, M., and Kenyon, C. (2008). A role for autophagy in the extension of lifespan by dietary restriction in C. elegans. *PLoS Genet.* 4. doi:10.1371/journal.pgen.0040024.

Hao, J. C., Yu, T. W., Fujisawa, K., Culotti, J. G., Gengyo-Ando, K., Mitani, S., et al. (2001). C. elegans slit acts in midline, dorsal-ventral, and anterior-posterior guidance via the SAX-3/Robo receptor. *Neuron* 32, 25–38. doi:10.1016/S0896-6273(01)00448-2.

Harding, H. P., Zhang, Y., Zeng, H., Novoa, I., Lu, P. D., Calfon, M., et al. (2003). An Integrated Stress Response Regulates Amino Acid Metabolism and Resistance to Oxidative Stress. *Mol. Cell* 11, 619–633. doi:10.1016/S1097-2765(03)00105-9.

Hartman, P. S., Ishii, N., Kayser, E. B., Morgan, P. G., and Sedensky, M. M. (2001). Mitochondrial mutations differentially affect aging, mutability and anesthetic sensitivity in Caenorhabditis elegans. *Mech. Ageing Dev.* 122, 1187–1201. doi:10.1016/S0047-6374(01)00259-7.

Heimbucher, T., Liu, Z., Bossard, C., McCloskey, R., Carrano, A. C., Riedel, C. G., et al. (2015). The Deubiquitylase MATH-33 Controls DAF-16 Stability and Function in Metabolism and Longevity. *Cell Metab.* 22, 151–163. doi:10.1016/j.cmet.2015.06.002.

Hirsch, C., Blom, D., and Ploegh, H. L. (2003). A role for N-glycanase in the cytosolic turnover of glycoproteins. *EMBO J.* 22, 1036–1046. doi:10.1093/emboj/cdg107.

Holmes, E. C. (2003). Patterns of Intra- and Interhost Nonsynonymous Variation Reveal Strong Purifying Selection in Dengue Virus. *J. Virol.* 77, 11296–11298. doi:10.1128/JVI.77.20.11296-11298.2003.

Holt, I. J., Speijer, D., and Kirkwood, T. B. L. (2014). The road to rack and ruin: selecting deleterious mitochondrial DNA variants. *Philos. Trans. R. Soc. B Biol. Sci.* 369, 20130451–20130451. doi:10.1098/rstb.2013.0451.

Honda, Y., and Honda, S. (1999). The daf-2 gene network for longevity regulates oxidative stress resistance and Mn-superoxide dismutase gene expression in Caenorhabditis elegans. *FASEB J.* 13, 1385–1393.

Honda, Y., and Honda, S. (2002). Oxidative stress and life span determination in the nematode Caenorhabditis elegans. *Ann.N.Y.Acad.Sci.* 959, 466–474. Available at: http://www.ncbi.nlm.nih.gov/entrez/query.fcgi?cmd=Retrieve&db=PubMed&dopt=Citation&list_uids=11976220.

Honjoh, S., Yamamoto, T., Uno, M., and Nishida, E. (2009). Signalling through RHEB-1 mediates intermittent fasting-induced longevity in C. elegans. *Nature* 457, 726–730. doi:10.1038/nature07583.

Howe, D. K., Baer, C. F., and Denver, D. R. (2010). High rate of large deletions in Caenorhabditis briggsae mitochondrial genome mutation processes. *Genome Biol. Evol.* 2, 29–38. doi:10.1093/gbe/evp055.

Howe, D. K., and Denver, D. R. (2008). Muller's Ratchet and compensatory mutation in Caenorhabditis briggsae mitochondrial genome evolution. *BMC Evol. Biol.* 8, 62. doi:10.1186/1471-2148-8-62.

Hsu, A.-L., Murphy, C. T., and Kenyon, C. (2003). Regulation of Aging and Age-Related Disease by DAF-16 and Heat-Shock Factor. *Science (80-.).* 300, 1142–1145. doi:10.1126/science.1083701.

Hu, J.-P., Xu, X.-Y., Huang, L.-Y., Wang, L., and Fang, N.-Y. (2015). Freeze–thaw Caenorhabditis elegans freeze–thaw stress response is regulated by the insulin/IGF-1 receptor daf-2. *BMC Genet.* 16, 139. doi:10.1186/s12863-015-0298-5.

Huang, C., Harada, Y., Hosomi, A., Masahara-Negishi, Y., Seino, J., Fujihira, H., et al. (2015). Endo-β-N-acetylglucosaminidase forms N-GlcNAc protein aggregates during ER-associated degradation in Ngly1-defective cells. *Proc. Natl. Acad. Sci.*, 201414593. doi:10.1073/pnas.1414593112.

Illumina Sequencing (2010). Available at: http://www.illumina.com/documents/products/techspotlights/techspotlight_sequencing.pdf [Accessed April 1, 2016].

Iser, W. B., and Wolkow, C. A. (2007). DAF-2/Insulin-Like Signaling in C. elegans Modifies Effects of Dietary Restriction and Nutrient Stress on Aging, Stress and Growth. *PLoS One* 2, e1240. doi:10.1371/journal.pone.0001240.

Jenuth, J. P., Peterson, a C., and Shoubridge, E. a (1997). Tissue-specific selection for different mtDNA genotypes in heteroplasmic mice. *Nat. Genet.* 16, 93–95. doi:10.1038/ng0597-93.

Johri, A., and Beal, M. F. (2012). Mitochondrial dysfunction in neurodegenerative diseases. *J. Pharmacol. Exp. Ther.* 342, 619–630. doi:10.1124/jpet.112.192138.

Joyner-Matos, J., Hicks, K. A., Cousins, D., Keller, M., Denver, D. R., Baer, C. F., et al. (2013). Evolution of a Higher Intracellular Oxidizing Environment in Caenorhabditis elegans under Relaxed Selection. *PLoS One* 8, e65604. doi:10.1371/journal.pone.0065604.

Jun, A. S., Trounce, I. A., Brown, M. D., Shoffner, J. M., and Wallace, D. C. (1996). Use of transmitochondrial cybrids to assign a complex I defect to the mitochondrial DNA-encoded NADH dehydrogenase subunit 6 gene mutation at nucleotide pair 14459 that causes Leber hereditary optic neuropathy and dystonia. *Mol. Cell. Biol.* 16, 771–777. Available at:

http://mcb.asm.org/cgi/reprint/16/3/771?view=long&pmid=8622678\npapers3://publication/uuid/0723095B-18F7-4D3C-8753-FEEF567AB8EA.

Kamran-Disfani, A., and Agrawal, A. F. (2014). Selfing, adaptation and background selection in finite populations. *J. Evol. Biol.* 27, 1360–1371. doi:10.1111/jeb.12343.

Kann, L. M., Rosenblum, E. B., and Rand, D. M. (1998). Aging, mating, and the evolution of mtDNA heteroplasmy in Drosophila melanogaster. *Proc. Natl. Acad. Sci. U. S. A.* 95, 2372–7. doi:10.1073/pnas.95.5.2372.

Karthikeyan, G., and Resnick, M. A. (2005). Impact of mitochondria on nuclear genome stability. *DNA Repair (Amst).* 4, 141–148. doi:10.1016/j.dnarep.2004.07.004.

Kayser, E. B., Morgan, P. G., Hoppel, C. L., and Sedensky, M. M. (2001a). Mitochondrial expression and function of GAS-1 in Caenorhabditis elegans. *J. Biol. Chem.* 276, 20551–20558. doi:10.1074/jbc.M011066200.

Kayser, E. B., Morgan, P. G., Hoppel, C. L., and Sedensky, M. M. (2001b). Mitochondrial Expression and Function of GAS-1 in Caenorhabditis elegans. *J. Biol. Chem.* 276, 20551–20558. doi:10.1074/jbc.M011066200.

Kayser, E. B., Morgan, P. G., and Sedensky, M. M. (1999a). GAS-1: a mitochondrial protein controls sensitivity to volatile anesthetics in the nematode Caenorhabditis elegans. *Anesthesiology* 90, 545–554. doi:10.1097/00000542-199902000-00031.

Kayser, E. B., Sedensky, M. M., and Morgan, P. G. (2004a). The effects of complex I function and oxidative damage on lifespan and anesthetic sensitivity in Caenorhabditis elegans. *Mech. Ageing Dev.* 125, 455–464. doi:10.1016/j.mad.2004.04.002.

Kayser, E. B., Suthammarak, W., Morgan, P. G., and Sedensky, M. M. (2011). Isoflurane selectively inhibits distal mitochondrial complex i in caenorhabditis elegans. *Anesth. Analg.* 112, 1321–1329. doi:10.1213/ANE.0b013e3182121d37.

Kayser, E.-B., Hoppel, C. L., Morgan, P. G., and Sedensky, M. M. (2003). A mutation in mitochondrial complex I increases ethanol sensitivity in Caenorhabditis elegans. *Alcohol. Clin. Exp. Res.* 27, 584–92. doi:10.1097/01.ALC.0000060524.62805.D2.

Kayser, E.-B., Morgan, P. G., and Sedensky, M. M. (1999b). GAS-1. *Anesthesiology* 90, 545–554. doi:10.1097/00000542-199902000-00031.

Kayser, E.-B., Sedensky, M. M., and Morgan, P. G. (2004b). The effects of complex I function and oxidative damage on lifespan and anesthetic sensitivity in Caenorhabditis elegans. *Mech. Ageing Dev.* 125, 455–464. doi:10.1016/j.mad.2004.04.002.

Keightley, P. D., and Otto, S. P. (2006). Interference among deleterious mutations favours sex and recombination in finite populations. *Nature* 443, 89–92. doi:10.1038/nature05049.

Keightley, P. D., Trivedi, U., Thomson, M., Oliver, F., Kumar, S., and Blaxter, M. L. (2009). Analysis of the genome sequences of three Drosophila melanogaster spontaneous mutation accumulation lines. *Genome Res.* 19, 1195–1201. doi:10.1101/gr.091231.109.

Kennedy, S. R., Loeb, L. A., and Herr, A. J. (2012). Somatic mutations in aging, cancer and neurodegeneration. *Mech. Ageing Dev.* 133, 118–126. doi:10.1016/j.mad.2011.10.009.

Kenyon, C. (2011). The first long-lived mutants: discovery of the insulin/IGF-1 pathway for ageing. *Philos. Trans. R. Soc. B Biol. Sci.* 366, 9–16. doi:10.1098/rstb.2010.0276.

Khopp, K., Zaidenshnur, G., Beier, R., Kheinrikh, I., and Germann, K. (1977). [Cardiotocographic and electroencephalographic studies in early diagnosis of fetal hypoxia]. *Akush Ginekol (Mosk)*, 27–31.

Kim, E. H., Koh, E. H., Park, J.-Y., and Lee, K.-U. (2010). Adenine Nucleotide Translocator as a Regulator of Mitochondrial Function: Implication in the Pathogenesis of Metabolic Syndrome. *Korean Diabetes J.* 34, 146. doi:10.4093/kdj.2010.34.3.146.

Kim, Y., Schumaker, K. S., and Zhu, J.-K. (2006). EMS mutagenesis of Arabidopsis. *Methods Mol. Biol.* 323, 101–103. doi:10.1101/pdb.prot4621.

Kimura, M. (1984). *The neutral theory of molecular evolution*. doi:http://dx.doi.org/10.1017/CBO9780511623486.

Kiriyama, Y., and Nochi, H. (2015). The Function of Autophagy in Neurodegenerative Diseases. *Int. J. Mol. Sci.* 16, 26797–26812. doi:10.3390/ijms161125990.

Knott, A. B., Perkins, G., Schwarzenbacher, R., and Bossy-Wetzel, E. (2008). Mitochondrial fragmentation in neurodegeneration. *Nat. Rev. Neurosci.* 9, 505–518. doi:10.1038/nrn2417.

Kondo, M., Senoo-Matsuda, N., Yanase, S., Ishii, T., Hartman, P. S., and Ishii, N. (2005). Effect of oxidative stress on translocation of DAF-16 in oxygen-sensitive mutants, mev-1 and gas-1 of Caenorhabditis elegans. *Mech. Ageing Dev.* 126, 637–641. doi:10.1016/j.mad.2004.11.011.

Kondrashov, A. S. (1988). Deleterious mutations and the evolution of sexual reproduction. *Nature* 336, 435–440. doi:10.1038/336435a0.

Kovacs, A. L., and Zhang, H. (2010). Role of autophagy in Caenorhabditis elegans. *FEBS Lett.* 584, 1335–1341. doi:10.1016/j.febslet.2010.02.002.

Kryazhimskiy, S., and Plotkin, J. B. (2008). The Population Genetics of dN/dS. *PLoS Genet.* 4, e1000304. doi:10.1371/journal.pgen.1000304.

Księzakowska-Łakoma, K., Zyła, M., and Wilczyński, J. R. (2014). Mitochondrial dysfunction in cancer. *Prz. Menopauzalny* 18, 136–144. doi:10.5114/pm.2014.42717.

Kurki, S., Zickermann, V., Kervinen, M., Hassinen, I., and Finel, M. (2000). Mutagenesis of three conserved Glu residues in a bacterial homologue of the ND1 subunit of complex I affects ubiquinone reduction kinetics but not inhibition by dicyclohexylcarbodiimide. *Biochemistry* 39, 13496–13502. doi:10.1021/bi001134s.

Lande, R. (1995). Mutation and Conservation. *Conserv. Biol.* 9, 782–791. doi:10.1046/j.1523-1739.1995.09040782.x.

Lane, N. (2011). Mitonuclear match: Optimizing fitness and fertility over generations drives ageing within generations. *Bioessays* 33, 860–869. doi:10.1002/bies.201100051.

Lane, N. (2014). Bioenergetic constraints on the evolution of complex life. *Cold Spring Harb. Perspect. Biol.* 6. doi:10.1101/cshperspect.a015982.

Lapierre, L. R., and Hansen, M. (2012). Lessons from C. elegans: Signaling pathways for longevity. *Trends Endocrinol. Metab.* 23, 637–644. doi:10.1016/j.tem.2012.07.007.

Laplante, M., and Sabatini, D. M. (2012). mTOR Signaling in Growth Control and Disease. *Cell* 149, 274–293. doi:10.1016/j.cell.2012.03.017.

Lemasters, J. J., and Sowers, A. E. (1979). Phosphate dependence and atractyloside inhibition of mitochondrial oxidative phosphorylation. The ADP-ATP carrier is rate-limiting. *J. Biol. Chem.* 254, 1248–1251.

Lenski, R. E. (2001). "Evolutionary Rate," in *Encyclopedia of Genetics* (Elsevier), 671–672. doi:10.1006/rwgn.2001.0432.

Leung, M. C. K., Rooney, J. P., Ryde, I. T., Bernal, A. J., Bess, A. S., Crocker, T. L., et al. (2013). Effects of early life exposure to ultraviolet C radiation on mitochondrial DNA content, transcription, ATP production, and oxygen consumption in developing Caenorhabditis elegans. *BMC Pharmacol. Toxicol.* 14, 9. doi:10.1186/2050-6511-14-9.

Li, Y., Inoki, K., and Guan, K.-L. (2004). Biochemical and Functional Characterizations of Small GTPase Rheb and TSC2 GAP Activity. *Mol. Cell. Biol.* 24, 7965–7975. doi:10.1128/MCB.24.18.7965-7975.2004.

Lindahl, T. (1993). Instability and decay of the primary structure of DNA. *Nature* 362, 709–715. doi:10.1038/362709a0.

Lithgow, G. J., White, T. M., Melov, S., and Johnson, T. E. (1995). Thermotolerance and extended life-span conferred by single-gene mutations and induced by thermal stress. *Proc. Natl. Acad. Sci. U. S. A.* 92, 7540–7544. doi:10.1073/pnas.92.16.7540.

Liu, C.-S., Tsai, C.-S., Kuo, C.-L., Chen, H.-W., Lii, C.-K., Ma, Y.-S., et al. (2003). Oxidative stress-related alteration of the copy number of mitochondrial DNA in human leukocytes. *Free Radic. Res.* 37, 1307–1317.

Loewe, L., and Hill, W. G. (2010). The population genetics of mutations: good, bad and indifferent. *Philos. Trans. R. Soc. B Biol. Sci.* 365, 1153–1167. doi:10.1098/rstb.2009.0317.

Loman, N. J., Misra, R. V, Dallman, T. J., Constantinidou, C., Gharbia, S. E., Wain, J., et al. (2012). Performance comparison of benchtop high-throughput sequencing platforms. *Nat. Biotechnol.* 30, 434–9. doi:10.1038/nbt.2198.

Lynch, M., Blanchard, J., Houle, D., Kibota, T., Schultz, S., Vassilieva, L., et al. (1999). Perspective: Spontaneous Deleterious Mutation. *Evolution (N. Y).* 53, 645. doi:10.2307/2640707.

Lynch, M., Bürger, R., Butcher, D., and Gabriel, W. (1993). The mutational meltdown in asexual populations. *J. Hered.* 84, 339–44. Available at: http://www.ncbi.nlm.nih.gov/pubmed/8409355.

Lynch, S. M., Weinstein, S. J., Virtamo, J., Lan, Q., Liu, C.-S., Cheng, W.-L., et al. (2011). Mitochondrial DNA copy number and pancreatic cancer in the alpha-tocopherol beta-carotene cancer prevention study. *Cancer Prev. Res. (Phila).* 4, 1912–1919. doi:10.1158/1940-6207.CAPR-11-0002.

Maeda, I., Kohara, Y., Yamamoto, M., and Sugimoto, A. (2001). Large-scale analysis of gene function in Caenorhabditis elegans by high-throughput RNAi. *Curr. Biol.* 11, 171–176. doi:10.1016/S0960-9822(01)00052-5.

Maisnier-Patin, S., Berg, O. G., Liljas, L., and Andersson, D. I. (2002). Compensatory adaptation to the deleterious effect of antibiotic resistance in Salmonella typhimurium. *Mol. Microbiol.* 46, 355–366. doi:10.1046/j.1365-2958.2002.03173.x.

Martin, D. E., and Hall, M. N. (2005). The expanding TOR signaling network. *Curr. Opin. Cell Biol.* 17, 158–166. doi:10.1016/j.ceb.2005.02.008.

Martin, T. D., Chen, X. W., Kaplan, R. E. W., Saltiel, A. R., Walker, C. L., Reiner, D. J., et al. (2014). Ral and Rheb GTPase Activating Proteins Integrate mTOR and GTPase Signaling in Aging, Autophagy, and Tumor Cell Invasion. *Mol. Cell* 53, 209–220. doi:10.1016/j.molcel.2013.12.004.

Martin, W., and Müller, M. (1998). The hydrogen hypothesis for the first eukaryote. *Nature* 392, 37–41. doi:10.1038/32096.

Mates, J. M., and Sanchez-Jimenez, F. M. (2000). Role of reactive oxygen species in apoptosis: implications for cancer therapy. *Int. J. Biochem. Cell Biol.* 32, 157–170. doi:10.1016/S1357-2725(99)00088-6.

Mayr, J. A. (2014). Lipid metabolism in mitochondrial membranes. *J. Inherit. Metab. Dis.* 38, 137–144. doi:10.1007/s10545-014-9748-x.

McDonald, M. J., Rice, D. P., and Desai, M. M. (2016). Sex speeds adaptation by altering the dynamics of molecular evolution. *Nature*. doi:10.1038/nature17143.

Meléndez, A., Tallóczy, Z., Seaman, M., Eskelinen, E.-L., Hall, D. H., and Levine, B. (2003). Autophagy genes are essential for dauer development and life-span extension in C. elegans. *Science* 301, 1387–91. doi:10.1126/science.1087782.

Melser, S., Chatelain, E. H., Lavie, J., Mahfouf, W., Jose, C., Obre, E., et al. (2013). Rheb regulates mitophagy induced by mitochondrial energetic status. *Cell Metab.* 17, 719–730. doi:10.1016/j.cmet.2013.03.014.

Michelakis, E. D. (2008). Mitochondrial medicine: A new era in medicine opens new windows and brings new challenges. *Circulation* 117, 2431–2434. doi:10.1161/CIRCULATIONAHA.108.775163.

Mittler, R., Vanderauwera, S., Suzuki, N., Miller, G., Tognetti, V. B., Vandepoele, K., et al. (2011). ROS signaling: The new wave? *Trends Plant Sci.* 16, 300–309. doi:10.1016/j.tplants.2011.03.007.

Montooth, K. L., and Rand, D. M. (2008). The Spectrum of Mitochondrial Mutation Differs across Species. *PLoS Biol.* 6, e213. doi:10.1371/journal.pbio.0060213.

Moreira, P. I., Carvalho, C., Zhu, X., Smith, M. A., and Perry, G. (2010). Mitochondrial dysfunction is a trigger of Alzheimer's disease pathophysiology. *Biochim. Biophys. Acta - Mol. Basis Dis.* 1802, 2–10. doi:10.1016/j.bbadis.2009.10.006.

Morgan, P. G., and Sedensky, M. M. (1994). Mutations conferring new patterns of sensitivity to volatile anesthetics in Caenorhabditis elegans. *Anesthesiology* 81, 888–898. Available at: http://www.ncbi.nlm.nih.gov/entrez/query.fcgi?cmd=Retrieve&db=PubMed&dopt=Citation&list_uids=7943840.

Morran, L. T., Cappy, B. J., Anderson, J. L., and Phillips, P. C. (2009). Sexual partners for the stressed: Facultative outcrossing in the self-fertilizing nematode Caenorhabditis elegans. *Evolution (N. Y).* 63, 1473–1482. doi:10.1111/j.1558-5646.2009.00652.x.

Mukai, T. (1964). THE GENETIC STRUCTURE OF NATURAL POPULATIONS OF DROSOPHILA MELANOGASTER. I. SPONTANEOUS MUTATION RATE OF POLYGENES CONTROLLING VIABILITY. *Genetics* 50, 1–19.

Mulder, N. J. (2003). The InterPro Database, 2003 brings increased coverage and new features. *Nucleic Acids Res.* 31, 315–318. doi:10.1093/nar/gkg046.

Muller, H. J. (1964). The relation of recombination to mutational advance. *Mutat. Res.* 106, 2–9. Available at: http://www.ncbi.nlm.nih.gov/pubmed/14195748.

Munkacsy, E., and Rea, S. L. (2014). The paradox of mitochondrial dysfunction and extended longevity. *Exp. Gerontol.* 56, 221–233. doi:10.1016/j.exger.2014.03.016.

Murphy, M. P. (2009). How mitochondria produce reactive oxygen species. *Biochem. J.* 417, 1–13. doi:10.1042/BJ20081386.

Nagaraja, P., Alexander, H. K., Bonhoeffer, S., and Dixit, N. M. (2015). Influence of recombination on acquisition and reversion of immune escape and compensatory mutations in HIV-1. *Epidemics*. doi:10.1016/j.epidem.2015.09.001.

Neher, R. A., and Shraiman, B. I. (2012). Fluctuations of Fitness Distributions and the Rate of Muller's Ratchet. *Genetics* 191, 1283–1293. doi:10.1534/genetics.112.141325.

Ness, R. W., Morgan, A. D., Colegrave, N., and Keightley, P. D. (2012). Estimate of the spontaneous mutation rate in Chlamydomonas reinhardtii. *Genetics* 192, 1447–1454. doi:10.1534/genetics.112.145078.

Nielsen, R., Bustamante, C., Clark, A. G., Glanowski, S., Sackton, T. B., Hubisz, M. J., et al. (2005). A scan for positively selected genes in the genomes of humans and chimpanzees. *PLoS Biol.* 3, 0976–0985. doi:10.1371/journal.pbio.0030170.

Nishant, K. T., Singh, N. D., and Alani, E. (2009). Genomic mutation rates: what high-throughput methods can tell us. *BioEssays* 31, 912–920. doi:10.1002/bies.200900017.

Nisoli, E., and Carruba, M. O. (2006). Nitric oxide and mitochondrial biogenesis. *J. Cell Sci.* 119, 2855–2862. doi:10.1242/jcs.03062.

O'Brien, K. P., Remm, M., and Sonnhammer, E. L. L. (2005). Inparanoid: A comprehensive database of eukaryotic orthologs. *Nucleic Acids Res.* 33. doi:10.1093/nar/gki107.

Okimoto, R., Macfarlane, J. L., Clary, D. O., and Wolstenholme, D. R. (1992). The mitochondrial genomes of two nematodes, Caenorhabditis elegans and Ascaris suum. *Genetics* 130, 471–498.

Orr, H. A. (1998). The Population Genetics of Adaptation: The Distribution of Factors Fixed during Adaptive Evolution. *Evolution (N. Y).* 52, 935. doi:10.2307/2411226.

Orr, H. A. (2005). The genetic theory of adaptation: a brief history. *Nat. Rev. Genet.* 6, 119–127. doi:10.1038/nrg1523.

Ow, Y.-L. P., Green, D. R., Hao, Z., and Mak, T. W. (2008). Cytochrome c: functions beyond respiration. *Nat. Rev. Mol. Cell Biol.* 9, 532–542. doi:10.1038/nrm2434.

Park, C. B., and Larsson, N.-G. (2011). Mitochondrial DNA mutations in disease and aging. *J. Cell Biol.* 193, 809–818. doi:10.1083/jcb.201010024.

Patananan, A. N., Budenholzer, L. M., Eskin, A., Torres, E. R., and Clarke, S. G. (2015). Ethanol-induced differential gene expression and acetyl-CoA metabolism in a longevity model of the nematode Caenorhabditis elegans. *Exp. Gerontol.* 61, 20–30. doi:10.1016/j.exger.2014.11.010.

Pätsi, J., Kervinen, M., Finel, M., and Hassinen, I. E. (2008). Leber hereditary optic neuropathy mutations in the ND6 subunit of mitochondrial complex I affect ubiquinone reduction kinetics in a bacterial model of the enzyme. *Biochem. J.* 409, 129–137. doi:10.1042/BJ20070866.

De Paula, W. B. M., Lucas, C. H., Agip, A.-N. a, Vizcay-Barrena, G., and Allen, J. F. (2013). Energy, ageing, fidelity and sex: oocyte mitochondrial DNA as a protected genetic template. *Philos. Trans. R. Soc. Lond. B. Biol. Sci.* 368, 20120263. doi:10.1098/rstb.2012.0263.

Pellegrino, M. W., and Haynes, C. M. (2015). Mitophagy and the mitochondrial unfolded protein response in neurodegeneration and bacterial infection. *BMC Biol.* 13, 22. doi:10.1186/s12915-015-0129-1.

Phillips, W. S., Coleman-Hulbert, A. L., Weiss, E. S., Howe, D. K., Ping, S., Wernick, R. I., et al. (2015). Selfish Mitochondrial DNA Proliferates and Diversifies in Small, but not Large, Experimental Populations of Caenorhabditis briggsae. *Genome Biol. Evol.* 7, 2023–37. doi:10.1093/gbe/evv116.

Podlesniy, P., Figueiro-Silva, J., Llado, A., Antonell, A., Sanchez-Valle, R., Alcolea, D., et al. (2013). Low cerebrospinal fluid concentration of mitochondrial DNA in preclinical Alzheimer disease. *Ann. Neurol.* 74, 655–668. doi:10.1002/ana.23955.

Poon, A., Davis, B. H., and Chao, L. (2005). The coupon collector and the suppressor mutation: Estimating the number of compensatory mutations by maximum likelihood. *Genetics* 170, 1323–1332. doi:10.1534/genetics.104.037259.

Pópulo, H., Lopes, J. M., and Soares, P. (2012). The mTOR Signalling Pathway in Human Cancer. *Int. J. Mol. Sci.* 13, 1886–1918. doi:10.3390/ijms13021886.

Pujol, C., Bratic-Hench, I., Sumakovic, M., Hench, J., Mourier, A., Baumann, L., et al. (2013). Succinate dehydrogenase upregulation destabilize complex I and limits the lifespan of gas-1 mutant. *PLoS One* 8, e59493. doi:10.1371/journal.pone.0059493.

Pyle, A., Anugrha, H., Kurzawa-Akanbi, M., Yarnall, A., Burn, D., and Hudson, G. (2016). Reduced mitochondrial DNA copy number is a biomarker of Parkinson's disease. *Neurobiol. Aging* 38, 216.e7–216.e10. doi:10.1016/j.neurobiolaging.2015.10.033.

Quail, M., Smith, M. E., Coupland, P., Otto, T. D., Harris, S. R., Connor, T. R., et al. (2012). A tale of three next generation sequencing platforms: comparison

of Ion torrent, pacific biosciences and illumina MiSeq sequencers. *BMC Genomics* 13, 1. doi:10.1186/1471-2164-13-341.

Van Raamsdonk, J. M., and Hekimi, S. (2011). FUdR causes a twofold increase in the lifespan of the mitochondrial mutant gas-1. *Mech. Ageing Dev.* 132, 519–521. doi:10.1016/j.mad.2011.08.006.

Ramis, M. R., Esteban, S., Miralles, A., Tan, D.-X., and Reiter, R. J. (2015). Protective effects of melatonin and mitochondria-targeted antioxidants against oxidative stress: A review. *Curr. Med. Chem.* 22. doi:10.2174/0929867322666150619104143.

Rand, D. M. (2001). The Units of Selection on Mitochondrial DNA. *Annu. Rev. Ecol. Syst.* 32, 415–448. doi:10.1146/annurev.ecolsys.32.081501.114109.

Reddi, A. R., Jensen, L. T., Naranuntarat, A., Rosenfeld, L., Leung, E., Shah, R., et al. (2009). The overlapping roles of manganese and Cu/Zn SOD in oxidative stress protection. *Free Radic. Biol. Med.* 46, 154–162. doi:10.1016/j.freeradbiomed.2008.09.032.

Reinke, S. N., Hu, X., Sykes, B. D., and Lemire, B. D. (2010). Caenorhabditis elegans diet significantly affects metabolic profile, mitochondrial DNA levels, lifespan and brood size. *Mol. Genet. Metab.* 100, 274–282. doi:10.1016/j.ymgme.2010.03.013.

Ribas, V., GarcÃa-Ruiz, C., and FernÃ¡ndez-Checa, J. C. (2014). Glutathione and mitochondria. *Front. Pharmacol.* 5. doi:10.3389/fphar.2014.00151.

Rice, A. C., Keeney, P. M., Algarzae, N. K., Ladd, A. C., Thomas, R. R., and Bennett, J. P. (2014). Mitochondrial DNA copy numbers in pyramidal neurons are decreased and mitochondrial biogenesis transcriptome signaling is disrupted in Alzheimer's disease hippocampi. *J. Alzheimer's Dis.* 40, 319–330. doi:10.3233/JAD-131715.

Riddle, Donald L. Blementhal, Thomas. Meyer, Barbara J. Priess, J. R. ed. (1997). *C. elegans II.* 2nd editio. New York: Cold Spring Harbor Laboratory Press.

Rossignol, R., Faustin, B., Rocher, C., Malgat, M., Mazat, J.-P., and Letellier, T. (2003). Mitochondrial threshold effects. *Biochem. J.* 370, 751–62. doi:10.1042/BJ20021594.

Rutter, M. T., Roles, A., Conner, J. K., Shaw, R. G., Shaw, F. H., Schneeberger, K., et al. (2012). Fitness of arabidopsis thaliana mutation accumulation lines whose spontaneous mutations are known. *Evolution (N. Y).* 66, 2335–2339. doi:10.1111/j.1558-5646.2012.01583.x.

Safdar, A., Khrapko, K., Flynn, J. M., Saleem, A., De Lisio, M., Johnston, A. P. W., et al. (2015). Exercise-induced mitochondrial p53 repairs mtDNA mutations in mutator mice. *Skelet. Muscle* 6, 7. doi:10.1186/s13395-016-0075-9.

Santos, D., Esteves, A. R., Silva, D., Januário, C., and Cardoso, S. (2015). The Impact of Mitochondrial Fusion and Fission Modulation in Sporadic Parkinson's Disease. *Mol. Neurobiol.* 52, 573–586. doi:10.1007/s12035-014-8893-4.

Santos, R. X., Correia, S. C., Carvalho, C., Cardoso, S., Santos, M. S., and Moreira, P. I. (2011). Mitophagy in neurodegeneration: an opportunity for therapy? *Curr. Drug Targets* 12, 790–799. doi:10.2174/138945011795528813.

Saxer, G., Havlak, P., Fox, S. A., Quance, M. A., Gupta, S., Fofanov, Y., et al. (2012). Whole Genome Sequencing of Mutation Accumulation Lines Reveals a Low Mutation Rate in the Social Amoeba Dictyostelium discoideum. *PLoS One* 7. doi:10.1371/journal.pone.0046759.

Saxton, W. M., and Hollenbeck, P. J. (2012). The axonal transport of mitochondria. *J. Cell Sci.* 125, 2095–2104. doi:10.1242/jcs.053850.

Sazanov, L. A. (2015). A giant molecular proton pump: structure and mechanism of respiratory complex I. *Nat. Rev. Mol. Cell Biol.* 16, 375–388. doi:10.1038/nrm3997.

Schadt, E. E., Turner, S., and Kasarskis, A. (2010). A window into third-generation sequencing. *Hum. Mol. Genet.* 19. doi:10.1093/hmg/ddq416.

Schloss, P. D., Gevers, D., and Westcott, S. L. (2011). Reducing the effects of PCR amplification and sequencing Artifacts on 16s rRNA-based studies. *PLoS One* 6. doi:10.1371/journal.pone.0027310.

Schon, E. A., DiMauro, S., and Hirano, M. (2012). Human mitochondrial DNA: roles of inherited and somatic mutations. *Nat. Rev. Genet.* 13, 878–890. doi:10.1038/nrg3275.

Schulz, K. L., Eckert, A., Rhein, V., Mai, S., Haase, W., Reichert, A. S., et al. (2012). A new link to mitochondrial impairment in tauopathies. *Mol. Neurobiol.* 46, 205–216. doi:10.1007/s12035-012-8308-3.

Sedensky, M. M., and Morgan, P. G. (2006). Mitochondrial respiration and reactive oxygen species in C. elegans. *Exp. Gerontol.* 41, 957–967. doi:10.1016/j.exger.2006.06.056.

Serra-Pages, C. (1998). Liprins, a Family of LAR Transmembrane Protein-tyrosine Phosphatase-interacting Proteins. *J. Biol. Chem.* 273, 15611–15620. doi:10.1074/jbc.273.25.15611.

Shaw, R. G., Shaw, F. H., and Geyer, C. (2003). WHAT FRACTION OF MUTATIONS RED.UCES FITNESS? A REPLY TO KEIGHTLEY AND LYNCH. *Evolution (N. Y).* 57, 686–689. doi:10.1111/j.0014-3820.2003.tb01562.x.

Shiraishi, Y., Murai, M., Sakiyama, N., Ifuku, K., and Miyoshi, H. (2012). Fenpyroximate Binds to the Interface between PSST and 49 kDa Subunits in Mitochondrial NADH-Ubiquinone Oxidoreductase. *Biochemistry* 51, 1953–1963. doi:10.1021/bi300047h.

Silander, O. K., Tenaillon, O., and Chao, L. (2007). Understanding the evolutionary fate of finite populations: The dynamics of mutational effects. *PLoS Biol.* 5, 922–931. doi:10.1371/journal.pbio.0050094.

Smith, J. M. (1978). *The Evolution of Sex*. Cambridge: Cambridge University Press.

Solignac, M., Gnermont, J., Monnerot, M., and Mounolou, J.-C. (1987). Drosophila mitochondrial genetics: Evolution of heteroplasmy through germ line cell divisions. *Genetics* 117, 687–696.

Solon-Biet, S. M., Mitchell, S. J., de Cabo, R., Raubenheimer, D., Le Couteur, D. G., and Simpson, S. J. (2015). Macronutrients and caloric intake in health and longevity. *J. Endocrinol.* 226, R17–R28. doi:10.1530/JOE-15-0173.

Song, I.-S., Kim, H.-K., Jeong, S.-H., Lee, S.-R., Kim, N., Rhee, B. D., et al. (2011). Mitochondrial Peroxiredoxin III is a Potential Target for Cancer Therapy. *Int. J. Mol. Sci.* 12, 7163–7185. doi:10.3390/ijms12107163.

De Souza, N., Vallier, L. G., Fares, H., and Greenwald, I. (2007). SEL-2, the C. elegans neurobeachin/LRBA homolog, is a negative regulator of lin-12/Notch activity and affects endosomal traffic in polarized epithelial cells. *Development* 134, 691–702. doi:10.1242/dev.02767.

Stewart, J. B., and Chinnery, P. F. (2015). The dynamics of mitochondrial DNA heteroplasmy: implications for human health and disease. *Nat. Rev. Genet.* 16, 530–42. doi:10.1038/nrg3966.

Stiernagle, T. (2006). Maintenance of C. elegans. *WormBook*. doi:10.1895/wormbook.1.101.1.

Swan, K. A., Curtis, D. E., McKusick, K. B., Voinov, A. V., Mapa, F. A., and Cancilla, M. R. (2002). High-throughput gene mapping in Caenorhabditis elegans. *Genome Res.* 12, 1100–1105. doi:10.1101/gr.208902.

Szamecz, B., Boross, G., Kalapis, D., Kovács, K., Fekete, G., Farkas, Z., et al. (2014). The Genomic Landscape of Compensatory Evolution. *PLoS Biol.* 12, e1001935. doi:10.1371/journal.pbio.1001935.

Taylor, R. W., and Turnbull, D. M. (2005). Mitochondrial DNA mutations in human disease. *Nat. Rev. Genet.* 6, 389–402. doi:10.1038/nrg1606.

Thu, V. T., Kim, H. K., Ha, S. H., Yoo, J.-Y., Park, W. S., Kim, N., et al. (2010). Glutathione peroxidase 1 protects mitochondria against hypoxia/reoxygenation damage in mouse hearts. *Pflugers Arch.* 460, 55–68. doi:10.1007/s00424-010-0811-7.

Tsang, W. Y., and Lemire, B. D. (2002a). Mitochondrial genome content is regulated during nematode development. *Biochem. Biophys. Res. Commun.* 291, 8–16. doi:10.1006/bbrc.2002.6394.

Tsang, W. Y., and Lemire, B. D. (2002b). Stable heteroplasmy but differential inheritance of a large mitochondrial DNA deletion in nematodes. *Biochem. Cell Biol.* 80, 645–654. doi:10.1139/o02-135.

Tsang, W. Y., and Lemire, B. D. (2003). The role of mitochondria in the life of the nematode, Caenorhabditis elegans. *Biochim. Biophys. Acta - Mol. Basis Dis.* 1638, 91–105. doi:10.1016/S0925-4439(03)00079-6.

Tuppen, H. A. L., Blakely, E. L., Turnbull, D. M., and Taylor, R. W. (2010a). Mitochondrial DNA mutations and human disease. *Biochim. Biophys. Acta - Bioenerg.* 1797, 113–128. doi:10.1016/j.bbabio.2009.09.005.

Tuppen, H. A. L., Hogan, V. E., He, L., Blakely, E. L., Worgan, L., Al-Dosary, M., et al. (2010b). The p.M292T NDUFS2 mutation causes complex I-deficient Leigh syndrome in multiple families. *Brain A J. Neurol.* 133, 2952–2963. doi:10.1093/brain/awq232.

Twig, G., and Shirihai, O. S. (2011). The interplay between mitochondrial dynamics and mitophagy. *Antioxid. Redox Signal.* 14, 1939–51. doi:10.1089/ars.2010.3779.

Vanduyn, N., Settivari, R., Levora, J., Zhou, S., Unrine, J., and Nass, R. (2013). The metal transporter SMF-3/DMT-1 mediates aluminum-induced dopamine neuron degeneration. *J. Neurochem.* 124, 147–157. doi:10.1111/jnc.12072.

Vasseur, E., and Quintana-Murci, L. (2013). The impact of natural selection on health and disease: uses of the population genetics approach in humans. *Evol. Appl.* 6, 596–607. doi:10.1111/eva.12045.

Vasta, V., Sedensky, M., Morgan, P., and Hahn, S. H. (2011a). Altered redox status of coenzyme Q9 reflects mitochondrial electron transport chain deficiencies in Caenorhabditis elegans. *Mitochondrion* 11, 136–138. doi:10.1016/j.mito.2010.09.002.

Vasta, V., Sedensky, M., Morgan, P., and Hahn, S. H. (2011b). Altered redox status of coenzyme Q9 reflects mitochondrial electron transport chain deficiencies in Caenorhabditis elegans. *Mitochondrion* 11, 136–138. doi:10.1016/j.mito.2010.09.002.

Vendelbo, M. H., and Nair, K. S. (2011). Mitochondrial longevity pathways. *Biochim. Biophys. Acta - Mol. Cell Res.* 1813, 634–644. doi:10.1016/j.bbamcr.2011.01.029.

Ventura, N., and Rea, S. L. (2007). Caenorhabditis elegans mitochondrial mutants as an investigative tool to study human neurodegenerative diseases associated with mitochondrial dysfunction. *Biotechnol. J.* 2, 584–595. doi:10.1002/biot.200600248.

Vinothkumar, K. R., Zhu, J., and Hirst, J. (2014). Architecture of mammalian respiratory complex I. *Nature* 515, 80–84. doi:10.1038/nature13686.

Wallace, D. C. (2005). A mitochondrial paradigm of metabolic and degenerative diseases, aging, and cancer: a dawn for evolutionary medicine. *Annu. Rev. Genet.* 39, 359–407. doi:10.1146/annurev.genet.39.110304.095751.

Wallace, D. C. (2007). Why do we still have a maternally inherited mitochondrial DNA? Insights from evolutionary medicine. *Annu. Rev. Biochem.* 76, 781–821. doi:10.1146/annurev.biochem.76.081205.150955.

Wallace, D. C., and Chalkia, D. (2013a). Mitochondrial DNA Genetics and the Heteroplasmy Conundrum in Evolution and Disease. *Cold Spring Harb. Perspect. Biol.* 5, a021220–a021220. doi:10.1101/cshperspect.a021220.

Wallace, D. C., and Chalkia, D. (2013b). Mitochondrial DNA genetics and the heteroplasmy conundrum in evolution and disease. *Cold Spring Harb. Perspect. Biol.* 5. doi:10.1101/cshperspect.a021220.

Wallace, D. C., and Youle, R. eds. (2013). *Mitochondria*. Cold Spring Harbor, New York: Cold Spring Harbor Laboratory Press.

Wang, A. D., Sharp, N. P., and Agrawal, A. F. (2014). Sensitivity of the distribution of mutational fitness effects to environment, genetic background, and adaptedness: A case study with Drosophila. *Evolution (N. Y).* 68, 840–853. doi:10.1111/evo.12309.

Wang, J. W., Howson, J., Haller, E., and Kerr, W. G. (2001). Identification of a novel lipopolysaccharide-inducible gene with key features of both A kinase anchor proteins and chs1/beige proteins. *J. Immunol.* 166, 4586–4595. doi:10.4049/jimmunol.166.7.4586.

Wang, J.-W., Gamsby, J. J., Highfill, S. L., Mora, L. B., Bloom, G. C., Yeatman, T. J., et al. (2004). Deregulated expression of LRBA facilitates cancer cell growth. *Oncogene* 23, 4089–4097. doi:10.1038/sj.onc.1207567.

Wang, Y., and Hekimi, S. (2015). Mitochondrial dysfunction and longevity in animals: Untangling the knot. *Science (80-.).* 350, 1204–1207. doi:10.1126/science.aac4357.

Whitlock, M. C. (2000). Fixation of new alleles and the extinction of small populations: drift load, beneficial alleles, and sexual selection. *Evolution* 54, 1855–1861. doi:10.2144/05384CI01.

Wicks, S. R., Yeh, R. T., Gish, W. R., Waterston, R. H., and Plasterk, R. H. (2001). Rapid gene mapping in Caenorhabditis elegans using a high density polymorphism map. *Nat. Genet.* 28, 160–164. doi:10.1038/88878.

Williams, B. D., Schrank, B., Huynh, C., Shownkeen, R., and Waterston, R. H. (1992). A genetic mapping system in Caenorhabditis elegans based on polymorphic sequence-tagged sites. *Genetics* 131, 609–624.

Wloch, D. M., Szafraniec, K., Borts, R. H., and Korona, R. (2001). Direct estimate of the mutation rate and the distribution of fitness effects in the yeast Saccharomyces cerevisiae. *Genetics* 159, 441–452.

Wong, A., Boutis, P., and Hekimi, S. (1995). Mutations in the clk-1 gene of Caenorhabditis elegans affect developmental and behavioral timing. *Genetics* 139, 1247–1259. doi:10.1007/s11033-011-0852-9.

Wood, W. B. (1988). *The Nematode Caenorhabditis elegans*. Cold Spring Harbor, N.Y.: Cold Spring Harbor Laboratory.

Wood, and WB (1988). *The Nematode Caenohabditis Elegans*. Cold Spring Harbor, New York: Cold Spring Harbor Laboratory doi:10.1101/087969307.17.1.

WormBase *WS242*. Available at: http://www.wormbase.org/#01-23-6 [Accessed June 20, 2004].

Wright, S. (1931). Evolution in Mendelian Populations. *Genetics* 16, 97–159. Available at: http://www.pubmedcentral.nih.gov/articlerender.fcgi?artid=1201091&tool=pmcentrez&rendertype=abstract.

Yanase, S., Yasuda, K., and Ishii, N. (2002). Adaptive responses to oxidative damage in three mutants of Caenorhabditis elegans (age-1, mev-1 and daf-16) that affect life span. *Mech. Ageing Dev.* 123, 1579–1587. doi:10.1016/S0047-6374(02)00093-3.

Zeyl, C., Mizesko, M., and de Visser, J. a (2001). Mutational meltdown in laboratory yeast populations. *Evolution* 55, 909–917. doi:10.1111/j.0014-3820.2001.tb00608.x.

Zhang, P., Lu, Y., Yu, D., Zhang, D., and Hu, W. (2015). TRAP1 Provides Protection Against Myocardial Ischemia-Reperfusion Injury by Ameliorating Mitochondrial Dysfunction. *Cell. Physiol. Biochem.* 36, 2072–2082. doi:10.1159/000430174.

Zhang, Y., Zou, X., Ding, Y., Wang, H., Wu, X., and Liang, B. (2013). Comparative genomics and functional study of lipid metabolic genes in Caenorhabditis elegans. *BMC Genomics* 14, 164. doi:10.1186/1471-2164-14-164.

Zhen, M., and Jin, Y. (1999). The liprin protein SYD-2 regulates the differentiation of presynaptic termini in C. elegans. *Nature* 401, 371–375. doi:10.1038/43886.

Zhong, W., and Sternberg, P. W. (2006). Genome-wide prediction of C. elegans genetic interactions. *Science* 311, 1481–1484. doi:10.1126/science.1123287.

Zhu, Y. O., Siegal, M. L., Hall, D. W., and Petrov, D. A. (2014). Precise estimates of mutation rate and spectrum in yeast. *Proc. Natl. Acad. Sci. U. S. A.* 111, E2310–8. doi:10.1073/pnas.1323011111.

Ziegler, D. V., Wiley, C. D., and Velarde, M. C. (2015). Mitochondrial effectors of cellular senescence: beyond the free radical theory of aging. *Aging Cell* 14, 1–7. doi:10.1111/acel.12287.